

**DEVELOPMENT OF A BLOWOUT  
INTERVENTION METHOD AND DYNAMIC  
KILL SIMULATOR FOR BLOWOUTS  
OCCURRING IN ULTRA-DEEPWATER**

by

**Dr. Jerome J. Schubert, Texas A&M University  
Dr. Peter Valko, Texas A&M University  
Dr. Serguei Jourine, Texas A&M University  
Dr. Ray T. Oskarsen, John Wright Company  
Mr. Sam Noynaert, Texas A&M University  
Mr. Hector Meyer, Texas A&M University  
Mr. Steve Walls, Cherokee Offshore Engineering  
Mr. Curtis Weddle, III, Cherokee Offshore Engineering**

**Final Project Report – Phase One  
Prepared for the Minerals Management Service  
Under the MMS/OTRC Cooperative Research Agreement  
1435-01-99-CA-31003  
Task Order 18132  
Project Number 408**

**December 2004**

OTRC Library Number: 12/04-A147

“The views and conclusions contained in this document are those of the authors and should not be interpreted as representing the opinions or policies of the U.S. Government. Mention of trade names or commercial products does not constitute their endorsement by the U. S. Government”.



*For more information contact:*

**Offshore Technology Research Center**

Texas A&M University  
1200 Mariner Drive  
College Station, Texas 77845-3400  
(979) 845-6000

or

**Offshore Technology Research Center**

The University of Texas at Austin  
1 University Station C3700  
Austin, Texas 78712-0318  
(512) 471-6989

*A National Science Foundation Graduated Engineering Research Center*

# **Development of a Blowout Intervention Method and Dynamic Kill Simulator for Blowouts Occurring in Ultra-Deepwater.**

## **Executive Summary**

**Project Description:** This project originally included five tasks

- Task 1: Bridging tendencies in ultra-deepwater blowouts
- Task 2: Dynamic kill investigation of ultra-deepwater blowouts and simulator development.
- Task 3: Development of ultra-deepwater blowout control methods.
- Task 4: Cost of intervention
- Task 5: Final report, progress meetings, and workshops.

Tasks 3 and 5 will be completed in Phase II. Task 4 has been cancelled.

### **Task 1 – Bridging of blowouts in the GOM and tools for evaluation**

In this part of the project, a study of current wellbore bridging concepts was performed, and an approach for the prediction of blowout self-killing based on the numerical analysis of reservoir performance data, wellbore hydraulics, and wellbore stability was accomplished. The model can describe a wide variety of geological conditions and it can be used to define the parameters for evaluation of bridging, including conditions with openhole drilling and cased hole completions.

Several computer subroutines were built to assist in this analysis. The model elements were partially tested on published data and laboratory experiments. The advantages, important shortcomings, and design problems were identified. The model will be verified on two groups of blowout scenarios to simulate and analyze the control of each.

The bridging model concept assumes that the well is originally filled with drilling mud and the open part of the hole is in stable condition; then, for some reason, fluid starts flowing from the reservoir pushing the mud out of the well. The hole becomes unstable due to the pressure decline and hole starts to produce debris from the weakened rock layers. If the wellbore can collapse or falling particles can be stuck at an arbitrary point, the bridging will occur and wellbore will be self-killed. However, pressure below packed part of the well builds up. The pressure can exceed the shear strength of the rock bridge. In this case the plug can be pushed out of the well and the well will blow periodically. Depending on the pressure at which the fracturing occurs within the weakest zone the flowing formation will continue to flow and losses continue to occur in the fractured zone (underground blowout). This simplification of the real physical system with conservation of all important phenomena and processes represent the basis of developed model.

#### **Model Elements**

##### *1. Reservoir performance prediction subroutines.*

Well known reliable inflow performance relationships (IPR) have been used to model the flow of fluids from the reservoir, through the formation, and into the well

## *2. Wellbore hydraulic performance subroutines.*

The wellbore bridging model will be integrated into a dynamic kill simulator and it will use the output results of its pressure distribution prediction. However, currently we have developed a stand alone subroutine to calculate pressure drop along the wellbore. The components of the overall system pressure drop include the pressure drop associated with conveying the gas, liquid and solids.

## *3. Wellbore stability analysis and solid production subroutines*

To predict formation failure, stability in the packed wellbore, and solid mass rate under blowout conditions, three applicable geomechanics models were selected; shear failure, tensile failure and erosion failure. These models were coupled with the developed fluid flow model through solid mass flow rate.

- Failure model 1: Shear failure. The most conservative linear elastic deformational model was used to predict the stress concentrations and onset of shear failure. The laboratory tests were performed to estimate the influence of selected failure criteria on model prediction results.
- Failure model 2: Tensile failure. To predict the tensile failure mode we have developed an extended poroelastic solution for axisymmetrical plane strain problems with time dependent boundary conditions. The solution was developed in Laplace space and it was verified with published results for the special cases of boundary conditions for finite and infinite cylinders using numerical Laplace inversion.

Computational results successfully describe the occurrence of tensile radial stresses due to rapid and intensive decrease in pressure at the inner boundary. The results show that by changing the rate of the pressure descent, a failure can be avoided or triggered when so desired. The general solution can be used to calculate the stress and pore pressure distributions around boreholes under infinite/finite boundary conditions with gradually changing pore pressure. The proposed solution was verified with laboratory tests.

- Failure Model 3: Erosion failure. The solid production was analyzed with a sand erosion model that couples the fluid flow and rock erosion behavior during fluid production. The fluid flow and solid transport are coupled through the fluid flow rate. The model was tested using published data.

The final results of this task will be submitted upon completion in early 2005.

## **Task 2- Dynamic kill model for conventional and dual density Deep Water Blowouts (surface and underground) and investigation of pump rates to kill wells**

In this section of the project a preliminary dynamic kill simulator is complete and functional. The program is written in Java. Java is chosen because of its versatility, modularity, and reusability. Java is an object-orientated language which is a favored programming approach that has largely replaced the standard procedure-based programming techniques over the last decade.

The program's main features and advantages include user friendliness, a choice between stand alone or web application, surface, sub surface and underground blowout capabilities and simple dual-gradient drilling. The program also has the capability to model both Newtonian and non-Newtonian kill fluids, oil and gas reservoirs, rigid temperature models, fluid properties adjusted for pressure and temperature effects, it takes into account sonic flow considerations and has three multiphase models accounting for slip between phases. The interface is clear and simple to work with and is easy to navigate. The inputs and results panel can be viewed at the same time. The layout contains four frames, the menu bar, the results bar, the inputs panel and the results panel

The dynamic kill simulator comprises of four main sections, an input data section, estimation of the initial blowing condition such as temperature, pressure and flowrates, calculation of the minimum kill rate and standpipe pressure needed for successful intervention with a given fluid and well configuration and graphical output of the results.

This early version of the program focuses on simulating dynamic kills for vertical wells in ultra-deep water. The simulator applies to both gas and liquid reservoirs and has the option of using a relief well or a drillstring in the blowing wellbore. The blowing wellbore may include both pipe flow and annular flow, depending on whether a drillstring is present in the wellbore. The computer program is also capable of simulating a dynamic kill using either a Newtonian or a non-Newtonian kill fluid. For pressure, temperature and fluid-property predictions, the simulator incorporates state-of-the-art models that have been extensively used and verified by the industry. No new correlations were developed for this task. The computer program was tested against multiphase-pressure data to identify and prevent potential coding bugs and conceptual errors.

The program calculates the initial conditions, then calculates the required flow rate of kill fluid for a dynamic kill. The initial conditions are based on multiphase calculations and use the concept of system or nodal analysis. Once the IPR curve has been determined for a blowing wellbore, the kill rate can be determined. Successive iterations of a system curve encompassing the blowing wellbore during the kill operation will lead to an answer. The initial inflow performance relationship curve or IPR curve is calculated using a multiphase model.

A full discussion of the Dynamic Kill simulator can be found in Appendix A.

### **Task 3: Development of ultra-deepwater blowout control methods.**

The investigation of mechanical intervention techniques has ranged into all envisioned failure points which would require some form of intervention at the mudline. This naturally led to the exploring of extremely detailed and divergent scenarios, many of them requiring unique solutions in order that the goal of recovering primary well control be met. Even with this detail and divergence, the types of interventions rapidly evolved into two different areas: presently workable and not workable using today's methods and techniques.

Discussions with the well control companies which have had personnel aboard the rare blowouts and potential blowouts to date in water depths greater than 1000 feet have enabled the research team to create a list of lessons learned and best practices to add to the normal suite of well-fighting techniques. These techniques range from rather obscure details, such as capping off unused control lines inside the purely hydraulic BOP control systems, to selecting rig and service contractors based upon their ability to provide manpower and resources during an emergency management event.

This project differs from typical industry well control efforts. The entire approach of prevention of well control events, or safely handling any occurrences, is the focus of well control training and certification. This particular project assumes that those efforts have failed, for whatever reason, and explores the various failure scenarios to determine whether or not primary well control can be recovered using presently-available tools and techniques.

In certain failure scenarios which do not involve influx flow outside the blowout preventer stack, control may well be restored with simple mechanical interventions or repairs using ROVs (Remotely Operated Vehicles) or in very limited situations, one-atmosphere diving suits.

In failure scenarios where there has been a catastrophic failure either of the surface equipment, the wellhead system or high casing, or at almost any point where influx is flowing outside of the blowout preventers, options become very rapidly non-existent. Even higher-horsepower ROVs can do little but stay outside an area of turbulence, and visibility could well be reduced anyway. Mudline mechanical intervention becomes an impossibility at this point with present tools and techniques. Specifically, there are no tools available which can hold station in a blowout with influx moving through the desired intervention area. ROVs also do not possess the horsepower required to consider some of the work tasks involved in a given scenario, particularly when affecting repairs on damaged blowout preventers. When viewed individually, the endpoints reached while developing the various scenarios seem widely varied. Closer examination has revealed that the inability to perform a task after a certain point in a failure scenario actually defines the scope of work for developing new tools and equipment.

Dialogues with top industry professionals helped produce several ideas, two of which may seem workable. For instance, to avoid the inherent weakness of trying to perform operations while floating lead to the possibility that the intervention tools may need to be based on the bottom of the seafloor, much like seabed tractors used in offshore pipeline and cable operations. Developing a vehicle such as this would enable the maximum horsepower to be used to perform hydraulic operations instead of diverting power to remaining on station.

An even more intriguing idea has been gleaned from experienced ROV specialists who envision hydraulically coupling today's most powerful ROV units to a slightly-negative-buoyed lower tractor unit which has been designed, built and deployed by a consortium similar to the present clean-up contractors such as Clean Seas Inc. This tractor unit could be designed to take advantage of mobility, maximum flexibility and redundancies, using the ROV's control systems to view, operate or repair equipment during mechanical interventions at the mudline.

This concept, carried to its most efficient utilization, envisions a fleet of similar ROVs conducting normal surveillance or control operations on a unit sub as a multiple template, or group of subsea trees or completions. This type of unit would be in continual use for routine operations with operating spares in place for maintenance, upgrades or for deployment during well control emergencies. The most efficient use of this type of system would most likely require a dedicated tender vessel.

The decision of which concept to pursue for design, development and deployment of the envisioned Deepwater Intervention System (DIS) needs to be made early during Phase II of this project with the input of the project partners, top subsea and well control companies and with the input of respected industry consultants. After this decision has been agreed upon, design of the DIS should proceed with the goal of presenting a complete development plan at the conclusion of Phase II.

A full description of the “Best Practices” for deepwater blowout containment can be found in Appendix B. Upon completion of Phase II, a final report will be provided which describes any new kill techniques developed by the research team via a supplemental report

**Task 5: Final Report, Progress meetings, and workshops.**

Will be completed in Phase II.

**Reports and Publications:**

Jourine, S., Karner, S L, Kronenberg, A K, Chester, F M.: Influence of Intermediate Stress on Yielding of Berea Sandstone Eos Trans. AGU, 84(46), Fall Meet. Suppl., Abstract T41D-0249, 2003.

Jourine, S., Schubert J.J, Valko P.P.: Saturated Poroelastic Hollow Cylinder Subjected To Non-stationary Boundary Pressure – Model and Laboratory Test. Submitted to Gulf Rocks '04, 6th North American Rock Mechanics Symposium (NARMS).

Oskarsen, R.T., and Schubert, J.J., “Development of a Dynamic Kill Simulator for Drilling in Ultradeep Water,” Presented at the AADE National Technical Conference.

Jourine, S., and Schubert, J. J., “Wellbore Bridging as a Possible Alternative to Blowout Control in Ultra-Deepwater Wells,” Presented at the 2003 AADE National Technical Conference, Houston, TX. April 1-3, 2003.

Noynaert, S.F., “ULTRADEEP WATER BLOWOUTS: COMASIM Dynamic Kill Simulator Validation and Best Practices Recommendations,” Masters Thesis at TAMU, December 2004.

# **Appendix A**

**Final Report for Task 2.**

## **DEVELOPMENT OF A DYNAMIC-KILL SIMULATOR FOR ULTRADEEP WATER**

**By**

**Dr. Ray T. Oskarsen, TAMU (currently John Wright Company)**

**DEVELOPMENT OF A DYNAMIC-KILL SIMULATOR FOR  
ULTRADEEP WATER**

A Dissertation

by

RAY TOMMY OSKARSEN

Submitted to the Office of Graduate Studies of  
Texas A&M University  
in partial fulfillment of the requirements for the degree of

DOCTOR OF PHILOSOPHY

August 2004

Major Subject: Petroleum Engineering

**DEVELOPMENT OF A DYNAMIC-KILL SIMULATOR FOR  
ULTRADEEP WATER**

A Dissertation

by

RAY TOMMY OSKARSEN

Submitted to Texas A&M University  
in partial fulfillment of the requirements  
for the degree of

DOCTOR OF PHILOSOPHY

Approved as to style and content by:

---

Hans C. Juvkam-Wold  
(Co-Chair of Committee)

---

Jerome J. Schubert  
(Co-Chair of Committee)

---

James E. Russell  
(Member)

---

Ann E. Jochens  
(Member)

---

Stephen A. Holditch  
(Head of Department)

August 2004

Major Subject: Petroleum Engineering

## ABSTRACT

Development of a Dynamic-Kill Simulator for Ultradeep Water.

(August 2004)

Ray Tommy Oskarsen, B.S., University of Surrey, England;

M.S., Texas A&M University

Co-Chairs of Advisory Committee: Dr. Hans C. Juvkam-Wold

Dr. Jerome J. Schubert

Over the last decades exploration for hydrocarbons has been rapidly moving into unconventional reservoirs such as ultradeep water. Because no guidelines and procedures for blowout containment in ultradeep water are currently available, a project has been undertaken to develop them. Developing and validating the procedures requires a dynamic-kill simulator, but no available dynamic-kill simulator can perform all the simulations necessary. Therefore, the project chose to develop its own simulator that can model dynamic kills for surface, subsurface, and underground blowouts for modern drilling techniques. This dissertation describes the development of that simulator.

Some of the main features and advantages of this dynamic-kill simulator include:

- A user-friendly interface.
- Choice between stand-alone or Web application.
- Surface, subsurface and underground blowout capability.
- Simple dual-gradient drilling.
- Both Newtonian and non-Newtonian kill fluids.
- Oil and gas reservoirs.
- Rigid temperature models.
- Fluid properties adjusted for pressure and temperature effects.
- Sonic flow considerations.
- Three multiphase models accounting for slip between phases.

The simulator is validated using simple analytical solutions and production data. In all cases the simulator gives reasonable and meaningful results.

The simulator is also used to study the effect on blowout intervention as drilling is moved into deeper and deeper water. Results show that as water depth increases, the intervention requirements become more demanding. Because of the high flowrates and horsepower needed, a blowout in ultradeep water will likely require more than one relief well for successful blowout intervention.

## **DEDICATION**

This work is dedicated to my parents, who let me become a Texan and be a student for way too long, and to my wife Marissa, who rescued me from the cold dark hole I grew up in, cleaned me, fed me, and waited patiently for me to graduate without expecting anything in return.

## ACKNOWLEDGMENTS

I wish to express “mange tusen hjertelig” thanks to Dr. Hans “I Speak Norwegian, but You Don’t” Juvkam-Wold for being my advisor and a good friend throughout my many years at A&M. Good luck with your retirement; only another 15 years to go.

My most sincere thanks to Dr. Jerome “Bury Me 6 Feet Under, Not 2 Meters” Schubert for being my co-chair, mentor, the principal investigator, the guy who signs my paychecks, and a friend.

Great big ’ol thanks to my committee members Dr. James Russell and Dr. Ann Jochens, and to my colleagues Curtis Weddle III, Steve Walls, Serguei Jourine, Sam “I Broke Your Simulator” Noynaert, Bjorn Gjorv, Max Long and all of ADR.

A big bow and heaps of thanks to Kai Capps, Allen Biehle, Kevin Smith and Dori Edens at Capsher. Without your help I’d still be working on a graphics package.

Warm thanks to John “Let the Adventure Begin” Wright, for teaching me some basic blowout skills and giving me something to look forward to beyond graduation.

Many thanks to Dr. Otto Santos for enlightening me in my sonic confusion. There should be a good position available for you at A&M in about 15 years.

Mucho gracias to Dr. Tom “Me Big Chief, You Little Indian” Blasingame for accepting me into A&M and keeping education interesting.

Last but not least, I would like to thank my wife’s Longhorn family, the Forbuses of fun, for making me a proud brAggie.

## TABLE OF CONTENTS

	Page
ABSTRACT .....	iii
DEDICATION .....	v
ACKNOWLEDGMENTS.....	vi
TABLE OF CONTENTS .....	vii
LIST OF FIGURES.....	x
LIST OF TABLES .....	xii
 CHAPTER	
I INTRODUCTION.....	1
1.1 Blowouts.....	2
1.2 Types of Blowouts .....	2
1.3 Blowout Trends and Statistics.....	6
1.4 Blowout Intervention Methods.....	8
1.5 Modeling of a Dynamic Kill .....	12
1.6 Objective of the Study.....	14
1.7 Expected Contributions From Study .....	16
II THE DYNAMIC-KILL SIMULATOR .....	17
2.1 Java.....	17
2.2 Layout and Features .....	18
2.2.1 The Menu Bar.....	19
2.2.2 The Result Bar.....	19
2.2.3 The Results Panel.....	20
2.2.4 The Inputs Panel.....	20
III MODELING.....	28
3.1 Flow Rates and Velocities.....	28
3.2 Pressure Calculations .....	29
3.2.1 Moody Friction Factor for Newtonian Flow .....	34
3.2.2 Fanning Friction Factor for Non-Newtonian Flow .....	35
3.2.3 Multiphase Flow Calculation .....	37

CHAPTER	Page
3.2.4 Single-Phase Liquid Flow .....	42
3.2.5 Single-Phase Gas Flow.....	44
3.2.6 Annular Flow.....	44
3.2.7 Sonic Flow.....	45
3.3 Temperature Calculations .....	46
3.3.1 Wellbore-Heat Transfer Below the Mudline.....	50
3.3.2 Wellbore-Heat Transfer Above the Mudline .....	53
3.3.3 Overall Heat-Transfer Coefficient .....	54
3.4 Inflow Performance Relationship.....	57
3.4.1 Oil Reservoir IPR .....	59
3.4.2 Gas Reservoir IPR.....	61
3.5 Properties of Reservoir Fluids.....	64
3.5.1 $z$ -Factor of Natural Gases.....	64
3.5.2 Gas Density .....	65
3.5.3 Gas Formation Volume Factor.....	65
3.5.4 Gas Viscosity.....	66
3.5.5 Oil Density .....	66
3.5.6 Oil Formation Volume Factor and Oil Compressibility.....	67
3.5.7 Solution-Gas/Oil Ratio.....	68
3.5.8 Oil Viscosity.....	68
3.5.9 Water Density.....	69
3.5.10 Water Formation Volume Factor .....	69
3.5.11 Solution-Gas/Water Ratio .....	69
3.5.12 Water Viscosity .....	70
3.5.13 Gas/Oil and Gas/Water Interfacial Tension .....	70
3.6 Nodal Analysis .....	70
3.7 Dynamic Kill Single-Phase Solution.....	71
3.8 Dynamic Kill Multiphase Solution .....	74
IV ALGORITHMS.....	77
4.1 Pressure Algorithm.....	79
4.2 Temperature Algorithm.....	81
4.3 Wellbore-Profile Algorithm .....	82
4.4 Initial-Condition Algorithm .....	84
4.5 Single-Phase Solution Algorithm.....	84
4.6 Multiphase Solution Algorithm.....	86
4.7 Global Iteration Scheme.....	88
V TESTING AND RESULTS .....	90
5.1 Initial Condition .....	90

CHAPTER	Page
5.2 Minimum Kill Rate .....	95
VI DISCUSSION AND CONCLUSIONS .....	98
6.1 Suggestion for Further Work.....	99
NOMENCLATURE.....	101
REFERENCES .....	106
APPENDIX A: TWO-PHASE FLOW CORRELATIONS .....	111
A.1 Hagendorn and Brown.....	111
A.2 Beggs and Brill.....	116
A.3 Duns and Ros.....	121
APPENDIX B: EMPIRICAL FLUID PROPERTY CORRELATIONS .....	134
B.1 z-Factor .....	134
B.2 Gas Viscosity .....	137
B.3 Oil Formation-Volume Factor .....	137
B.4 Oil Compressibility Above the Bubblepoint .....	138
B.5 Solution-Gas/Oil Ratio .....	139
B.6 Oil Viscosity .....	139
B.7 Water Formation-Volume Factor .....	140
B.8 Solution-Gas/Water Ratio.....	141
B.9 Water Viscosity .....	142
B.10 Gas/Oil Interfacial Tension .....	143
B.11 Gas/Water Interfacial Tension.....	143
VITA .....	145

## LIST OF FIGURES

FIGURE	Page
1.1 Blowout pyramid for GOM drilling .....	8
2.1 Simulator interface .....	18
2.2 Mixture-velocity graph displayed in separate window .....	21
2.3 Blowout case with returns to the surface using a drillstring to circulate the kill fluid .....	22
2.4 Blowout case with returns to the mudline using a relief well to circulate the kill fluid .....	23
2.5 Drillstring options for wild well.....	24
2.6 Drillstring hanging from BOP .....	25
2.7 Drillstring dropped to the bottom.....	26
2.8 Pop-up message indicating an input error .....	27
3.1 Small element of fluid in a pipe .....	31
3.2 Rheological models .....	33
3.3 Apparent viscosity for a power-law fluid.....	35
3.4 Temperature fluxes for an element of fluid below the mudline .....	51
3.5 Temperature fluxes for an element of fluid above the mudline .....	55
3.6 Radial flow from a reservoir to a wellbore .....	58
3.7 Determining the initial flowrate and bottomhole flowing pressure using nodal-analysis .....	71
3.8 System-intake curves for different kill rates .....	72
3.9 Relationship between single-phase, multiphase and zero-derivative solution for the minimum kill rate .....	76
4.1 Blowing well with exit to the mudline separated into finite elements .....	78
4.2 Two adjacent elements in the wellbore .....	79
4.3 Pressure algorithm.....	80
4.4 Temperature algorithm.....	82

FIGURE	Page
4.5 Wellbore-profile algorithm .....	83
4.6 Initial-condition algorithm .....	85
4.7 Single-phase solution for the minimum kill rate.....	86
4.8 Multiphase solution for the minimum kill rate.....	87
4.9 Global iteration scheme.....	89
5.1 System-intake curves from the simulator with varying gas/liquid ratios.....	91
5.2 Comparing the multiphase models with tubing size of 1.995 in. and GLR of 100 scf/STBL .....	93
5.3 Comparing the multiphase models with tubing size of 8.921 in. and GLR of 300 scf/STBL .....	94
5.4 Comparing the multiphase models with tubing size of 8.921 in. and GLR of 300 scf/STBL in 10,000 ft of water depth.....	95
5.5 Minimum-kill rate and standpipe-pressure requirement with increasing water depth.....	97
A.1 Hagendorn and Brown correlation for $N_{LC}$ .....	113
A.2 Hagendorn and Brown correlation for $H_L/\psi$ .....	114
A.3 Hagendorn and Brown correlation for $\psi$ .....	117
A.4 Duns and Ros bubble/slug transition parameters .....	123
A.5 Duns and Ros bubble-flow, slip-velocity parameter $F_1$ .....	124
A.6 Duns and Ros bubble-flow, slip-velocity parameter $F_2$ .....	124
A.7 Duns and Ros bubble-flow, slip-velocity parameter $F_3$ .....	125
A.8 Duns and Ros bubble-flow, slip-velocity parameter $F_4$ .....	125
A.9 Duns and Ros slug-flow, slip-velocity parameter $F_5$ .....	126
A.10 Duns and Ros slug-flow, slip-velocity parameter $F_6$ .....	127
A.11 Duns and Ros slug-flow, slip-velocity parameter $F_7$ .....	127
A.12 Duns and Ros bubble-flow, friction-factor parameter $f_2$ .....	129

## LIST OF TABLES

TABLE	Page
1.1 Potential Sources for Uncontrolled Flow Above the Mudline .....	4
1.2 Potential Sources for Uncontrolled Flow Below the Mudline .....	5
5.1 Absolute Error Between Beggs Curves and Simulation Results	
With Tubing Size of 1.995 in. and Liquid Rate of 700 STBL/D .....	92
5.2 Absolute Error Between Beggs Curves and Simulation Results	
With Tubing Size of 3.958 in. and Liquid Rate of 8,000 STBL/D .....	92
5.3 Blowout Data for Calculation Example .....	96
A.1 Horizontal Flow-Pattern Coefficients, Beggs and Brill Method.....	118
A.2 Deviated Flow-Pattern Coefficients for Beggs and Brill Method.....	119
B.1 A Constants for the Dranchuk and Abou-Kassem Correlation for z-Factor.....	136
B.2 Constants for the Vasquez and Beggs Correlation for Oil	
Formation Volume Factor .....	138

## CHAPTER I

### INTRODUCTION

The trend for the oil industry has been to explore for hydrocarbon reservoirs in deeper and deeper water. This trend is a result of depleting oil reserves on land, an increase in demand for hydrocarbons, and promising potential for deepwater reservoirs.<sup>1</sup> With the current technology available, drilling for reservoirs in ultradeep water—where ultradeep water is defined in this text as water depths greater than 5,000 ft—encounters many problems. Numerous wells in such water depths have been plugged and abandoned, leading to huge financial losses for the company. It is predicted that many reservoirs cannot be reached with current technology, or they can be reached but the production tubing will be of such a small diameter that the well will be uneconomical.

The call for new technology is being heard from the industry, and several new methods for drilling in ultradeep water are being proposed. One such method that is showing great potential is dual-gradient drilling.<sup>2-4</sup> Several variations on how to obtain a dual-pressure gradient in the annulus include using a subsea pump to lift the drilling mud from the seafloor to the rig or injecting hollow glass spheres at the seafloor. Either way, the annular pressure at the seafloor is reduced to approximate the seawater hydrostatic pressure. The result is a virtually smaller hydrostatic column of mud in the annulus, which enables drilling with a higher-density drilling fluid, hence increasing the hydrostatic gradient in the annulus. The wellbore-pressure profile will thus follow the fracture and pore-pressure gradients more closely. Several of the major problems encountered with conventional drilling are thereby overcome, and other positive factors that may enhance well control have been found by using this method.

---

This dissertation follows the style and format of *SPE Drilling and Completion*.

## **1.1 Blowouts**

A kick is defined as an unscheduled influx of formation fluid into the wellbore. Kicks occur when the rig crew fails to control the pressures in the well. A blowout occurs when the rig crew fails to control the kick and regain pressure control, and can be defined as an uncontrolled flow of formation fluids. A blowout will always cause large unplanned expenses to the company, but may also result in loss of lives and damage to the environment.

The most recent deepwater blowout containment study can be found in Drilling Engineering Association (DEA)–63, Joint Industry Project (JIP) for evaluating floating vessel blowout control, which was released in September 1990.<sup>5</sup> Ultradeepwater drilling activity has increased dramatically in the last decade. Operations that were once exceptional and characterized by several man-years of well, operations, and contingency planning are now being done routinely several times each rig year. The report, DEA–63, did not contemplate operations in water as deep as we commonly operate in now. Nor did DEA–63 describe any of the recent deepwater drilling techniques such as dual-gradient drilling and appropriate blowout intervention procedures for them.

## **1.2 Types of Blowouts**

For offshore operations blowouts can be classified in three groups:

- Surface Blowouts.
- Subsurface Blowouts.
- Underground Blowouts.

Surface blowouts are characterized by fluid flow from a permeable formation to the rig floor, where atmospheric conditions exist. For subsurface blowouts the flow typically exits the well at the mudline, where the exit conditions are controlled by the seawater. Surface blowouts have been given the most attention, as they are usually

associated with large-scale fires. The most famous surface blowout is the Piper Alpha incident on the UK sector of the North Sea, 1988.<sup>6,7</sup> The explosion that occurred after the gas was ignited resulted in a fire that completely destroyed the platform and cost 167 lives and approximately \$1.48 billion in lost revenue. For subsurface blowouts, the plume of the reservoir fluid may cause loss of buoyancy to the point where a floating rig would sink. The likelihood of this scenario depends on the water depth, the flowing rate, and the density of the formation fluid. In deepwater the plume could be dispersed before reaching the surface or could be carried with the ocean currents to a location away from the rig.

An underground blowout occurs as fluids flow from one formation zone to another, typically by using the wellbore as a flow path. In the industry an underground blowout is also referred to as a cross flow between formations. Although underground blowouts are not as frequently discussed, they occur approximately 1.5 times<sup>6</sup> as frequently as surface and subsurface blowouts together and can escalate into just as dangerous and costly situations. The total loss of revenue for the Saga 2/4-14 and the West Venture underground blowout exceeded \$500 million.<sup>6</sup> One problem with underground blowouts is that there is no visible sign of danger at the surface. However, if the rig were on fire or sinking, the situation would immediately demand respect and attention. An underground blowout has the potential of breaching to the surface, which results in a subsurface blowout that can be very difficult to kill. This is very likely in depths less than 3,000 ft below mudline,<sup>8</sup> and the chances increase in young sediments—unconsolidated sands that was deposited at a relative recent geologic time—such as the ones often encountered in offshore drilling. If the underground blowout breaches to the surface immediately beneath the rig, it may topple jackups and platform rigs in addition to sinking floating rigs by loss of buoyancy.

As earlier described, a blowout can be defined as uncontrolled flow of formation fluid. For surface, subsurface, and underground blowouts, the uncontrolled flow can



**Table 1.2 – Potential Sources for Uncontrolled Flow Below the Mudline**

	Non-drilling operations w/ open ended drillstring (coring, fishing)	Broach to surface on shut in up an old broach/fracture chimney	Stuck or packed off, back off and have a kick up the drillstring	Shoe failure and leak back to previous casing shoe/annulus	Casing failure and leak back to previous casing shoe/annulus	Bit plugging and inability to control well pressures	Failure of SSSV (sub surface safety valve)	Liner top failure, either flow or breakdown	Squeeze perforation in shoe leaking	Bridging and inability in shoe leaking	Failure of casing shoe	Underground blowout	Omni tool fail	Worn Casing
<b>Drilling</b>	X	X	X	X	X	X		X	X	X	X			
<b>Completion</b>	X		X	X	X	X		X			X	X		
<b>Production</b>		X					X		X		X			X

When a well-control situation is escalating into a blowout through a conventional riser, appropriate measures are called for to prevent the mud from being unloaded from the riser. Studies have shown that if the mud is ejected from the riser and replaced by a low-density reservoir fluid such as gas, the pressure difference to the hydrostatic pressure of the seawater may be sufficient to collapse the riser.<sup>9</sup> Additionally, if the riser is filled with gas instead of mud, the flowing bottomhole pressure will be lower, creating a better flow-potential for the formation influx. In comparison, the hydrostatic pressure of seawater will create additional backpressure in the blowing well, which may aid in

controlling the formation-influx rate. If the well depth is greater than 3,000 ft below the mudline, the rig crew may choose to close the blowout preventer, which could potentially create an underground blowout. Otherwise, the riser should always be disconnected and the well vented to the seafloor.

### **1.3 Blowout Trends and Statistics**

A 1993 study by the Minerals Management Service (MMS) on the frequency of blowouts in the Gulf of Mexico (GOM) showed that from 1971 through 1991, 87 blowouts occurred during drilling operations.<sup>10</sup> During the same period, 21,436 wells were drilled. The number of blowouts per year in this period seemed to follow a trend linearly proportional to the number of wells drilled.

Typically, a blowout happens after a series of events that can be traced back to human error and/or equipment failure. The two main causes for blowouts in the MMS study were swabbing and fracturing the formation. Swabbing occurs when the drillpipe is pulled out of the hole too fast and formation fluid is swabbed into the hole. Fracturing occurs when the pressure in the well exceeds the formation integrity and the mud in the annulus disappears into a permeable formation. Because the mud level in the annulus will drop as mud exits the wellbore, the static bottomhole pressure will decrease, which allows formation fluid to enter the wellbore at any other permeable zone in the open-hole section.

Small gas pockets at shallow depths were the most common sources of formation fluid for the blowouts. These blowouts are typically short in duration, but the gas pockets may contain sulfur in the form of hydrogen sulfide, which is dangerous for the rig crew. Also, most blowouts occurred during drilling operations.

In 1998 Skalle and Podio<sup>11</sup> published a study on the frequency of blowouts for all operations covering both onshore Texas and offshore in the GOM over 36 years. This study found that on average there is a blowout per 285 wells drilled.

As for the MMS study, Skalle and Podio found that the frequency of blowouts offshore GOM follows the number of wells drilled. However, they found that for onshore Texas the frequency of blowouts remained flat and independent of the number of wells being drilled for the 36 years studied.

In 1990 Wylie and Visram<sup>12</sup> found that on average there is a blowout for every 110 kicks. A reliability study of blowout preventers found an average of 52 kicks for every 100 wells drilled,<sup>7</sup> 79 % of the kicks caused significant problems and 21 % resulted in loss of all or part of the well.

Using the data presented above, a blowout pyramid as shown in **Fig. 1.1** can be constructed for blowouts in the GOM. There are many ways to interpret the blowout-frequency data, which would lead to slightly different numbers in the pyramid. The number of at-risk operations is typically not reported and is therefore left blank.

This type of pyramid, which shows 1 blowout for every 285 wells drilled, is often used with a work-from-the-bottom analysis to avoid or moderate the most severe events. Reducing the number of wells drilled would obviously reduce the chances of a blowout. However, a more practical solution would be to limit at-risk operations and the occurrence of kicks to decrease the chances of a blowout.

At the time of writing this dissertation, no ultradeep-water blowout has been recorded. However the trend and history for blowout frequency show that ultradeep drilling is clearly at risk, and an ultradeep water blowout will be very difficult to avoid in the future.

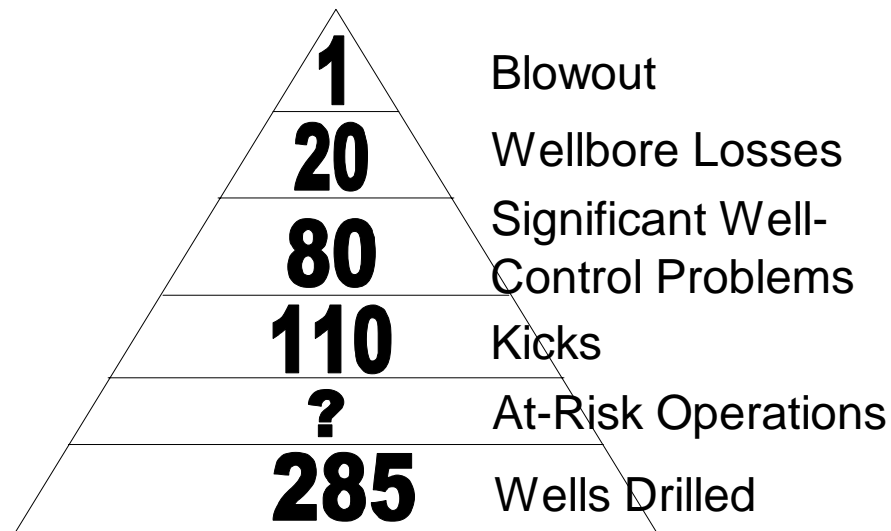


**Fig. 1.1—Blowout pyramid for GOM drilling.**

#### **1.4 Blowout Intervention Methods**

A number of blowout-intervention methods are available to bring a wild well under control. They can be classified in two groups<sup>8</sup> depending on the intervention location:

- Surface intervention.
- Relief well methods.

Surface intervention aims to control the blowout by direct access to the wellhead or exit point of the wild well. Relief wells are used to gain control of blowouts in situations where direct-surface intervention is impossible or impractical. Instead, the relief-well methods involve killing the uncontrolled well downhole, using a surface location at a

safe distance away from the wild well. A major drawback of relief-well killing is that it may take a long time to drill the relief well.

Blowout intervention can also be grouped depending on the intervention method. Some of the most common methods are:

- Capping.
- Momentum kill/bullheading.
- Dynamic kill.
- Gunk plugs.
- Flooding or relieving the pressure in the reservoir

Surface intervention typically focuses on capping and variations of capping the well. Capping refers to stopping the uncontrolled flow by closing in the flowpath exit point at the surface. The simplest capping equipment consists of a pipe fitted with a ball valve or blind rams and a diverter line. With the valve or rams in open position, the capping equipment is stabbed into the wellhead—if the wellhead is intact—or into the remaining pipe components. Once the capping stack is in place and the connection to the wild well has been sealed properly, the valve or rams are closed and the uncontrolled flow is stopped. There are many variations to this method that all require access to the exit point of the wild well.

Capping can be performed relatively quickly under the right circumstances. However, the disadvantages and limitations of this method are many. First, the pipe has to be guided over the exit point of the wild well, which may be on fire. For a gas blowout that did not ignite, the explosive danger may be high. Either way, capping the well may be dangerous for the personnel. For a shallow-water gas blowout, it may be difficult to access the wellhead because of the reduced buoyancy in the area. In deeper water, buoyancy may not be a problem because of currents and the length of the plume

of gas. However, the capping equipment would have to be guided over the wild well using a remote operated vehicle (ROV). Currently, no ROV is designed to navigate through the plume of a blowing well. Capping a well in deepwater is thus considered to be difficult or impossible. Some cases have been reported where capping techniques have been successfully applied to subsurface blowouts, but only in relatively shallow water of less than 300 ft depth.<sup>8</sup>

Furthermore, when the uncontrolled flow is abruptly stopped at the surface, the pressure in the well will increase almost instantaneously. This may induce an underground blowout, which may broach to the surface. If the wellhead craters, a surface intervention method is close to impossible.

Momentum kill, which is also sometimes called bullheading, is also done by surface intervention. If a drillstring is not present in the blowing well, it would need to be snubbed down the wellbore using a snubbing unit.<sup>13</sup> An advantage of momentum kill is that the drillstring does not need to be all the way to the bottom of the well. The method involves circulating a kill fluid down the drillstring with greater momentum than the flow of formation fluid coming up the wellbore. A momentum kill is equivalent to a head-to-head collision of two cars. The slower and smaller car will immediately halt and be pushed backwards. This method is also frequently used to prevent sour-gas kicks from reaching the surface as the hydrogen sulfide may cause harm to the personnel. The major disadvantage of the momentum kill method is that it is likely to cause an underground blowout.

Relief wells are used to gain control of blowouts in situations where direct surface intervention is impossible or impractical. Conceptually, in the late 19<sup>th</sup> century, relief wells were drilled parallel to the blowing well and used to relieve pressure by producing from the flowing formation.<sup>14</sup> Operators later discovered that flooding the reservoir with water was a more effective intervention method. The relief well would

connect with the wild well through fractures and vugs in the formation and further flood it with water until it was dead. This method had many limitations, particularly in deep wells, in formations with very low permeability such as tight gas reservoirs, or in cases where a relief well could not be drilled in close proximity to the blowing well. With the introduction of directional drilling, the relief well could intersect the wild well, which is the preferred method today. An electromagnetic tool is used in the relief well to detect the casing of the blowing well. After milling a hole in the casing, or intersecting just below the last casing string, the kill fluid can be injected directly into the wild well from the relief well.

If a kill fluid with density sufficient to hydrostatically stop and control the formation influx is injected directly into the blowing well, it may be difficult to avoid fracturing the formation. The dynamic-kill procedure<sup>8,14</sup> was introduced to give more control throughout the course of the intervention. A dynamic kill involves circulating a kill fluid, such as seawater, with density resulting in a hydrostatic-column pressure less than the static reservoir pressure before the weighted fluid. The lighter fluid is circulated at a rate that will generate sufficient frictional pressure in the blowing well to stop the influx of formation fluid. Once the formation influx is stopped, a weighted mud is circulated to statically control the well. If the formation is fractured, the kill rate may be decreased to reduce the pressure in the well. A thick, viscous, special kill fluid may also be used to reduce the chance of fracturing the formation.

Dynamic kill is one of the oldest and most widely used intervention methods. In the early 1960s, dynamic kills were commonly used in the Arkoma basin where air drilling was popular.<sup>8</sup> Every productive zone that was encountered would result in a blowout, which was later contained by dynamic-kill intervention. Unfortunately, since the physics behind the dynamic kills was not fully understood at the time, a trial-and-error approach was the only method to succeed.

A dynamic kill can also be done in combination with capping intervention. While the dynamic kill is initiated, the capping stack can be used as a choke to give additional backpressure. Another flexibility of the dynamic-kill method is that it can be performed either through a relief well or by surface intervention. The decision of whether to use a relief well or a drillstring in the wild well depends on the kill rate required and the likelihood of successfully snubbing a drillstring into the wild well. Because of the small inner diameter of a drillstring, significant pressure will be lost inside the drillstring during a high kill rate. For a relief well the annulus may be used to circulate down the kill fluid, which would result in less frictional-pressure drop and less pumping power required for the same kill rate.

Typically, if all of the approaches above fail, a gunk plug is attempted. Gunk is a combination of diesel and gel, and this intervention method is equivalent to putting bubble gum down the hole. An alternative to gunk material is using a fast-reacting cement. If the plug is set high, a weak formation below the plug could fracture, creating an underground blowout. After a gunk plug is set, it may be difficult to ever regain control of the well.

### **1.5 Modeling of a Dynamic Kill**

Proper planning is the key to a successful dynamic kill. Without proper planning, the logistics for the task at hand is almost guaranteed to escalate into complete chaos. Furthermore, an unsuccessful dynamic kill could worsen the situation.

Blount and Soeiinah<sup>15</sup> are credited as the pioneers of dynamic-kill modeling. In 1978 their engineering concepts were applied to a blowout in the Arun field, which at the time was the world's biggest gas field. The well was blowing at a rate of 400 MMscf/D, and was under control after only one hour and fifty minutes of pumping using a relief well. The kill rate required to control the wild well was calculated from a single-phase solution. Kouba *et al.*<sup>16</sup> showed that a single-phase solution may in some cases

underpredict the kill rate required. They presented a simple analytical multiphase solution that can be used to check the validity of the single-phase solution.

Over the last couple of decades, the industry has created several dynamic-kill simulators to assist in the planning process. These dynamic-kill simulators aim to:

- Determine the initial downhole conditions of a blowing well such as pressures, temperature, and flowrates.
- Determine the requirements for a dynamic kill such as pump rate, power requirement, and mud volumes.
- Gain a better understanding of the task at hand and evaluate the best plan of action.

Some of the most recent and most popular dynamic-kill simulators include:

- Olga-Well-Kill.
- Sidekick.
- Dyn-X.
- Santos Simulator.

In 1980 a full-scale flow loop was built in Norway to develop a model—named OLGA 2000—capable of simulating slow transients in two-phase hydrocarbon transport pipelines. In 1989 a blowout occurred in the Norwegian North Sea and OLGA 2000 was used in developing a dynamic-kill simulator named OLGA-WELL-KILL.<sup>17</sup> Since then OLGA-WELL-KILL has evolved to become the industry's leading dynamic-kill simulator and has been used successfully to plan an extensive number of blowout interventions.

Sidekick<sup>18</sup> was originally developed as an advanced kick simulator for all the events that lead up to a blowout. Sidekick can also be used to simulate a dynamic kill for a gas blowout. The dynamic-kill simulator cannot be used to simulate circulation through a relief well and the simulator would require tweaking to simulate a subsurface or underground blowout.

A spreadsheet program, named Dyn-X, that can be used to study dynamic kills was developed at Louisiana State University.<sup>19</sup> The program incorporated a steady-state, system-analysis approach and a model for sonic flow of gas/mud mixtures. The program contains a reservoir fluid-property calculator, which enables the program to be used for complex mixtures of formation fluids. The program also has the features to be used for directional wells, off-bottom kills, and underground blowouts.

Santos<sup>9</sup> presented a FORTRAN computer program developed to study blowouts in ultradeep water. The dynamic-kill simulator was developed from an experimental study on riser and diverter unloading during blowouts. Using piston-like displacement and no slip between the phases as assumptions, the simulator has transient capabilities.

## **1.6 Objective of the Study**

Schubert and Weddle<sup>20</sup> proposed to expand on the 1990 DEA-63 report.<sup>5</sup> The purpose of their project is to create procedures and guidelines for blowout containment in ultradeep water. Developing and validating the procedures will require a dynamic-kill simulator. None of the current dynamic-kill simulators are either available or designed for this particular purpose and therefore the project decided to develop one. This simulator—which is presented in this dissertation—is different from those already existing in that it can simulate bridging predictions and dual-gradient drilling. It is also the first simulator written in Java code, which enables a Web-based application. New versions of the program will be updated automatically and the program can be run from

any location with Internet access. The program can also be used as a stand-alone application.

The final dynamic-kill simulator will accommodate a fully transient analysis with all possible blowout scenarios. Because of the complexity and extensive quantity of work required, developing the simulator requires several phases. The primary objective of this dissertation was to develop an early version of this dynamic-kill simulator.

The dynamic-kill simulator comprises four main sections:

- Input data.
- Estimate of the initial blowing condition such as temperature, pressure and flowrates.
- Calculation of the minimum kill rate and standpipe pressure needed for successful intervention with a given kill fluid and well configuration.
- Graphical output of the results.

The early version of the program focuses on simulating dynamic kills for vertical wells in ultradeep water. The simulator applies to both gas and liquid reservoirs and has the option of using a relief well or a drillstring in the blowing wellbore. The blowing wellbore may include both pipe flow and annular flow, depending on whether a drillstring is present in the wellbore. The computer program is also capable of simulating a dynamic kill using either a Newtonian or a non-Newtonian kill fluid.

For pressure, temperature and fluid-property predictions, the simulator incorporates state-of-the-art models that have been extensively used and verified by the industry. No new correlations were developed for this study. The computer program was tested against multiphase-pressure data to identify and prevent potential coding bugs and conceptual errors.

### **1.7 Expected Contributions From Study**

The dynamic-kill simulator is expected to be a valuable tool in developing and validating general blowout procedures and for planning blowout interventions on a case-by-case basis. It can also help give a better understanding of blowouts and improve training of personnel, and it has the ability to model significant components of the well system:

- Conventional and dual-density wells.
- Circulation paths through a drillstring located in the blowout well or relief wells.
- Returns to the surface via the drilling riser, choke and kill line, seafloor pumps and return line, or returns to the ocean at the seafloor.
- Surface, subsurface, and underground blowouts.

## CHAPTER II

### THE DYNAMIC-KILL SIMULATOR

The simulator presented here for dynamic kills was written in Java. The layout of the program is designed to make it as user-friendly as possible with few operations necessary to achieve the desired results. This chapter will give an overview of the different features available and the layout of the program.

#### 2.1 Java

Java was chosen as the programming language because of its versatility, modularity, and reusability. Java is an object-oriented language, which is a favored programming approach that has largely replaced the standard procedure-based programming techniques over the last decade. A thorough discussion of the benefits of object-oriented programming versus procedure-based programming is beyond the scope of this study.<sup>21</sup>

Platform independence, popularity, and simplicity are just some of the benefits that Java offers. Platform independence enables the user to run a Java application on any operating system and still get the same results. This has earned Java the recognition as *the* Internet programming language. A Java application has the option of being used as an applet, which is an application that can be run over the World Wide Web, or as a stand-alone application. Java's popularity has generated an abundance of source-code information and examples and plenty of programmers who are familiar with reading the code. Compared to other object-oriented languages such as C++, Java is an improvement. Several of the complicated features of C++ such as memory management, pointers, and multiple-inheritance that can easily lead to confusion are greatly simplified in Java.

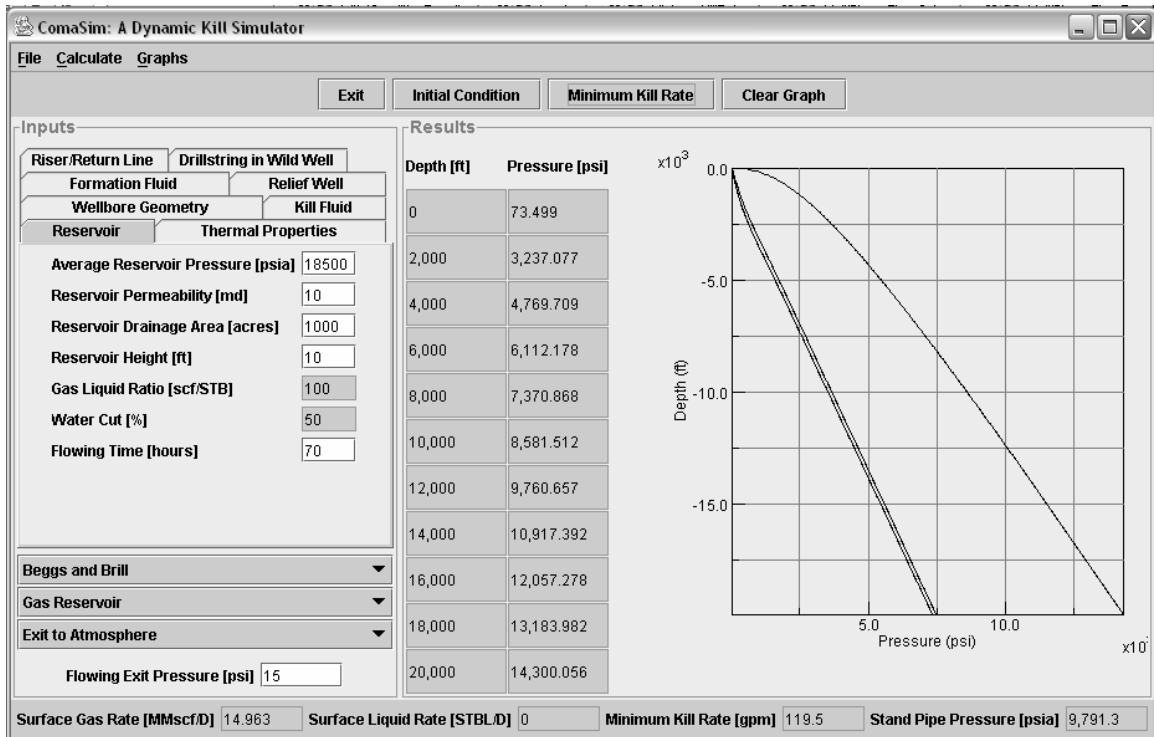


Fig. 2.1—Simulator interface.

## 2.2 Layout and Features

The interface was developed to be clear and simple to work with and to enable easy navigation. **Fig. 2.1** shows the main page of the computer program. As shown, both the inputs and results panel can be viewed at the same time. This is particularly useful when working with an applet to minimize the amount of page downloading and information sent over the Internet.

The layout of the interface is separated into four frames:

- Menu bar.
- Result bar.
- Inputs panel.
- Results panel.

### **2.2.1 The Menu Bar**

The menu bar is located at the top of the interface and currently stores four buttons:

- Exit.
- Initial Condition.
- Minimum Kill Rate.
- Clear Graph.

The exit button will close the application. The initial-condition button calculates the pressure and flowrates of the wild well before a dynamic kill is attempted. The minimum-kill-rate button will calculate the kill rate and the standpipe pressure required for successful blowout containment.

Multiple curves can be plotted in the result panel as seen in Fig. 2.1, where three curves are shown. This can be useful for comparing different scenarios. However, the clear graph button will clean up the result panel and display only the last curve.

### **2.2.2 The Result Bar**

The result bar is located at the bottom of the interface and displays the single-result values. The surface-gas rate and surface-liquid rate are the rates of the reservoir fluid at standard conditions before a dynamic kill is attempted. During the initial

conditions for a gas reservoir, the liquid rate will always be assumed zero. For a liquid reservoir, the gas rate is calculated as the liquid rate times the gas/liquid ratio, which is defined by the user. Also located in the result bar are the minimum kill rate and the corresponding standpipe pressure results.

### **2.2.3 The Results Panel**

The results panel displays a table and a graph of the wellbore pressure at the initial conditions before the dynamic kill is attempted. Additional graphs, such as the temperature profile and mixture velocity, can be found in the graph menu at the top. **Fig. 2.2** shows a separate window with the mixture velocity.

### **2.2.4 The Inputs Panel**

The inputs panel is grouped in tabs and drop-down menus. All of the input cells, except for the flowing-exit pressure, are located in the tabs. As seen in Fig. 2.1, some of the input cells are gray and some are white. A gray input cell indicates that the input is not needed and the cell is un-editable. As an example, in Fig. 2.1 a gas reservoir has been chosen. For this case it is assumed that the reservoir produces dry-gas only and, thus, the gas/liquid ratio and water cut are not necessary as inputs.

Below the tabs, drop-down menus allow the user to choose the multiphase model, the reservoir-fluid type, and the blowout type. The choices of multiphase models are Hagendorn and Brown, Beggs and Brill, and Duns and Ros.

The reservoir-fluid type is grouped as either liquid reservoir or gas. For an oil well in ultradeep water, the reservoir pressure is always assumed above the bubblepoint pressure, so a compositional reservoir is not featured in this simulator.

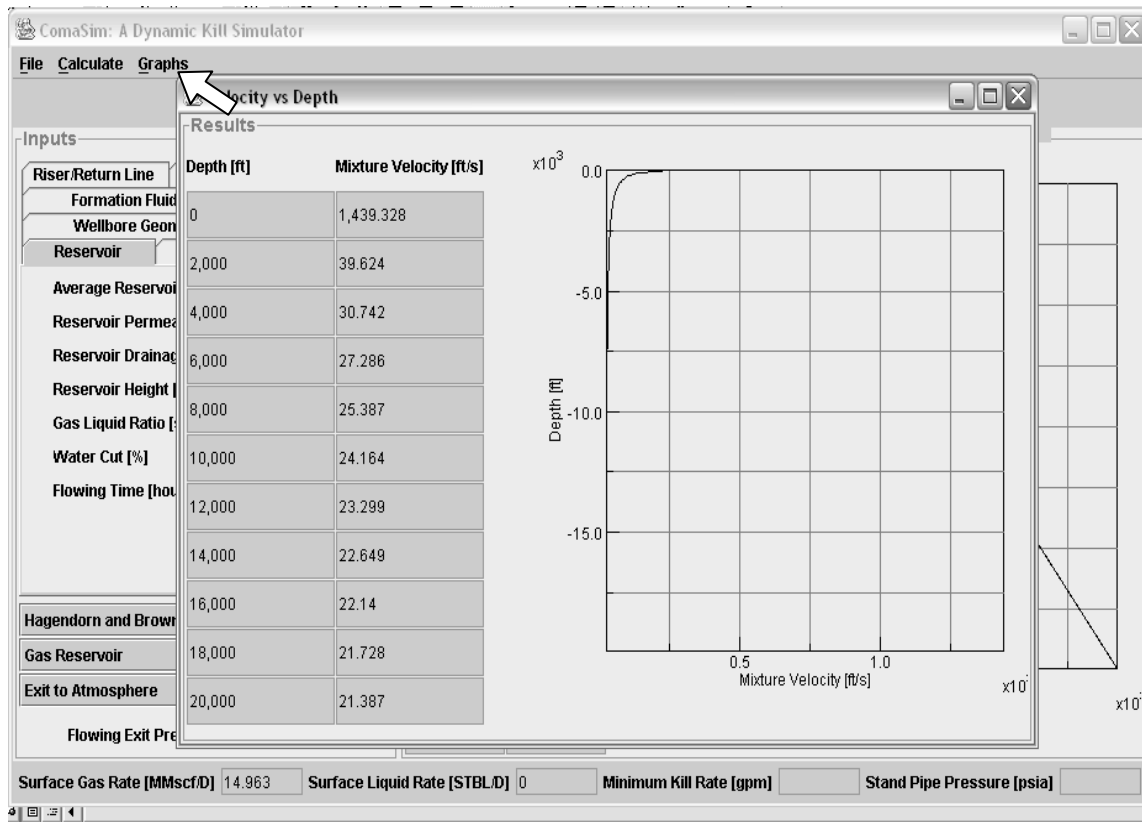


**Fig. 2.2—Mixture-velocity graph displayed in separate window.**

With the last drop-down menu, the user may choose the blowout type, which is either exit to the surface or exit to the mudline.

“Exit to the surface” indicates a surface blowout where the exit of the blowout is to atmospheric conditions. This could be the case where the formation flow is using either the drillstring or the riser as a medium, as seen in **Fig. 2.3**. The option of exit to the mudline can be used for either subsurface or underground blowouts. A case where the wild well is blowing to the mudline is shown in **Fig. 2.4**. This option can also be used for dual-gradient drilling, where the pressure at the seafloor remains constant during the intervention.

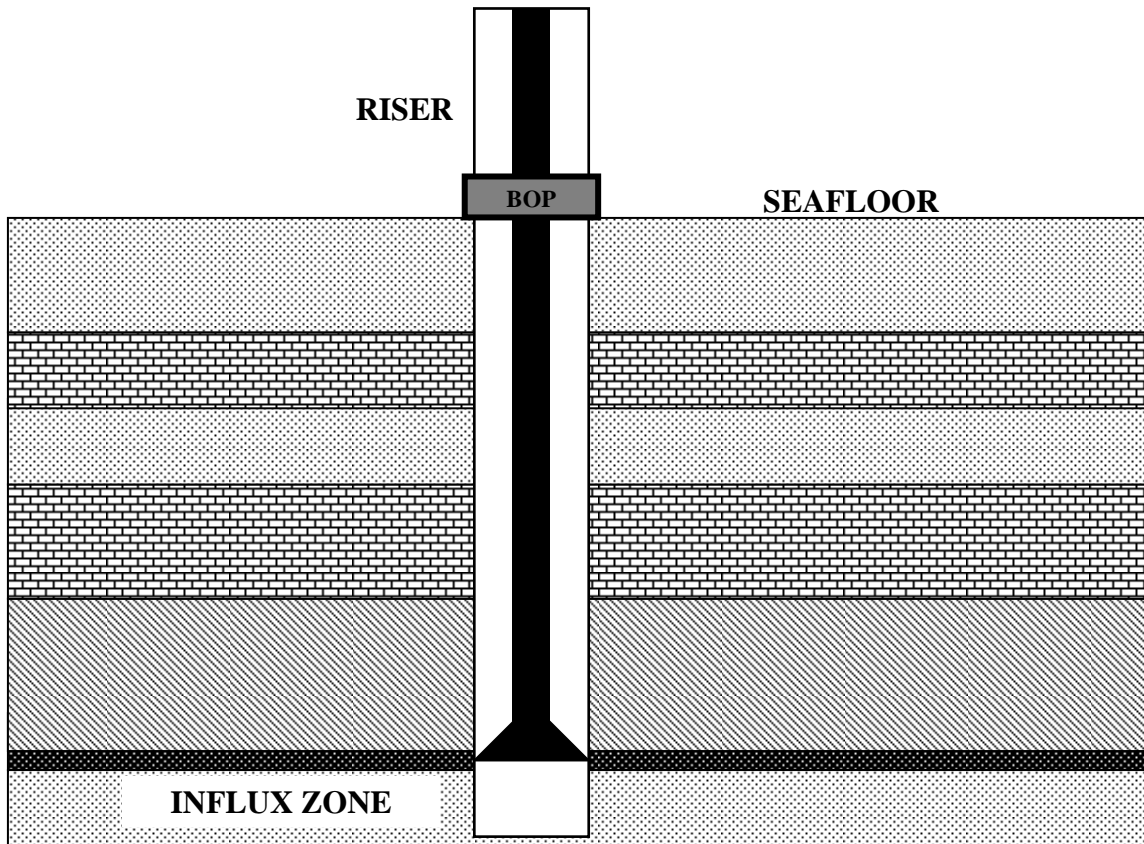


**Fig. 2.3—Blowout case with returns to the surface using a drillstring to circulate the kill fluid.**

As seen in Fig. 2.1, an input cell for the flowing-exit pressure is located below the drop-down menus. If Exit to the surface is chosen, the default value for the flowing-exit pressure is 15 psia. If Exit to the mudline is chosen, the program will calculate the seawater hydrostatic and display it in this input cell. For an underground blowout, the user would have to enter the fracture pressure of the formation as the exit pressure.

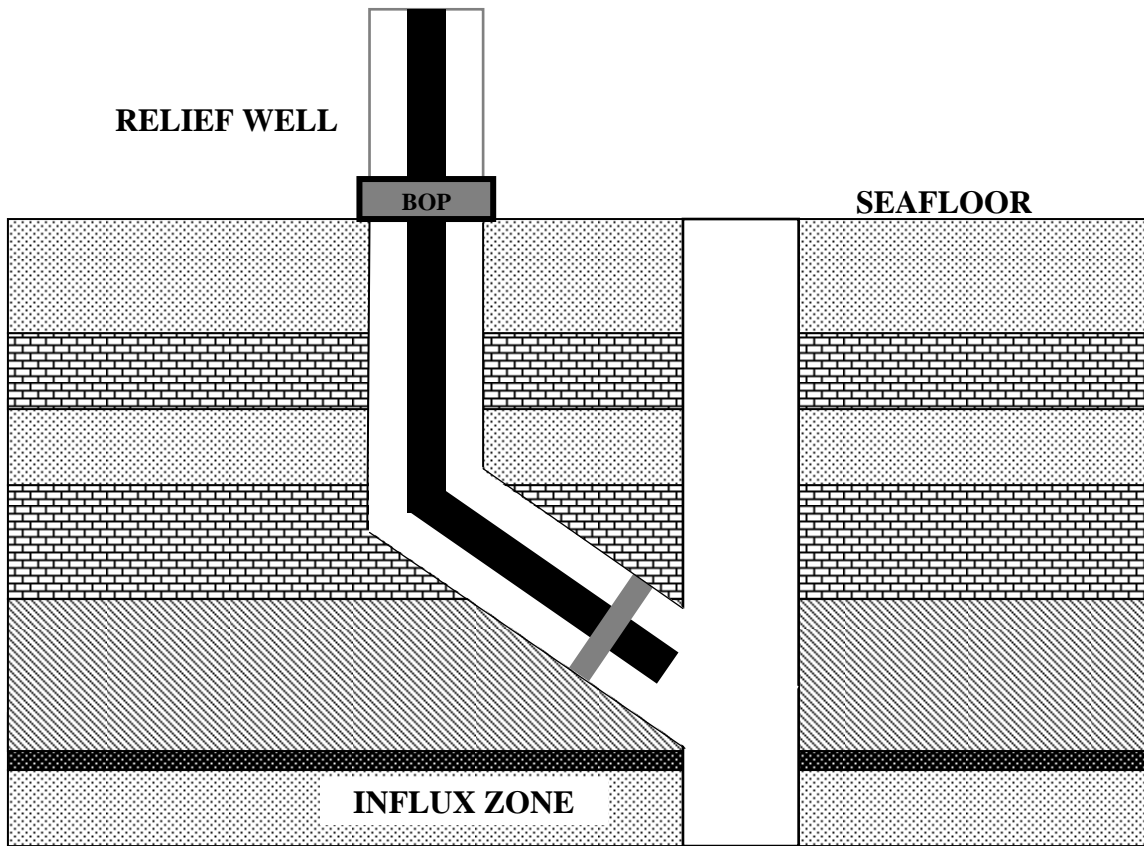


**Fig. 2.4—Blowout case with returns to the mudline using a relief well to circulate the kill fluid.**

The kill fluid can be circulated into the wild well either by using a relief well as shown in Fig. 2.4, or by using a drillstring inside the wild, well as seen in Fig. 2.3. The default circulation method is using a relief well. If circulation using a drillstring is desired, the user must navigate to the Drillstring in Wild Well tab and choose Kill With Drillstring from the drop-down menu (**Fig. 2.5**).

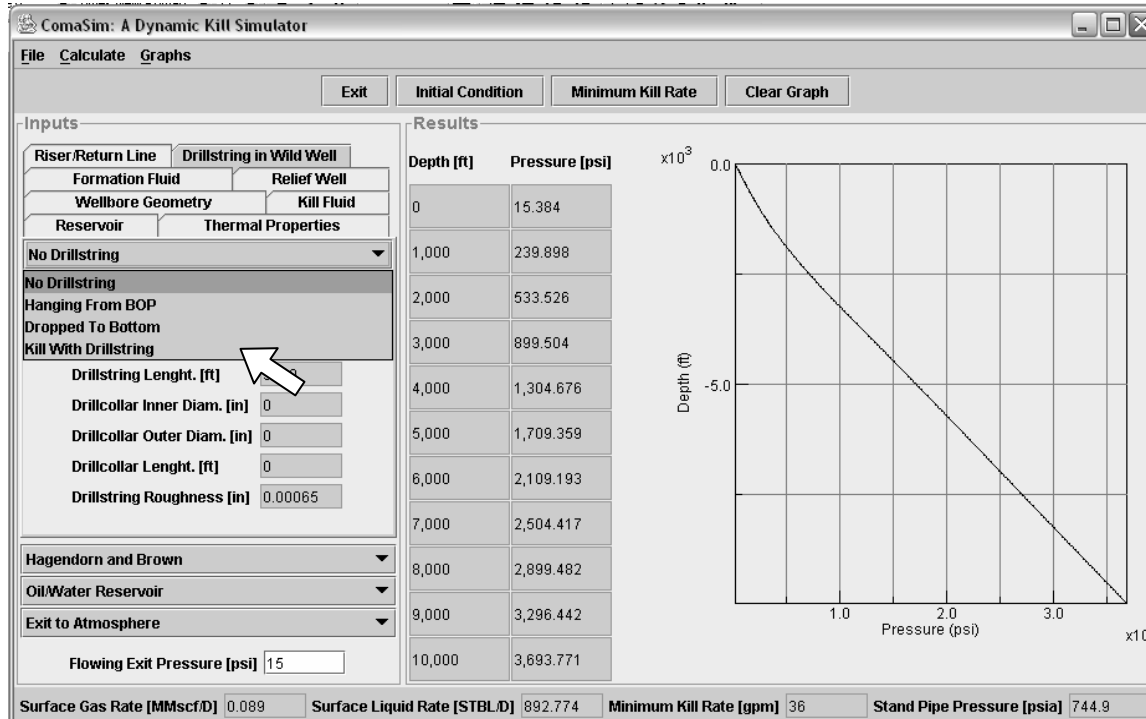


**Fig. 2.5—Drillstring options for wild well.**

Fig. 2.5 shows three other options for the drillstring inside the wild well. No Drillstring is the default case shown in Fig. 2.4. Hanging From BOP (blowout preventer) is shown in **Fig. 2.6**. Here, a pipe ram is closed below a tool joint before the drillstring is sheared off above the tool joint. This will suspend the drillstring from the BOP. The third option is a drillstring dropped to the bottom, **Fig. 2.7**.

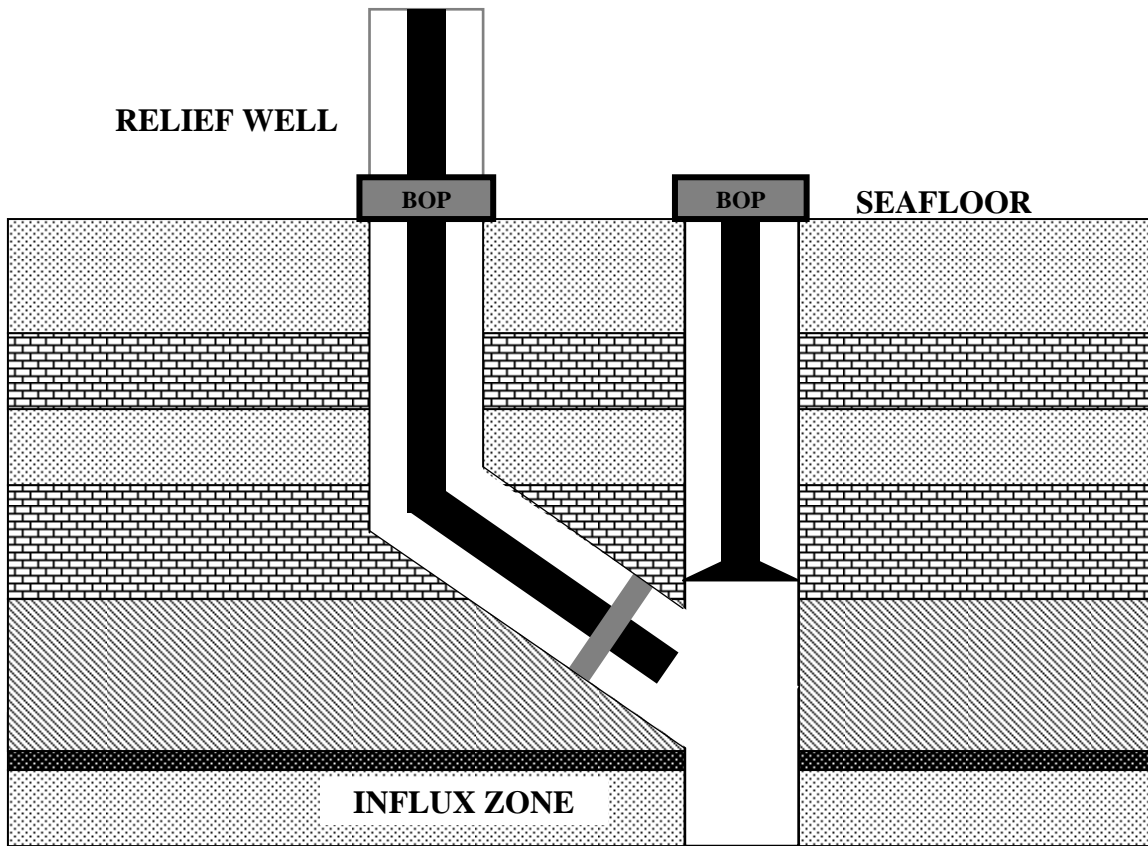


**Fig. 2.6—Drillstring hanging from BOP.**

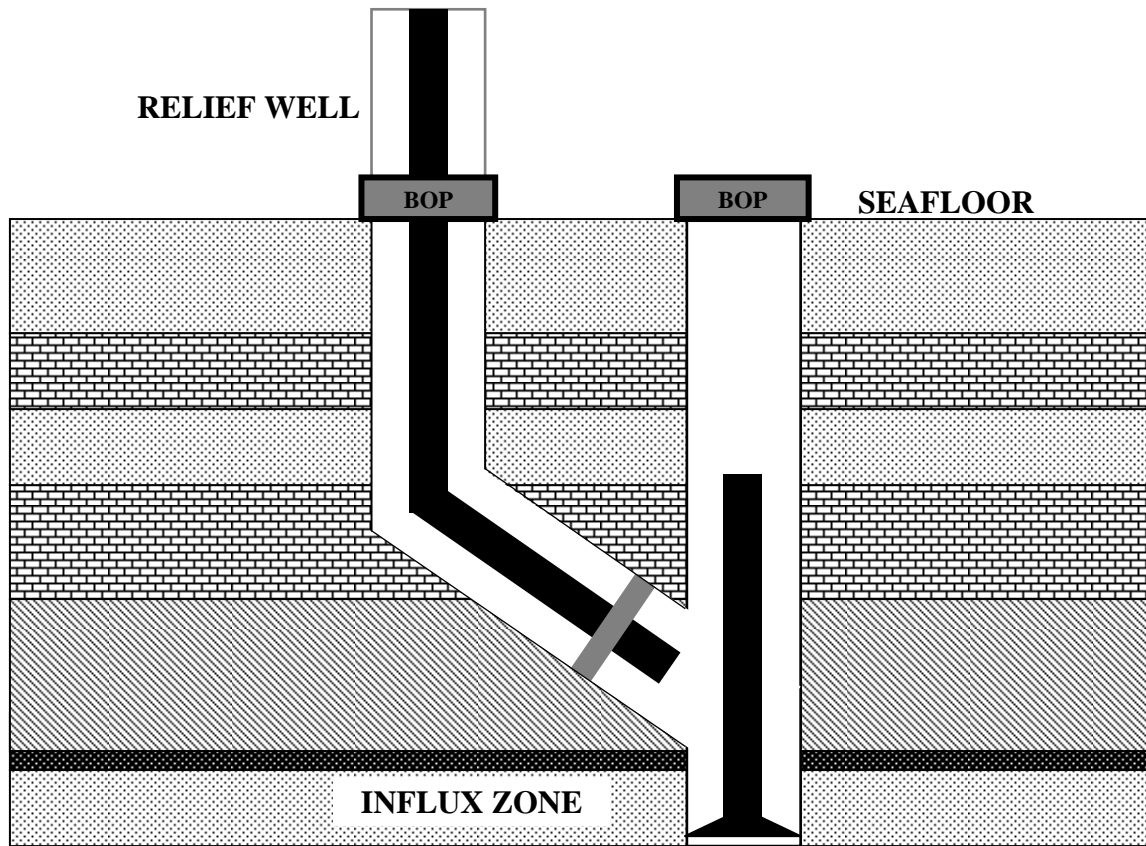


**Fig. 2.7—Drillstring dropped to the bottom.**

The user may in some cases input values that the program will not compile or can't handle. This could happen for example if the kill-fluid weight entered would result in a hydrostatic column larger than the average reservoir pressure, which would not be considered a dynamic kill. In this case, a pop-up window will display a message explaining the error, as seen in **Fig. 2.8**. Several obvious input checks like this are included in the program. Thorough testing of an extensive variety of cases will be necessary to identify all possible input errors. Testing is scheduled as part of a future study in this project.

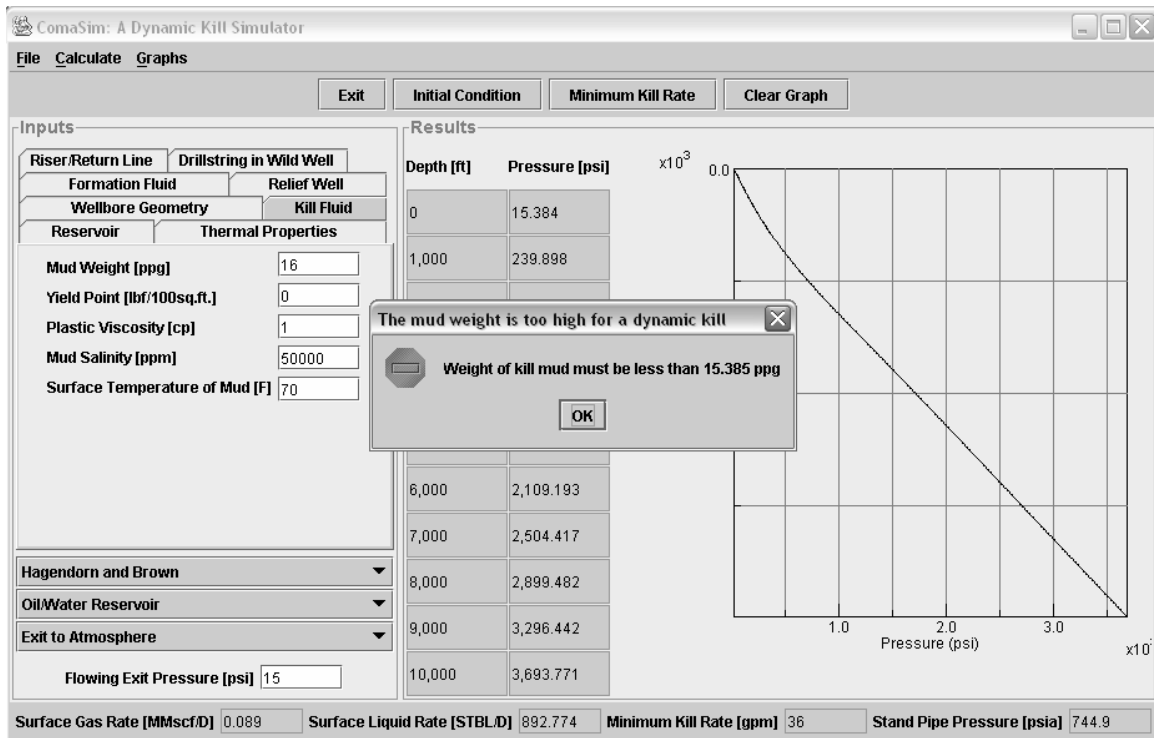


**Fig. 2.8—Pop-up message indicating an input error.**

## CHAPTER III

### MODELING

The two main objectives of the dynamic-kill simulator are to determine the initial blowing condition of the wild well and the minimum kill rate required to stop the influx of formation fluid into the wellbore. During both evaluations, the pressure and temperature must be calculated throughout the wellbore. The pressure and temperature calculations also require that the fluid properties be determined. One of the main assumptions used for the modeling here is that data available during a blowout are very limited. The correlations used to determine the pressure, temperature, and fluid properties must therefore require a minimum of inputs, yet they must yield accurate results, which were the two deciding factors used to choose the correlations. The following sections in this chapter will describe the modeling and assumptions for each of these components.

#### 3.1 Flow Rates and Velocities

The fluids in the wellbore may be highly compressed. Because the pressure and temperature change with depth, the fluids will expand as they approach the surface. This will change the rates at which the gas and liquid phases are flowing. The flow rate for each phase can be calculated throughout the wellbore if the surface rates, formation volume factor,  $B_o$  and  $B_w$ , and solution ratios,  $R_s$  and  $R_{sw}$ , are all known. The rates can then be calculated as

$$q_o = q_{osc} B_o, \dots\dots\dots (3.1)$$

$$q_w = q_{wsc} B_w, \dots\dots\dots (3.2)$$

and

$$q_g = (q_{gsc} - q_{osc} R_s - q_{wsc} R_{sw}) B_g \dots\dots\dots (3.3)$$

The area inside the pipe is

$$A_p = \frac{\pi}{4} d^2 \dots\dots\dots (3.4)$$

The superficial velocity is defined as the velocity for a given phase if it occupied the entire pipe area alone. The superficial velocities of the oil, water, and gas phases are then

$$v_{so} = \frac{q_o}{A_p}, \dots\dots\dots (3.5)$$

$$v_{sw} = \frac{q_w}{A_p}, \dots\dots\dots (3.6)$$

and

$$v_{sg} = \frac{q_g}{A_p} \dots\dots\dots (3.7)$$

### 3.2 Pressure Calculations

Conservation of mass for a small element of fluid implies that mass in minus mass out must equal to the mass accumulation.<sup>22</sup> For flow in a pipe with constant area, the mass balance equation is

$$\frac{\partial p}{\partial t} + \frac{\partial(\rho v)}{\partial L} = 0. \dots\dots\dots (3.8)$$

For steady-state flow with no mass accumulation, Eq. 3.8 becomes

$$\frac{\partial(\rho v)}{\partial L} = 0. \dots\dots\dots (3.9)$$

Conservation of momentum implies that the momentum out minus the momentum in, plus the rate of momentum accumulation must equal to the sum of all the forces. By applying Newton's first law to **Fig 3.1** we get

$$\frac{\partial(\rho v)}{\partial t} + \frac{\partial(\rho v^2)}{\partial L} = -\frac{\partial p}{\partial L} - \tau \frac{\pi d}{A} - \rho g \sin \theta. \dots\dots\dots (3.10)$$

For steady state the rate of momentum accumulation is eliminated. Combining the mass balance Eq. 3.9 and the momentum balance Eq. 3.10 and solving for the pressure gradient, we get

$$\frac{dp}{dL} = -\tau \frac{\pi d}{A} - \rho g \sin \theta - \rho v \frac{dv}{dL}. \dots\dots\dots (3.11)$$

Thus, we see that the pressure gradient can be calculated for a single element in the wellbore according to

$$\left(\frac{dp}{dL}\right)_t = \left(\frac{dp}{dL}\right)_f + \left(\frac{dp}{dL}\right)_{el} + \left(\frac{dp}{dL}\right)_{acc}, \dots\dots\dots (3.12)$$

where *f* denotes the friction term, *el* denotes the elevation term or hydrostatic head, *acc* denotes the acceleration term, and *t* denotes the total pressure gradient at a given well

depth. The sign convention depends on which direction the elements in the wellbore are added and the direction of the flow. The friction and acceleration term will be positive in the opposite direction of the flow. The hydrostatic term will be positive if the elements in the wellbore are added with increasing wellbore depth. The acceleration term is often ignored. However, if compressed gas is present in the wellbore, the acceleration term can become significant as the gas expands close to the surface.

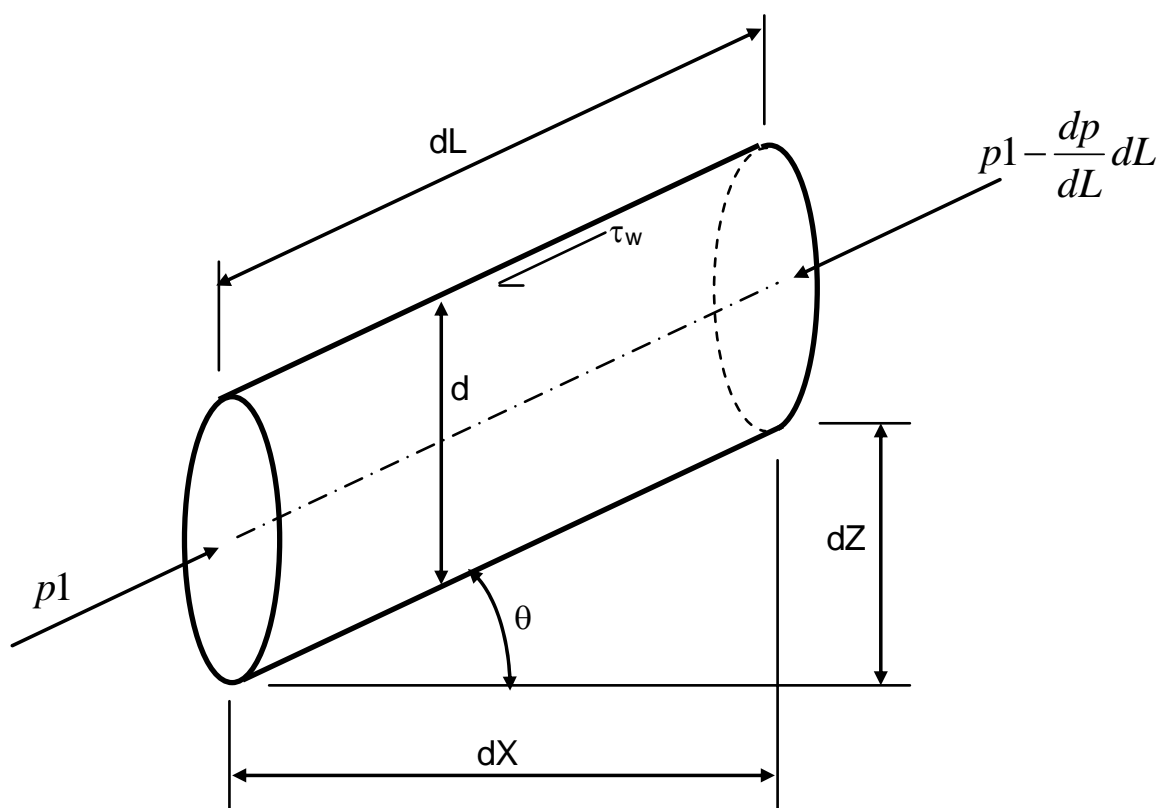


**Fig. 3.1—Small element of fluid in a pipe.**

The shear stress is a function of shear rate. The relationship between shear stress and shear rate depends on the rheologic properties of the fluid as seen in **Fig 3.2**.<sup>23,24</sup> The flow of oil and water is assumed to follow the Newtonian model, where

$$\tau = \mu\gamma, \dots\dots\dots (3.13)$$

while the flow of a drilling mud is assumed to follow the power-law model,

$$\tau = K\gamma^n . \dots\dots\dots (3.14)$$

Thus, if the flow behavioral index,  $n$ , is unity and the fluid consistency index,  $K$ , is equal to the viscosity,  $\mu$ ,—which is normally the assumption for seawater—then the power-law model will reduce to the Newtonian model.

To determine the friction term, a dimensionless friction factor is used. Evaluating ratio of shear stress at the wall to the kinetic energy defines the Fanning friction factor,

$$f' = \frac{\tau}{\rho v^2 / 2g_c} . \dots\dots\dots (3.15)$$

The Fanning friction factor is used in this study when drilling mud is present in the wellbore and the flow is assumed to follow the power-law model. However, for Newtonian flow the Moody friction factor,<sup>25</sup> which is four times larger than the Fanning friction factor, is used to preserve the original equations.

The shear stress as a function of the Moody friction factor is thus

$$\tau = f \frac{\rho v^2}{8g_c} . \dots\dots\dots (3.16)$$

Substituting Eq. 3.16 into the pressure gradient Eq. 3.11 the friction term becomes

$$\left(\frac{dp}{dL}\right)_f = \frac{f\rho v^2}{2g_c d} \dots\dots\dots (3.17)$$

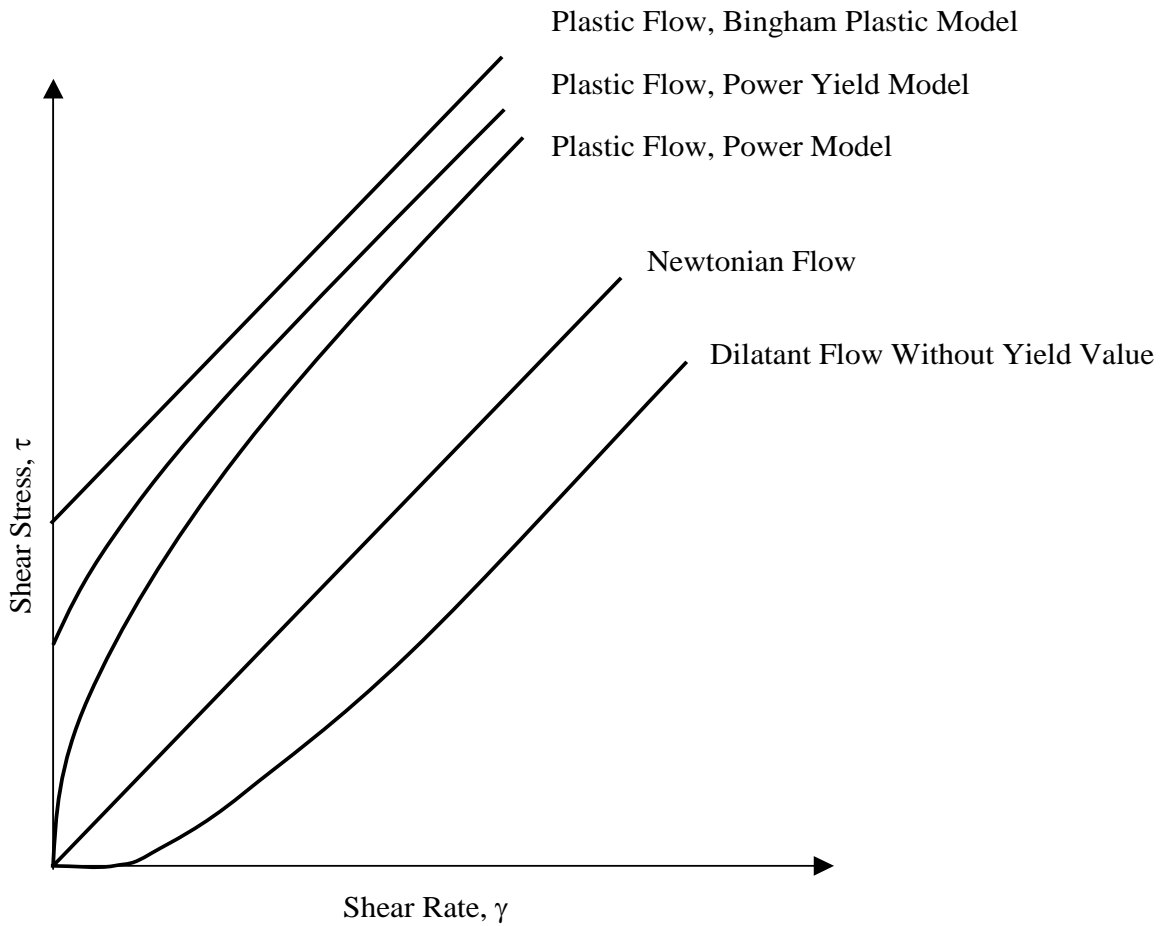


**Fig. 3.2—Rheological models.**

### 3.2.1 Moody Friction Factor for Newtonian Flow

The friction factor is a function of whether the flow is in a laminar or a turbulent flow regime. Laminar flow is assumed when Reynolds number,  $N_{Re}$ , is less than 2,100. Reynolds number is defined as

$$N_{Re} = \frac{\rho v d}{\mu} \dots\dots\dots (3.18)$$

For laminar flow the Moody friction factor can be derived analytically as:

$$f = \frac{64}{N_{Re}} \dots\dots\dots (3.19)$$

For turbulent flow an analytical expression is not available. Colebrook<sup>26</sup> proposed the empirical-implicit expression in Eq. 3.20, which requires an iterative solution.

$$f_c = \left[ 1.74 - 2 \log \left( \frac{2\varepsilon}{d} + \frac{18.7}{N_{Re} \sqrt{f_{est}}} \right) \right]^{-2} \dots\dots\dots (3.20)$$

A guess is made for the estimated friction factor,  $f_{est}$ , and the friction factor,  $f_c$ , is calculated. The calculated friction factor is then used as the next estimated value until the two values agree within a certain tolerance. The initial guess is estimated using the Drew *et al.*<sup>27</sup> correlation for smooth pipe.

$$f_{est} = 0.0056 + 0.5 N_{Re}^{-0.32} \dots\dots\dots (3.21)$$

For fully established turbulent flow with Reynolds number larger than 5,000, the Jain<sup>28</sup> friction factor correlation is used to avoid iterations.

$$f_c = \left[ 1.14 - 2 \log \left( \frac{\varepsilon}{d} + \frac{21.25}{N_{Re}^{0.9}} \right) \right]^{-2} \dots \dots \dots (3.22)$$

### 3.2.2 Fanning Friction Factor for Non-Newtonian Flow

For non-Newtonian flow the viscosity is not the derivative of shear stress as a function of shear rate. Thus for a given condition an apparent or effective viscosity, as seen from **Fig 3.3**, has to be determined before calculating the Reynolds number.

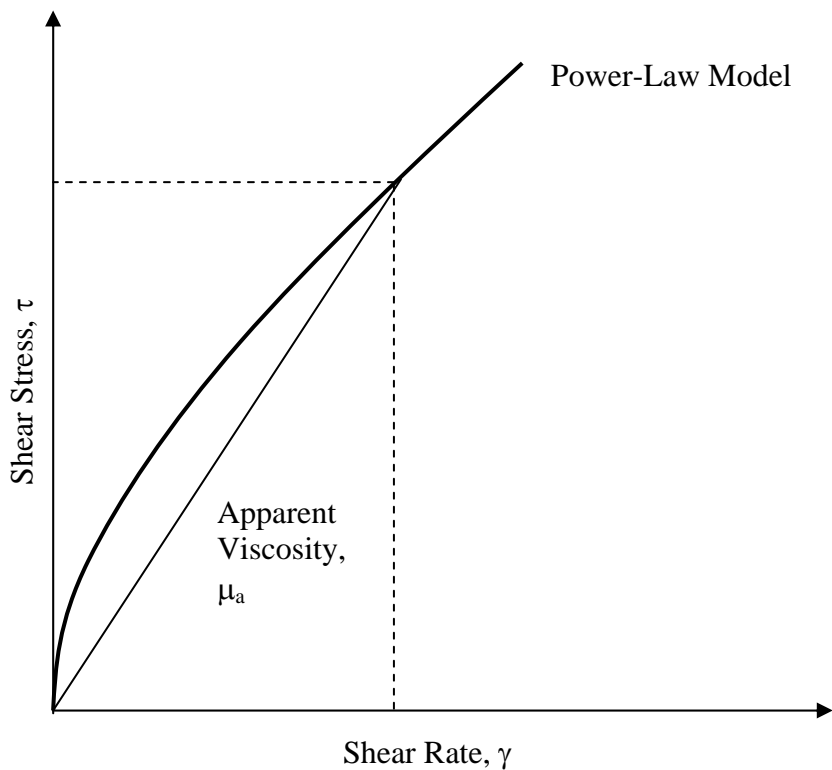


**Fig. 3.3—Apparent viscosity for a power-law fluid.**

The effective viscosity in centipoises is calculated according to the API RP13D<sup>29</sup> as

$$\mu_e = 100K \left( \frac{96v}{d} \right)^{n-1} \left( \frac{3n+1}{4n} \right)^n \dots\dots\dots (3.23)$$

The Reynolds number can be calculated with  $\mu_e$  as for Newtonian flow using Eq. 3.18. Similarly to the Moody friction factor, but four times smaller, the Fanning friction factor for laminar flow is:

$$f' = \frac{16}{N_{Re}} \dots\dots\dots (3.24)$$

For turbulent flow, Dodge and Metzner<sup>30</sup> propose the implicit Fanning-friction factor in Eq. 3.25 for smooth pipes:

$$f'_c = \left[ \frac{4.0}{n^{0.75}} \log \left( N_{Re} f'_{est} \right)^{(1-n/2)} - \frac{0.4}{n^{1.2}} \right]^{-2} \dots\dots\dots (3.25)$$

Govier and Aziz<sup>31</sup> suggest Eq. 3.26 for non-Newtonian friction factor in rough pipes:

$$f' = f_{M-R} \left( \frac{f'_r}{f'_s} \right) \dots\dots\dots (3.26)$$

where  $f_{M-R}$  is the Fanning friction factor calculated according to Dodge and Metzner (Eq. 3.25),  $f'_r$  is the Fanning friction factor for Newtonian flow in rough pipe, and  $f'_s$  is the Fanning friction factor for Newtonian flow in smooth pipe. Because  $f'_r/f'_s$  is a ratio, the Moody-friction factor from Eq. 3.20 and Eq. 3.21 can be used.

Once the Fanning friction factor is calculated the friction component of the pressure gradient can be calculated. However, because the Fanning friction factor is being used Eq. 3.17 now becomes

$$\left(\frac{dp}{dL}\right)_f = \frac{2f' \rho v^2}{g_c d} \dots\dots\dots (3.27)$$

### 3.2.3 Multiphase Flow Calculation

The multiphase flow calculations in this study assume steady-state behavior, which has been found to give good agreement with actual field cases.<sup>15,16</sup> Over the last decades, significant development in modeling of transient multiphase-flow has resulted in commercial simulators such as the OLGA-WELL-KILL.<sup>17</sup> Currently, however, all the multiphase models that describe the transient phenomena are proprietary.

The multiphase flow models can be classified as either mechanistic or empirical models. The mechanistic models seek to apply basic physical laws to describe the multiphase flow behavior. Because of the complexity of multiphase flow, the mechanistic models still require some empiricism to predict certain flow mechanisms. They are also typically much more complex and time consuming than empirical models, yet they have not been reported to yield any significant increase in accuracy. This study focuses on empirical multiphase models.

Currently little research has reported the relationship between oil, gas, and brine flowing simultaneous with a non-Newtonian drilling mud. In the empirical multiphase models used in this study, the entire liquid phase is treated as a homogeneous fluid where the liquid density  $\rho_L$ , viscosity  $\mu_L$ , and surface tension  $\sigma_L$  is calculated as

$$\rho_L = f_o \rho_o + f_w \rho_w, \dots\dots\dots (3.28)$$

$$\mu_L = f_o \mu_o + f_w \mu_w, \dots\dots\dots (3.29)$$

and

$$\sigma_L = f_o \sigma_o + f_w \sigma_w. \dots\dots\dots (3.30)$$

The water fraction may consist of both produced brine and the kill fluid, which is assumed to be either seawater or a water-based mud with low density. The fraction of oil is calculated as

$$f_o = \frac{q_o}{q_L} = \frac{v_{so}}{v_{sL}}, \dots\dots\dots (3.31)$$

where the liquid flow rate is

$$q_L = q_o + q_w, \dots\dots\dots (3.32)$$

and the superficial liquid velocity is

$$v_{sL} = v_{so} + v_{sw}. \dots\dots\dots (3.33)$$

The fraction of water is

$$f_w = 1 - f_o. \dots\dots\dots (3.34)$$

If the gas and the liquid phase travel at equal phase velocities and no slip exist between the phases—which is the assumption during sonic flow in this study—the volume fraction of liquid in the pipe can be calculated as

$$\lambda_L = \frac{q_L}{q_t} = \frac{v_{sL}}{v_m}, \dots\dots\dots (3.35)$$

where the total flow rate is

$$q_t = q_L + q_g, \dots\dots\dots (3.36)$$

and the mixture velocity is

$$v_m = v_{sL} + v_{sg} \dots\dots\dots (3.37)$$

The no-slip gas holdup is defined by

$$\lambda_g = 1 - \lambda_L \dots\dots\dots (3.38)$$

$\lambda_L$  is the no-slip liquid holdup, sometimes called the input liquid content. If slip between the phases occurs—which is the assumption for all except sonic velocities—the actual liquid holdup,  $H_L$ , or void fraction is defined as the fraction of an element of pipe that is occupied by a liquid.

$$H_L = \frac{V_L}{V_p} \dots\dots\dots (3.39)$$

The gas holdup is then expressed as

$$H_g = 1 - H_L \quad \dots\dots\dots (3.40)$$

The slip velocity and liquid holdup are calculated differently depending on the investigators. The different models proposed by these investigators will be discussed in more detail later. The multiphase mixture density and viscosity are calculated, depending on which multiphase model used, as

$$\rho_s = H_L \rho_L + H_g \rho_g, \quad \dots\dots\dots (3.41)$$

$$\rho_n = \lambda_L \rho_L + \lambda_g \rho_g, \quad \dots\dots\dots (3.42)$$

$$\mu_s = H_L \mu_L + H_g \mu_g, \quad \dots\dots\dots (3.43)$$

$$\mu_s = \mu_L^{H_L} \mu_g^{H_g}, \quad \dots\dots\dots (3.44)$$

and

$$\mu_n = \lambda_L \mu_L + \lambda_g \mu_g \quad \dots\dots\dots (3.45)$$

The pressure gradient equation is given in Eq. 3.12. For two-phase flow the elevation or hydrostatic component can be calculated as

$$\left( \frac{dp}{dZ} \right)_{el} = \frac{g}{g_c} \rho_s \cos \theta \quad \dots\dots\dots (3.46)$$

For vertical flow the  $\cos \theta$ -term is unity. The friction component is calculated as

$$\left(\frac{dp}{dZ}\right)_f = \frac{f\rho v^2}{2g_c d}, \dots\dots\dots (3.47)$$

where  $f$ ,  $\rho$  and  $v$  are also defined differently by the various investigators. Finally the acceleration component is often ignored for bubble and slug flow. However, the acceleration component may be significant for mist flow. The acceleration component<sup>32</sup> is calculated as

$$\left(\frac{dp}{dZ}\right)_{acc} = \frac{v_m v_{sg} \rho_s}{p} \left(\frac{dp}{dZ}\right)_t \dots\dots\dots (3.48)$$

Three multiphase models—Hagendorn and Brown, Duns and Ros, and Beggs and Brill—were used to determine the liquid holdup and the pressure gradient in this study.

Hagendorn and Brown<sup>33</sup> presented a method based on extensive testing using a vertical well, instrumented 1,500 ft deep. The nominal diameter of the tubing was 1.0, 1.25, and 1.5 in. Air was used as the gas phase, and both water and crude oil were used as the liquid phase. The Hagendorn and Brown method accounts for slip, but makes no consideration for which flow pattern exists. The procedure to calculate pressure gradients using Hagendorn and Brown is listed in Appendix A.

Duns and Ros<sup>34</sup> published a method after conducting about 4,000 tests in an experimental study of vertical two-phase flow. They used a 185-ft-high vertical flow loop with pipe diameters ranging from 1.26 to 5.6 in. They used air as the gas phase and liquid hydrocarbon or water as the liquid phase, performing the tests at near-atmospheric pressure. Duns and Ros identified four separate flow patterns for computational purposes: bubble, slug, transition, and mist flow. The procedure to calculate pressure gradients using Duns and Ros is listed in Appendix A.

The Beggs and Brill<sup>32</sup> method was the first attempt to predict multiphase flow behavior for all wellbore inclinations. They used 90 ft of acrylic pipe with 1- and 1.5-in. diameters. The fluid mixture consisted of water and air. The flow patterns were determined from horizontal flow and grouped as segregated, intermittent, and distributed flow. The procedure to calculate pressure gradients using Beggs and Brill is listed in Appendix A.

Many comparisons have been made by different investigators to determine which of the multiphase models is the most accurate. From the literature<sup>24, 35, 36</sup> the Hagendorn and Brown method appears to be the most accurate for vertical flow. However, for inclined flow the Beggs and Brill method seems to perform better. The literature suggests that engineers should gather as much data as possible from similar wells and do a comparison study to determine which method to use. If data from nearby wells are not available, the most conservative results should be used.

Given the pressure at a boundary condition, one of the three models described above can be used to calculate the pressure gradient. The pressure gradient can then be used to calculate the pressure in the adjacent element. The full algorithm used to calculate the pressure profile will be described in Chapter IV.

### **3.2.4 Single-Phase Liquid Flow**

The three multiphase-flow correlations described above will reduce to a Newtonian flow model when no gas is present, which is used in this study for the case when all the gas is dispersed into the solution of the liquid phase.

For a non-Newtonian model the flow behavioral index,  $n$ , and fluid consistency index,  $K$ , for the mud have to be determined. The  $n$  and  $K$  value can be determined from a six-speed Fann viscometer according to

$$n = 3.32 \log \left( \frac{R600}{R300} \right) \dots\dots\dots (3.49)$$

and

$$K = \frac{5.11R300}{511^n}, \dots\dots\dots (3.50)$$

where  $R600$  and  $R300$  are the viscometer readings at 300 and 600-rev/min respectively. Alternatively, if the yield point,  $\tau_y$ , and plastic viscosity,  $\mu_p$ , are given,  $n$  and  $K$  can be calculated as follows:

$$n = 3.32 \log \left( \frac{2\mu_p + \tau_y}{\mu_p + \tau_y} \right) \dots\dots\dots (3.51)$$

and

$$K = \frac{5.11(\mu_p + \tau_y)}{511^n} \dots\dots\dots (3.52)$$

Once  $n$  and  $K$  values are determined, the effective viscosity is calculated according to Eq. 3.23 and the Fanning friction is calculated according to Eq. 3.25. Finally, the friction gradient can be calculated using Eq. 3.26.

The acceleration term is in this study considered negligible for single-phase liquid flow.

### 3.2.5 Single-Phase Gas Flow

If only gas is present in the wellbore, all of the multiphase models above reduce to the same single-phase gas-flow correlation that was used in this study.

### 3.2.6 Annular Flow

The hydraulic diameter concept was used to model annular flow in this study. According to this concept the hydraulic diameter is four times the area for flow divided by the wetted perimeter. For pipe flow we have

$$r_h = \frac{\pi d^2 / 4}{\pi d} = \frac{d}{4} \dots\dots\dots (3.53)$$

For annular flow, Eq. 3.54 is modified to

$$r_h = \frac{\pi(d_i^2 - d_o^2)/4}{\pi(d_i - d_o)} = \frac{(d_i - d_o)}{4} \dots\dots\dots (3.54)$$

Substituting for  $r_h$  in Eq. 3.54 and Eq. 3.55 implies that the hydraulic diameter,  $d_h$  must be:

$$d_h = d_i - d_o \dots\dots\dots (3.55)$$

Using this concept, any of the previously described multiphase and single-phase flow models can be used for annular flow.

The hydraulic diameter has been found to yield good results for large annular flow areas. For single-phase flow, the concept is assumed valid if  $d_o/d_i \leq 0.3$ .<sup>35</sup> This limitation has not been confirmed for two-phase flow. Langlais *et al.*<sup>36</sup> reported an experimental study comparing different equivalent-diameter concepts and annular

multiphase flow. They found that Hagendorn and Brown together with the hydraulic diameter concept gave the overall best performance. However, the hydraulic concept has been found to yield poor representation of deviated annular wellbores with high eccentricity.<sup>24</sup>

Kouba et al.<sup>16</sup> suggested using the area-equivalent diameter,

$$d_A = \sqrt{d_i^2 - d_o^2} \dots\dots\dots (3.56)$$

The area-equivalent diameter,  $d_A$ , in Eq. 3.56 will always be larger than the hydraulic diameter concept in Eq. 3.55. Using  $d_A$  will therefore always yield a more conservative result for the minimum-kill requirement.

### 3.2.7 Sonic Flow

For compressible flow the velocity of the fluid may reach the speed of sound, which is also called sonic flow in the fluids. When sonic flow is reached, it is impossible for the multiphase mixture to flow any faster. The sonic flow velocity is therefore called the critical velocity. At the critical velocity it is assumed that there is no slip between the phases. Wallis<sup>37</sup> presented an equation for the critical velocity,  $v_m^*$ , for a multiphase mixture as

$$v_m^* = \frac{1}{\sqrt{(\rho_g \lambda_g + \rho_L \lambda_L) \left( \frac{\lambda_g}{\rho_g v_g^{*2}} + \frac{\lambda_L}{\rho_L v_L^{*2}} \right)}}, \dots\dots\dots (3.57)$$

where the critical velocity for the liquid,  $v_L^*$ , in English field units is

$$v_L^* = \frac{68.73}{\sqrt{\rho_L \cdot c_L}}, \dots\dots\dots (3.58)$$

where  $c_L$  is the compressibility of the liquid mixture. The critical velocity for the gas,  $v_g^*$ , in English field units is

$$v_g^* = 41.4 \cdot \sqrt{\frac{k \cdot z \cdot T}{\gamma_g}}, \dots\dots\dots (3.59)$$

where  $z$  is the compressibility factor and  $k$  is the ratio of specific heats, calculated as

$$k = \frac{C_p}{C_v}, \dots\dots\dots (3.60)$$

where  $C_p$  is the specific heat at constant pressure and  $C_v$  is the specific heat at constant volume.  $k$  is typically 1.3 for hydrocarbon gases.

Eq. 3.58 implies that the smallest critical velocity occurs for the no-slip liquid holdup,  $\lambda_L$ , of 0.5.

For certain conditions such as a small pipe diameter and atmospheric conditions, a surface blowout may reach critical velocity at the exit point. Under these conditions a nozzle effect will appear at the exit point as the fluid is ejected from the pipe to the atmosphere. The pressure at the exit point will therefore be higher than atmospheric pressure. This increase in pressure is not considered in the simulator, although an estimate can be made for this pressure differential and entered as the input value for the exit pressure.

### 3.3 Temperature Calculations

In a multiphase composition, the fluid properties will change as a function of pressure and temperature. Conservation of energy for an element of fluid implies that the

energy in minus the energy out, plus the heat energy transferred to or from the surroundings, must equal the rate of energy accumulation.<sup>38</sup> For a small element of fluid this can be expressed as

$$\frac{\partial}{\partial t}(\rho e) = \frac{\partial}{\partial L} \left[ \rho v \left( e + \frac{p}{\rho g_c J} \right) \right] + \frac{U \pi d (T_f - T_e)}{A}, \dots \quad (3.61)$$

where  $U$  is the overall heat-transfer coefficient,  $T_f$  is the temperature of the fluid and  $T_e$  is the formation temperature. For steady-state flow this equation reduces to

$$\frac{\partial}{\partial L} \left[ \rho v \left( e + \frac{p}{\rho g_c J} \right) \right] = \frac{-U \pi d (T_f - T_e)}{A}, \dots \quad (3.62)$$

where  $J$  is a constant to convert units and  $e$  is the intrinsic specific energy, which is defined as

$$e = \frac{gL \sin \theta}{g_c J} + \frac{v^2}{2g_c J} + u \dots \quad (3.63)$$

Combining Eq. 3.62 and Eq. 3.63 with the mass conservation Eq. 3.9 we get

$$\rho v \frac{d}{dL} \left[ \frac{gL \sin \theta}{g_c J} + \frac{v^2}{2g_c J} + u + \frac{p}{\rho g_c J} \right] = \frac{-U \pi d (T_f - T_e)}{A} \dots \quad (3.64)$$

The specific enthalpy,  $h$ , is defined as

$$h = u + \frac{p}{\rho g_c J} \dots \quad (3.65)$$

By substituting Eq. 3.65 into Eq. 3.64 and rearranging for the enthalpy gradient, we get

$$\frac{dh}{dL} = \frac{-U\pi d(T_f - T_e)}{w} - \frac{v}{g_c J} \frac{dv}{dL} - \frac{g \sin \theta}{g_c J} \quad \dots \quad (3.66)$$

Clearly just as for the pressure gradient in Eq. 3.11 the enthalpy gradient is made up of three components:

$$\left(\frac{dh}{dL}\right)_t = \left(\frac{dh}{dL}\right)_{HT} + \left(\frac{dh}{dL}\right)_{acc} + \left(\frac{dh}{dL}\right)_{el}, \quad \dots \quad (3.67)$$

where  $HT$  denotes the heat transfer to the surroundings.

A change in enthalpy can be calculated by evaluating the change in temperature and pressure separately such that

$$dh = \left(\frac{\partial h}{\partial T}\right)_p dT + \left(\frac{\partial h}{\partial p}\right)_T dp = c_p dT + \left(\frac{\partial h}{\partial p}\right)_T dp \quad \dots \quad (3.68)$$

For an isenthalpic process where  $dh = 0$ , we have

$$\left(\frac{\partial h}{\partial p}\right)_T = -c_p \left(\frac{dT}{dp}\right)_h = -c_p \eta, \quad \dots \quad (3.69)$$

where  $\eta$  is the Joule-Thompson coefficient for cooling by expansion. By combining Eq. 3.68 and Eq. 3.69 we get

$$dh = c_p dT + c_p \eta dp \quad \dots \quad (3.70)$$

Combining Eq. 3.70 and 3.66 and simplifying for the temperature gradient, we get

$$\frac{dT_f}{dL} = \frac{(T_e - T_f)}{C_1} + C_2, \dots\dots\dots (3.71)$$

where

$$C_1 = \frac{c_p w}{U \pi d}, \dots\dots\dots (3.72)$$

and

$$C_2 = \eta \frac{dp}{dL} - \frac{v}{J g_c c_p} \frac{dv}{dL}. \dots\dots\dots (3.73)$$

$C_1$  is called the relaxation distance and is in units of length.  $C_2$  accounts for acceleration and Joule-Thompson effects, which is necessary for accurate modeling of multiphase and single-phase gas flow. In English field units  $C_1$  in Eq. 3.72 and  $C_2$  in Eq. 3.73 become

$$C_1 = \frac{229.183 w c_p}{U d} \dots\dots\dots (3.74)$$

and

$$C_2 = \eta \frac{dp}{dL} - \frac{v}{25036 \cdot c_p} \frac{dv}{dL}. \dots\dots\dots (3.75)$$

The mass rate,  $w$ , in Eq. 3.74 can be calculated as

$$w = q_o \rho_o + q_g \rho_g + q_w \rho_w + q_m \rho_m \dots \dots \dots (3.76)$$

Eq. 3.71 is a generalized differential equation with no limiting assumptions that can be used to calculate the temperature gradient both below and above the mudline. A boundary condition, such as the reservoir temperature, must be given. The temperature gradient can then be calculated and used to predict the temperature for an adjacent element. The full procedure will be described as an algorithm in the algorithm Chapter IV.

The most difficult parameter to determine when calculating the temperature gradient in Eq. 3.71 is the overall heat-transfer coefficient,  $U$ . This is particularly difficult below the mudline, where  $U$  will vary depending on the type of completion and the flowing time. The following sections will describe a method to calculate  $U$  for completions above and below the mudline.

### 3.3.1 Wellbore-Heat Transfer Below the Mudline

**Fig 3.4** shows a typical wellbore cross-section below the mudline. The heat transfer within the flowing fluid in the tubing and the fluid-filled annulus is primarily a result of convection, while heat transfer in the cement-filled annulus and the tubing and casing walls is primarily a result from conduction.<sup>24</sup>

Heat transfer in the production tubing resulting from convection can be described by

$$T_f - T_i = \frac{q}{2\pi\Delta L} \frac{1}{r_i h_f}, \dots \dots \dots (3.77)$$

where  $q$  is the radial heat transfer and  $h$  is the local convective-film coefficient.

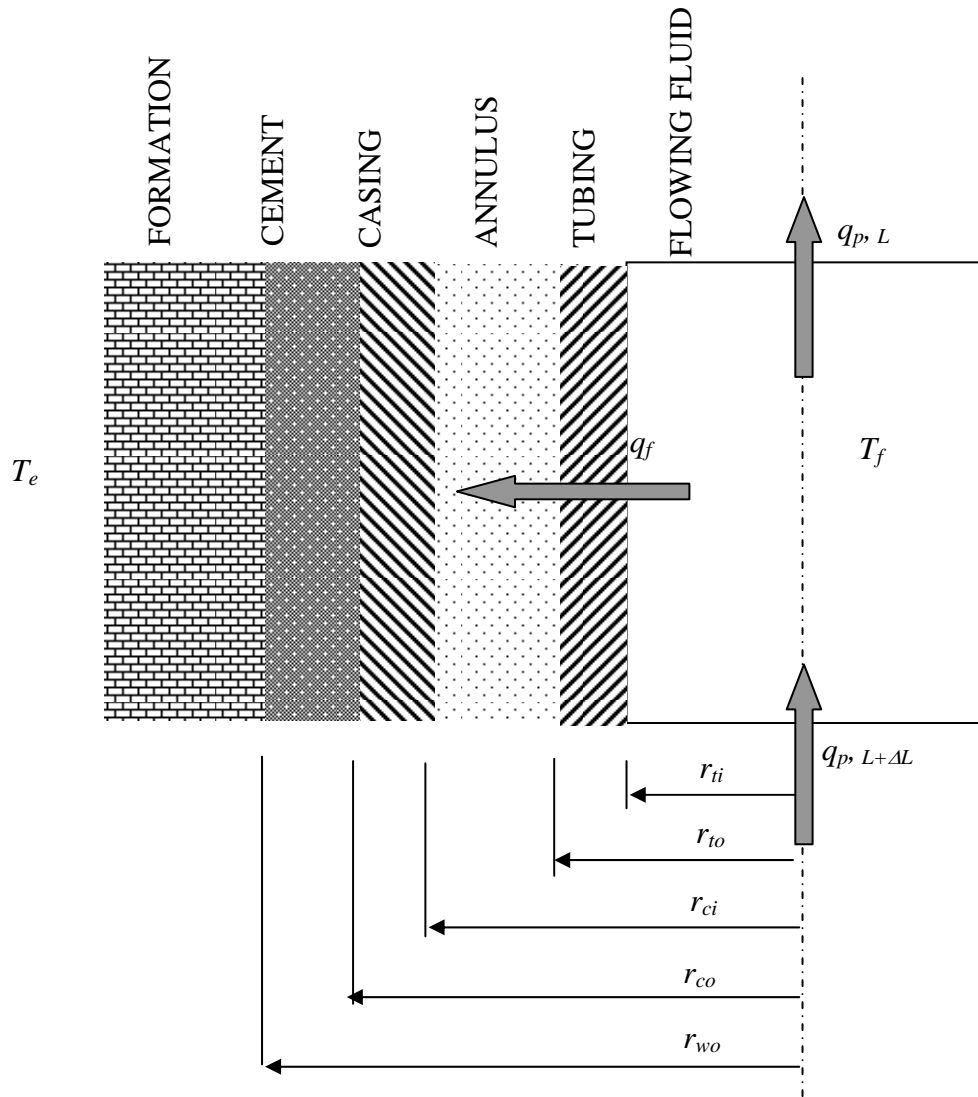


Fig. 3.4—Temperature fluxes for an element of fluid below the mudline.

Heat transfer through the production tubing resulting from conduction can be described according to Fourier's equation

$$T_{ii} - T_{io} = \frac{q}{2\pi\Delta L} \frac{\ln\left(\frac{r_{io}}{r_{ii}}\right)}{k_t}, \dots\dots\dots (3.78)$$

where  $k$  is the thermal conductivity of the tubing. Convection through the annulus is

$$T_{io} - T_{ci} = \frac{q}{2\pi\Delta L} \frac{1}{r_{ci} h_{an}}. \dots\dots\dots (3.79)$$

Conduction through the casing is

$$T_{ci} - T_{co} = \frac{q}{2\pi\Delta L} \frac{\ln\left(\frac{r_{co}}{r_{ci}}\right)}{k_c}. \dots\dots\dots (3.80)$$

Conduction through the cement is

$$T_{co} - T_w = \frac{q}{2\pi\Delta L} \frac{\ln\left(\frac{r_{cw}}{r_{co}}\right)}{k_{cem}}. \dots\dots\dots (3.81)$$

Heat transfer into the surrounding rock is described by the infinite-reservoir line-source solution,

$$T_w - T_e = \frac{q}{2\pi\Delta L} \frac{f(t)}{k_e}. \dots\dots\dots (3.82)$$

where  $f(t)$  is calculated as proposed by Hasan and Kabir.<sup>39</sup> A dimensionless time is defined as

$$t_{Dw} = \frac{\alpha t}{r_w^2}, \dots\dots\dots (3.83)$$

where  $\alpha$  is the thermal diffusivity of the formation.  $f(t)$  is then calculated for  $t_{Dw} \leq 1.5$  as

$$f(t) = 1.1281\sqrt{t_{Dw}}(1 - 0.3\sqrt{t_{Dw}}) \dots\dots\dots (3.84)$$

and for  $t_{Dw} > 1.5$  as

$$f(t) = [0.4603 + 0.5 \ln(t_{Dw})] \left( 1 + \frac{0.6}{t_{Dw}} \right) \dots\dots\dots (3.85)$$

Combining the temperature from the fluid inside production tubing to the formation temperature, Eq. 3.77 to 3.82, gives

$$T_f - T_e = \frac{q}{2\pi\Delta L} \left( \frac{1}{r_{ii}h_f} + \frac{\ln\left(\frac{r_{to}}{r_{ii}}\right)}{k_t} + \frac{1}{r_{ci}h_{an}} + \frac{\ln\left(\frac{r_{co}}{r_{ci}}\right)}{k_c} + \frac{\ln\left(\frac{r_w}{r_{co}}\right)}{k_{cem}} + \frac{f(t)}{k_e} \right) \dots\dots\dots (3.86)$$

### 3.3.2 Wellbore-Heat Transfer Above the Mudline

A similar analysis as for the wellbore-heat transfer below the mudline can be made for transfer above the mudline (**Fig. 3.5**). The heat transfer in the flowing fluid is again described by Eq. 3.77, the heat transfer through the tubing is described by Eq.

3.78, and the heat transfer through the fluid filled annulus is described by Eq. 3.79. The conduction through the riser is

$$T_{Ri} - T_{sw} = \frac{q_f}{2\pi\Delta z} \frac{\ln\left(\frac{r_{Ro}}{r_{Ri}}\right)}{k_R} \dots\dots\dots (3.87)$$

If buoyancy material is put on the riser, which is typical for deep and ultradeep water drilling, the outer radius,  $r_{Ro}$ , of the riser will increase and the thermal conductivity,  $k_R$ , will decrease.

Again, combining the temperature from inside the production tubing to the temperature of the seawater, Eq. 3.78 to 3.79 with Eq. 3.87, we get

$$T_f - T_{sw} = \frac{q}{2\pi\Delta L} \left( \frac{1}{r_{ii} h_f} + \frac{\ln\left(\frac{r_{to}}{r_{ii}}\right)}{k_t} + \frac{1}{r_{Ri} h_{an}} + \frac{\ln\left(\frac{r_{Ro}}{r_{Ri}}\right)}{k_R} \right) \dots\dots\dots (3.88)$$

In Eq. 3.86 and 3.88  $k$  is thermal conductivity and  $h$  is the convective film coefficient.

### 3.3.3 Overall Heat-Transfer Coefficient

Both Eq. 3.86 and Eq. 3.88 are equivalent to Newton's law of cooling<sup>33</sup> given by

$$T_f - T_e = \frac{q}{2\pi\Delta L r_{to} U} \dots\dots\dots (3.89)$$

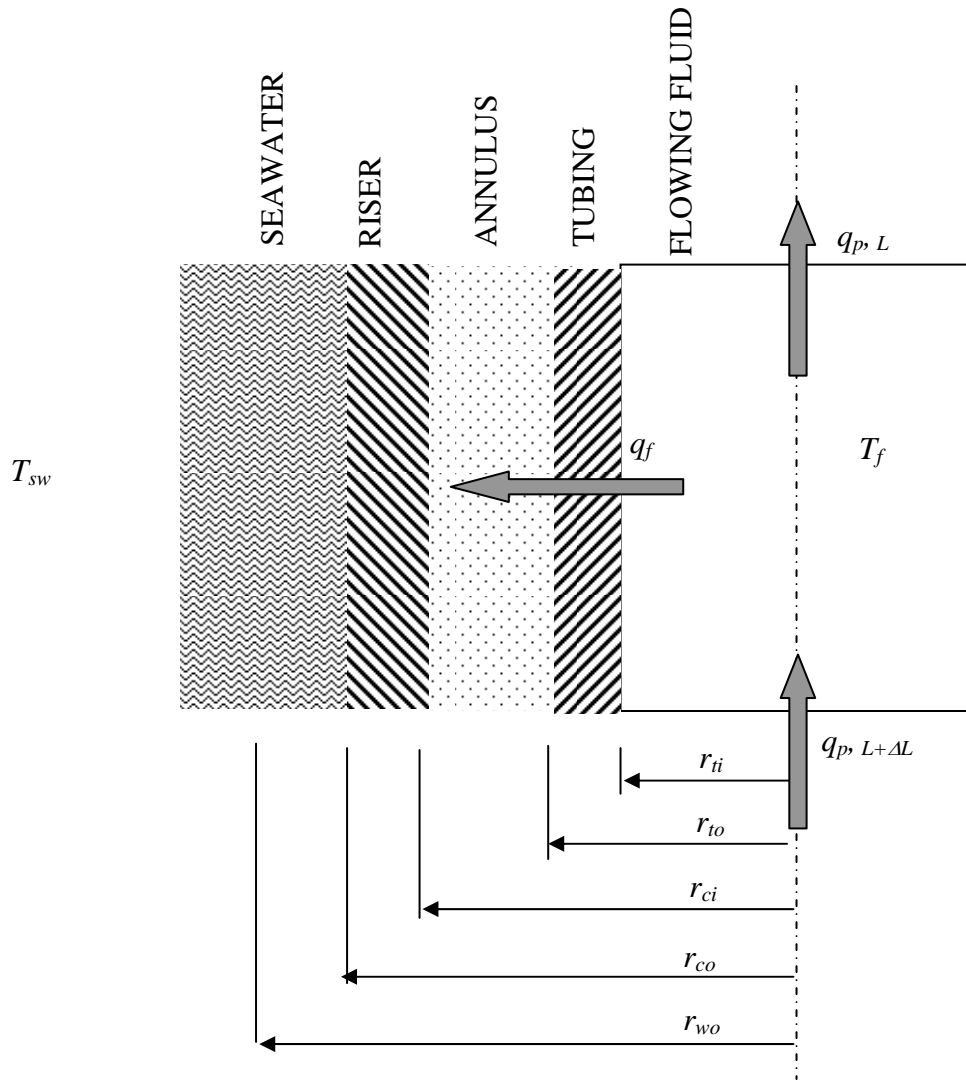


**Fig. 3.5—Temperature fluxes for an element of fluid above the mudline.**

By inspection, the bracket component in Eq. 3.86 and Eq. 3.88 is equal to the  $(r_{to}U)^{-1}$  term in Eq. 3.89. Thus, for below the mudline

$$(r_{to}U)^{-1} = \frac{1}{r_{ti}h_f} + \frac{\ln\left(\frac{r_{to}}{r_{ti}}\right)}{k_t} + \frac{1}{r_{ci}h_{an}} + \frac{\ln\left(\frac{r_{co}}{r_{ci}}\right)}{k_c} + \frac{\ln\left(\frac{r_w}{r_{co}}\right)}{k_{cem}} + \frac{f(t)}{k_e}, \dots \quad (3.90)$$

and above the mudline

$$(r_{io}U)^{-1} = \frac{1}{r_{ii}h_f} + \frac{\ln\left(\frac{r_{io}}{r_{ii}}\right)}{k_t} + \frac{1}{r_{ci}h_{an}} + \frac{\ln\left(\frac{r_{Ro}}{r_{Ri}}\right)}{k_R} \dots\dots\dots (3.91)$$

Eq. 3.90 and Eq.3.91 can be used to calculate the overall heat transfer coefficient,  $U$ , which is necessary when using Eq. 3.71 to calculate the thermal gradient in wellbores. In many cases it will be nearly impossible to make a sound estimate of some of the variables in  $U$ , such as the local convective-film coefficient of the annulus and the thermal conductivity of the cement. Ramey's<sup>40</sup> derivation of the wellbore heat-transmission for incompressible fluids also arrived at Eq. 3.71. However,  $C_1$  became

$$C_1 = \frac{c_p w [k + rUf(t)]}{2U\pi r k} \dots\dots\dots (3.92)$$

and

$$C_2 = 0. \dots\dots\dots (3.93)$$

Ramey assumed that  $U$  included heat transfer from outer casing wall to inside the tubing, excluding the heat transfer in the formation. The heat transfer in the formation is included separately in the relaxation distance,  $C_1$ . For a case such as injecting liquid down the casing or fluid flow in an openhole section, the thermal resistance of the wellbore can be assumed negligible. Thus,  $U$  would in this case be infinite and Eq. 3.92 would reduce to

$$C_1 = \frac{c_p w f(t)}{2\pi k} \dots\dots\dots (3.94)$$

Shiu and Beggs<sup>41</sup> proposed an empirical correlation (Eq. 3.95) for  $C_1$  developed from a broad range of temperature surveys:

$$C_1 = 0.0149(w)^{0.5253} (d_{ii})^{-0.2904} (\gamma_{API})^{0.2608} (\gamma_g)^{4.4146} (\rho_L)^{2.9303}, \dots \quad (3.95)$$

where  $w$  is the total mass flow rate in lbm/sec,  $\rho_L$  is liquid density at standard condition in lbm/ft<sup>3</sup>,  $d$  is the inner diameter of the pipe in inches,  $\gamma_{API}$  is the API gravity of the oil in °API, and  $\gamma_g$  is the gas-specific gravity. Eq. 3.95 was developed for oil wells but has been found to give good results for dry-gas wells by using liquid density of 62.4 and oil API gravity of 50.<sup>35</sup>

Above the mudline  $C_1$  still has to be calculated using Eq. 3.74, either by estimating the overall heat-transfer coefficient or by calculation using Eq. 3.91.

### 3.4 Inflow Performance Relationship

The study at hand focuses on drilling in deep- and ultradeep water. It is assumed that under these conditions the pressures in an oil reservoir will exceed the bubblepoint pressure, and only a single-phase, liquid reservoir exists. Thus, the reservoir fluid in this study is grouped as either a pure-liquid or a dry-gas reservoir. If a mixture of phases existed then a compositional reservoir model would have to be developed, which would complicate the study.

The relationship between production rate and the bottomhole flowing pressure is called the inflow performance relationship (IPR). The most famous IPR is Darcy's Law.<sup>42</sup> In 1856, Darcy performed experiments for purifying water in sand-filter beds. His findings for linear flow can be expressed as

$$v = \frac{k}{\mu} \frac{dp}{dx}, \dots \quad (3.96)$$

where  $k$  is the permeability of the sand,  $\mu$  is the fluid viscosity, and  $dp/dx$  is the pressure gradient in the direction of the flow.

Darcy's law can be used for a radial system such as flow from a reservoir to a well as seen in **Fig. 3.6**. As the flow is radial,  $dp/dx$  becomes  $dp/dr$  and the cross-sectional area open to flow at any radius is  $A = 2\pi rh$ . Since the volumetric flow rate is  $q = vA$ , Darcy's law in Eq. 3.96 becomes

$$q = \frac{2\pi rhk}{\mu} \frac{dp}{dr} \dots\dots\dots (3.97)$$

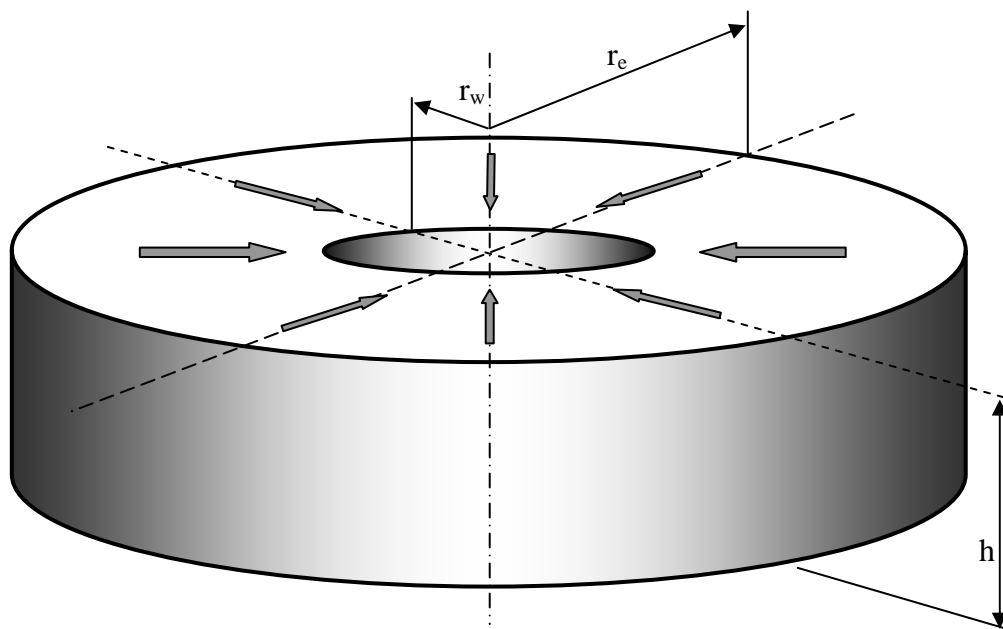


**Fig. 3.6—Radial flow from a reservoir to a wellbore.**

### 3.4.1 Oil Reservoir IPR

For an oil flow it is assumed that the reservoir fluid is only slightly compressible. This small compressibility is handled by the oil formation volume factor,  $B_o$ . Eq. 3.97 then becomes

$$q_o B_o = \frac{2\pi r h k_o}{\mu_o} \frac{dp}{dr} \dots\dots\dots (3.98)$$

or

$$q_o \int_{r_w}^{r_e} \frac{dr}{r} = 2\pi h \int_{p_{wf}}^{p_e} \frac{k_o}{\mu_o B_o} dp \dots\dots\dots (3.99)$$

By assuming that the permeability,  $k$ , the viscosity,  $\mu$ , and the oil formation volume factor are not functions of pressure, by integration we get

$$q_o = \frac{2\pi k_o h (p_e - p_{wf})}{\mu_o B_o \ln\left(\frac{r_e}{r_w}\right)} \dots\dots\dots (3.100)$$

Eq. 3.100 applies to steady state where  $p_e$  is constant. During pseudosteady state,  $\bar{p}_R - p_{wf} = \text{constant}$ . Thus, Eq. 3.100 can be rewritten as

$$q_o = \frac{2\pi k_o h (\bar{p}_R - p_{wf})}{\mu_o B_o \ln\left(\frac{0.472 r_e}{r_w}\right)} \dots\dots\dots (3.101)$$

During a blowout the rates may be very high and turbulence effects may become significant. A turbulence factor can be added as

$$q_o = \frac{2\pi k_o h (\bar{p}_R - p_{wf})}{\mu_o B_o \ln\left(\frac{0.472r_e}{r_w} + Dq_o\right)} \dots\dots\dots (3.102)$$

where  $D$  is the turbulence factor. Forchheimer<sup>43</sup> presented a derivation for the turbulence factor. Eq. 3.102 was written in the following form:

$$\bar{p}_R - p_{wf} = Aq_o + Bq_o^2 \dots\dots\dots (3.103)$$

The  $Aq_o$  term in Eq. 3.103 accounts for the laminar flow while  $Bq_o^2$  is the turbulence contribution to IPR. In field units

$$A = \frac{141.2\mu_o B_o}{k_o h} \ln\left(\frac{0.472r_e}{r_w}\right) \dots\dots\dots (3.104)$$

and  $B$ , assuming  $r_e$  is much greater than  $r_w$ , is

$$B = \frac{141.2\mu_o B_o}{k_o h} D = \frac{2.3 \times 10^{-14} \beta B_o^2 \rho_o}{h^2 r_w} \dots\dots\dots (3.105)$$

The field units of the variables in Eq. 3.104 and 3.105 are:

- $q_o$  = inflow rate, STBO/D,
- $k_o$  = effective oil permeability, md,
- $h$  = reservoir thickness, ft,
- $\bar{p}_R$  = average reservoir pressure, psia,
- $p_{wf}$  = wellbore flowing pressure, psia,

- $r_e$  = wells drainage radius, ft,  
 $r_w$  = wellbore radius, ft,  
 $\mu_o$  = oil viscosity, cp,  
 $B_o$  = oil formation volume factor, res. bbl/STB, and  
 $\beta$  = velocity coefficient, ft<sup>-1</sup>.

All the fluid properties should be evaluated at the reservoir temperature and at the average pressure of  $0.5(\bar{p}_R + p_{wf})$ . The velocity coefficient can be calculated as a function of permeability and the formation type.<sup>35</sup> For an unconsolidated formation

$$\beta = \frac{1.47 \times 10^7}{k_o^{0.55}}, \dots\dots\dots (3.106)$$

and for consolidated formations

$$\beta = \frac{2.329 \times 10^{10}}{k_o^{1.2}} \dots\dots\dots (3.107)$$

The user has the option to specify if the formation rock is consolidated or unconsolidated.

### 3.4.2 Gas Reservoir IPR

For a gas reservoir the reservoir fluid is going to be highly compressible and the assumption that density is independent of pressure is no longer valid. According to the equation of state, the density is

$$\rho = \frac{pM}{zRT} \dots\dots\dots (3.108)$$

For a gas reservoir it is also assumed that  $\rho q$  is constant. Applying this assumption and substituting Eq. 3.108 into Eq. 3.97 we get

$$q_{sc} = \frac{p_{sc} T_{sc}}{p_{sc} T_z} \frac{2\pi r h k_g}{\mu_g} \frac{dp}{dr}, \dots\dots\dots (3.109)$$

or

$$\int_{p_{wf}}^{p_e} p dp = \frac{q_{sc} \mu_g T_{sc} z}{2\pi h k_g T_{sc}} \int_{r_w}^{r_e} \frac{dr}{r} \dots\dots\dots (3.110)$$

By integration eq 3.109 becomes

$$p_e^2 - p_{wf}^2 = \frac{q_{sc} \mu_g T_{sc} z}{\pi h k_g T_{sc}} \ln \left[ \frac{r_e}{r_w} \right] \dots\dots\dots (3.111)$$

$p_{sc}$  and  $T_{sc}$  is the pressure and temperature at standard condition, which is assumed to be 14.7 psia and 65 °F respectively. For pseudo-steady state using the average reservoir pressure, Eq. 3.111 can be written in field units as

$$q_{sc} = \frac{703 \times 10^{-6} h k_g (p_R^2 - p_{wf}^2)}{\mu_g z T \ln \left[ \frac{0.472 r_e}{r_w} \right]} \dots\dots\dots (3.112)$$

As for the oil reservoir analysis a turbulence factor can be added. Thus, Eq. 3.111 can be written

$$p_R^2 - p_{wf}^2 = A q_{sc} + B q_{sc}^2, \dots\dots\dots (3.113)$$

where

$$A = \frac{1422\mu_g zT}{k_g h} \ln\left(\frac{0.472r_e}{r_w}\right), \dots\dots\dots (3.114)$$

and

$$B = \frac{1422\mu_g zT}{k_g h} D = \frac{3.161 \times 10^{-12} \beta \gamma_g zT}{h^2 r_w}, \dots\dots\dots (3.115)$$

The variables in Eq. 3.113 and their respective field units are:

- $q_{sc}$  = gas flow rate at standard conditions, Mscf/D,
- $k_g$  = effective gas permeability, md,
- $h$  = reservoir thickness, ft,
- $\bar{p}_R$  = average reservoir pressure, psia,
- $p_{wf}$  = wellbore flowing pressure, psia,
- $r_e$  = well's drainage radius, ft,
- $r_w$  = wellbore radius, ft,
- $\mu_g$  = gas viscosity, cp,
- $T$  = reservoir temperature, °R,
- $z$  = z factor, dimensionless, and
- $\beta$  = velocity coefficient, ft<sup>-1</sup>.

As for an oil reservoir, the fluid properties should be evaluated at the reservoir temperature and at the average pressure of  $0.5(\bar{p}_R + p_{wf})$ .

### 3.5 Properties of Reservoir Fluids

The properties of a reservoir fluid such as viscosity and formation-volume factor are best determined from a laboratory analysis using a fluid sample. However, during a blowout a fluid sample may not be available and correlations must be used to estimate the fluid properties. The correlations used in this analysis were chosen because they are easy to implement in a computer program and because of their accuracy and consistency.

#### 3.5.1 $z$ -Factor of Natural Gases

To determine the  $z$ -factor the pseudoreduced temperature,  $T_{pr}$ , and pressure,  $p_{pr}$ , must first be estimated. Piper *et al.*<sup>44</sup> presented a correlation for the pseudocritical temperature,  $T_{pc}$ , and pseudocritical pressure,  $p_{pc}$ , based on 1,482 data points using natural gases ranging in composition from lean sweet to rich acid gases. The correlation was fitted to their data points with an average error of 1.3 % and a maximum error of 7.3 %. Using  $T_{pc}$  and  $p_{pc}$ , the pseudoreduced temperature and pressure can be calculated as

$$T_{pr} = \frac{T}{T_{pc}} \dots\dots\dots (3.116)$$

and

$$p_{pr} = \frac{p}{p_{pc}} \dots\dots\dots (3.117)$$

Dranchuk and Abou-Kassem<sup>45</sup> presented a  $z$ -factor correlation primarily designed for a computer routine. The correlation was developed by fitting 1,500 data points with an average error of 0.486 %. The correlation is estimated to be accurate for engineering purposes in the ranges of  $0.2 \leq p_{pr} < 30$  for  $1.0 < T_{pr} \leq 3.0$  and  $p_{pr} < 1.0$  for  $0.7 < T_{pr} < 1.0$ .

The correlation must be solved numerically using a root solving technique such as Newton's method. The correlations for pseudoreduced pressure and temperature and the Dranchuk and Abou-Kassem  $z$ -factor correlation are listed in full detail in Appendix B.

### 3.5.2 Gas Density

The gas density can be calculated using the equation of state as

$$\rho_g = \frac{pM_g}{zRT} \quad \dots\dots\dots (3.118)$$

The specific gravity of a gas is defined as

$$\gamma_g = \left( \frac{\rho_g}{\rho_a} \right)_{sc} = \frac{M_g}{M_a}, \quad \dots\dots\dots (3.119)$$

where the subscript  $a$  denotes air. Substituting for the molecular weight of gas in Eq. 3.118 and using 28.96 for the molecular weight of air we get in field units

$$\rho_g = 2.7 \frac{p\gamma_g}{zT} \quad \dots\dots\dots (3.120)$$

### 3.5.3 Gas Formation Volume Factor

The gas formation volume can also be calculated using the equation of state. The definition of gas formation volume factor is the gas volume at reservoir conditions divided by the volume of gas at standard conditions for the same mass (Eq. 3.121).

$$B_g = \frac{V_R}{V_{sc}} \quad \dots\dots\dots (3.121)$$

Using the equation of state and substituting for the volumes, we get

$$B_g = \frac{\frac{znRT}{p}}{\frac{z_{sc}nRT_{sc}}{P_{sc}}} = \frac{zTp_{sc}}{z_{sc}T_{sc}p} \dots\dots\dots (3.122)$$

In field units Eq. 3.122 becomes

$$B_g = 0.0282 \frac{zT}{p}, \dots\dots\dots (3.123)$$

where  $T$  is in °Rankin,  $p$  in psia, and  $B_g$  is in cu.ft/scf.

### 3.5.4 Gas Viscosity

The simulator uses Lee *et al.*'s<sup>46</sup> semi empirical method to calculate gas viscosity. This method is accurate within 9 % for pressure in the range of  $100 < p$  (psia)  $< 8000$ , temperature in the range of  $100 < T$  (°F)  $< 340$ , and carbon dioxide content of  $0.9 < CO_2$  (mole percent)  $< 3.2$ .

Lee *et al.*'s method is given in Appendix B.

### 3.5.5 Oil Density

The oil gravity is often given in °API, which is the input unit used in the simulator. The oil specific gravity referenced to water gravity can be calculated as

$$\gamma_o = \frac{141.5}{131.5 + \gamma_{API}} \dots\dots\dots (3.124)$$

The oil density below the bubblepoint can be calculated as

$$\rho_o = \frac{62.4\gamma_o + 0.0136R_s\gamma_g}{B_o}, \dots\dots\dots (3.125)$$

where  $R_s$  is the solution-gas/oil ratio in scf/STB,  $B_o$  is the oil formation volume factor in res. bbl/STB, and the oil density is lbm/ft<sup>3</sup>. For saturated oils above the bubblepoint pressure, the density can be calculated as

$$\rho_o = \rho_{ob} \exp[c_o(p - p_b)]. \dots\dots\dots (3.126)$$

A correlation for calculating oil compressibility,  $c_o$ , is discussed below. The oil density at the bubblepoint,  $\rho_{ob}$ , can be calculated using Eq. 3.125 with the values for  $R_s$  and  $B_o$  calculated at the bubblepoint pressure.

### 3.5.6 Oil Formation Volume Factor and Oil Compressibility

Above the bubblepoint the formation volume factor of the oil,  $B_o$ , decreases as the oil becomes more compressed. Below the bubblepoint the  $B_o$  increases with pressure as more gas is dissolved in the oil. Two correlations for the oil formation volume factor are therefore required, one for above and one below the bubblepoint.

The compressibility of oil above the bubble point may be defined as

$$c_o = -\frac{1}{B_o} \left( \frac{\partial B_o}{\partial p} \right)_T. \dots\dots\dots (3.127)$$

Integration of Eq. 3.127 from the bubblepoint pressure to a higher pressure yields

$$B_o = B_{ob} \exp[c_o(p_b - p)]. \dots\dots\dots (3.128)$$

Eq. 3.128 is valid only for pressures above the bubblepoint pressure. An empirical correlation is necessary for pressures below the bubblepoint. Based on more than 6,000 measured values in a pressure, volume, temperature (PVT) analysis Vasquez and Beggs<sup>47</sup> presented correlations for several fluid properties, including a correlation for the oil compressibility,  $c_o$ , to be used with Eq. 3.128. The  $B_o$  correlation had an average error of 0.284 percent, and the  $c_o$  correlation would be expected to yield better or equal accuracy. The ranges of validity for the  $c_o$  and  $B_o$  correlations were  $126 < p$  (psia)  $< 9,500$ ,  $9.3 < R_s$  (scf/STB)  $< 2,199$ ,  $15.3 < \gamma_{API} < 59.5$ ,  $0.511 < \gamma_g < 1.351$ , and  $1.006 < B_o$  (bbl/STB)  $< 2.226$ .

The Vasquez and Beggs correlation for oil formation volume factor at and below the bubblepoint and the oil compressibility correlation are listed in Appendix B.

### 3.5.7 Solution-Gas/Oil Ratio

For pressures above the bubblepoint the solution-gas/oil ratio,  $R_s$ , is constant. Standing<sup>48</sup> developed a correlation for  $R_s$  below the bubblepoint. The average error of this correlation was 4.8 % for 105 sample points. The correlation was developed for the ranges of  $130 < p$  (psia)  $< 7,000$ ,  $100 < T$  (°F)  $< 258$ ,  $20 < R_s$ (scf/STB)  $< 1,425$ ,  $16.5 < \gamma_{API} < 63.8$ ,  $0.59 < \gamma_g < 0.95$ , and  $1.024 < B_o$  (bbl/STB)  $< 2.05$ .

The Standing correlation for solution-gas/oil ratio is listed in Appendix B.

### 3.5.8 Oil Viscosity

The dead-oil viscosity below the bubblepoint pressure is calculated using a correlation developed by Egbogah,<sup>49</sup> which is an extension of work done by Beggs and Robinson.<sup>50</sup> Egbogah used 394 oil systems to determine his correlation. The average error of this correlation was 6.6 % with the ranges of  $0 < p$  (psia)  $< 5250$ ,  $59 < T$  (°F)  $< 176$ ,  $20 < R_s$  (scf/STB)  $< 1425$ , and  $16 < \gamma_{API} < 58.0$ .

The oil viscosity for pressures above the bubblepoint is estimated using the Vasquez and Beggs correlation for  $\mu_o$ . The average error for this correlation was 7.54 % for 3143 sample points. The range of data for this correlation is the same as for the oil formation volume factor correlation by Vasquez and Beggs. The Egbogah and the Vasquez and Beggs correlation for  $\mu_o$  are listed in Appendix B.

### 3.5.9 Water Density

If the water is assumed incompressible, the water density can be calculated as

$$\rho_w = \frac{62.4\gamma_w + 0.0136R_{ws}\gamma_g}{B_w} \dots\dots\dots (3.129)$$

### 3.5.10 Water Formation Volume Factor

McCain<sup>51</sup> developed a correlation for water formation volume factor with an average error within 1 %. This correlation is listed in Appendix B.

### 3.5.11 Solution-Gas/Water Ratio

McCain<sup>51</sup> also developed a correlation for the solution-gas/water ratio. This correlation had an average error of less than 5 %. The range of applicability for this correlation is  $1,000 < p \text{ (psia)} < 10,000$  and  $100 < T \text{ (°F)} < 340$ .

McCain pointed out that this correlation should never be used for pressures below 1,000 psia. At these conditions the solution-gas/water ratio is ignored. This correlation is summarized in Appendix B.

### 3.5.12 Water Viscosity

A correlation for water viscosity was also presented by McCain.<sup>51</sup> The correlation has a maximum error of 7 % and was developed for a very limited temperature range of  $86 < T \text{ (}^\circ\text{F)} < 167$ .

The correlation is listed in Appendix B.

### 3.5.13 Gas/Oil and Gas/Water Interfacial Tension

The interfacial tension has a very small effect on the pressure and temperature gradient. However the multiphase flow models require values for the interfacial tensions. A model<sup>35</sup> for gas/oil and gas/water interfacial tension is therefore listed in Appendix B.

## 3.6 Nodal Analysis

The simulator models the initial condition using a system-analysis method—also called nodal analysis—which has already been discussed extensively in the literature.<sup>35,52</sup> A node is selected at the bottom of the blowing well. The bottomhole flowing pressure,  $p_{wf}$ , at this node can be calculated from two sets of equations upstream and downstream of the flow. The inflow to the node is

$$p_{wf} = \bar{p}_R - \Delta p_{res}, \dots\dots\dots (3.130)$$

and the outflow of the node is

$$p_{wf} = p_{exit} + \Delta p_f + \Delta p_h + \Delta p_{acc} \cdot \dots\dots\dots (3.131)$$

These two equations can be graphed as functions of flow rate as seen in **Fig 3.7**. Since two different pressures cannot exist at the same node at the same time, the pressure and rate at the node will be where the two system-curves intersect. The algorithm used to calculate  $p_{wf}$  and the blowing rate will be described in the next chapter.

The inflow curve is calculated according to the inflow-performance relationship and the outflow curve—also called system-intake curve—is calculated from pressure correlations, both of which are described earlier in this chapter.

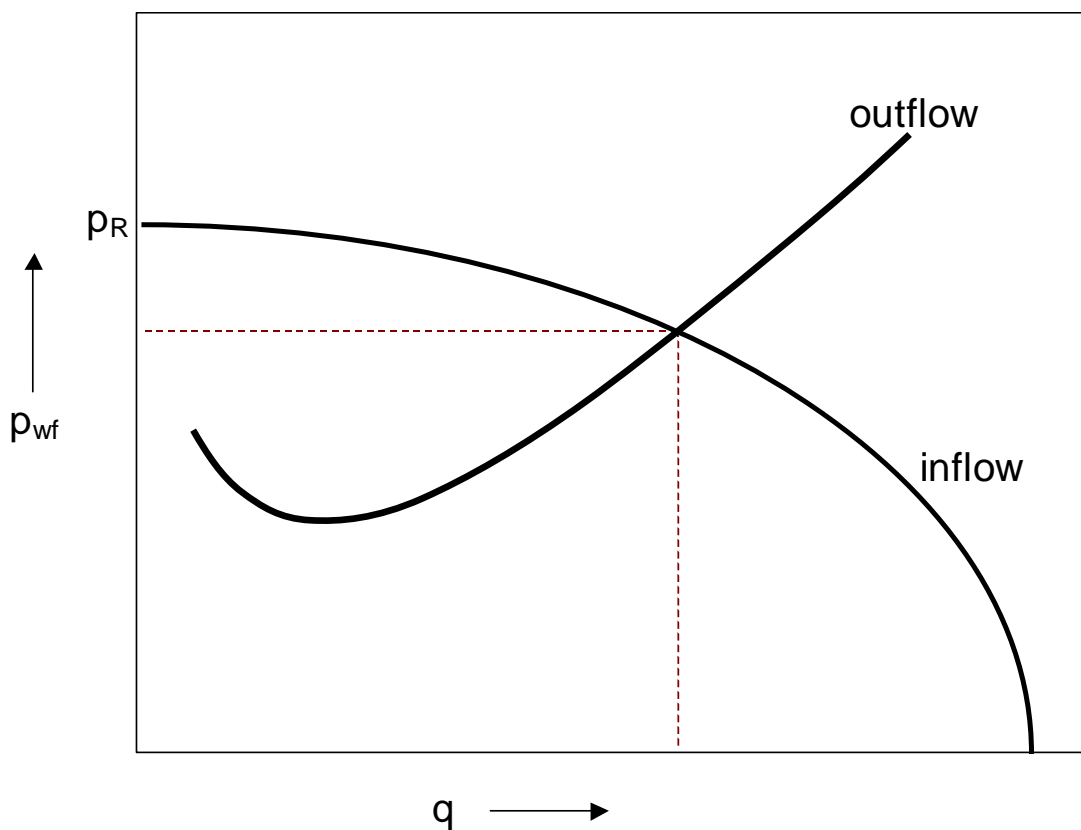


**Fig. 3.7—Determining the initial flowrate and bottomhole flowing pressure using nodal-analysis.**

### 3.7 Dynamic Kill Single-Phase Solution

As kill fluid is injected into the wellbore, the system-intake curve will change while the inflow-performance curve will remain the same. **Fig. 3.8** illustrates the effect

on the system-intake curve as the injection rate of the kill fluid is increased. The minimum kill rate that will successfully stop the influx of formation fluid is the minimum rate that gives a system-intake curve, which is always above the inflow-performance curve. For the case in Fig 3.8, the minimum kill rate would be 80 bbl/min.

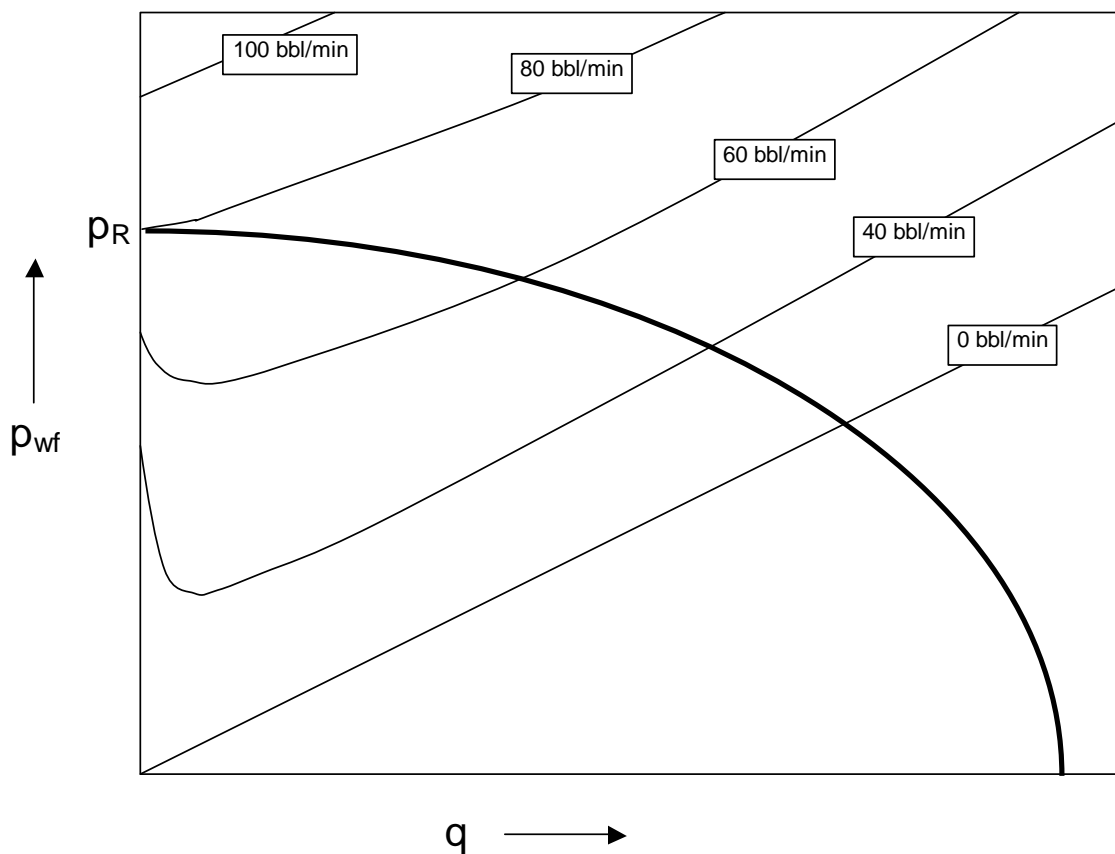


**Fig. 3.8—System-intake curves for different kill rates.**

When the influx of formation fluid is zero, the bottomhole flowing pressure is equal to the average reservoir pressure for the minimum kill rate. At this point the well will be filled with kill fluid only and the complication of multiphase does not need to be

considered in the calculations. The single-phase solution is thus the kill rate that will give a flowing bottomhole pressure equal to the average reservoir pressure when the well is filled with kill fluid only.

Blount and Soeiinah<sup>15</sup> presented a simple analytical solution for the single-phase solution. They started with Eq. 3.131. Assuming an incompressible kill fluid and ignoring acceleration, the flowing bottomhole pressure is

$$p_{wf} = p_{wh} + \rho h + \frac{f\rho v^2 L}{2g_c d}, \dots\dots\dots (3.132)$$

where

$$v = \frac{4q_L}{\pi d^2} \dots\dots\dots (3.133)$$

Substituting Eq. 3.133 into Eq. 3.132 and rearranging for the kill rate,  $q_L$ , gives

$$q_L = 0.592d^{2.5} \left( \frac{p_{wf} - p_{wh} - \rho h}{f\rho L} \right) \dots\dots\dots (3.134)$$

The minimum kill is calculated where the flowing bottomhole pressure is equal to the average reservoir pressure; thus,

$$(q_L)_{\min} = 0.592d^{2.5} \left( \frac{p_R - p_{wh} - \rho h}{f\rho L} \right) \dots\dots\dots (3.135)$$

The solution to equation 3.135 requires an iterative solution since the Moody friction factor is a function of  $q_L$ .

### 3.8 Dynamic Kill Multiphase Solution

As seen for the system-intake curves in Fig. 3.8, with kill rates of 40 and 60 bbl/min the flowing bottomhole pressure increases with decreasing influx rate as the influx rate approaches zero. This dip in the system-intake curves occurs when the flow in the wellbore is unstable and the liquid is loading.

If liquid loading occurs for the case of 80 bbl/min, the system-intake curve would fall below the inflow-performance curve and this kill rate would not successfully kill the well. Thus, the single-phase solution may in some cases underpredict the minimum kill rate. The multiphase solution is the minimum kill rate that gives a system-intake curve that is always above the inflow-performance curve. The procedure to calculate the multiphase solution will be described in detail in the next chapter.

Kouba *et al.*<sup>16</sup> presented an analytical derivation for the zero-derivative curve. The zero-derivative curve is the minimum kill rate that will give stable flow and no liquid loading for any influx rate. They started with Eq. 3.131; however, in this case the density and velocity include both kill fluid and reservoir fluid. Assuming a gas reservoir and no slippage between the phases, the mixture velocity and density can be written

$$v_m = v_{sL} + v_{sg} = \frac{4(q_L + q_g)}{\pi d^2}, \dots\dots\dots (3.136)$$

and

$$\rho_m = \lambda_L \rho_L + \lambda_g \rho_g = \frac{q_L \rho_L + q_g \rho_g}{q_L + q_g}. \dots\dots\dots (3.137)$$

Substituting Eq. 3.136 and 3.137 into Eq. 3.131, we get

$$p_{wf} = p_{wh} + \left( \frac{q_L \rho_L + q_g \rho_g}{q_L + q_g} \right) h + \left( \frac{q_L \rho_L + q_g \rho_g}{q_L + q_g} \right) \left( \frac{4[q_L + q_g]}{\pi d} \right)^2 \frac{fL}{2g_c d} \dots \dots \dots (3.138)$$

The conditions for the zero-derivative curve is

$$\left( \frac{\partial p_{wf}}{\partial q_g} \right) \rightarrow 0 \quad \text{as} \quad q_g \rightarrow 0. \dots \dots \dots (3.139)$$

Taking the derivative of Eq. 3.137 with respect to  $q_g$ , setting all the  $q_g$  terms to zero, and rearranging for the kill rate yields

$$(q_L)_{\min} = 0.135 \left[ \frac{(\rho_L - \rho_g) d^5 h}{(\rho_L + \rho_g) fL} \right] \dots \dots \dots (3.140)$$

Kouba also showed that if the gas density is small compared to the kill-fluid density, then the zero-derivative condition is met for the kill rate that gives frictional pressure equal to the hydrostatic pressure.

If simple hand-calculation is the only method available to estimate the minimum kill rate, the recommended procedure is to calculate the single-phase solution according to Eq. 3.135 and the zero-derivative solution from Eq. 3.140. The larger of the two should be considered as the design requirement.

**Fig. 3.9** illustrates the relationship between the single-phase solution, the zero-derivative curve, and the actual multiphase solution for the minimum kill rate. If the zero-derivative solution is larger than the single-phase solution, then the actual solution will be located as an intermediate value. However, the actual solution for the minimum kill rate can never fall below the single-phase solution.

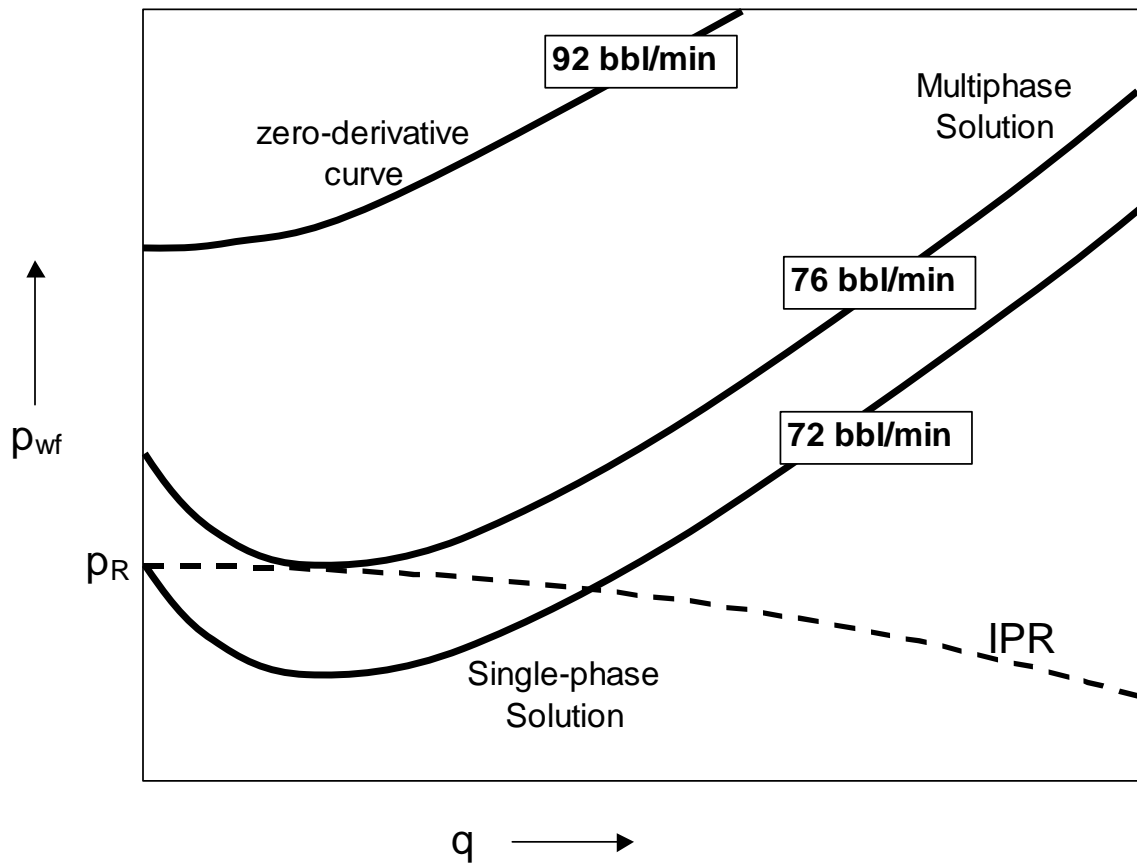


**Fig. 3.9—Relationship between single-phase, multiphase, and zero-derivative solution for the minimum kill rate.**

## CHAPTER IV

### ALGORITHMS

One of the major accomplishments of this work—which also took most of the time—was developing the algorithms for the simulator.

The simulator considers a case where the average reservoir pressure,  $\bar{p}_R$ , and the exit pressure,  $p_{\text{exit}}$ , are constant. The fluid from the blowing well may in some cases flow to the surface, which would make the exit pressure equal to atmospheric pressure, or in other cases the flow may be exiting at the mudline (**Fig. 4.1**), which would make the exit pressure equal to the seawater hydrostatic,  $p_{sw}$ . The average reservoir pressure and the exit pressure are the boundary conditions for the simulations.

The well is separated into small elements as shown in Fig 4.1. As will be described in this chapter, a value for the bottomhole flowing pressure,  $p_{wf}$ , is estimated. This estimate is used to calculate the surface flow rate of formation fluid from the inflow-performance relationship. The user sets the gas/liquid ratio and the water cut at the surface conditions, and the fluid properties are calculated for each element using fluid-property correlations as described in the previous chapter. From the fluid properties, the pressure and temperature in the well are calculated using a nodal-analysis approach.

This chapter describes in close detail how the initial blowing conditions and the dynamic-kill requirements are calculated in the computer program. These two main objectives are separated into two global algorithms that share similar subalgorithms. The global algorithms are the initial condition and dynamic kill.

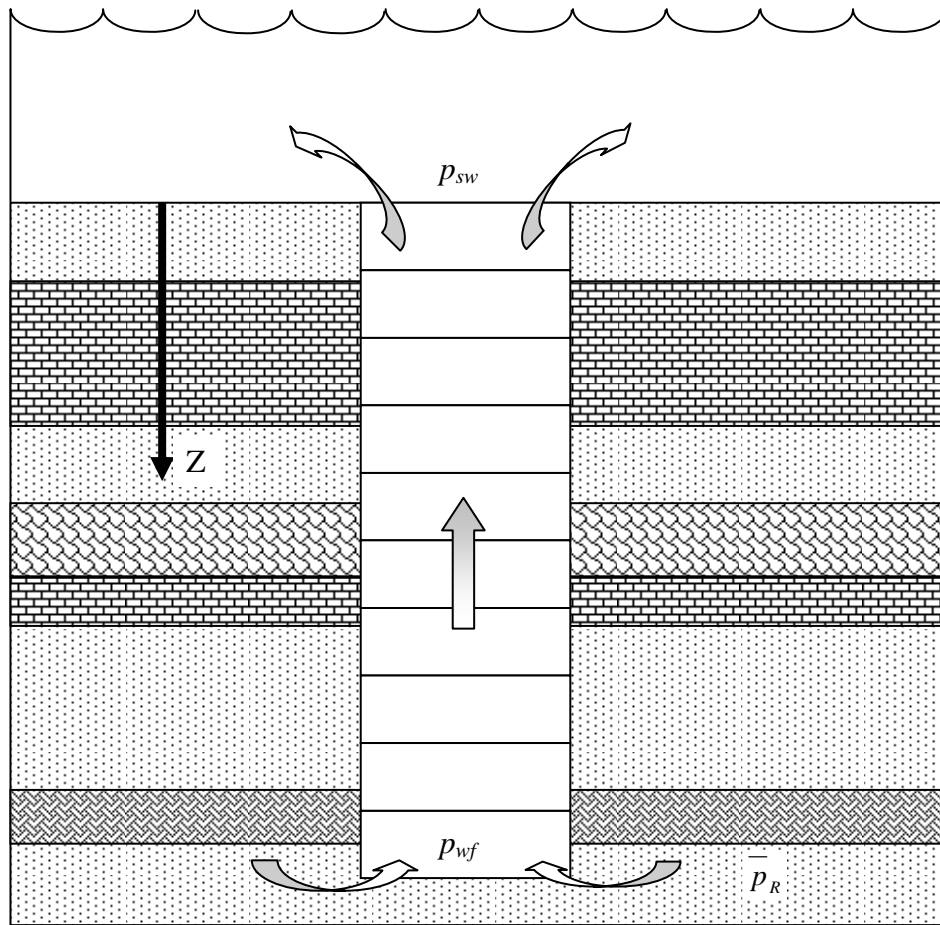


**Fig. 4.1—Blowing well with exit to the mudline separated into finite elements.**

The sub algorithms, which the global algorithm shares, are pressure, temperature, and wellbore profile.

The dynamic-kill algorithm is further separated into a single-phase solution and a multiphase solution algorithm as described in the previous chapter.

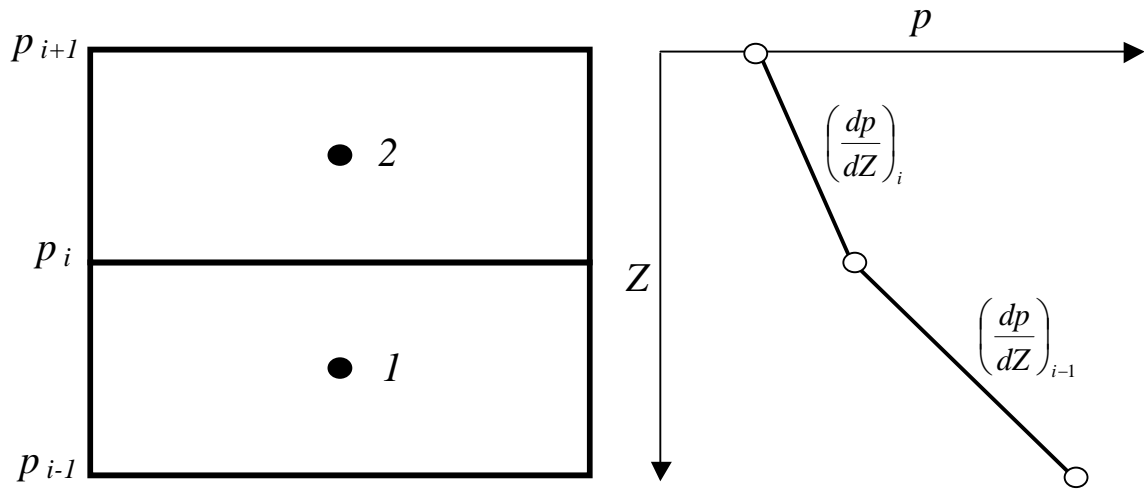


**Fig. 4.2—Two adjacent elements in the wellbore.**

#### 4.1 Pressure Algorithm

As seen in Fig. 4.1, the wellbore is separated into a finite number of elements. In **Fig. 4.2** two neighboring elements are shown with a chart for the pressure plotted with depth. The pressure at the boundary of each element is denoted as  $p_{i-1}$ ,  $p_i$  and  $p_{i+1}$ . The pressure gradients between the boundaries are calculated at the center of each element, which is marked with a filled dot.

The flow chart in **Fig. 4.3** is the algorithm used to calculate the pressure at  $p_{i+1}$ . Given the pressure  $p_i$  and the pressure gradient  $(dp/dZ)_{i-1}$ , an estimate for  $p_{i+1}$  is made (Eq. 4.1).

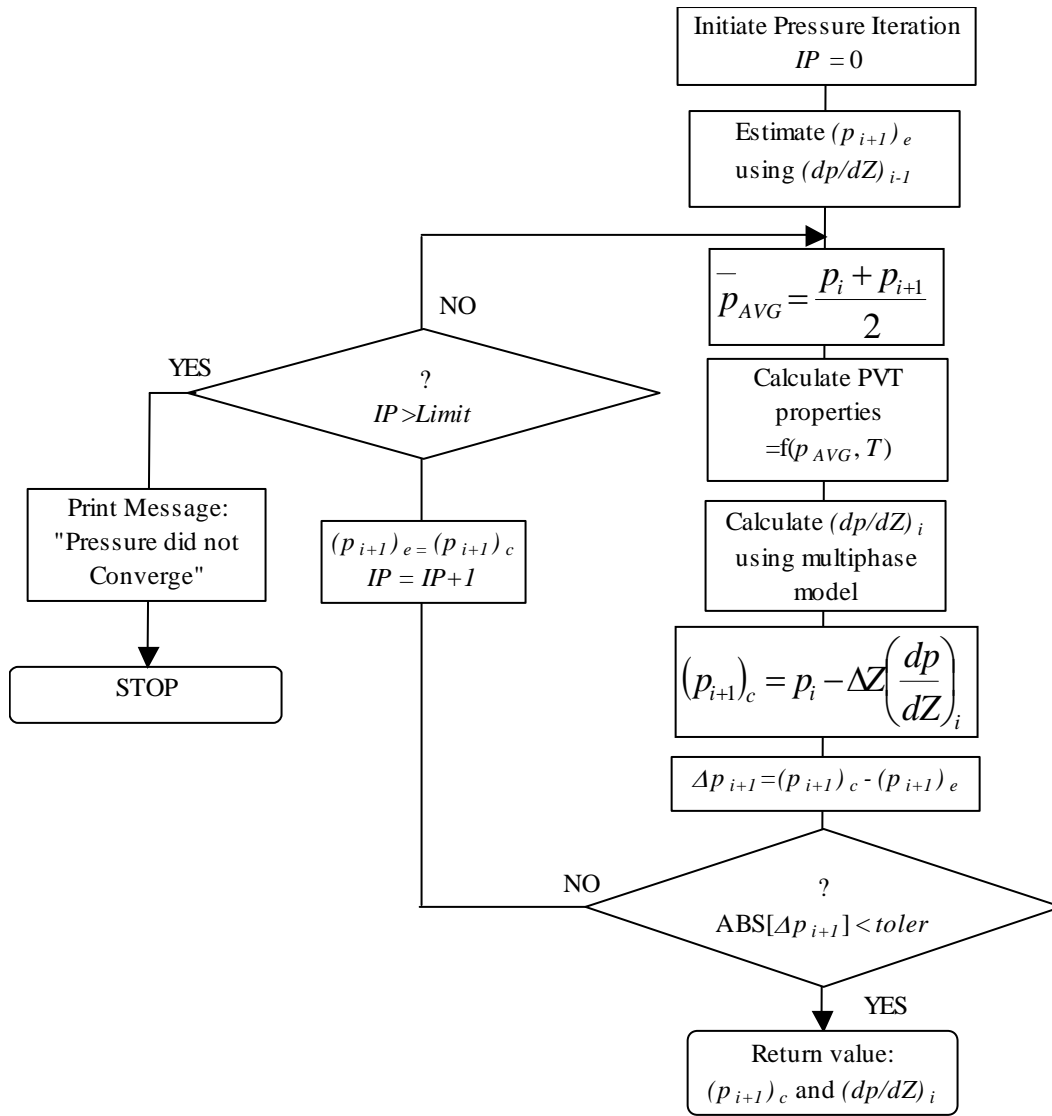


**Fig. 4.3—Pressure algorithm.**

$$(p_{i+1})_e = p_i - \Delta Z \left( \frac{dp}{dZ} \right)_{i-1} \dots \dots \dots (4.1)$$

The average pressure between  $p_{i+1}$  and  $p_i$  is calculated and used to determine all the fluid properties of the element. One of the three multiphase models described earlier in the modeling chapter and listed in Appendix A is then used to calculate the pressure gradient  $(dp/dZ)_i$ . A new value for  $p_{i+1}$  is then calculated as

$$(p_{i+1})_c = p_i - \Delta Z \left( \frac{dp}{dZ} \right)_i \dots\dots\dots (4.2)$$

The estimated pressure  $(p_{i+1})_e$  is compared with the new calculated pressure  $(p_{i+1})_c$ . If the difference is within a specified tolerance, the value of the calculated pressure is returned from the algorithm. If the difference is not within the range of the tolerance (*toler*), the calculated pressure is entered as the new initial guess and iterations are performed. If the number of iterations exceed a specific limit (*Limit*) the algorithm returns a message indicating that convergence was not obtained and the simulation is stopped.

The tolerance, *toler*, and the limit, *Limit*, is defined at the start of the main algorithm and can easily be changed throughout the program. The current default value for *toler* and *Limit* is  $10^{-8}$  % and 100 iterations respectively.

#### 4.2 Temperature Algorithm

The temperature algorithm is illustrated in **Fig. 4.4**. As shown, the temperature algorithm resembles the pressure algorithm. As for the pressure algorithm, an estimate for  $T_{i+1}$  is made using an equation of the same form as Eq. 4.1. This estimate is used to calculate the pressure and fluid properties as described in the pressure algorithm. The temperature gradient is then calculated as described in the previous chapter and the temperature,  $T_{i+1}$ , is again calculated. The procedure is repeated until either the solution is found or the no-convergence criterion is fulfilled.

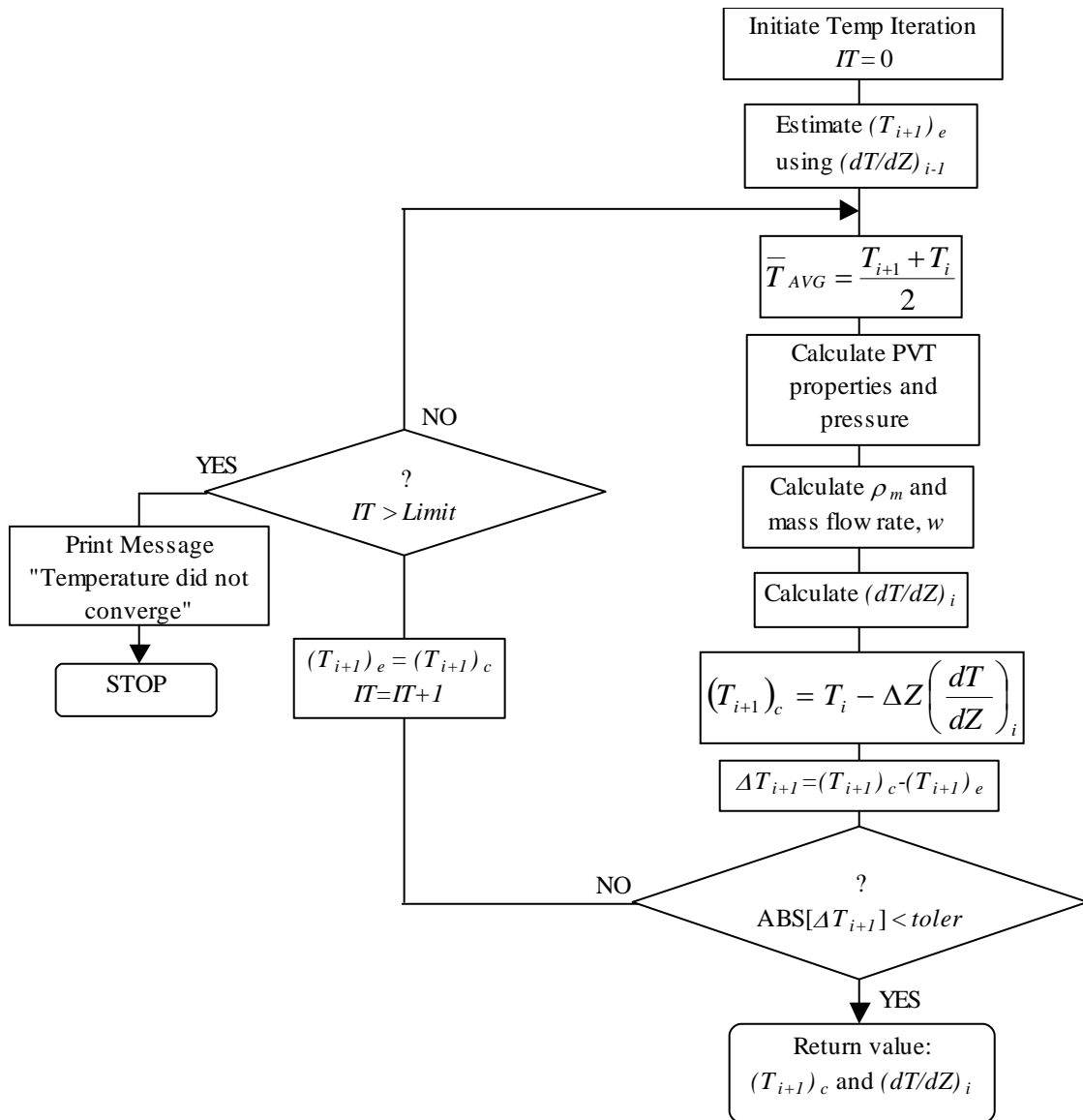


**Fig. 4.4—Temperature algorithm.**

### 4.3 Wellbore-Profile Algorithm

The wellbore-profile algorithm calculates the temperature and pressure with depth for a given flow rate. For boundary conditions given at the bottom of the well,

where  $Z$  equals the total-vertical depth, the algorithm steps upward until the pressure and temperature are determined for every element in the wellbore. The wellbore-profile algorithm appears as **Fig. 4.5**. The algorithm then returns an array for the pressure ( $p[i]$ ) and the temperature ( $T[i]$ ).

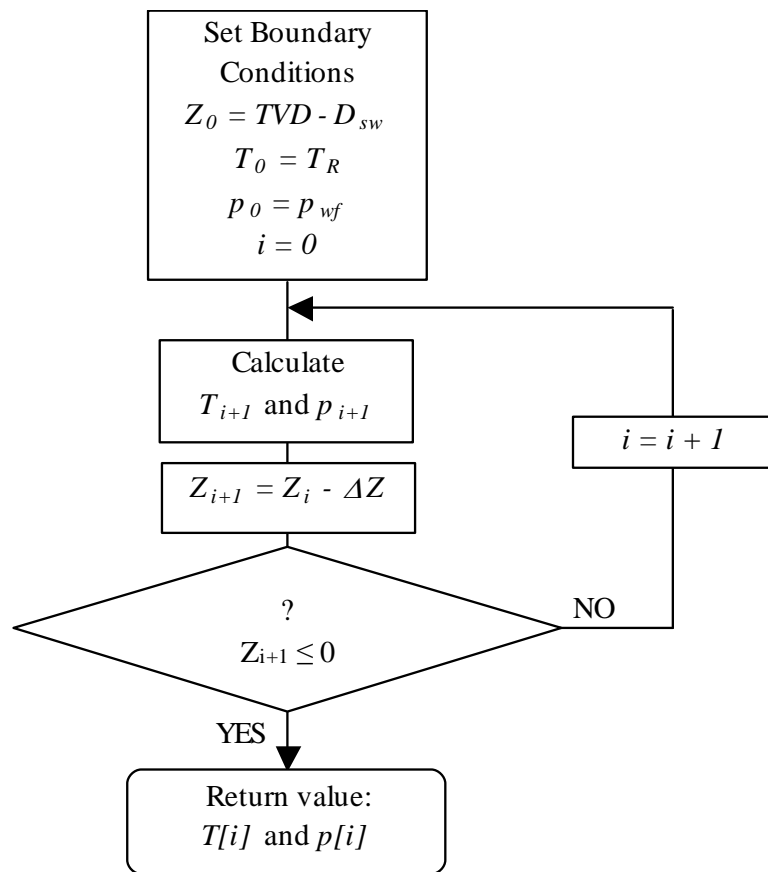


**Fig. 4.5—Wellbore-profile algorithm.**

#### 4.4 Initial-Condition Algorithm

The initial-condition algorithm calculates the influx rate of formation fluid at standard conditions with the corresponding pressure and temperature in the wild well before a dynamic kill is attempted. The methodology is a nodal analysis. Following the chart in **Fig 4.6**, the actual exit pressure,  $(p_{\text{exit}})_a$ , must be set by the user or calculated as explained in Chapter II. An initial guess is made for the flowing bottomhole pressure, which enables the calculation of influx rate at standard surface conditions using the IPR equation given as Eq. 3.103 for oil wells or Eq. 3.113 for gas wells. The pressure and temperature profile can then be calculated using the wellbore-profile algorithm.

*SIZE* is a variable for the number of elements in the wellbore, and  $p_{\text{SIZE}}$  is the pressure of the last element, which is also the calculated exit pressure,  $(p_{\text{exit}})_c$ . The calculated exit pressure is compared with actual exit pressure,  $(p_{\text{exit}})_a$ , and iteration commences until a desired tolerance is obtained.

#### 4.5 Single-Phase Solution Algorithm

The minimum kill rate calculated from the single-phase solution is the kill rate that gives a flowing bottom-hole pressure equal to the average reservoir pressure when only kill fluid is present in the wellbore. The procedure to calculate the single-phase solution is illustrated in **Fig 4.7**. A kill rate is estimated and the flowing bottomhole pressure is calculated until the solution is found. The actual iteration scheme will be explained later.

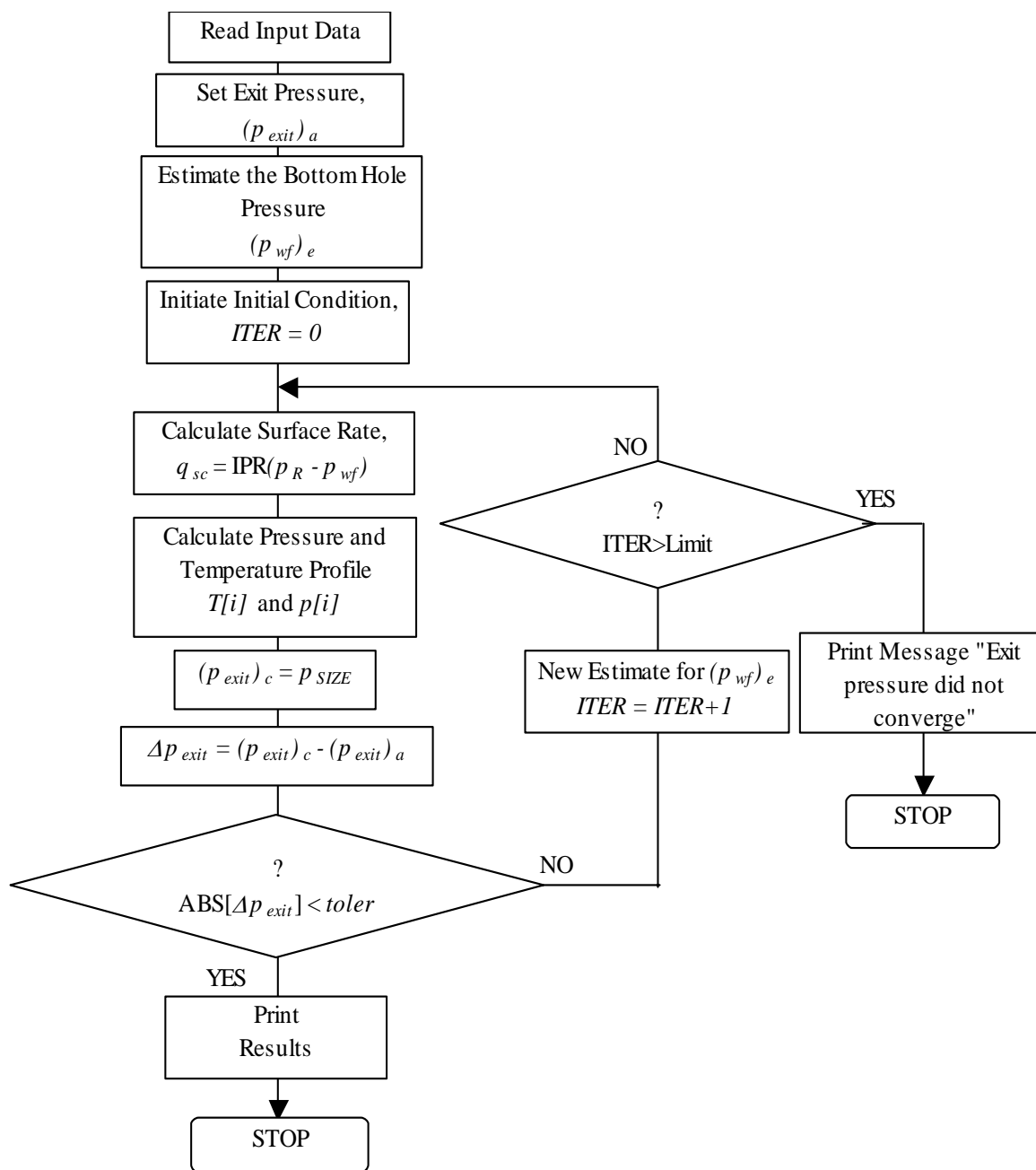


**Fig. 4.6—Initial-condition algorithm.**

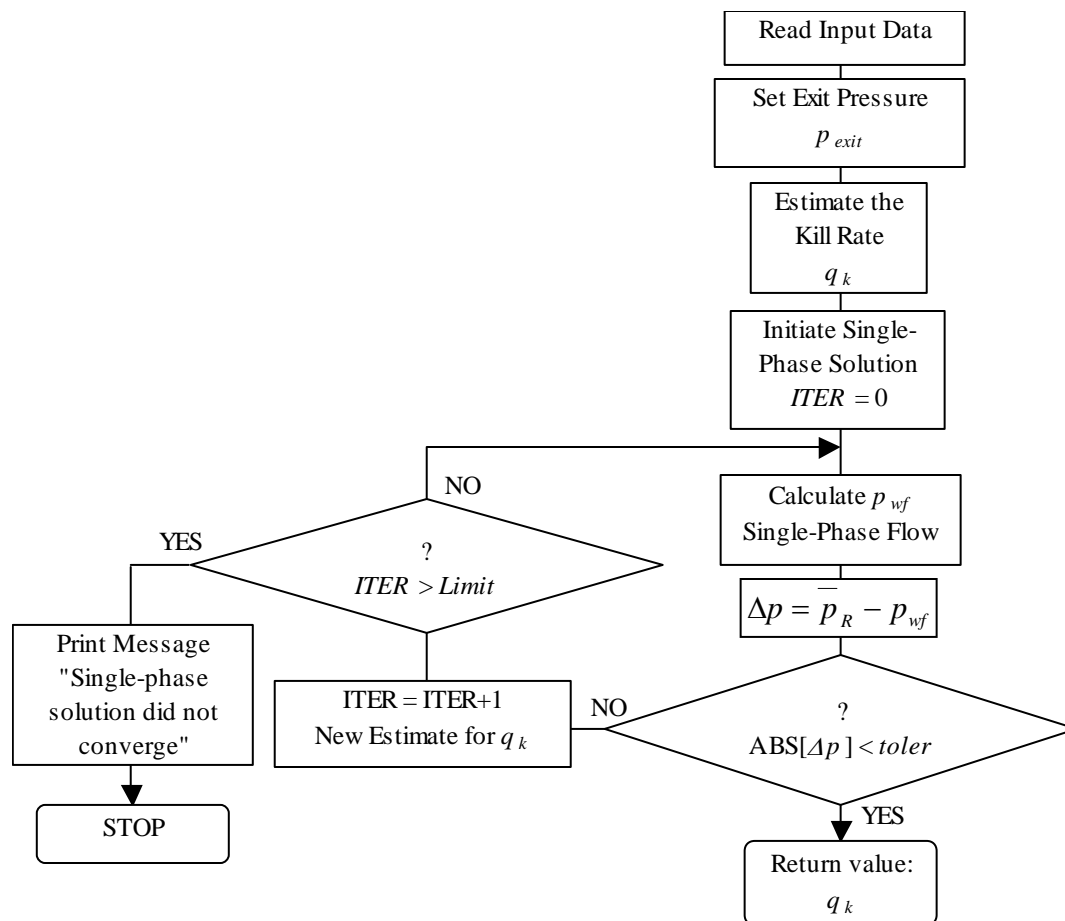


**Fig 4.7—Single-phase solution for the minimum kill rate.**

#### 4.6 Multiphase Solution Algorithm

The multiphase solution for the minimum kill rate is much more complicated than the single-phase solution. The flow diagram in **Fig. 4.8** illustrates the multiphase solution. First, the single-phase solution is calculated and used as an initial guess. A small influx,  $\Delta q_{isc}$ , is assumed in the wellbore, and the system-intake curve is calculated.

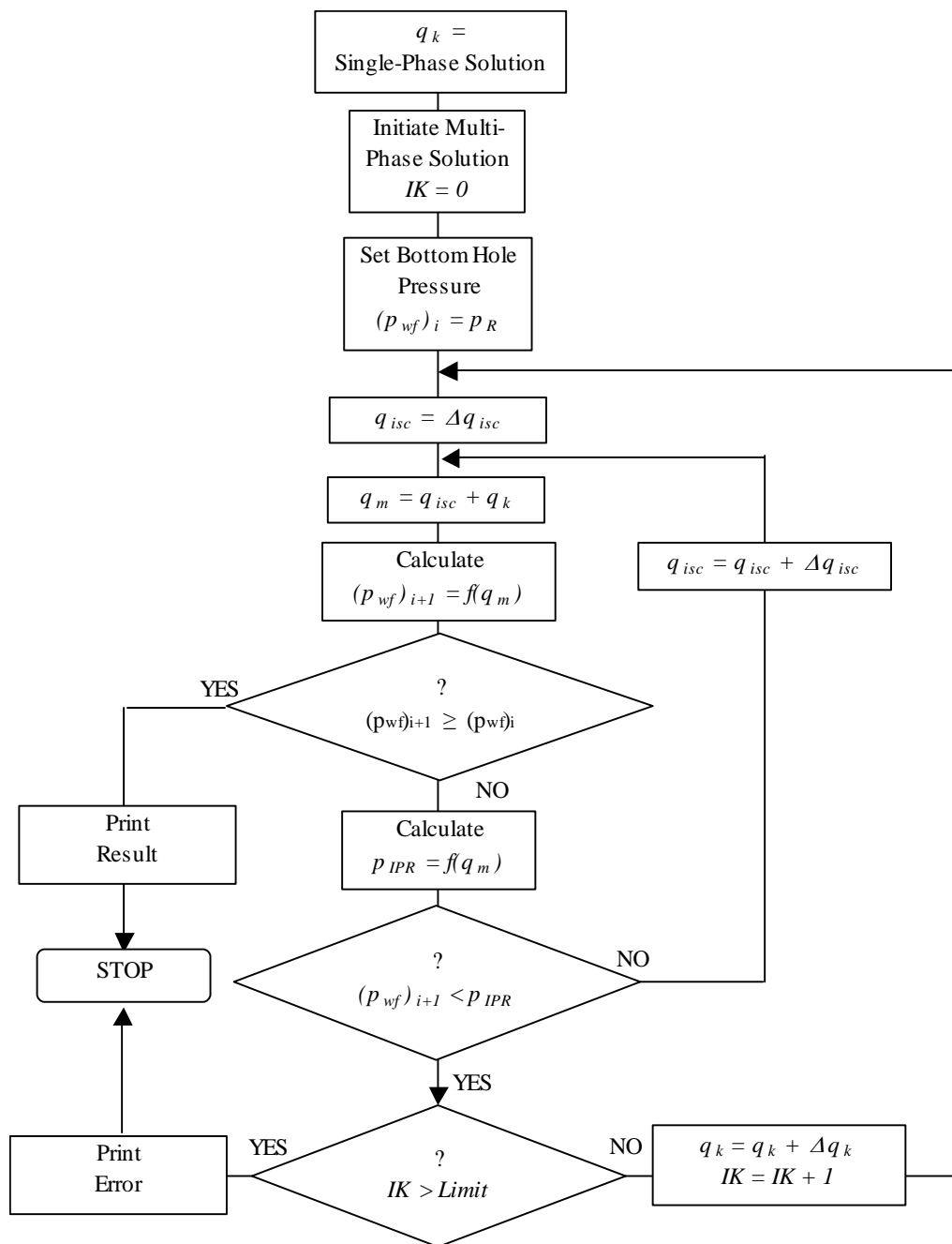


**Fig. 4.8—Multiphase solution for minimum kill rate.**

If the flowing bottomhole pressure increased compared to the average reservoir pressure, then the assumption is that no liquid loading exists under the current conditions and the single-phase solution is valid.

However, if the flowing bottomhole pressure decreased, a comparison between the system-intake curve and the inflow-performance curve must be made. If the system-intake curve falls below the inflow-performance, the kill rate must be increased and a new single-phase system-intake curve must be calculated. Or, if the system-intake curve remains above the inflow-performance curve, a new system-intake curve is calculated for a slightly larger influx. The procedure is repeated until the flowing bottomhole pressure increases for a larger influx, which will give the final solution.

While calculating the multiphase solution, it is assumed that the kill fluid dominates the friction factor. Thus, in the case of a non-Newtonian kill fluid, the friction factor is calculated as for the single-phase, non-Newtonian case. A further assumption is also made for liquid reservoirs. In the later stage of a dynamic kill, the influx of formation fluid decreases towards zero as the pressures in the wellbore increase. Most likely the gas/liquid ratio (GLR) will decrease under these conditions. However, during the simulation it is assumed that the GLR remains the same to simplify the analysis.

#### 4.7 Global Iteration Scheme

Both for the single-phase solution and for the initial-condition algorithm, iteration is performed with estimates of the solution until an error is minimized. Here, the method for choosing the estimate for every iteration will be described. The case considered is that of the initial condition, but the same methodology is used for the single-phase solution algorithm. ....

Following the flowchart in **Fig. 4.6**, two values for the flowing bottomhole pressure,  $(p_{wf})_1$  and  $(p_{wf})_2$ , are randomly chosen, and the exit pressure,  $(p_{exit})_1$  and  $(p_{exit})_2$ ,

is calculated for both  $p_{wf}$  values. The absolute error,  $\Delta p_{exit}$ , between the calculated surface pressure and actual surface pressure can be plotted for the two values of flowing bottomhole pressures. A linear trend line is fitted through the two points, x-y coordinates, as seen in **Fig. 4.9**. A new estimate for the flowing bottomhole pressure,  $(p_{wf})_3$ , is then extrapolated to where the linear trend line crosses the x-axis and the error is zero, which is given by

$$(p_{wf})_3 = (p_{wf})_1 - \left( \frac{(p_{wf})_2 - (p_{wf})_1}{(\Delta p_{exit})_2 - (\Delta p_{exit})_1} \right) (\Delta p_{exit})_1 \dots\dots\dots (4.3)$$

A new value for the error,  $(\Delta p_{exit})_3$ , is calculated as a function of  $(p_{wf})_3$ , and a new linear trend line is fitted through the two last calculated points. This procedure is repeated until a desired tolerance for the absolute error,  $\Delta p_{exit}$ , is achieved.

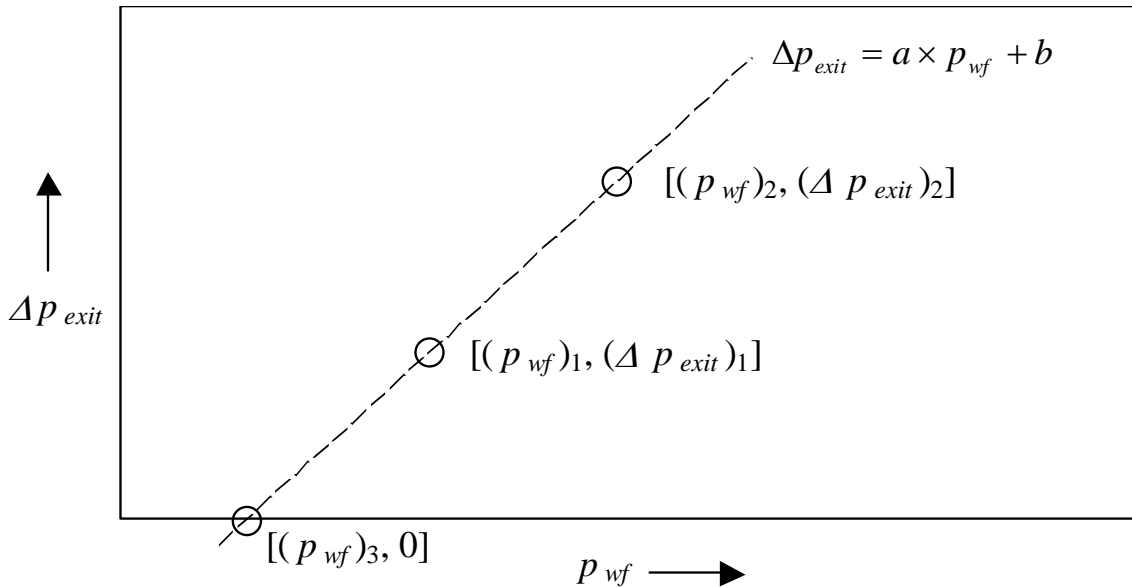


**Fig. 4.9—Global iteration scheme.**

## CHAPTER V

### TESTING AND RESULTS

The most challenging part in testing and verifying a dynamic-kill model is to overcome the sparse quantity of good field data. A separate part of this project—not included in this dissertation—is gathering blowout-field data that can be used for a thorough evaluation of all the models used in this study.

The simulator comprises empirical and analytical models that have been used extensively by the industry. No testing of the actual models should be necessary. However, the range of application for the simulator must be determined, and potential coding bugs must be found. In this section a brief comparison of the simulator is made to calculated data and analytical solutions found in the literature. Some observation and results from the simulator are included.

#### 5.1 Initial Condition

The initial condition part of the simulator is a system-analysis calculator as described in the modeling chapter. **Fig. 5.1** shows the initial-condition result for a case where the GLR is varied from zero to 300 scf/STBL in increments of 100, while all other variables remain unchanged. Beggs<sup>35</sup> published a large set of prepared system-intake curves just like these. He used the Hagendorn and Brown model with the assumption of smooth pipe and negligible acceleration. A comparison between the results from the simulator presented here and the Beggs curves are shown in **Table 5.1** and **Table 5.2**.

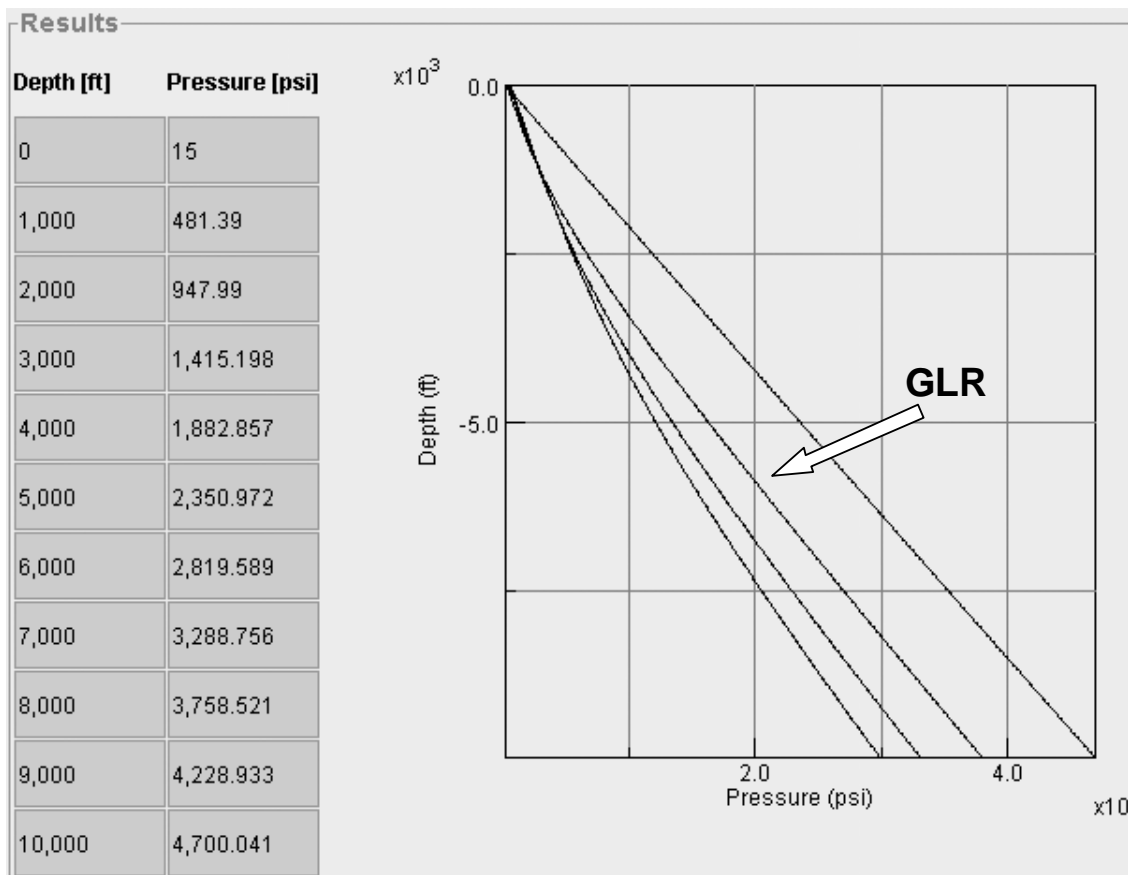


**Fig. 5.1—System-intake curves from the simulator with varying gas/liquid ratios.**

The absolute errors between Begg's results and the simulator are within reasonable agreement. The major source of discrepancy can most likely be attributed to reading the pressure results from Begg's charts. Other sources of error include the pipe roughness, which was set at 0.00065 ft for the simulation runs, and the acceleration term, which was included in the simulation runs.

**Table 5.1—Absolute Error Between Beggs Curves and Simulation Results With  
Tubing Size of 1.995 in and Liquid Rate of 700 STBL/D**

	Tubing Size	1.995 in.		
	Liquid Rate	700 STBL/D		
	Depth	10,000 ft		
	Gas Gravity	0.65		
	API Gravity	35		
	Water Gravity	1.07		
	Average Temperature	150 °F		
	<b>GLR</b>	<b>Water Cut = 0%</b>	<b>Water Cut = 50%</b>	<b>Water Cut = 100%</b>
	0	4.6	2.7	0.3
	100	6.3	1.7	0.3
	200	0.5	1.0	3.8
	300	2.9	4.0	5.7

**Table 5.2—Absolute Error Between Beggs Curves and Simulation Results With  
Tubing Size of 3.958 in and Liquid Rate of 8,000 STBL/D**

	Tubing Size	3.958 in.		
	Liquid Rate	8000 STBL/D		
	Depth	10,000 ft		
	Gas Gravity	0.65		
	API Gravity	35		
	Water Gravity	1.07		
	Average Temperature	150 °F		
	<b>GLR</b>	<b>Water Cut = 0%</b>	<b>Water Cut = 50%</b>	<b>Water Cut = 100%</b>
	0	3.3	1.9	2.2
	100	6.9	2.9	3.7
	200	5.7	3.6	2.5
	300	5.5	4.5	3.4

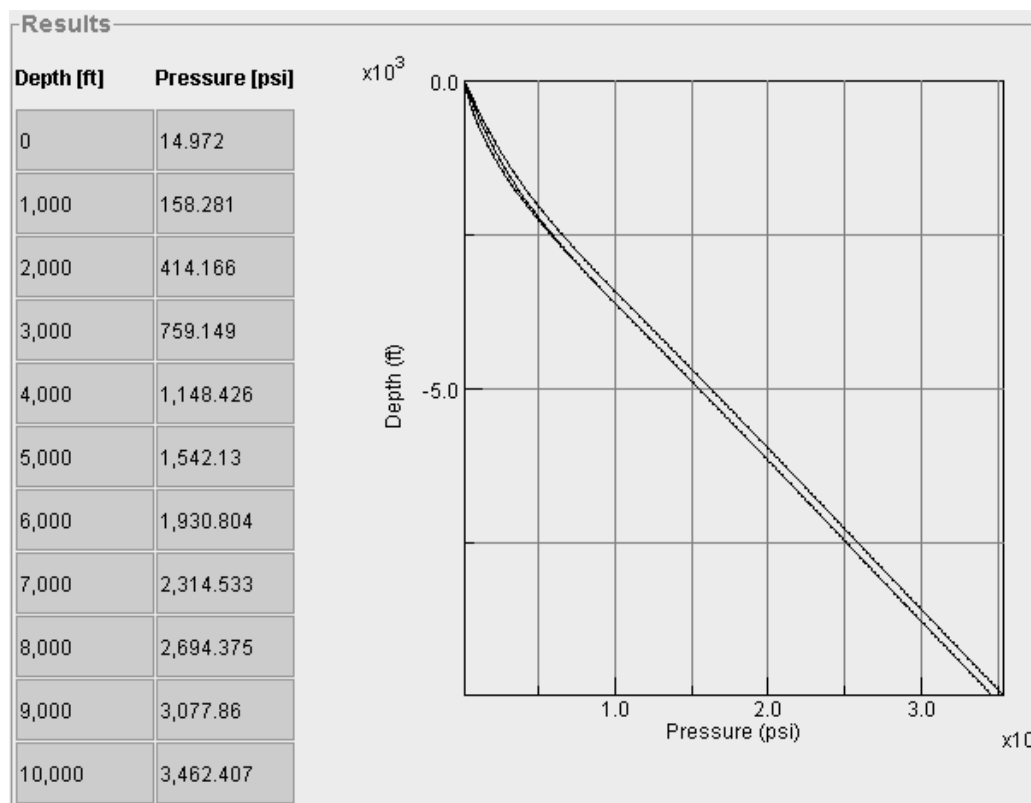


**Fig. 5.2—Comparing the multiphase models with tubing size of 1.995 in. and GLR of 100 scf/STBL.**

The multiphase models featured in the simulator can also be compared with each other. **Fig. 5.2** shows the comparison for a case with a small tubing size and low gas/liquid ratio. The Beggs and Brill model predicts the highest pressures, while the Duns and Ros and the Hagendorn and Brown models overlap each other. Another comparison between the multiphase models, with larger tubing size and higher GLR, is shown in **Fig. 5.3**. Clearly the models do not match at all. Again, Beggs and Brill predicted the highest pressure, while Hagendorn and Brown predicted substantially lower pressure.

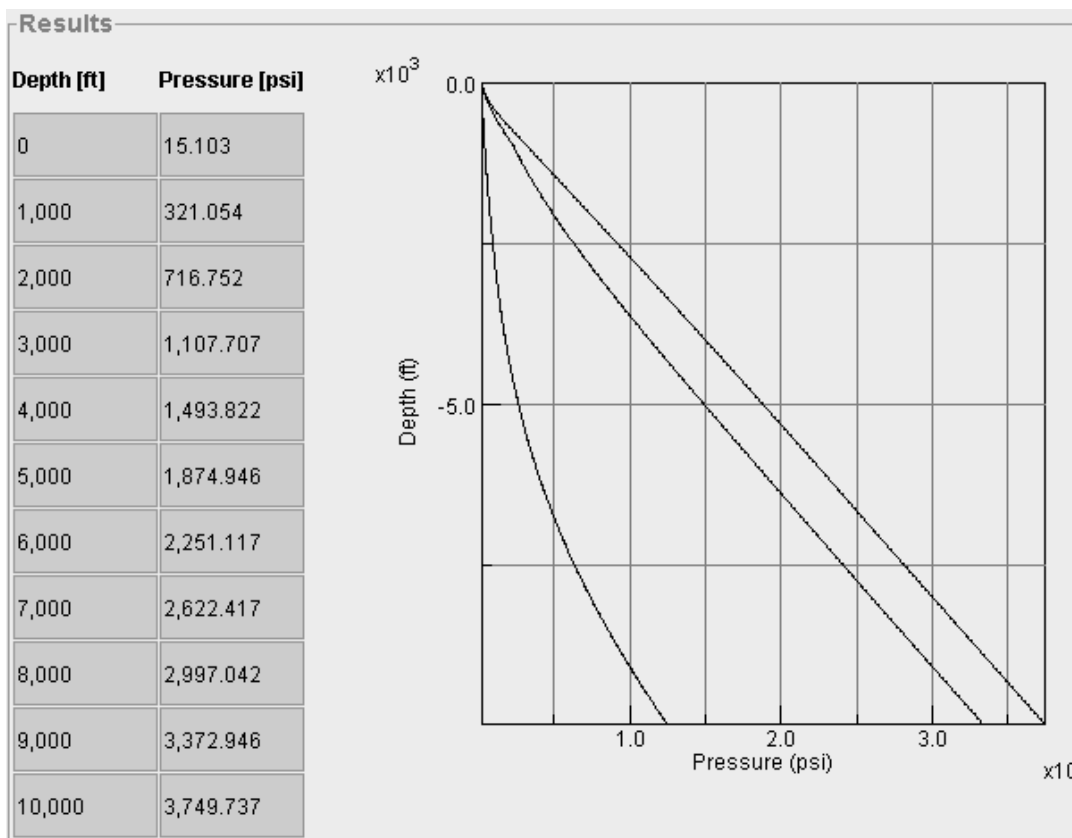


**Fig. 5.3—Comparing the multiphase models with tubing size of 8.921 in. and GLR of 300 scf/STBL.**

Both Fig. 5.2 and Fig. 5.3 illustrate the case of a surface blowout with well depth of 10,000 ft. The same case as in Fig. 5.3, but in 10,000 ft of water and a blowout to the mudline, is seen in **Fig. 5.4**. As seen with the 10,000 ft of hydrostatic backpressure at the exit point of the flow, all the multiphase models overlap and give identical results. The obvious reason for this is that the additional backpressure will always retain the gas within the liquid solution throughout the wellbore, and no multiphase flow will occur.

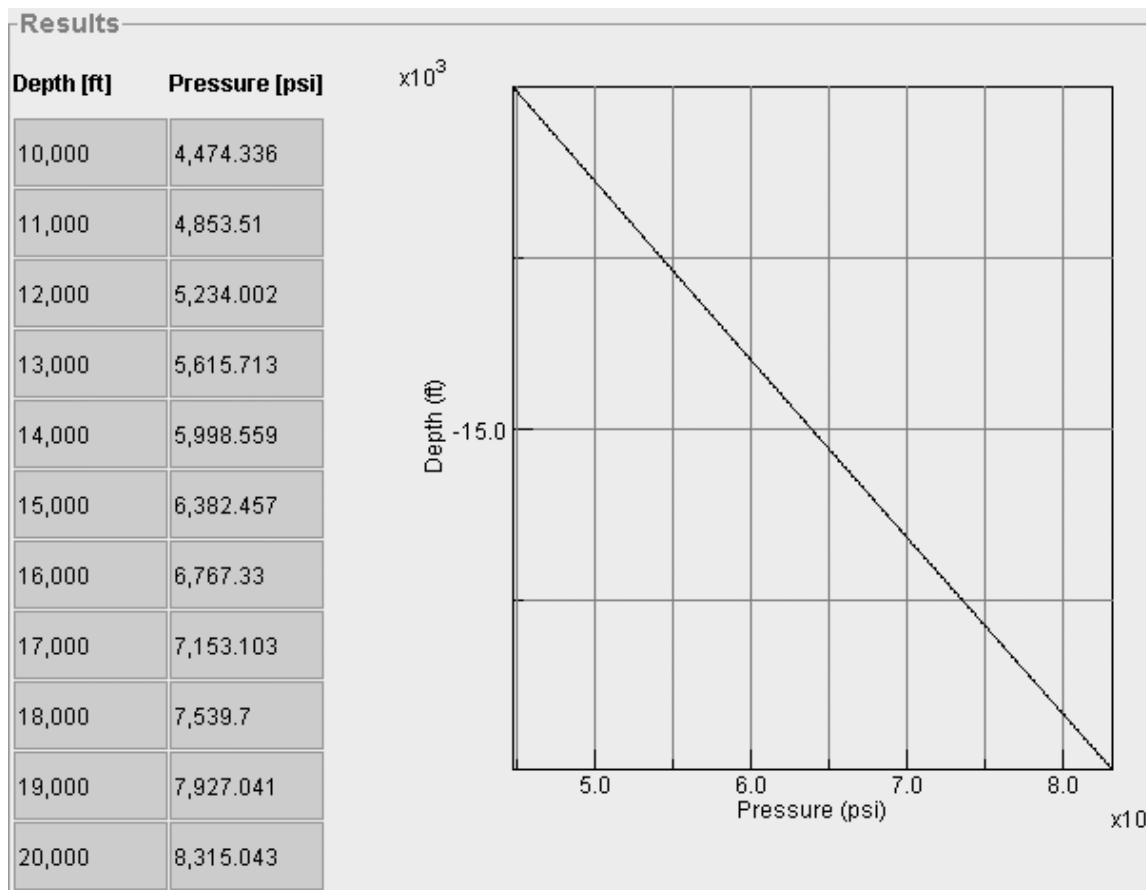


**Fig. 5.4—Comparing the multiphase models with tubing size of 8.921 in. and GLR of 300 scf/STBL in 10,000 ft of water depth.**

## 5.2 Minimum Kill Rate

As described in Chapter IV, simple analytical solutions for the minimum kill rate are available. Considering the case listed in **Table 5.3**, the result from the dynamic-kill simulator can be compared to the analytical models.

The calculated example here follows an example presented by Watson *et al.*<sup>13</sup> The single-phase solution from Eq. 3.135 is

**Table 5.3 – Blowout Data for Calculation Example**

<b>Wellbore</b>	
Wellbore Depth	11500 ft
Casing Nominal Inner Diameter	6.184 in.
Casing Roughness	0.00065 in.
<b>Blowout Data</b>	
Formation Fluid	Single-Phase Gas
Specific Gravity	0.6
Kill Fluid	Water
Kill Fluid Weight	8.5 ppg
Average Reservoir Pressure	7,177 psia
Exit Pressure	15 psia

$$(q_L)_{\min} = 0.592(6.184)^{2.5} \left( \frac{7,177 - 15 - 0.052(8.5)(11,500)}{(0.01208)(8.5)(11,500)} \right)^{0.5} = 71.7 \text{ bbl} / \text{min} \dots\dots\dots (5.1)$$

The friction factor is calculated using Jain's correlations in Eq. 3.22. Iterations, not included here, were necessary to find the solution above.

The zero-derivative solution according to Kouba can be calculated from Eq. 3.140 as

$$(q_L)_{\min} = 0.135 \left[ \frac{(8.5 - 1.7)(6.184)^5(11,500)}{(8.5 + 1.7)(0.01311)(11,500)} \right] = 91.6 \text{ bbl} / \text{min} \dots\dots\dots (5.2)$$

Since the zero-derivative solution is larger than the single-phase solution, the multiphase solutions should lie somewhere in the range between 72 and 92 bbl/min.

The result using the simulator is 3,210 gal/min or 76.4 bbl/min. The relationships between the results are illustrated in Fig. 3.9, where the multiphase solution from the simulator is in the correct range.

One of the immediate questions that arises when studying offshore blowouts is the consequence of moving drilling into ultradeep water. **Fig. 5.5** illustrates the effect of increasing water depth, while all other factors remain the same, on the case listed in Table 5.3. If the total vertical depth and the average reservoir pressure remain the same, while the water depth increases, the intervention requirements will, not surprisingly, become more demanding.

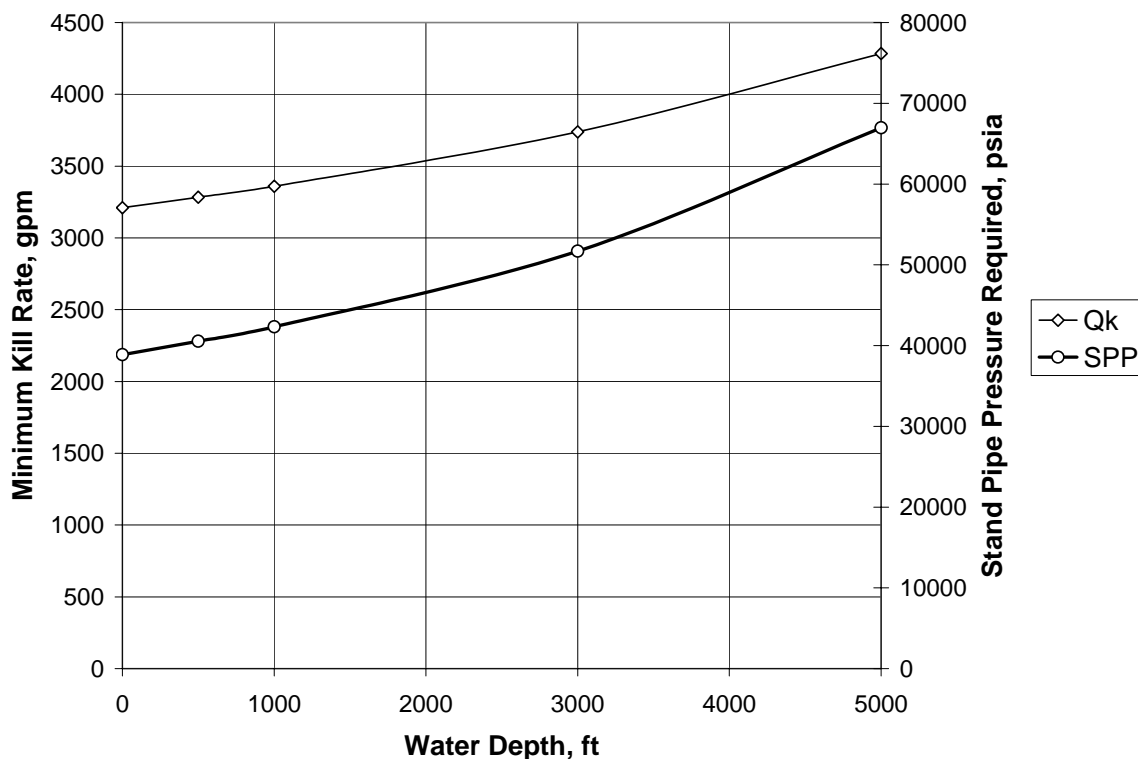


**Fig. 5.5—Minimum-kill rate and standpipe-pressure requirement with increasing water depth.**

## CHAPTER VI

### DISCUSSION AND CONCLUSIONS

A simulator specially designed to study blowouts and dynamic kills has been presented. The simulator will be used to develop new procedures for blowouts in ultradeep water, but can also be used to plan dynamic-kill intervention on a case-by-case basis and as a training tool.

Some of the main features and advantages of this dynamic-kill simulator include

- A user-friendly interface.
- Web application.
- Surface, subsurface and underground blowout capability.
- Simple dual-gradient drilling.
- Both Newtonian and non-Newtonian kill fluids.
- Oil and gas reservoirs.
- Rigid temperature models.
- Fluid properties adjusted for pressure and temperature effects.
- Sonic flow considerations.
- Three multiphase models accounting for slip between phases.

Some of the current limitations and assumptions are

- Steady-state flow behavior with no transient effects.
- Only vertical wells.
- No leak-off to the formation.
- No compositional reservoirs.

- Only pseudosteady-state reservoirs.
- Only one formation flowing.
- No counter flow for off-bottom kills.
- No wellbore restrictions or chokes.

The simulator was modeled using correlations that have been widely used and validated by the industry. The results from the simulator were also compared to simple analytical solutions and published production data. In all cases, reasonable agreement was obtained.

Three empirical multiphase models included in the simulator for calculating the pressure gradient agreed under the conditions for which they were developed. These conditions correspond to typical production conditions, where the tubing-inner diameter is less than 5 in. and the separator pressure and temperature are greater than atmospheric conditions. In the case of a large nominal pipe inner diameter and the exit point set at atmospheric conditions, the multiphase models disagreed substantially. For a blowout in ultradeep water, where the exit conditions are at the mudline, no multiphase occurs, because the pressures in the well are always above the bubblepoint pressures. If the three models give different results, the most conservative result should be used.

Finally, the consequence on blowout intervention as drilling is moved into deeper and deeper water depths showed that the intervention requirements become more demanding as water depth increases. For ultradeep water this means that multiple relief wells may be necessary to bring a wild well under control.

### **6.1 Suggestion for Further Work**

The most important task for further work will be to test and validate the dynamic-kill simulator with actual field data. Not much field data has been published on

blowouts. A current project, in parallel with this study, aims to collect field data that can be used for this purpose.

One of the major limitations in this study is the assumption of steady-state behavior. During a dynamic-kill, the influx rates will change and transient effects are likely to occur. The few transient multiphase models that are available are all proprietary. A simplified approximate transient model for blowouts is available.<sup>8</sup> Such a model coupled with a full-scale composite reservoir model should be incorporated into the simulator.

Currently, most ultradeepwater wells are drilled vertically. As drilling in these water depths becomes more routine, more complex wellbore geometries will be common. The simulator should therefore be updated to include deviated wellbores.

## NOMENCLATURE

$A$	=	area, $L^2$
$B$	=	formation volume factor, $L^3/L^3$
$c$	=	compressibility, $L^2/m$
$C$	=	specific heat, $L^2/t^2T$
$d$	=	pipe diameter, $L$
$D$	=	turbulence coefficient
$D$	=	depth, $L$
DEA	=	Drilling Engineering Association
$e$	=	intrinsic specific energy, $L^2/t^2$
$f$	=	Moody friction factor
$f'$	=	Fanning friction factor
$g$	=	acceleration of gravity, $L/t^2$
GLR	=	gas/liquid ratio, $L^3/L^3$
GOM	=	Gulf of Mexico
$h$	=	convective film coefficient, $m/t^3T$
$h$	=	specific enthalpy, $L^2/t^2$
$h$	=	reservoir thickness, $L$
$H$	=	slip volume fraction, $L^3/L^3$
IPR	=	inflow performance relationship
$J$	=	unit conversion constant
JIP	=	joint industry project
$k$	=	thermal conductivity, $mL/t^3T$
$k$	=	ratio of specific heats
$k$	=	effective permeability, $L^2$
$K$	=	fluid consistency index, $m/Lt$
$L$	=	length, $L$
$m$	=	mass, $m$

$M$	=	molecular weight, m
MMS	=	Mineral Management Service
$n$	=	power-law flow behavioral index
$N$	=	dimensionless number
$P$	=	pressure, $m/Lt^2$
$q$	=	volumetric flow rate, $L^3/t$
$q$	=	heat flow rate, $mL^2/t^3$
$r$	=	radius, L
$R$	=	gas constant, $mL^2/t^2T$
$R$	=	solution gas-liquid ratio, $L^3/L^3$
$S$	=	slip velocity number
<i>size</i>	=	total number of elements
<i>SPP</i>	=	stand pipe pressure
$t$	=	time, t
<i>toler</i>	=	tolerance, %
$T$	=	temperature, T
$u$	=	specific internal energy, $L^2/t^2$
$U$	=	overall heat-transfer coefficient, $m/t^3T$
$v$	=	velocity, L/t
$v^*$	=	sonic velocity, L/t
$V$	=	volume, $L^3$
$w$	=	mass rate, $L^3/t$
$z$	=	z-factor of gas
$Z$	=	vertical distance, L
$\alpha$	=	formation thermal diffusivity, $L^2/t$
$\beta$	=	velocity coefficient, $L^{-1}$
$\Delta$	=	difference
$\varepsilon$	=	absolute pipe roughness, L
$\phi$	=	angle from vertical

$\gamma$	=	shear rate, 1/t
$\gamma$	=	specific gravity
$\eta$	=	Joule-Thompson coefficient, TLt <sup>2</sup> /m
$\lambda$	=	no-slip coefficient
$\mu$	=	viscosity, m/Lt
$\mu_p$	=	plastic viscosity, m/Lt
$\theta$	=	inclination from horizontal
$\rho$	=	density, m/L <sup>3</sup>
$\sigma$	=	surface tension, m/t <sup>2</sup>
$\tau$	=	shear stress, m/Lt <sup>2</sup>
$\tau_y$	=	yield point, m/Lt <sup>2</sup>

### Subscripts

$a$	=	actual
$a$	=	air
$a$	=	annulus
$acc$	=	acceleration
$AVG$	=	average
$b$	=	bubblepoint
$c$	=	calculated
$c$	=	casing
$c$	=	conversion constant
$cem$	=	cement
$D$	=	dimensionless
$e$	=	environment
$e$	=	estimated
$el$	=	elevation
$exit$	=	fluid exit conditions

<i>f</i>	=	fluid
<i>g</i>	=	gas
<i>h</i>	=	hydrostatic
<i>HT</i>	=	heat transfer
<i>i</i>	=	element number
<i>i</i>	=	inner
<i>L</i>	=	liquid
<i>m</i>	=	mixture
<i>M-R</i>	=	Metzner and Reed
<i>o</i>	=	oil
<i>o</i>	=	outer
<i>p</i>	=	pipe
<i>pc</i>	=	pseudocritical
<i>pr</i>	=	pseudoreduced
<i>r</i>	=	rough
<i>res</i>	=	reservoir
<i>R</i>	=	average reservoir
<i>R</i>	=	riser
<i>Re</i>	=	Reynold
<i>s</i>	=	smooth
<i>s</i>	=	superficial
<i>sc</i>	=	standard condition
<i>sw</i>	=	seawater
<i>t</i>	=	total
<i>w</i>	=	wall
<i>w</i>	=	wellbore
<i>wf</i>	=	flowing bottom-hole
<i>wh</i>	=	well head

$W$  = Weber

$\mu$  = viscosity

## REFERENCES

1. Lawrence, D.T and Anderson, R.N.: "Details Confirm Gulf of Mexico Deepwater as Significant Province," *Oil & Gas J.* (1993) **91**, No. 18, 93.
2. Choe, J. and Juvkam-Wold, H.C.: "Riserless Drilling: Concepts, Applications, Advantages, Disadvantages and Limitations," paper CADE/CAODC 97-140 presented at the 1997 CADE/CAODC Spring Drilling Conference, Calgary, 8-10 April.
3. Choe, J. and Juvkam-Wold, H.C.: "Riserless Drilling and Well Control for Deep Water Applications," *Proc. 1997 IADC International Deep Water Well Control Conference and Exhibition*, Houston, 15-16 September.
4. Gault, A.D.: "Riserless Drilling: Circumventing the Size/Cost Cycle in Deepwater," *Offshore* (1996) **56**, No. 5, 49-54.
5. Adams, N.: "JIP for Floating Vessel Blowout Control—Final Report," DEA-63, available from Mineral Management Service, Houston (1991).
6. Adams, N. and Young, R.: "Underground Blowouts: What You Need To Know," *World Oil* (January 2004).
7. Holand, P.: *Offshore Blowout Causes and Control*, Gulf Publishing Company, Houston (1997).
8. Grace, R.D.: *Blowout and Well Control Handbook*, Gulf Professional Publishing, Burlington, Massachusetts (2003).
9. Santos, O.L.A: "A Study on Blowouts in Ultra Deep Waters," paper SPE 69530 presented at the 2001 SPE Latin American and Caribbean Petroleum Engineering Conference, Buenos Aires, Argentina, 25-28 March.
10. Daneberger, E.P.: "Outer Continental Shelf Drilling Blowouts, 1971-1991," paper OTC 7248 presented at the 1993 Offshore Technology Conference, Houston, 3-6 May.
11. Skalle, P. and Podio, A.L.: "Trends Extracted From 1,200 Gulf Coast Blowouts During 1960-1996," *World Oil* (June 1998) 67-72.

12. Wylie, W.W. and Visram, A.S.: "Drilling Kick Statistics", paper SPE 19914 presented at the 1990 IADC/SPE Drilling Conference, Houston, February 27-March 2.
13. Watson, D., Brittenham, T., and Moore, P.L.: *Advanced Well Control*, Text Book Series, SPE, Richardson, Texas (2003).
14. Flak, L.H. and Wright, J. W.: "Part 11 Blowout Control: Response, Intervention and Management–Relief Wells," *World Oil* (December 1994), 59.
15. Blount, E.M. and Soeimah, E.: "Dynamic Kill: Controlling Wild Wells a New Way," *World Oil* (October 1981) 109-126.
16. Kouba, G.E., MacDougall, G.R., and Schumacher, B.W.: "Advancement in Dynamic Kill Calculations for Blowout Wells," paper SPE 22559 presented at the 1991 SPE Annual Technical Conference and Exhibition, Dallas, 6-9 October.
17. Rygg, O.B. and Gilhuus, T.: "Use of a Dynamic Two-Phase Pipe Flow Simulator in Blowout Kill Planning," paper SPE 20433 presented at the 1990 SPE Annual Technical Conference and Exhibition, New Orleans, 23-26 October.
18. Frigaard, I.A., Humphries, N.L., Rezmer-Cooper, I.M., and James, J.P.: "High Penetration Rates: Hazards and Well Control – A Case Study," paper SPE 37953 presented at the 1997 SPE/IADC Drilling Conference, Amsterdam, 4-6 March.
19. Flores-Avila, F.S., Smith, J.R., and Bourgoyne, A.T. Jr.: "New Dynamic Kill Procedure for Off-Bottom Blowout Wells Considering Counter-Current Flow of Kill Fluid," paper SPE 85292 presented at the 2003 SPE/IADC Middle East Drilling Technology Conference & Exhibition, Abu Dhabi, 20-22 October.
20. Schubert, J.J. and Weddle, C.E. III: "Development of a Blowout Intervention Method and Dynamic Kill Simulator for Blowouts Occurring in Ultra-Deepwater," JIP proposal available from Mineral Management Service, Houston (October 2000).
21. Liang, Y.D.: *Introduction to Java Programming with JBuilder 4*, second edition, Prentice Hall, Upper Saddle River, New Jersey (2002).
22. Knudsen, J.G. and Katz, D.L.: *Fluid Dynamic and Heat Transfer*, McGraw-Hill Book Co. Inc., New York (1958).

23. Bourgoyne, A.T. Jr., Cheenevert, M.E., Millheim, K.K., and Young F.S. Jr.: *Applied Drilling Engineering*, second printing, Texbook Series, SPE, Richardson, Texas (1991).
24. Brill, J.P. and Mukherjee, H.: *Multiphase Flow in Wells*, Henry L Doherty Series, SPE, Richardson, Texas (1999) 17.
25. Moody, L.F.: "Friction Factors for Pipe Flow," *Trans.*, ASME (1944) **66**, No. 8, 671.
26. Colebrook, C.F.: "Turbulent Flow in Pipes With Particular Reference to Transition Region Between the Smooth and Rough Pipe Laws," *J. Inst. Civil Eng.* (1939) **11**, 133.
27. Drew, T.B., Koo, E.C., and McAdams, W.H.: "The Friction Factors for Clean Round Pipes," *Trans.*, *AIChE J.* (1930) **28**, 56.
28. Jain, A.K.: "Accurate Explicit Equation for Friction Factor," *J. Hydraul. Div. ASCE* (May 1976) **102**, 674-677.
29. "Recommended Practice on the Rheology and Hydraulics of Oil-Well Drilling Fluids," *Recommended Practice 13D*, third edition, API, Washington, D.C. (1 June 1995).
30. Dodge, D.W. and Metzner, A.B.: "Turbulent Flow of Non-Newtonian Systems," *AIChE J.* (1959) **5**, 189.
31. Govier, G.W. and Aziz, K.: *The Flow of Complex Mixtures in Pipes*, Van Nostrand Reinhold Co., New York (1972).
32. Beggs, H.D. and Brill, J.P.: "A Study of Two-Phase Flow in Inclined Pipes," *JPT* (May 1973) 607; *Trans.*, AIME, **255**.
33. Hagendorn, A.R. and Brown, K.E.: "Experimental Study of Pressure Gradients Occurring During Continuous Two-Phase Flow in Small Diameter Vertical Conduits," *JPT* (April 1965) 475; *Trans.*, AIME, **234**.
34. Duns, H. Jr. and Ros, N.C.J.: "Vertical Flow of Gas and Liquid Mixtures in Wells," *Proc.*, Sixth World Pet. Cong., Tokyo (1963) 451.
35. Beggs, H.D.: *Production Optimization Using NODAL<sup>tm</sup> Analysis*, OGCI Publications, Tulsa, Oklahoma (2000).

36. Langlinais, A.T., Bourgoyne, A.T. Jr., and Holden, W.R.: "Frictional Pressure Losses for the Flow of Drilling Mud and Mud/Gas Mixtures," paper SPE 11993 presented at the 1983 SPE Annual Technical Conference and Exhibition, San Francisco, California, 5-8 October.
37. Wallis, G.B.: *One-Dimensional Two-Phase Flow*, McGraw Hill Book Co. Inc., New York (1969).
38. Bird, R.B., Stewart, W.E., and Lightfoot, E.N.: *Transport Phenomena*, John Wiley & Sons, New York (1960).
39. Hasan, A.R. and Kabir, C.S.: "Heat Transfer During Two-Phase Flow in Wellbores: Part I – Formation Temperatures," paper SPE 22866 presented at the 1991 SPE Annual Technical Conference and Exhibition, Dallas, 6-9 October.
40. Ramey, H. J. Jr.: "Wellbore Heat Transmission." *JPT* (April 1962) **14**, 427-435.
41. Shiu, K.C. and Beggs, H.D.: "Predicting Temperatures in Flowing Wells," *J. Energy Res. Tech.* (March 1980) **102**, 2.
42. Darcy, H.: *Les Fontaines Publiques de la Ville de Dijon*, Victor Dalmont, Paris (1856) 590-594.
43. Forchheimer, P.: "Wasserbewegung durch Boden," *Zeitschrift der Verein Deutscher Ingenieure* (1901) **45**, 1731.
44. Piper, L.D., McCain, W.D. Jr., and Corredor, J.H.: "Compressibility Factors for Naturally Occurring Petroleum Gases," paper SPE 26668 presented at the 1993 SPE Annual Technical Conference and Exhibition, Houston, 3-6 October
45. Dranchuk, P.M. and Abou-Kassem, J.H.: "Calculation of Z Factors for Natural Gases Using Equation of State," *J. Cdn. Pet. Tech.* (July-September 1975) 34-36.
46. Lee, A.L., Gonzalez, M.H., and Eakin, B.E.: "The Viscosity of Natural Gasses," *JPT* (Aug 1966) 997-1000, *Trans.*, AIME, **237**.
47. Vasquez, M. and Beggs, H.D.: "Correlations for Fluid Physical Property Prediction," *JPT* (June 1980) 968-970.
48. Standing, M.B.: "A Pressure-Volume-Temperature Correlation for Mixtures of California Oils and Gasses," *API Drill. & Prod. Prac.* (1947) 275-287.

49. Egbogah, E.O.: "An Improved Temperature-Viscosity Correlation for Crude Oil Systems," paper 83-34-32 presented at the 1983 Annual Technical Meeting of the Petroleum Society of CIM, Banff, Alberta, May 10-13, 1983.
50. Beggs, H.D. and Robinson, J.R.: "Estimating the Viscosity of Crude Oil Systems," *JPT* (September 1975) 1140-1141.
51. McCain, W.D. Jr.: *The Properties of Petroleum Fluids*, Second Edition, PennWell Publishing Co., Tulsa, Oklahoma (1988).
52. Gilbert, W.E.: "Flowing and Gas-Lift Well Performance," *API Drill. & Prod. Prac.* (1954) 143.
53. Payne, G.A., Palmer, C.M., Brill, J.P., and Beggs, H.D.: "Evaluation of Inclined-Pipe Two-Phase Liquid Holdup and Pressure-Loss Correlations Using Experimental Data," *JPT* (September 1979) 1198; *Trans.*, AIME, **267**.
54. Ayres, F. Jr. and Mendelson, E.: *Calculus*, Fourth Edition, McGraw-Hill, New York (1999).

## APPENDIX A

### TWO-PHASE FLOW CORRELATIONS

To keep the equations consistent with appropriate unit-conversion constants, the following variables and sets of units are used in this appendix.

$d$	=	pipe inner diameter, in.
$\rho_L$	=	liquid density, lbm/ft <sup>3</sup> .
$\rho_g$	=	gas density, lbm/ft <sup>3</sup> .
$\sigma_L$	=	liquid shear rate, dynes/cm.
$\mu_g$	=	gas viscosity, cp.
$\mu_L$	=	liquid viscosity, cp.
$\varepsilon$	=	pipe roughness, ft.
$v_{SL}$	=	superficial liquid velocity, ft/s.
$v_{Sg}$	=	superficial gas velocity, ft/s.
$v_m$	=	mixture velocity, ft/s.
$dp/dZ$	=	pressure gradient, psi/ft.

#### A.1 Hagendorn and Brown

The step-by-step procedure to calculate the pressure gradient using Hagendorn and Brown<sup>33</sup> method is:

1. Calculate the dimensionless numbers:

$$N_{Lv} = 1.938 v_{SL} \left( \frac{\rho_L}{\sigma} \right)^{0.25}, \dots\dots\dots (A.1)$$

$$N_{gv} = 1.938v_{sg} \left( \frac{\rho_L}{\sigma} \right)^{0.25}, \dots\dots\dots (A.2)$$

$$N_d = 120.872d \left( \frac{\rho_L}{\sigma} \right)^{0.5}, \dots\dots\dots (A.3)$$

and

$$N_L = 0.15726\mu_L \left( \frac{1.0}{\rho_L \sigma_L^3} \right)^{0.25} \dots\dots\dots (A.4)$$

2. Find the viscosity number coefficient,  $N_L C$ , from **Fig A.1**.

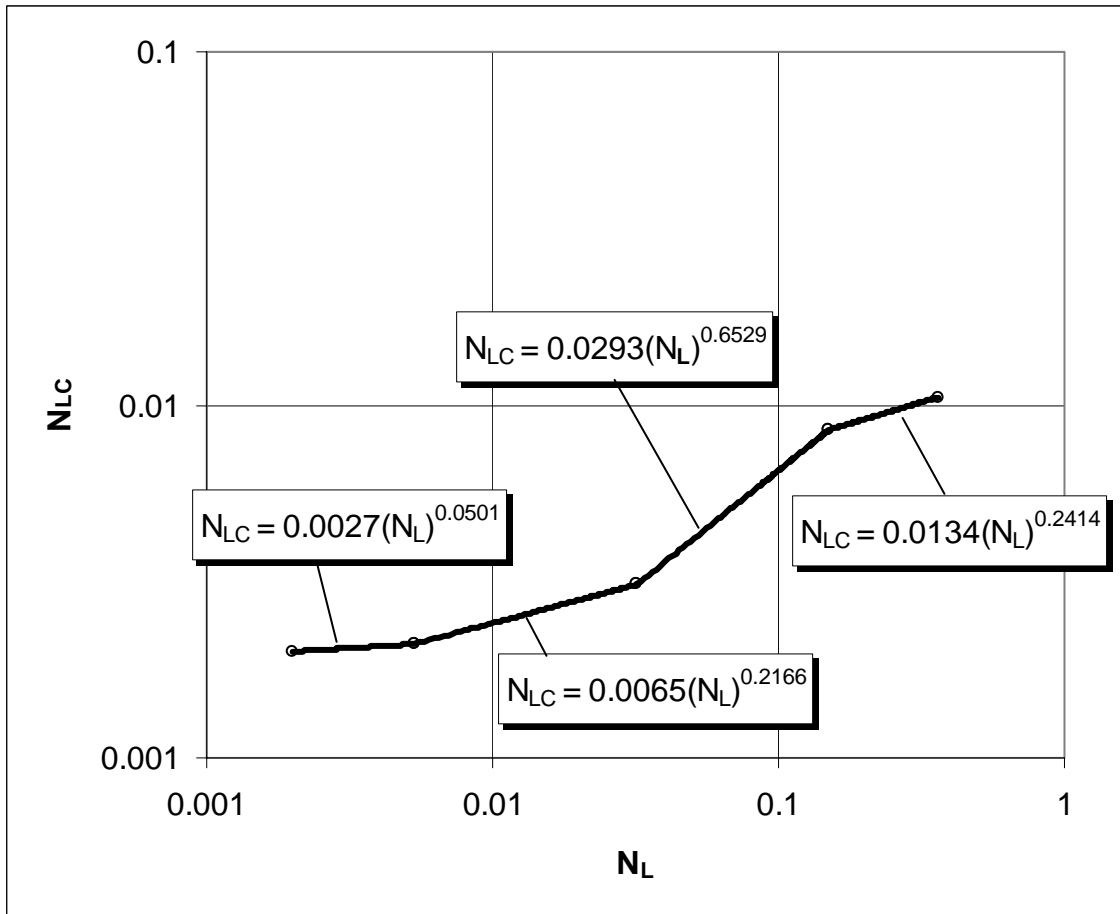


**Fig. A.1—Hagedorn and Brown correlation for  $N_{LC}$ .**

3. Calculate  $x_I$ :

$$x_I = \left( \frac{N_{Lv}}{N_{gv}^{0.575}} \right) \left( \frac{N_L C}{N_d} \right) \left( \frac{P}{14.7} \right)^{0.1} \cdot \dots \quad (\text{A.5})$$

4. Find the holdup factor  $H_L/\psi$  from **Fig. A.2**.

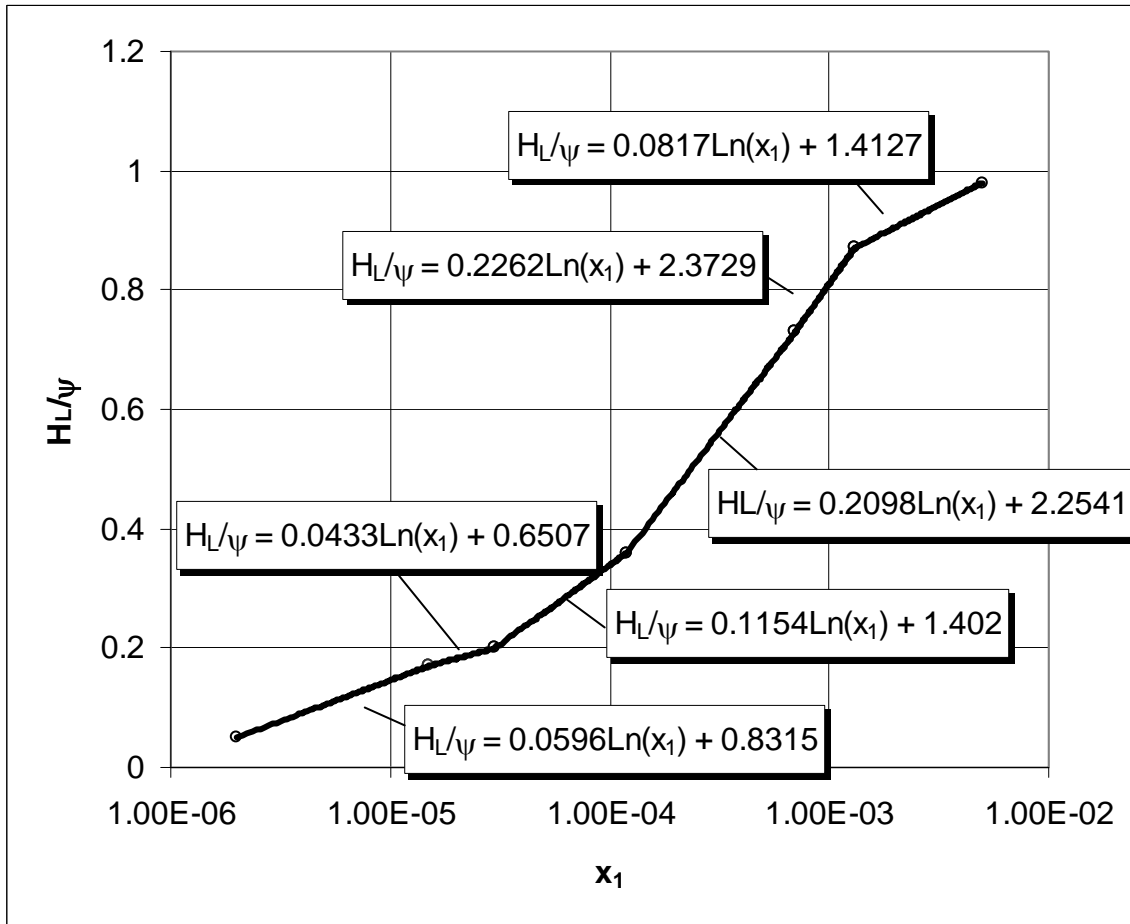


**Fig. A.2—Hagendorn and Brown correlation for  $H_L/\psi$ .**

5. Calculate  $x_2$ :

$$x_2 = \frac{N_{gv} N_L^{0.380}}{N_d^{2.14}} \dots\dots\dots (A.6)$$

6. Find  $\psi$  from **Fig. A.3**.

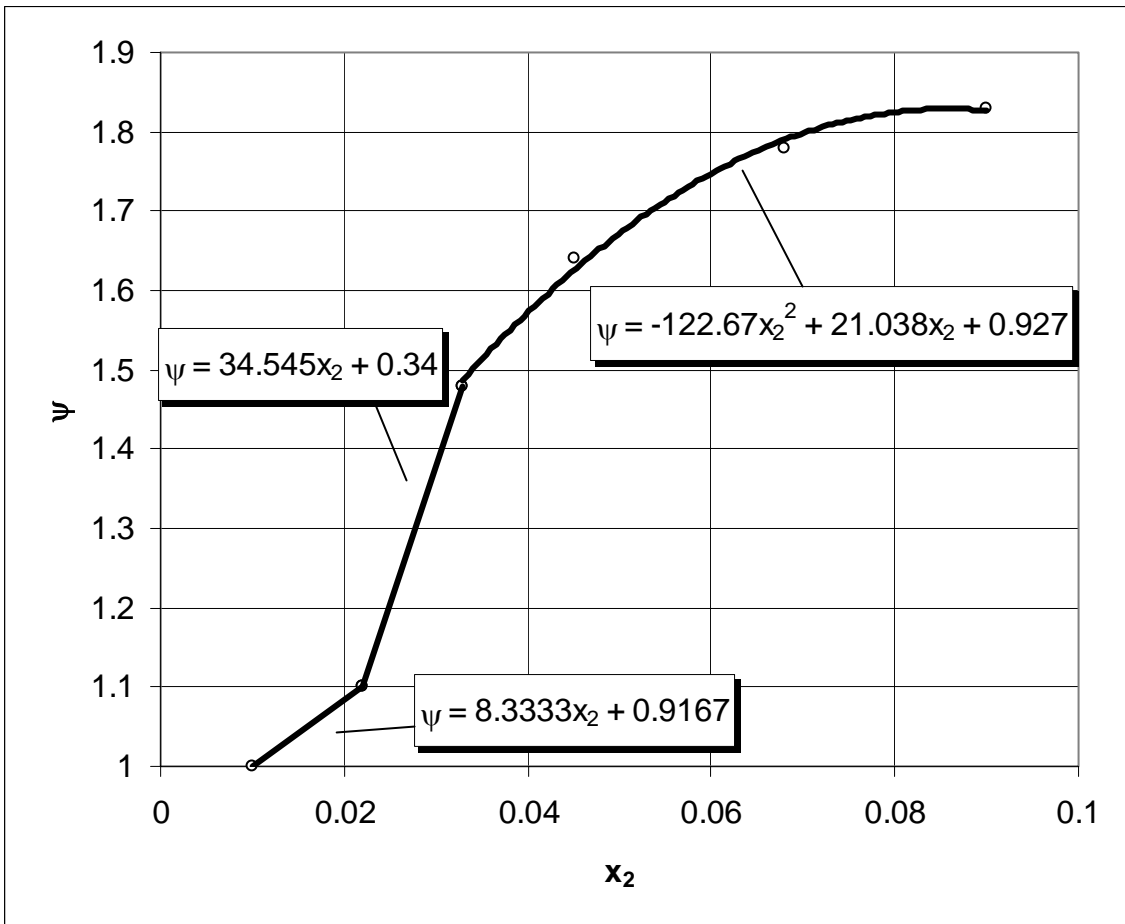


Fig. A.3—Hagendorn and Brown correlation for  $\psi$

7. Calculate the liquid holdup,  $H_L$ , and check that  $H_L$  is larger than  $\lambda_L$ :

$$H_L = \psi \left( \frac{H_L}{\psi} \right) \dots\dots\dots (A.7)$$

Check the validity of  $H_L$ : If  $H_L < \lambda_L$ , then set  $H_L = \lambda_L$ .

8. Calculate  $\rho_s$  from Eq. 1.32,  $\rho_n$  from Eq. 1.33 and  $\mu_s$  from Eq. 1.35.
9. Calculate Reynolds number,  $N_{Re}$ , and the friction factor from Eq. 1.13 if  $N_{Re} > 2,100$  and 1.12 if  $N_{Re} \leq 2100$ .

$$N_{Re} = \frac{1,488\rho_n v_m d}{\mu_s} \dots\dots\dots (A.8)$$

10. Calculate the pressure gradient:

$$\frac{dp}{dZ} = \frac{f\rho_n^2 v_m^2}{2g_c \rho_s d} + \frac{g}{g_c} \rho_s \cos \theta + \frac{\rho_s \Delta(v_m^2)}{2dZ} \dots\dots\dots (A.9)$$

Ignoring acceleration, for a vertical well in field units Eq. A.9 becomes

$$\frac{dp}{dZ} = \frac{f\rho_n^2 v_m^2}{9266\rho_s d} + \frac{\rho_s}{144} \dots\dots\dots (A.10)$$

## A.2 Beggs and Brill

The step-by-step procedure to calculate the pressure gradient using the Beggs and Brill<sup>32</sup> method follows:

1. Calculate the flow regime:

$$N_{FR} = \frac{v_m^2}{32.2d} \dots\dots\dots (A.11)$$

$$L_1 = 316\lambda_L^{0.302} \dots\dots\dots (A.12)$$

$$L_2 = 0.0009252\lambda_L^{-2.4684}, \dots\dots\dots (A.13)$$

$$L_3 = 0.10\lambda_L^{-1.4516}, \dots\dots\dots (A.14)$$

$$L_4 = 0.50\lambda_L^{-6.738}, \dots\dots\dots (A.15)$$

The limits for each flow regime are as follows:

Segregated:

$$\lambda_L < 0.01 \text{ and } N_{FR} < L_1. \text{ Or } \lambda_L \geq 0.02 \text{ and } N_{FR} < L_2$$

Transition:

$$\lambda_L \geq 0.01 \text{ and } L_2 < N_{FR} \leq L_3.$$

Intermittent:

$$0.01 \leq \lambda_L < 0.4 \text{ and } L_3 < N_{FR} \leq L_1. \text{ Or } \lambda_L \geq 0.4 \text{ and } L_3 < N_{FR} \leq L_4.$$

Distributed:

$$\lambda_L < 0.4 \text{ and } N_{FR} \geq L_1. \text{ Or } \lambda_L \geq 0.4 \text{ and } N_{FR} > L_4.$$

2. Calculate the liquid holdup,  $H_L$ :

For horizontal flow the liquid hold-up is

$$H_{L(0)} = \frac{a\lambda_L^b}{N_{FR}^c}, \dots\dots\dots (A.16)$$

where  $a$ ,  $b$  and  $c$  is determined from **Table A.1**.

**Table A.1 – Horizontal Flow-Pattern Coefficients, Beggs and Brill Method**

Flow Pattern	a	b	c
Segregated	0.98	0.4846	0.0868
Intermittent	0.845	0.5351	0.0173
Distributed	1.065	0.5824	0.0609

The correction factor,  $\psi$ , for pipe inclination is

$$\psi = 1 + C[\sin(1.8\phi) - 0.333\sin^3(1.8\phi)], \dots\dots\dots (A.17)$$

where  $\phi$  is the pipe inclination from horizontal, and  $C$  is given by

$$C = (1 - \lambda_L) \ln[(d)(\lambda_L)^e (N_{LV})^f (N_{FR})^g], \dots\dots\dots (A.18)$$

where  $d$ ,  $e$ ,  $f$ , and  $g$  are determined from **Table 1.2**.

The liquid holdup for any inclination is then

$$H_{L(\phi)} = \psi H_{L(0)}, \dots\dots\dots (A.19)$$

**Table A.2 – Deviated Flow-Pattern Coefficients for Beggs and Brill Method**

Flow Pattern	d	e	f	g
Segregated uphill	0.011	-3.768	3.539	-1.614
Intermittent uphill	2.96	0.305	-0.4473	0.0978
Distributed uphill	No Correction	C = 0, $\psi = 1$		$H_L \neq f(\phi)$
All flow patterns downhill	4.7	-0.3692	0.1244	-0.5056

If the flow regime is transition, the liquid holdup must be calculated using the liquid holdup estimated from segregated and intermittent flow (Eq. A.20).

$$H_{L(\text{transition})} = AH_{L(\text{segregated})} + BH_{L(\text{intermittent})}, \dots\dots\dots (A.20)$$

where

$$A = \frac{L_3 - N_{FR}}{L_3 - L_2} \dots\dots\dots (A.21)$$

and

$$B = 1 - A \dots\dots\dots (A.22)$$

Payne *et al.*<sup>53</sup> suggested a correction for the liquid holdup:

$$H_{L(\phi)} = 0.924H_{L(\phi)}; \text{ if } \phi > 0 \dots\dots\dots (A.23)$$

and

$$H_{L(\phi)} = 0.685H_{L(\phi)}; \text{ if } \phi < 0. \dots\dots\dots (\text{A.24})$$

Similarly to the Hagendorn and Brown method, the validity of the liquid holdup,  $H_L$ , must be checked. If  $H_L < \lambda_L$  then set  $H_L = \lambda_L$ .

3. Calculate  $\rho_s$  from Eq. 1.32,  $\rho_n$  from Eq. 1.33 and  $\mu_n$  from Eq. 1.36.
4. Calculate Reynolds number,  $N_{Re}$ , and the friction factor:

$$N_{Re} = \frac{1,488\rho_n v_m d}{\mu_n} \dots\dots\dots (\text{A.25})$$

The two-phase friction factor according to Beggs and Brill is calculated as

$$f_{tp} = f_n \left( \frac{f_{tp}}{f_n} \right), \dots\dots\dots (\text{A.26})$$

where  $f_n$  is the Moody friction factor calculated using Eq. 1.13 if  $N_{Re} > 2,100$  and 1.12 if  $N_{Re} \leq 2100$ . The ratio of friction factors in Eq. A.26 is calculated as

$$\left( \frac{f_{tp}}{f_n} \right) = e^s, \dots\dots\dots (\text{A.27})$$

where

$$s = \frac{\ln(y)}{-0.0523 + 3.182\ln(y) - 0.8725[\ln(y)]^2 + 0.01853[\ln(y)]^4}, \dots\dots\dots (\text{A.28})$$

and

$$y = \frac{\lambda_L}{[H_{L(\phi)}]^2} \dots\dots\dots (A.29)$$

Because of discontinuities in Eq. A.28, *s* must be calculated as

$$s = \ln(2.2y - 1.2), \dots\dots\dots (A.30)$$

when  $1 < y < 1.2$ . Also, *s* should be 0 for  $y = 1.0$  to ensure the correlation degenerates to single-phase liquid flow.

5. Calculate the pressure gradient:

$$\frac{dp}{dZ} = \frac{f_{tp} \rho_n v_m^2}{2g_c d} + \frac{g}{g_c} \rho_s \sin \phi + \left( \frac{\rho_s v_m v_{sg}}{g_c p} \right) \frac{dp}{dZ} \dots\dots\dots (A.31)$$

For a vertical well in field units, Eq. A.31 becomes

$$\frac{dp}{dZ} = \frac{f_{tp} \rho_n v_m^2}{9266d} + \frac{\rho_s}{144} + \left( \frac{\rho_s v_m v_{sg}}{2318.5(p_{i+1} + p_i)} \right) \left( \frac{p_{i+1} - p_i}{\Delta Z} \right) \dots\dots\dots (A.32)$$

The pressure gradient is found between two elements with pressure of  $p_{i+1}$  and  $p_i$  respectively.

**A.3 Duns and Ros**

The step-by-step procedure to calculate the pressure gradient using the Duns and Ros<sup>34</sup> method follows:

1. As for Hagedorn and Brown method, calculate the dimensionless numbers given in Eq. A.1, A.2, A.3 and A.4
2. Calculate the flow regime boundaries and the flow pattern:

Bubble/Slug Boundary

$$N_{gv_{B/S}} = L_1 + L_2 \cdot N_{Lv}, \dots\dots\dots (A.33)$$

where  $L_1$  and  $L_2$  is obtained from **Fig. A.4**.

Slug/Transition Boundary

$$N_{gv_{S/Tr}} = 50 + 36N_{Lv} \cdot \dots\dots\dots (A.34)$$

Transition/Mist Boundary

$$N_{gv_{Tr/M}} = 75 + 84N_{Lv}^{0.75} \cdot \dots\dots\dots (A.35)$$

Flow pattern is then:

- Bubble Flow:  $N_{gv} \leq N_{gv_{B/S}}$ .
- Slug Flow:  $N_{gv_{B/S}} < N_{gv} \leq N_{gv_{S/Tr}}$ .
- Transition Flow:  $N_{gv_{S/Tr}} < N_{gv} \leq N_{gv_{Tr/M}}$ .
- Mist Flow:  $N_{gv_{Tr/M}} < N_{gv}$ .

3. Calculate liquid holdup:

For bubble flow the dimensionless slip-velocity number is

$$S = F_1 + F_2 \cdot N_{Lv} + F'_3 \left( \frac{N_{gv}}{1 + N_{Lv}} \right)^2, \dots\dots\dots (A.36)$$

where  $F'_3$  is calculated as

$$F'_3 = F_3 - \frac{F_4}{N_d} \dots\dots\dots (A.37)$$

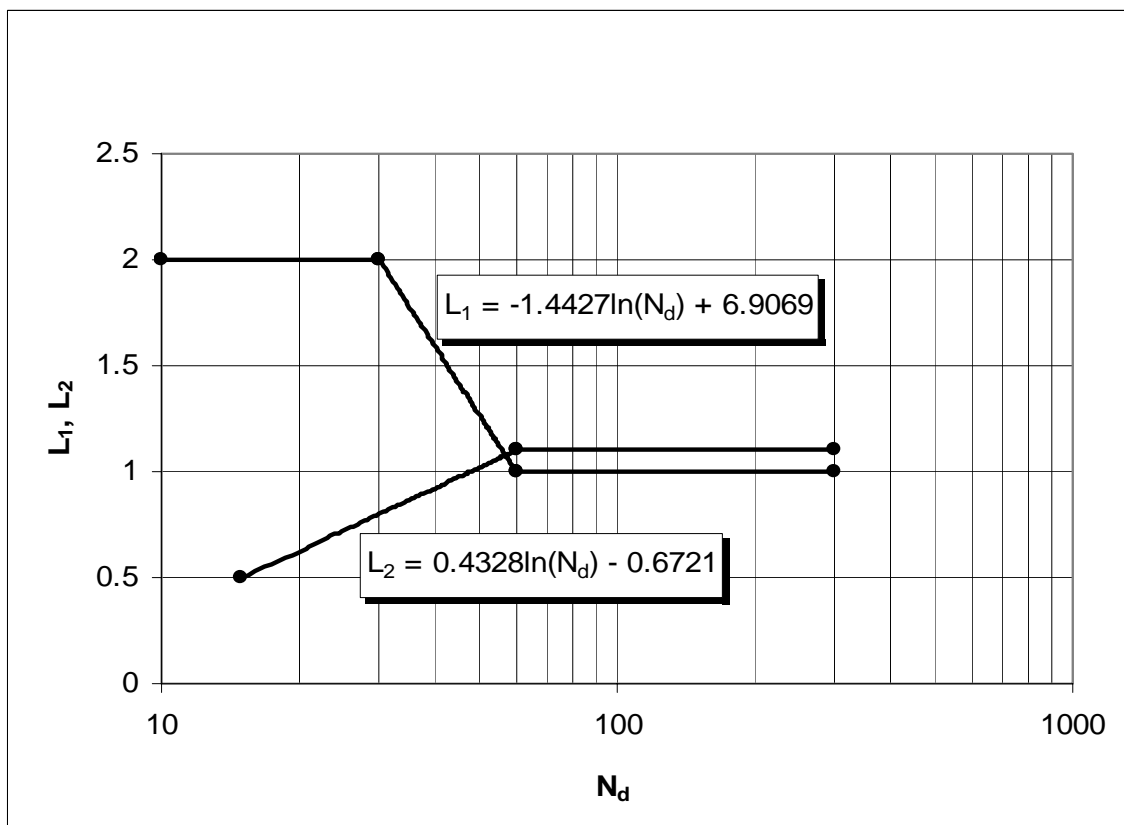


**Fig. A.4—Duns and Ros bubble/slug transition parameters.**

$F_1$  is given in **Fig. A.5**,  $F_2$  is given in **Fig. A.6**,  $F_3$  is given in **Fig. A.7** and  $F_4$  is given in **Fig. A.8**.

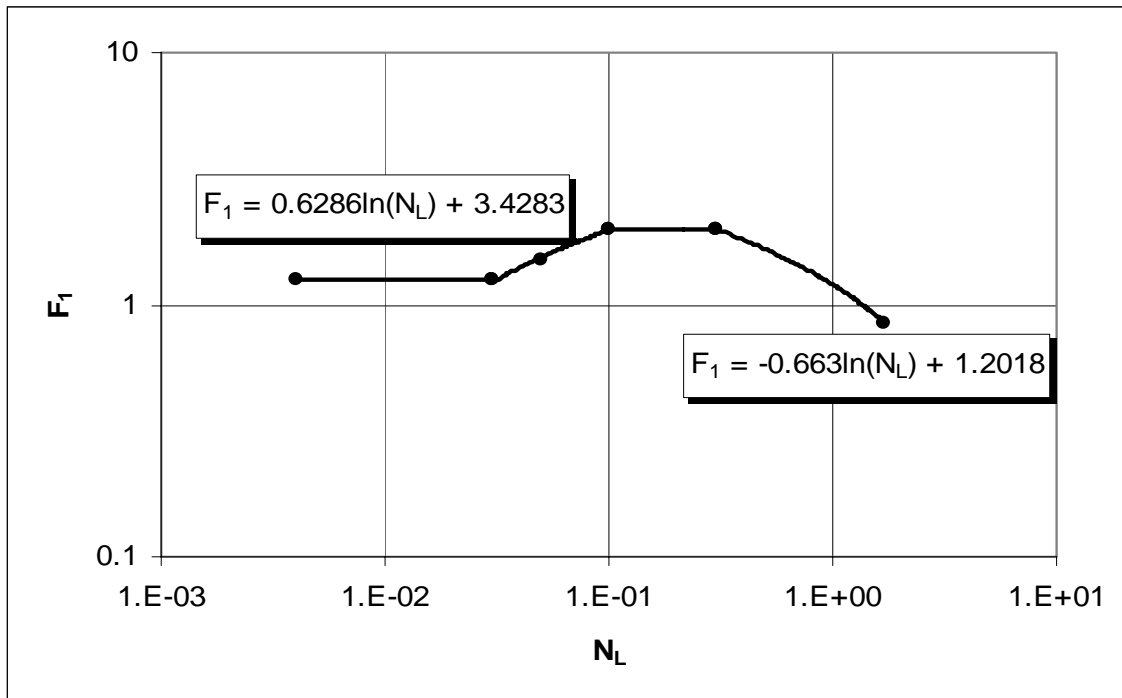


Fig. A.5—Duns and Ros bubble-flow, slip-velocity parameter  $F_1$ .

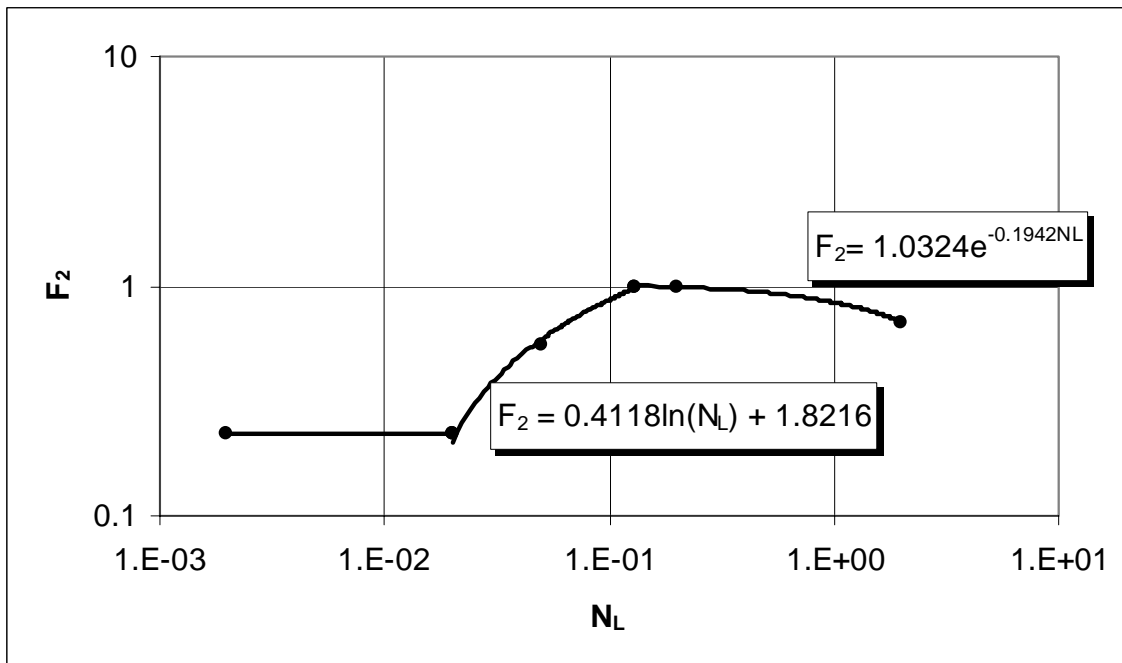


Fig. A.6—Duns and Ros bubble-flow, slip-velocity parameter  $F_2$ .

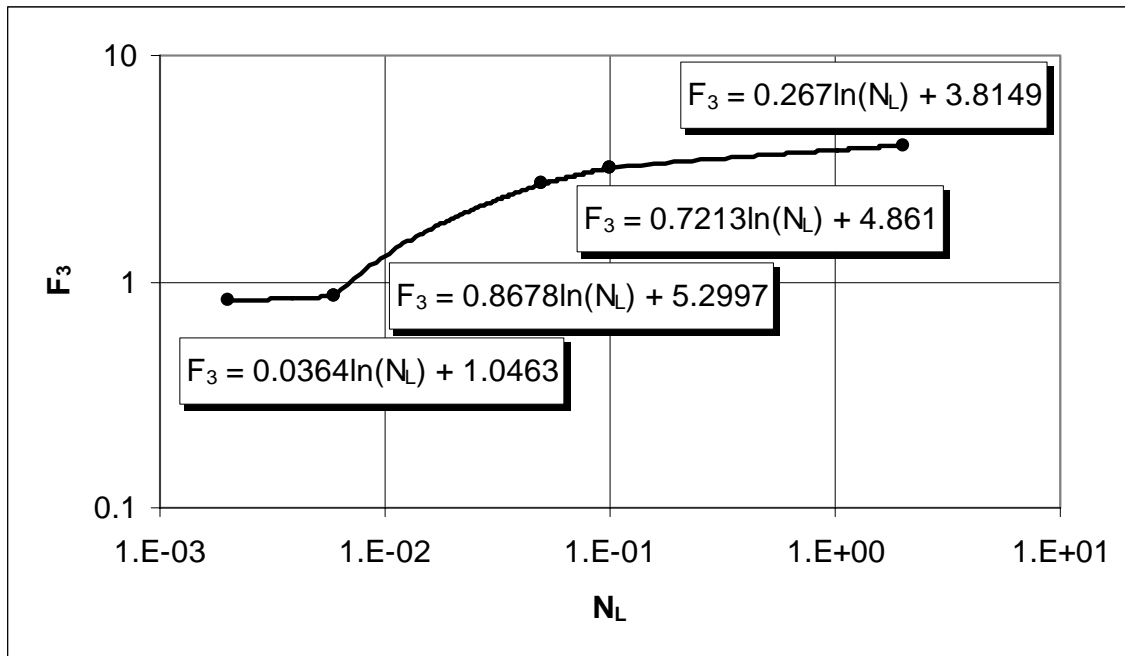


Fig. A.7—Duns and Ros bubble-flow, slip-velocity parameter  $F_3$ .

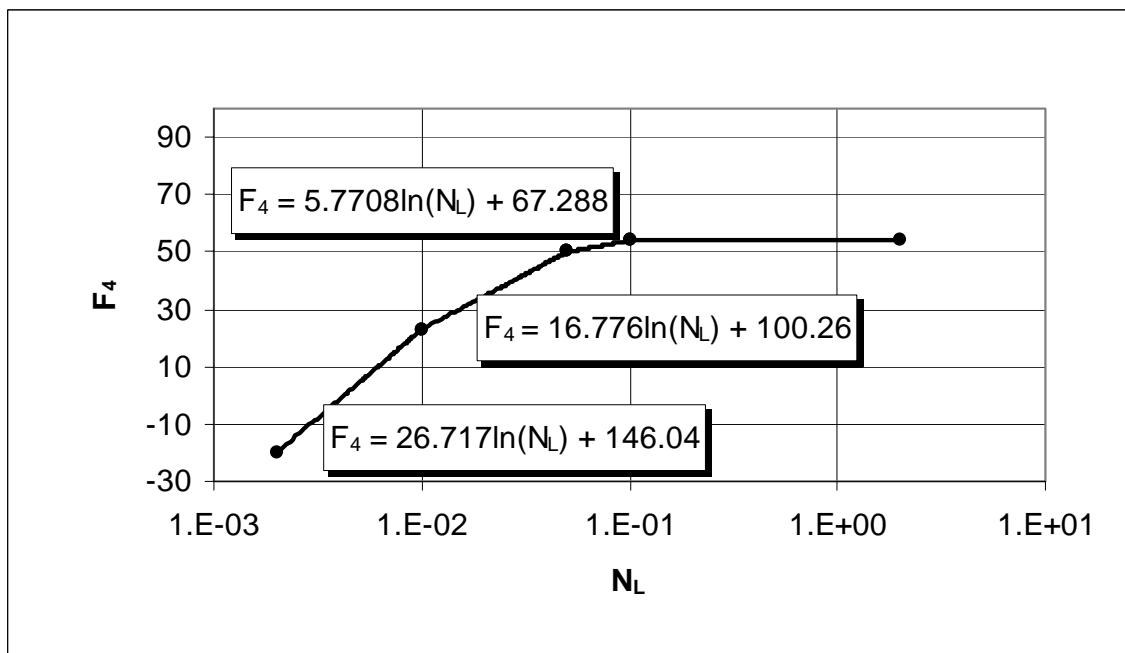


Fig. A.8 – Duns and Ros bubble-flow, slip-velocity parameter  $F_4$ .

For slug flow the dimensionless slip-velocity number is

$$S = (1 + F_5) \frac{(N_{gv})^{0.982} + F'_6}{(1 + F_7 \cdot N_{Lv})^2}, \dots\dots\dots (A.38)$$

where

$$F'_6 = F_6 + 0.029 \cdot N_d \dots\dots\dots (A.39)$$

$F_5$  is given in **Fig. A.9**,  $F_6$  is given in **Fig. A.10** and  $F_7$  is given in **Fig A.11**.

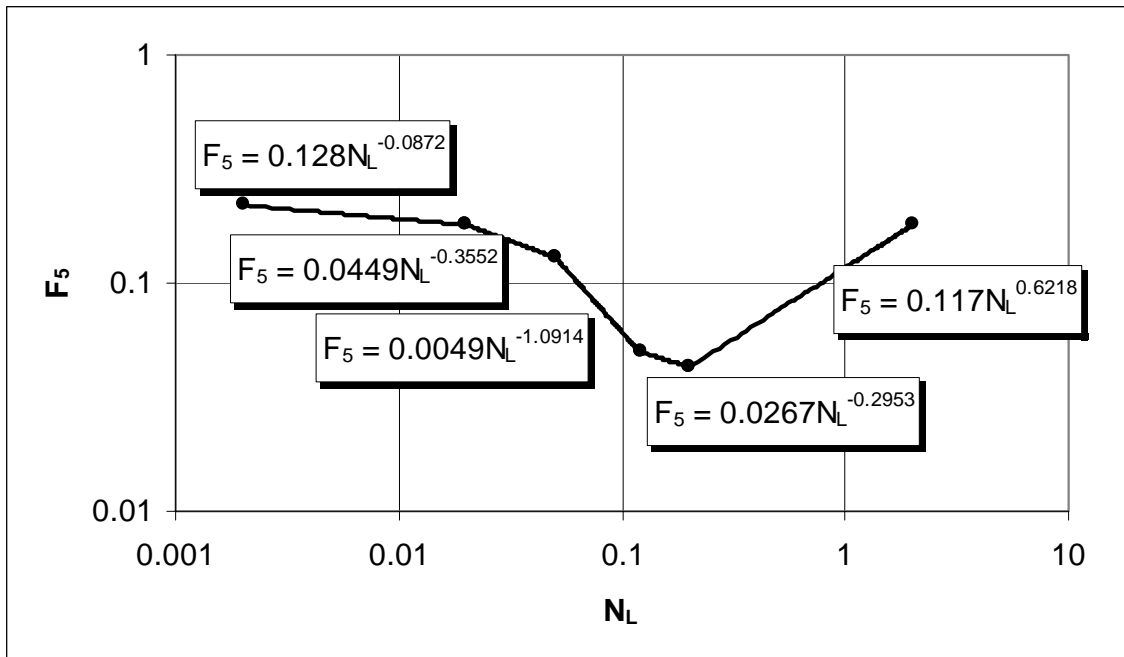


**Fig. A.9—Duns and Ros slug-flow, slip-velocity parameter  $F_5$ .**

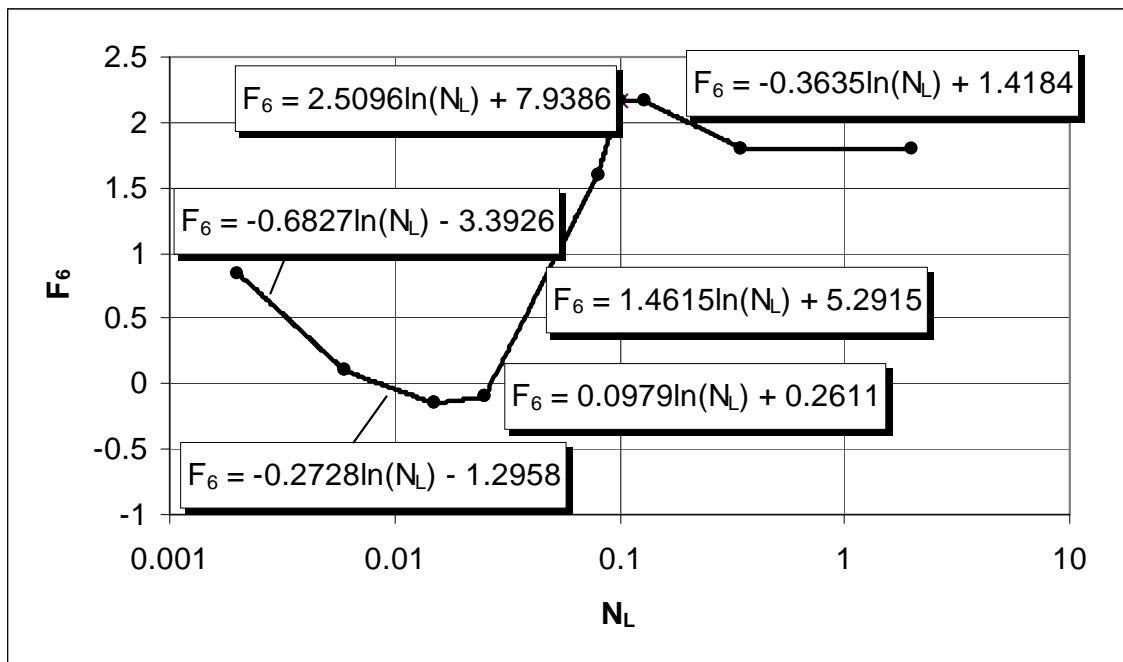


Fig. A.10—Duns and Ros slug-flow, slip-velocity parameter  $F_6$ .

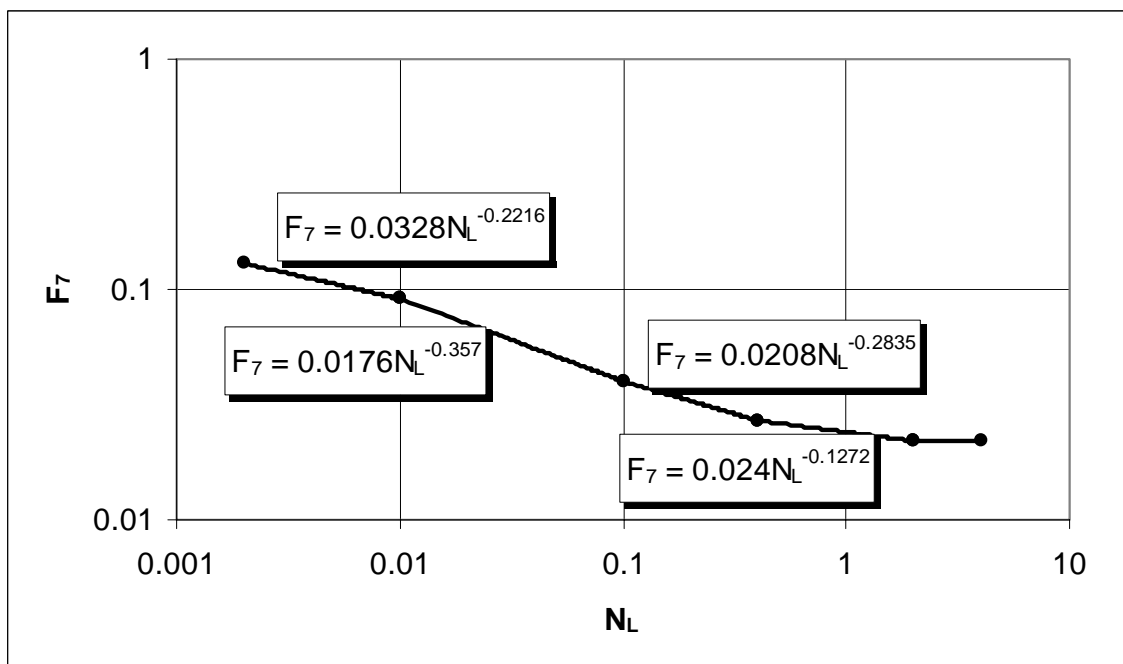


Fig. A.11—Duns and Ros slug-flow, slip-velocity parameter  $F_7$ .

For both slug and bubble flow, the liquid holdup can be calculated as

$$H_L = \frac{v_s - v_m + \sqrt{(v_m - v_s)^2 + 4 \cdot v_s \cdot v_{SL}}}{2 \cdot v_s}, \dots\dots\dots (A.40)$$

where the slip velocity is

$$v_s = \frac{S}{1.938 \left( \frac{\rho_L}{\sigma_L} \right)^{0.25}} \dots\dots\dots (A.41)$$

For mist flow

$$S = 0, \dots\dots\dots (A.42)$$

$$v_s = 0, \dots\dots\dots (A.43)$$

and

$$H_L = \lambda_L \dots\dots\dots (A.44)$$

#### 4. Calculate Reynolds number and the friction factor

For bubble flow:

$$N_{ReL} = \frac{\rho_L v_{sL} d}{\mu_L} \dots\dots\dots (A.45)$$

The friction factor is then calculated as

$$f = f_1 \frac{f_2}{f_3}, \dots\dots\dots (A.46)$$

where  $f_1$  is the Moody friction factor calculated using the Reynolds number from Eq. A.45.  $f_2$  is given in **Fig. A.12** where the x-axis is

$$x = \frac{f_1 v_{sg} N_d^{2/3}}{v_{SL}} \dots\dots\dots (A.47)$$

Finally,  $f_3$  in Eq. 4.46 is calculated as

$$f_3 = 1 + \frac{f_1}{4} \sqrt{\frac{v_{sg}}{50v_{SL}}} \dots\dots\dots (A.48)$$

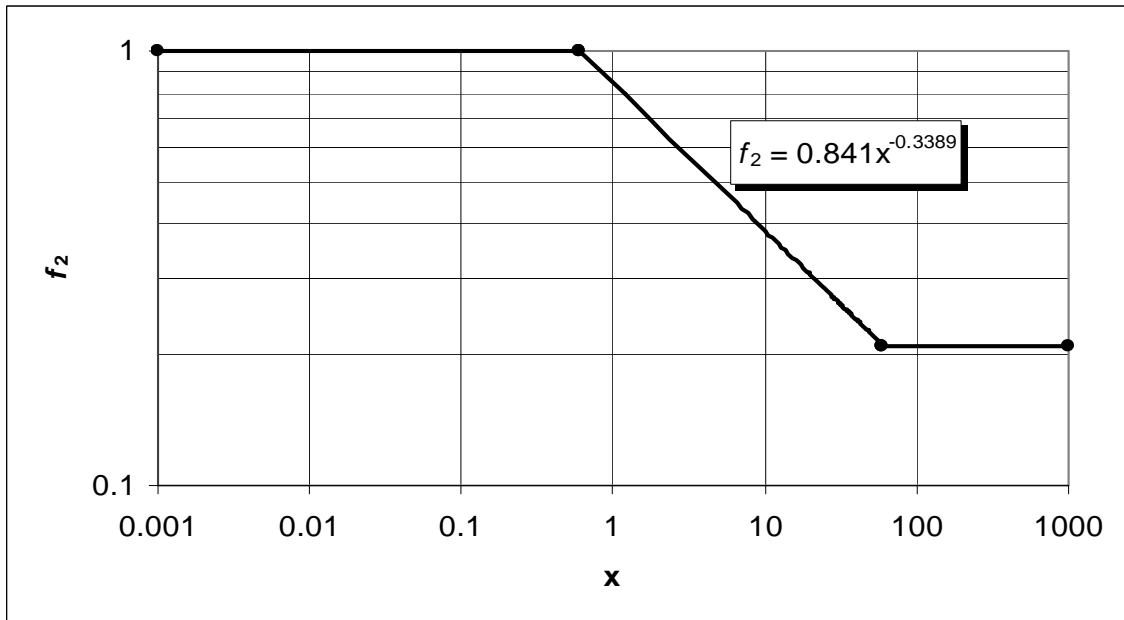


**Fig. A.12 – Duns and Ros bubble-flow, friction-factor parameter  $f_2$ .**

For slug flow the friction factor is calculated the same way as for bubble flow.

For mist flow Reynolds number is

$$N_{Re_g} = \frac{\rho_g v_{sg} d}{\mu_g} \dots\dots\dots (A.49)$$

Before the friction factor can be calculated the wall roughness must be corrected for the liquid film that covers the pipe. This is accomplished by calculating the Weber number as

$$N_{We} = \frac{453.59 \rho_g v_{sg}^2 \varepsilon}{\sigma_L} \dots\dots\dots (A.50)$$

and a dimensionless number with viscosity as

$$N_{\mu} = \frac{2.04817 \times 10^{-4} \mu_L^2}{\rho_L \sigma_L \varepsilon} \dots\dots\dots (A.51)$$

The ratio of pipe roughness to pipe diameter can be calculated as

$$\frac{\varepsilon}{d} = \frac{1.6534 \cdot 10^{-3} \sigma_L}{\rho_g \cdot v_{sg}^2 \cdot d}; \text{ if } N_{We} N_{\mu} \leq 0.05, \dots\dots\dots (A.52)$$

and

$$\frac{\varepsilon}{d} = \frac{9.3713 \cdot 10^{-3} \sigma_L}{\rho_g \cdot v_{sg}^2 \cdot d} (N_{We} N_{\mu})^{0.302}; \text{ if } N_{We} N_{\mu} > 0.05. \dots\dots\dots (A.53)$$

The friction factor for mist flow can now be calculated as

$$f = 4 \left( \frac{1}{4 \cdot \log_{10} \left( 0.027 \frac{\varepsilon}{d} \right)} + 0.067 \left( \frac{\varepsilon}{d} \right)^{1.73} \right); \text{ if } \frac{\varepsilon}{d} > 0.05. \dots\dots\dots (A.54)$$

If  $\frac{\varepsilon}{d} \leq 0.05$ , then the friction factor can be calculated as the normal Moody friction factor.

5. Calculate the pressure gradient

$$\left( \frac{dp}{dZ} \right)_t = \left( \frac{dp}{dZ} \right)_f + \left( \frac{dp}{dZ} \right)_{el} + \left( \frac{dp}{dZ} \right)_{acc} \dots\dots\dots (A.55)$$

For bubble and slug flow, Duns and Ros assumed that acceleration could be ignored. The friction and hydrostatic term for bubble and slug flow is

$$\left( \frac{dp}{dz} \right)_f = \frac{f \rho_L v_{sL} v_m}{9266d}, \dots\dots\dots (A.56)$$

and

$$\left( \frac{dp}{dz} \right)_{el} = \frac{\rho_s}{144} = \frac{[\rho_L H_L + \rho_g (1 - H_L)]}{144} \dots\dots\dots (A.57)$$

The pressure-gradient terms for mist flow are

$$\left(\frac{dp}{dZ}\right)_f = \frac{f\rho_g v_{sg}^2}{9266d}, \dots\dots\dots (A.58)$$

$$\left(\frac{dp}{dZ}\right)_{el} = \frac{\rho_s}{144}, \dots\dots\dots (A.59)$$

and

$$\left(\frac{dp}{dZ}\right)_{acc} = \left(\frac{\rho_s v_m v_{sg}}{2318.5(p_{i+1} + p_i)}\right) \left(\frac{p_{i+1} - p_i}{\Delta Z}\right). \dots\dots\dots (A.60)$$

The pressure gradient for transition flow is calculated by interpolating between the slug and mist flow pattern as

$$\left(\frac{dp}{dZ}\right)_t = A \left(\frac{dp}{dZ}\right)_{slug} + (1 - A) \left(\frac{dp}{dZ}\right)_{mist}, \dots\dots\dots (A.61)$$

where

$$A = \frac{N_{gvTr/M} - N_{gv}}{N_{gvTr/M} - N_{gvS/Tr}}. \dots\dots\dots (A.62)$$

An increase in accuracy for the transition region is obtained if the gas density is corrected as

$$\rho'_g = \frac{\rho_g N_{gv}}{N_{gvTr/M}} \dots\dots\dots (A.63)$$

throughout the mist-flow calculation.

## APPENDIX B

### EMPIRICAL FLUID PROPERTY CORRELATIONS

#### B.1 z-Factor

The pseudocritical temperature is calculated as<sup>44</sup>

$$T_{pc} = \frac{k^2}{j}, \dots\dots\dots (B.1)$$

and the pseudo-critical pressure is calculated as

$$p_{pc} = \frac{T_{pc}}{j} \dots\dots\dots (B.2)$$

In Eqs. B.1 and B.2 the  $j$  and  $k$  coefficients can be calculated as

$$j = 0.1158157 + (0.7072878 - 0.0993966\gamma_g)\gamma_g - 0.2368944n_{H_2S} - 0.4619311n_{CO_2} - 0.3041646n_{N_2}, \dots\dots\dots (B.3)$$

and

$$k = 3.821599 + (17.43771 - 3.219084\gamma_g)\gamma_g - 1.218021n_{H_2S} - 7.046435n_{CO_2} - 9.334518n_{N_2} \dots\dots\dots (B.4)$$

$n_{H_2S}$ ,  $n_{CO_2}$ , and  $n_{N_2}$  represent the molar fraction in percent of hydrogen sulfide, carbon dioxide, and nitrogen respectively.

The Dranchuk and Abou-Kassem<sup>45</sup>  $z$ -factor correlation is of the form

$$z = 1 + c_1(T_{pr})\rho_{pr} + c_1(T_{pr})\rho_{pr}^2 - c_3(T_{pr})\rho_{pr}^5 + c_4(\rho_{pr}, T_{pr}), \dots \quad (\text{B.5})$$

where

$$\rho_{pr} = 0.27 \frac{P_{pr}}{zT_{pr}}, \dots \quad (\text{B.6})$$

$$c_1(T_{pr}) = A_1 + \frac{A_2}{T_{pr}} + \frac{A_3}{T_{pr}^2} + \frac{A_4}{T_{pr}^4} + \frac{A_5}{T_{pr}^5}, \dots \quad (\text{B.7})$$

$$c_2(T_{pr}) = A_6 + \frac{A_7}{T_{pr}} + \frac{A_8}{T_{pr}^2}, \dots \quad (\text{B.8})$$

$$c_3(T_{pr}) = A_9 \left( \frac{A_7}{T_{pr}} + \frac{A_8}{T_{pr}^2} \right), \dots \quad (\text{B.9})$$

and

$$c_4(\rho_{pr}, T_{pr}) = A_{10} \left( 1 + A_{11} \rho_{pr}^2 \right) \left( \frac{\rho_{pr}^2}{T_{pr}^3} \right) e^{-A_{11} \rho_{pr}^2}. \dots \quad (\text{B.10})$$

The  $A$ -constants are listed in **Table B.1**.

Eq. B.5 has to be solved iteratively as  $z$  appears on both sides of the equation. The Newton-Raphson<sup>54</sup> method can be used by rearranging Eq. B.5 to the form

$$f(z) = z - \left[ 1 + c_1(T_{pr})\rho_{pr} + c_1(T_{pr})\rho_{pr}^2 - c_3(T_{pr})\rho_{pr}^5 + c_4(\rho_{pr}, T_{pr}) \right] = 0 \dots\dots\dots (B.11)$$

Using the Newton’s method to find the roots of Eq. B.11 requires the derivative, which is

$$f'(z) = \left[ \frac{\partial f(z)}{\partial z} \right]_{T_{pr}} = 1 - \frac{c_1(T_{pr})\rho_{pr} + 2c_1(T_{pr})\rho_{pr}^2 - 5c_3(T_{pr})\rho_{pr}^5}{z} + \dots\dots\dots (B.12)$$

$$\frac{2A_{10}\rho_{pr}^2}{T_{pr}^3 z} \left[ 1 + A_{11}\rho_{pr}^2 - (A_{11}\rho_{pr}^2)^2 \right] e^{-A_{11}\rho_{pr}^2}$$

The iterative procedure is then to estimate the z-factor,  $z_{est}$ , and calculate it as

$$z_{calc} = z_{est} - \frac{f(z_{est})}{f'(z_{est})} \dots\dots\dots (B.13)$$

The calculated value for the z-factor is used as the new estimate, and Eq. B.13 is calculated repeatedly until a reasonable agreement between the calculated and estimated value is obtained.

**Table B.1—A Constants for the Dranchuk and Abou-Kassem Correlation for z-Factor**

$A_1 = 0.3265$	$A_2 = -1.070$	$A_3 = -0.5339$	$A_4 = 0.01569$
$A_5 = -0.05165$	$A_6 = 0.5475$	$A_7 = -0.7361$	$A_8 = 0.1844$
$A_9 = 0.1056$	$A_{10} = 0.6134$	$A_{11} = 0.7210$	

## B.2 Gas Viscosity

The Lee, Gonzalez and Eakin<sup>46</sup> correlation for gas viscosity is

$$\mu_g = 10^{-4} K e^{X\rho_g^Y}, \dots\dots\dots (B.14)$$

where

$$\rho_g = 1.4935 \times 10^{-3} \frac{pM}{zT}, \dots\dots\dots (B.15)$$

$$K = \frac{(9.4 + 0.02M)T^{1.5}}{(209 + 19M + T)}, \dots\dots\dots (B.16)$$

$$X = 3.5 + \frac{986}{T} + 0.01M, \dots\dots\dots (B.17)$$

and

$$Y = 2.4 - 0.2X . \dots\dots\dots (B.18)$$

In these equations  $\mu_g$  is in cp, gas density,  $\rho_g$ , is in g/cc, and the temperature is in °R. The molecular weight can be calculated as

$$M = 28.9625\gamma_g . \dots\dots\dots (B.19)$$

## B.3 Oil Formation-Volume Factor

The Vasquez and Beggs<sup>47</sup> correlation for oil formation volume factor is of the form

$$B_o = 1 + C_1 R_s + (C_2 + C_3 R_s)(T - 60) \left( \frac{\gamma_{API}}{\gamma_g} \right), \dots\dots\dots (B.20)$$

where the constants are determined from **Table B.2**. In Eq. B.20 the temperature is in °F, solution-gas/oil ratio is in scf/STB, and the oil formation volume factor is in bbl/STB.

#### B.4 Oil Compressibility Above the Bubblepoint

The Vasquez and Beggs<sup>47</sup> correlation for the isothermal compressibility for and oil saturated with gas is of the form

$$c_o = \frac{5R_s + 17.2T - 1180\gamma_g + 12.61\gamma_{API} - 1433}{p \times 10^5} \dots\dots\dots (B.21)$$

In Eq. B.21 the temperature is in °F, the pressure is in psia and the compressibility is in 1/psia.

**Table B.2—Constants for the Vasquez and Beggs Correlation for Oil Formation Volume Factor**

Constant	API ≤ 30	API > 30
C <sub>1</sub>	4.677x10 <sup>-4</sup>	4.670x10 <sup>-4</sup>
C <sub>2</sub>	1.751x10 <sup>-5</sup>	1.100x10 <sup>-5</sup>
C <sub>3</sub>	-1.811x10 <sup>-8</sup>	1.337x10 <sup>-9</sup>

### B.5 Solution-Gas/Oil Ratio

Standing's correlation<sup>48</sup> for the solution-gas/oil ratio below the bubblepoint is

$$R_s = \gamma_g \left( \frac{P}{18 \times 10^{y_g}} \right)^{1.204}, \dots\dots\dots (B.22)$$

where

$$y_g = 0.00091T - 0.0125\gamma_{API} \dots\dots\dots (B.23)$$

The temperature is measured in °F.

### B.6 Oil Viscosity

The Egbogah<sup>49</sup> correlation for oil viscosity below the bubblepoint pressure is

$$\mu_o = A\mu_{od}^B, \dots\dots\dots (B.24)$$

where

$$A = 10.715(R_s + 100)^{-0.515}, \dots\dots\dots (B.25)$$

and

$$B = 5.44(R_s + 150)^{-0.338} \dots\dots\dots (B.26)$$

The dead-oil viscosity,  $\mu_{od}$ , can be calculated as

$$\log_{10}[\log_{10}(\mu_{od} + i)] = 1.8653 - 0.025086\gamma_{API} - 0.5644\log_{10}(T). \quad \text{..... (B.27)}$$

Above the bubblepoint, the Beggs and Robinson<sup>47</sup> correlation for oil viscosity is

$$\mu_o = \mu_{ob} \left( \frac{p}{p_b} \right)^m, \quad \text{..... (B.28)}$$

where

$$m = 2.6p^{1.187} e^{-11.513 - 8.98 \times 10^{-5} p}. \quad \text{..... (B.29)}$$

In Eq. B.28,  $\mu_{ob}$  is the oil viscosity at the bubblepoint, which can be calculated using Eq. B.24 with the bubblepoint pressure,  $p_b$ .

### B.7 Water Formation-Volume Factor

The McCain correlation<sup>51</sup> for water formation volume factor is

$$B_w = (1 + \Delta V_{wt})(1 + \Delta V_{wp}), \quad \text{..... (B.30)}$$

where

$$\Delta V_{wt} = -1.00010 \times 10^{-2} + 1.33391 \times 10^{-4} T + 5.50654 \times 10^{-7} T^2, \quad \text{..... (B.31)}$$

and

$$\begin{aligned} \Delta V_{wp} = & -1.95301 \times 10^{-9} pT - 1.72834 \times 10^{-13} p^2 T - 3.58922 \times 10^{-7} p \\ & - 2.25341 \times 10^{-10} p^2. \quad \text{..... (B.32)} \end{aligned}$$

The temperature here is in °F and pressure is in psia.

### B.8 Solution-Gas/Water Ratio

McCain's correlation<sup>51</sup> for solution-gas/water ratio for pure water is

$$R_{swp} = A + Bp + Cp^2, \dots\dots\dots (B.33)$$

where

$$A = 8.15839 - 6.12265 \times 10^{-2}T + 1.91663 \times 10^{-4}T^2 - 2.1654 \times 10^{-7}T^3, \dots\dots\dots (B.34)$$

$$B = 1.01021 \times 10^{-2} - 7.44241 \times 10^{-5}T + 3.05553 \times 10^{-7}T^2 - 2.94883 \times 10^{-10}T^3, \dots\dots (B.35)$$

and

$$C = -10^{-7} (9.02505 - 0.130237T + 8.53425 \times 10^{-4}T^2 - 2.34122 \times 10^{-6}T^3 + 2.37049 \times 10^{-9}T^4) \dots\dots\dots (B.36)$$

The solution-gas/water ratio for reservoir brines is

$$R_{sw} = R_{swp} \left( \frac{R_{sw}}{R_{swp}} \right), \dots\dots\dots (B.37)$$

where

$$\left( \frac{R_{sw}}{R_{swp}} \right) = 10^{(-0.0840655S \times T^{-0.285854})} \dots\dots\dots (B.38)$$

where  $S$  is the salinity in percent weight solids and the temperature is in °F.

**B.9 Water Viscosity**

McCain’s correlation<sup>51</sup> for water viscosity at atmospheric pressure and reservoir temperature is

$$\mu_{w1} = AT^B, \dots\dots\dots (B.39)$$

where

$$A = 109.574 - 8.40564S + 0.313314S^2 + 8.72213 \times 10^{-3} S^3, \dots\dots\dots (B.40)$$

and

$$B = -1.12166 + 2.63951 \times 10^{-2} S - 6.79461 \times 10^{-4} S^2 - 5.47119 \times 10^{-5} S^3 + 1.55586 \times 10^{-6} S^4 \dots\dots\dots (B.41)$$

The viscosity at reservoir pressure can be calculated as

$$\mu_w = \mu_{w1} \left( \frac{\mu_w}{\mu_{w1}} \right), \dots\dots\dots (B.42)$$

where

$$\left( \frac{\mu_w}{\mu_{w1}} \right) = 0.9994 + 4.0295 \times 10^{-5} p + 3.1062 \times 10^{-9} p^2 \dots\dots\dots (B.43)$$

### B.10 Gas/Oil Interfacial Tension

The dead-oil interfacial tension<sup>35</sup> at 68°F is

$$\sigma_{68} = 39 - 0.2571\gamma_{API}, \dots\dots\dots (B.44)$$

and the dead-oil interfacial tension at 100°F is

$$\sigma_{100} = 37.5 - 0.2571\gamma_{API} \cdot \dots\dots\dots (B.45)$$

The dead-oil interfacial tension for any temperature between 68° and 100°F can then be interpolated as

$$\sigma_T = \sigma_{68} - \frac{(T - 68)(\sigma_{68} - \sigma_{100})}{32} \cdot \dots\dots\dots (B.46)$$

If the temperature is higher than 100°F the  $\sigma_i$  should be used and if the temperature is below 68°F the  $\sigma_{68}$  should be used.

The interfacial tension at any pressure can then be calculated as

$$\sigma_o = (1.0 - 0.024p^{0.45})\sigma_T \cdot \dots\dots\dots (B.47)$$

### B.11 Gas/Water Interfacial Tension

The water interfacial tensions<sup>35</sup> at 74° and 280°F are

$$\sigma_{w(74)} = 75 - 1.108p^{0.349} \dots\dots\dots (B.48)$$

and

$$\sigma_{w(280)} = 53 - 0.1048 p^{0.637} \dots\dots\dots (B.49)$$

The dead-oil interfacial tension for any pressure and temperature between 68° and 100°F can then be interpolated as

$$\sigma_w = \sigma_{w(74)} - \frac{(T - 74)(\sigma_{w(74)} - \sigma_{w(280)})}{206} \dots\dots\dots (B.50)$$

If the temperature is higher than 280°F the  $\sigma_{w(280)}$  should be used, and if the temperature is below 74°F the  $\sigma_{w(74)}$  should be used.

## VITA

Name: Ray Tommy Oskarsen

Born: November 4, 1972, Stavanger, Norway

Address: Gravarverket 32A  
4327 Sandnes  
Norway

Education: College of Soer-Troendelag  
Norway, Technical Diploma - Mechanical Engineering (1997)

University of Surrey  
England, B.S. (Hon) – Mechanical Engineering (1999)

Texas A&M University  
USA, M.S. – Petroleum Engineering (2001)

## **Appendix B**

**Final Report for Phase I, Task 3.**

### **ULTRADEEP WATER BLOWOUTS: COMASIM DYNAMIC KILL SIMULATOR VALIDATION AND BEST PRACTICES RECOMMENDATIONS**

**By**

**Mr. Sam Noynaert, TAMU (currently BP)**

**ULTRADEEP WATER BLOWOUTS:  
COMASIM DYNAMIC KILL SIMULATOR VALIDATION  
AND BEST PRACTICES RECOMMENDATIONS**

A Thesis

by

SAMUEL F. NOYNAERT

Submitted to the Office of Graduate Studies of  
Texas A&M University  
in partial fulfillment of the requirements for the degree of

MASTER OF SCIENCE

December 2004

Major Subject: Petroleum Engineering

**ULTRADEEP WATER BLOWOUTS:  
COMASIM DYNAMIC KILL SIMULATOR VALIDATION  
AND BEST PRACTICES RECOMMENDATIONS**

A Thesis

by

SAMUEL F. NOYNAERT

Submitted to Texas A&M University  
in partial fulfillment of the requirements  
for the degree of

MASTER OF SCIENCE

Approved as to style and content by:

---

Jerome J. Schubert  
(Chair of Committee)

---

Hans C. Juvkam-Wold  
(Member)

---

Ann Kenimer  
(Member)

---

Stephen A. Holditch  
(Head of Department)

December 2004

Major Subject: Petroleum Engineering

## ABSTRACT

Ultradeep Water Blowouts:  
COMASim Dynamic Kill Simulator Validation and  
Best Practices Recommendations.

(December 2004)

Samuel F. Noynaert, B.S., Texas A&M University  
Chair of Advisory Committee: Dr. Jerome J. Schubert

The petroleum industry is in a constant state of change. Few industries have advanced as far technologically as the petroleum industry has in its relatively brief existence. The produced products in the oil and gas industry are finite. As such, the easier to find and produce hydrocarbons are exploited first. This forces the industry to enter new areas and environments to continue supplying the world's hydrocarbons. Many of these new frontiers are in what is considered ultradeep waters, 5000 feet or more of water.

While all areas of the oil and gas industry have advanced their ultradeep water technology, one area has had to remain at the forefront: drilling. Unfortunately, while drilling as a whole may be advancing to keep up with these environments, some segments lag behind. Blowout control is one of these areas developed as an afterthought. This lax attitude towards blowouts does not mean they are not a major concern. A blowout can mean injury or loss of life for rig personnel, as well as large economic losses, environmental damage and damage to the oil or gas reservoir itself. Obviously, up-to-date technology and techniques for the prevention and control of ultradeep water blowouts would be an invaluable part of any oil and gas company's exploration planning and technology suite.

To further the development of blowout prevention and control, COMASim (Cherokee Offshore, MMS, Texas A&M Simulator) was developed. COMASim

simulates the planning and execution of a dynamic kill delivered to a blowout. Through a series of over 800 simulation runs, we were able to find several key trends in both the initial conditions as well as the kill requirements.

The final phase of this study included a brief review of current industry deepwater well control best practices and how the COMASim results fit in with them. Overall, this study resulted in a better understanding of ultradeep water blowouts and what takes to control them dynamically. In addition to this understanding of blowouts, COMASim's strengths and weaknesses have now been exposed in order to further develop this simulator for industry use.

## **DEDICATION**

I would like to dedicate this thesis to my family: my wife Courtney who was the best wife, cheerleader and overall best support team I could ask for and who has been waiting for this moment for three long years. Her love and dedication was all that kept me going at times. To my study partners: Daisy, Shiner, Phoebe and Socks who stayed up every night with me making sure the work got done.

I also dedicate this work to my parents for imparting a love of knowledge to me at an early age. Particularly my mother who has demonstrated the fact that education is a lifelong process and doesn't have to be limited by number of degrees or time.

## ACKNOWLEDGEMENTS

I would like to acknowledge the following for the priceless help, advice and support I received during this endeavor:

I would first like to acknowledge my committee of Dr. Jerome J. Schubert, Dr. Hans Juvkam-Wold, and Dr. Ann Kenimer for helping this work be accurate and something that I can be proud of.

I would also like to acknowledge Dr. Stephen A. Holditch and Dr. Tom Blasingame for your advice and help concerning my decision on whether or not to even enter this department and industry.

In addition, I would like to acknowledge Curtis Weddle and Steve Walls for providing their time to give us an industry view of this study and tell us where the theory broke down.

I would be remiss if I did not acknowledge RPSEA (Research Partnership to Secure Energy for America) for funding this study.

And last but not least, I would like to acknowledge Dr. Ray T. Oskarsen for his tireless help with this project even after he finished his part and went out into the real world. Without Ray's help, this project would still be floundering towards a finish.

To all: Thank you for your help, Gig'em and God Bless

## TABLE OF CONTENTS

	Page
ABSTRACT .....	iii
DEDICATION .....	v
ACKNOWLEDGEMENTS .....	vi
TABLE OF CONTENTS .....	vii
LIST OF FIGURES.....	x
LIST OF TABLES .....	xiii
 CHAPTER	
I INTRODUCTION.....	1
1.1 Blowouts.....	1
1.2 Blowouts Historically.....	4
1.3 Blowouts Statistically.....	7
1.4 Blowout Control Measures.....	13
1.5 Kill Method Selection .....	25
II RESEARCH BACKGROUND.....	30
2.1 Proposal Background and Objectives .....	30
2.2 Thesis Objectives .....	31
2.3 COMASim Background.....	32
2.4 Simulator Calculations .....	33
III COMASIM RESULTS AND ANALYSIS.....	38
3.1 COMASim Simulation Input Values .....	38
3.2 COMASim Simulation Procedure.....	41
3.3 Validation of COMASim .....	42
3.4 COMASim Initial Condition Analyses .....	45
3.5 Effect of Casing Size and Drillstring Presence on Initial Conditions.....	49

CHAPTER	Page
3.6 Effect of Drillstring Length.....	53
3.7 Kill with Drillstring Initial Conditions.....	57
3.8 Dynamic Kill Requirements for Relief Well Necessary Situations.....	61
3.9 Dynamic Kill Requirement for Kill with the Drillstring Situation.....	67
 IV      ULTRA-DEEP WATER BLOWOUT PREVENTION AND CONTROL ..	 70
4.1 Ultra-deepwater Drilling Equipment.....	70
4.2 Ultra-deepwater Blowout Control Equipment .....	75
4.3 Ultra-deepwater Kicks and Well Control.....	78
4.4 Ultra-deepwater Well Control .....	82
4.5 Dynamic Kill Blowout Control .....	88
 V      CONCLUSIONS AND RECOMMENDED FUTURE RESEARCH .....	 96
5.1 Ultradeep Water Blowout Control Conclusions.....	96
5.2 Simple COMASim User Tasks and Extended Analysis Capability .....	97
5.3 Multilateral Capability .....	98
5.4 Fluid Fallback.....	98
5.5 Underground Blowout Capability .....	99
5.6 Linking to Dr. Jongguen Choe’s Simulator .....	99
5.7 Simulator Validation .....	99
5.8 Combination Vertical Intervention and Relief Well Dynamic Kill Operations.....	100
 NOMENCLATURE.....	 101
 REFERENCES .....	 103
 APPENDIX A: SIMULATION RUN MATRIX .....	 107
 APPENDIX B: RELIEF WELL INITIAL CONDITION RUNS .....	 124
 APPENDIX C: RELIEF WELL KILL REQUIREMENTS.....	 164
 APPENDIX D: KILL WITH DRILLSTRING INITIAL CONDITIONS .....	 176

	Page
APPENDIX E: KILL WITH DRILLSTRING KILL REQUIREMENTS .....	187
VITA .....	189

## LIST OF FIGURES

FIGURE	Page
1.1 Tripping in during bit change.....	3
1.2 Well blows out in seconds.....	3
1.3 Crew evacuation after blowout .....	3
1.4 The well is abandoned and out of control .....	3
1.5 Derrick collapses .....	4
1.6 Spindletop’s first well (Lucas well) was a blowout .....	4
1.7 Frequency of blowouts per 100 wells in the Outer Continental Shelf (OCS) did not show improvement from 1960-1996.....	5
1.8 Frequency of blowouts per 100 wells in onshore Texas increased from 1960-1996 .....	6
1.9 Frequency of blowouts per 10 <sup>6</sup> feet drilled in onshore Texas is erratic and shows no improvement from 1960 to 1996.....	6
1.10 Number of blowouts per phase in progress shows most blowouts occur in unfamiliar drilling situations.....	8
1.11 Percentage of OCS blowouts having a certain fluid composition indicates majority of blowouts were gas .....	12
1.12 Relative majority of OCS blowouts controlled by bridging .....	12
1.13 Typical capping stacks .....	14
1.14 Momentum kill theory.....	18
1.15 Blowout control through flooding is a lengthy process .....	19
1.16 Depletion kill or waterflood relief well bottomhole location.....	20
1.17 Relief intersection point allows maximum use of frictional pressure.....	22
1.18 Control of large blowout completed using dynamic kill in approximately 12 minutes.....	23
1.19a Example kill method selection flowchart I.....	26
1.19b Example kill method selection flowchart II .....	27

FIGURE	Page
1.19c Example kill method selection flowchart III.....	28
1.19d Example kill method selection flowchart IV.....	29
2.1 Screen shot of COMASim interface shows simplicity of operation .....	33
2.2 Graphical example of general nodal analysis calculation .....	34
2.3 Example of use of nodal analysis to find required dynamic kill rate.....	34
2.4 No drillstring in wild well .....	35
2.5 Drillstring dropped .....	35
2.6 Drillstring hanging from BOP.....	35
2.7 Drillstring used to kill well.....	35
3.1 Typical 15000 psi fracturing vessel .....	42
3.2 Comparison of solution types shows zero-derivative curve grossly over calculates the dynamic kill solution.....	44
3.3 Numerical output of COMASim is limited to 10 equally spaced points .....	46
3.4 Numerical output for a hanging drillstring at 13000 ft TVD, 13000 ft drillstring, 5000 ft of water, 10 ¾ casing.....	47
3.5 Close-up of graph from Fig. 3.3, a hanging drillstring at 13000 ft TVD, 13000 ft drillstring, 5000 ft of water, 10 ¾ inch casing .....	48
3.6 Hanging drillstring situations shows typical behavior for pressure profile .....	49
3.7 Dropped drillstring data matches hanging drillstring pressure profile .....	50
3.8 No drillstring in hole reduces pressure value and variation .....	51
3.9 Effect of drillstring length on hanging drillstring, 13000 ft TVD, 5000 ft water depth, 10 ¾ inch casing.....	54
3.10 Effect of drillstring length on dropped drillstring, 13000 ft. TVD, 5000 ft water depth, 10 ¾ inch casing.....	55
3.11 Difference between 3250 ft. of drillstring in 13000 ft TVD in 5000 ft of water with 10 ¾ inch casing.....	56

FIGURE	Page
3.12 13000 ft TVD, 5000 ft water depth, 10 ¾ inch casing, drillstring is 75% of TVD.....	58
3.13 Kill with drillstring, 13000 ft TVD, 5000 ft water depth, 10 ¾ inch casing shows decreasing bottom-hole pressures as drillstring length decreases.....	59
3.14 Kill with drillstring, 13000 ft TVD, 5000 ft water depth, drillstring length is 75% of TVD.....	61
3.15 Relief well flow path.....	62
3.16 Dynamic kill rates differ widely among drillstring statuses as drillstring length decreases.....	64
3.17 Increasing casing size in with no drillstring present increases number of relief wells required.....	66
3.18 Kill rates increase for larger casing sizes.....	69
4.1 Example of drillship.....	70
4.2 Example of semi-submersible.....	71
4.3 ABB Vetco Gray composite material riser increases water depth capability of floaters.....	72
4.4 Acoustic control system on lower marine riser package.....	75
4.5 Example of offshore dynamic kill pumping plant.....	76
4.6 Increasing kill fluid weight reduces the kill rate.....	77
4.7a Onshore gradients.....	78
4.7b Offshore gradients.....	79
4.8 Comparison of casing shoe pressures between Drillers method and Wait and Weight Method shows Drillers method causes lost circulation.....	86
4.9 Decision process for dynamic kill path.....	89
4.10 Data from Adams et al. shows minimal loss of buoyancy from blowout plume.....	91
4.11 Data from Adams et al. shows wide plume at surface for blowout in 10000 feet of water.....	91

## LIST OF TABLES

TABLE	Page
1.1 SINTEF database concurs with Skalle et al. database findings on blowout causes .....	8
1.2 Distribution of most frequent operation phase failures (Louisiana, Texas, OCS; 1960-96) shows majority of blowout causes are human error .....	9
1.3 Gulf of Mexico (GoM) development wells drilled twice as fast as Norwegian development wells .....	10
2.1 Input options for COMASim.....	36
3.1 Blowout information for COMASim validation problem.....	43
3.2 Hanging and dropped drillstrings allow almost identical flow rates.....	51
3.3 Blowing wellbores with no drillstring have higher $Q_{g,surface}$ .....	53
3.4 Kill with drillstring configuration yields higher $Q_{g,surface}$ .....	59
3.5 Kill with drillstring, 13000 ft TVD, 5000 ft water depth, 10 ¾ inch casing shows flow rate increases as drillstring length decreases .....	60
3.6 13000 ft TVD, 5000 ft water depth, kill rate increases with increasing casing size .....	64
3.7 Increasing relief well MD/TVD ratio increases relief well parameters .....	65
3.8 Kill with drillstring kill rates similar to dropped drillstring.....	67
3.9 Decreasing drillstring length increases kill requirements .....	68
4.1 Hang-off, shut-in, and flow-check procedure .....	83
4.2 Drillers method procedure for killing well.....	84
4.3 Wait and Weight method for killing well.....	85

# CHAPTER I

## INTRODUCTION

### 1.1 Blowouts

The petroleum industry constantly undergoes radical changes and progress. Few industries have advanced as far or as fast technologically as the petroleum industry has in the past century. This advancement has been caused by the lucrative nature of the oilfield business as well as the procurement of the product itself. Obviously as more money is put into an industry, technological advancement becomes easier and often a necessary part of competition. However, in the petroleum industry the technological advancement has actually been a forced issue. The products we as an industry are trying to produce, oil and natural gas, are a finite resource. As the easier to find and produce hydrocarbons are used up, the industry must move into new areas to continue supplying the world with hydrocarbons. Many of these areas are in what is considered ultra-deep waters, 5000 feet or more of water. This is a unique environment that requires many new techniques and technologies to explore and produce.

As the various areas of the oil and gas industry advance their ultra-deep water technology, one area has had to remain at the forefront: drilling. For example, geological exploration can be done with multi-billion dollar seismic projects or by using the map as a dartboard. Either way, drilling must be done to confirm and develop the discovery. Without drilling, there simply is no petroleum industry. However, much of the drilling done is on unknown frontiers for hydrocarbon exploration. Often these frontiers are harsh environments either downhole, on the surface or both. Ultra-deep water is a great example of a dangerous and unknown drilling environment.

It is on these frontiers however that the advancement of technology is often disjointed. While drilling as a whole may be advancing to keep up with these

---

This thesis follows the style of *SPE Drilling and Completion*.

environments, some parts lag behind. An example of this is the running of casing offshore. Until very recently, casing was run in the same manner, and often using the same tools, as a casing job done twenty to thirty years ago. It has only been in the past few years that the use of technology like automatic pipe handling equipment has become widespread. This change brought on by pure safety concerns. Another area that is seen the same stagnation and recent call for change has been blowout control in deep and ultradeep waters.

Blowout control is an area often put aside until the last minute for the industry. A blowout means that the drilling contractor and crew have failed in some way, and as is often the case in business, failure is not an option. However, in the case of drilling a well, failure in the form a blowout can mean injury or loss of life for rig personnel, large economic losses, environmental damage and damage to the oil or gas reservoir itself. Obviously, a contingency plan for the prevention and control of ultradeep water blowouts would be a valuable part of any oil and gas company's planning for the drilling of a well.

The following sequence of photographs (**Fig. 1.1-1.5**) show the rapidity and unexpectedness of blowouts as well as some of the dangers. In **Fig. 1.1**, the derrick is shown prior to the blowout. In this picture, the drill collars are racked back in the derrick and the derrick man is on the monkeyboard. **Fig. 1.2** occurs during a film change by the photographer immediately after taking **Fig. 1.1**. This shows how quickly the situation gets out of control. Once the blowout occurred, the crew began evacuation as shown in **Fig. 1.3**. In **Fig. 1.3**, the derrick man is seen just getting off of the geronimo line. In the same figure, a worker is shown narrowly avoiding falling drillpipe. As the crew left the location, the drill collars were ejected in **Fig. 1.4** and the blowout continues. Finally, **Fig. 1.5** shows the rig collapsing due to the weight of the racked-back drill collars. This is a dramatic series of pictures showing the potential dangers of a blowout. Fortunately no one was injured in this particular instance.

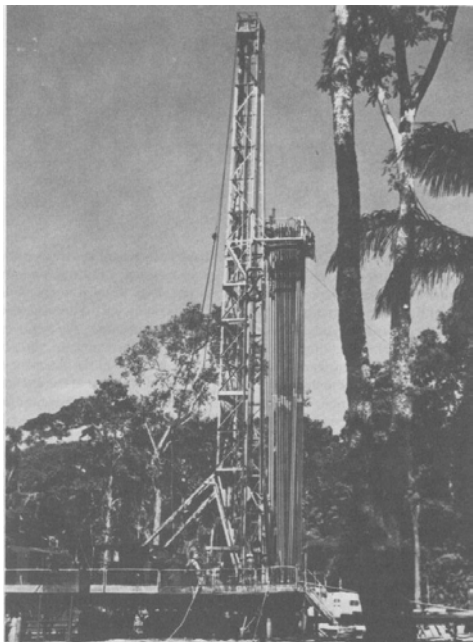


**Fig. 1.1-Tripping in during bit change.<sup>1</sup>**



**Fig. 1.2 – Well blows out in seconds.<sup>1</sup>**

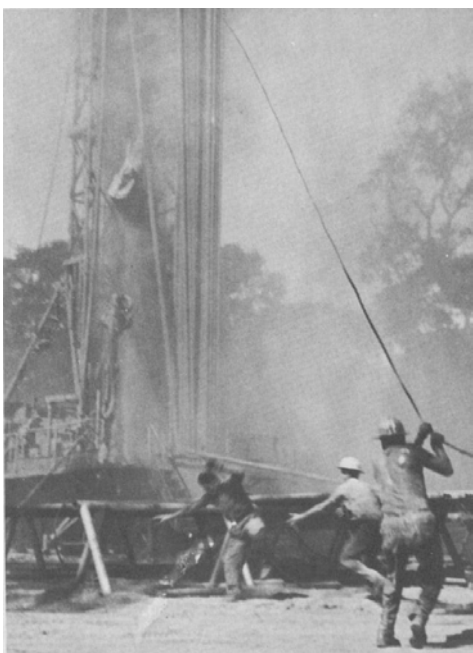


**Fig. 1.3 – Crew evacuation after blowout.<sup>1</sup>**



**Fig. 1.4 – The well is abandoned and out of control.<sup>1</sup>**



**Fig. 1.5 – Derrick collapses.<sup>1</sup>**

## **1.2 Blowouts Historically**

Blowouts have been a problem for this industry since its inception. A famous picture (Fig. 1.6) in the oil and gas industry is of the first Spindletop gusher. The drillers of the original



**Fig. 1.6 - Spindletop's first well (Lucas well) was a blowout.<sup>2</sup>**

Spindletop well, along with others in that era knew they had a good find when a blowout occurred. This was a dangerous situation which was eventually remedied with the invention of the BOP (Blowout preventer) in 1922 by the founders of Cooper Cameron.<sup>3</sup>

However, in spite of the development of many safety measures such as the aforementioned BOPs, as well as numerous types of equipment and drilling procedures, blowouts still occur. In fact, since 1960 blowouts have occurred at a fairly stable rate<sup>4</sup>. This rate has not changed even though blowout prevention equipment and procedures have drastically changed (Fig. 1.7-1.8).

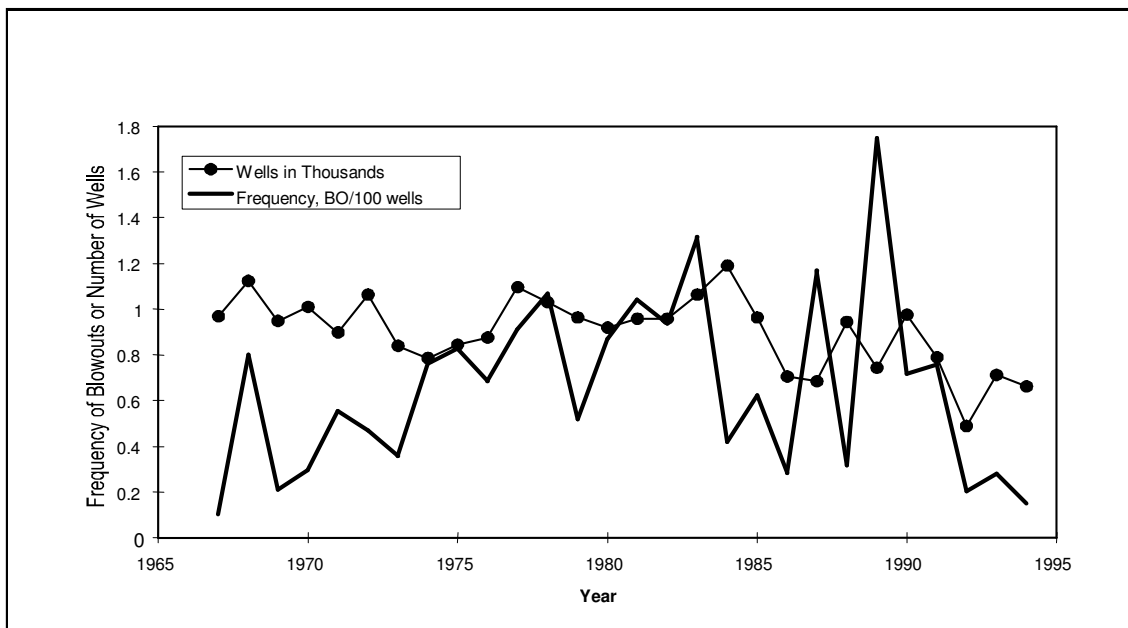


**Fig. 1.7-Frequency of blowouts per 100 wells in the Outer Continental Shelf (OCS) did not show improvement from 1960-1996.<sup>4</sup>**

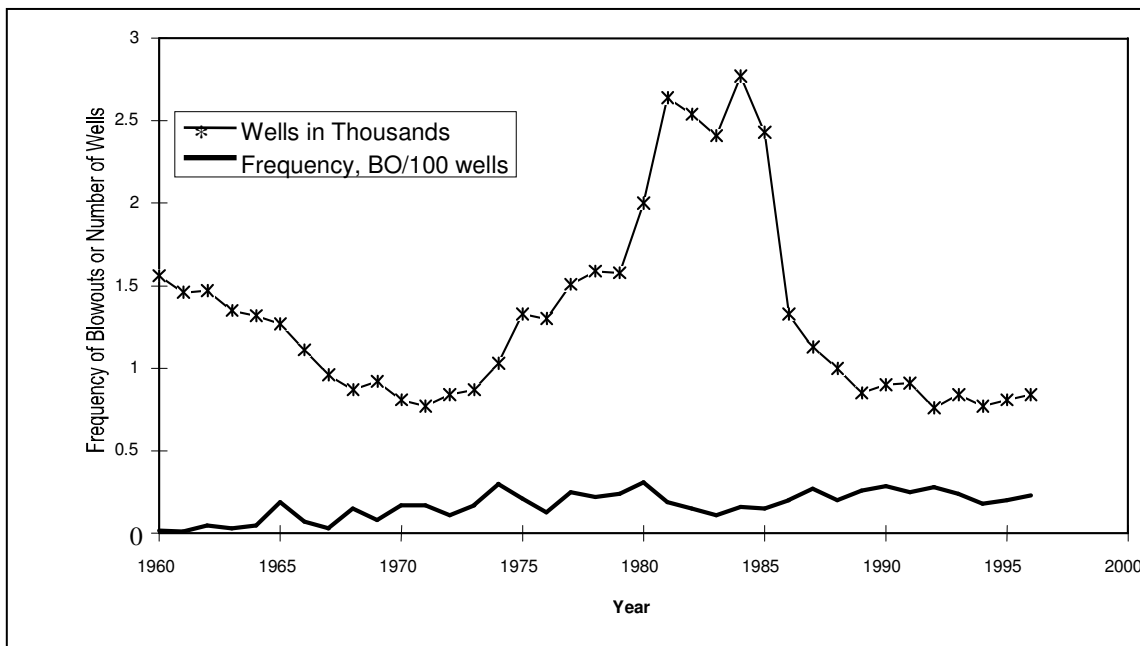


**Fig. 1.8 – Frequency of blowouts per 100 wells in onshore Texas increased from 1960-1996.<sup>4</sup>**

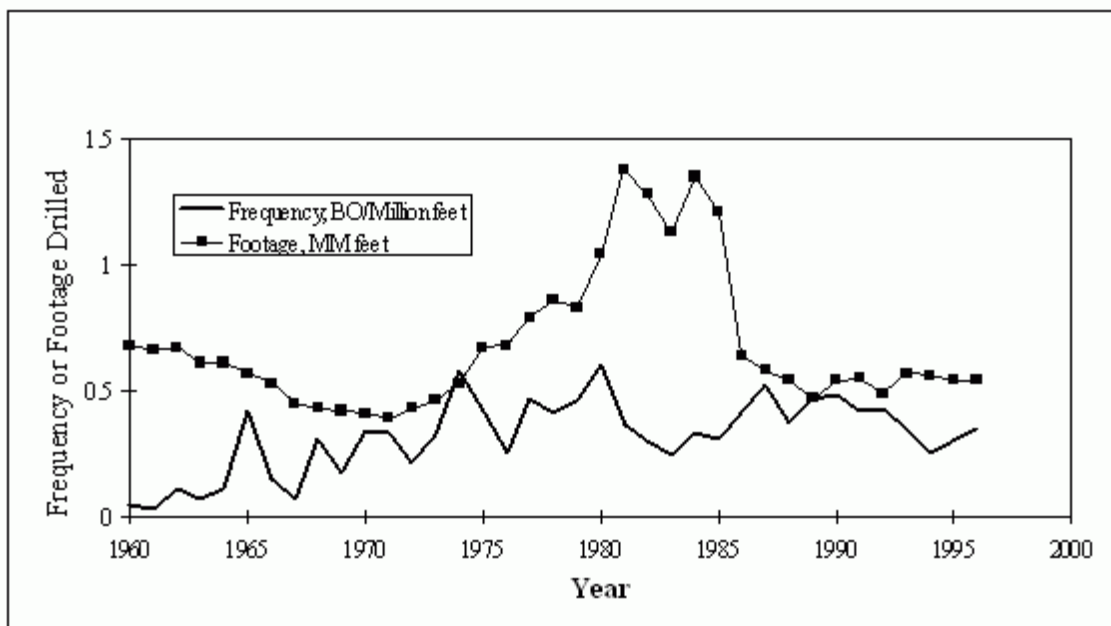


**Fig. 1.9-Frequency of blowouts per  $10^6$  feet drilled in onshore Texas is erratic and shows no improvement from 1960 to 1996.<sup>4</sup>**

As evidenced by **Figs. 1.7 – 1.8** the number of blowouts per feet drilled stayed relatively constant from 1960 to 1996. This was true for both the Outer Continental Shelf of the Gulf of Mexico (OCS) (**Fig. 1.7**) as well as for onshore Texas (**Fig. 1.8**). Further investigation shows that onshore Texas actually had several years in the mid-1980's in which drilled footage went up and blowout frequency went down (**Fig. 1.9**). This is a strange phenomenon, considering that in boom times the industry tends to hire inexperienced personnel and rush to explore or produce hydrocarbons. However, the data shows a contrarian trend that shows blowouts being reduced in the mid-1980's in spite of the boom occurring at the time. This is unexplainable based on the published data from the Skalle, et. al database.<sup>4</sup> Unfortunately, according to **Fig. 1.9**, this unique trend did not last. The drilled footage went down dramatically and the blowout frequency continued its steady climb. All of these numbers point to an irrefutable conclusion: blowouts will always happen no matter how far technology and training advance.

### **1.3 Blowouts Statistically**

Since we can reasonably expect blowouts to always occur in spite of technical advances, we must complete two tasks. First, we must conduct a quick study of why blowouts occur. Next, we must find ways to first prevent blowouts and in a worst case scenario, kill them. In the case of deepwater drilling, no studies have been undertaken. This is mostly due to lack of data. Therefore, this report uses data from onshore Texas and OCS wells to briefly discuss the causes of blowouts.

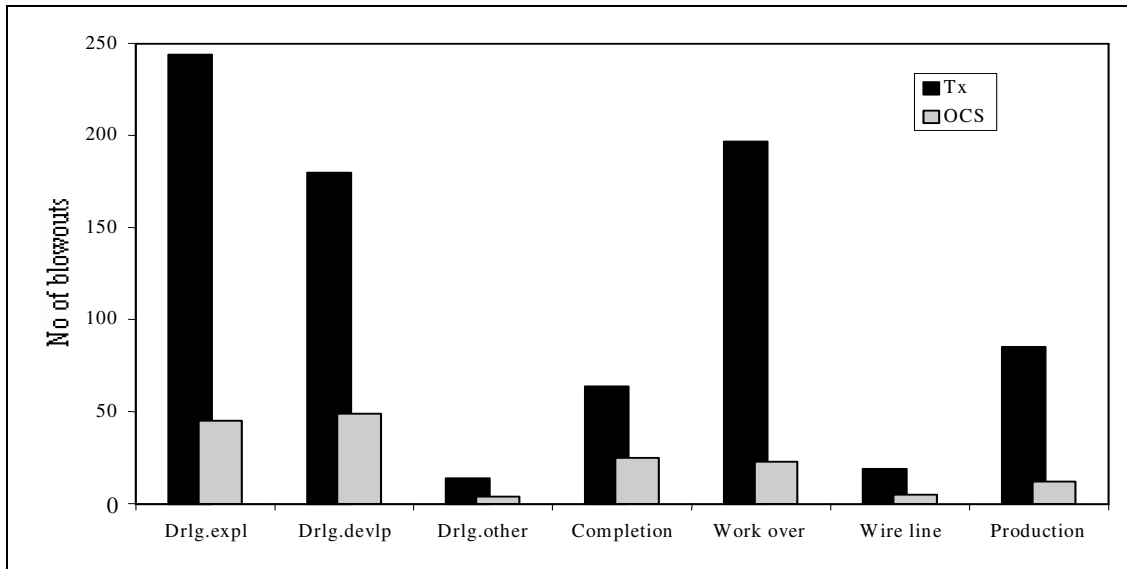


**Fig. 1.10 – Number of blowouts per phase in progress shows most blowouts occur in unfamiliar drilling situations.<sup>4</sup>**

**Table 1.1 – SINTEF database concurs with Skalle et al. database findings on blowout causes<sup>5,6</sup>.**

AREA	Develop. Drilling	Expl. Drilling	unknown Drilling	Completion	Workover	Production		Wireline	Unknown	Total
						External cause*	No ext. cause*			
North Sea (UK & Norway)	7	22	3	3	5	1	1	1	1	44
	15.9%	50.0%	6.8%	6.8%	11.4%	2.3%	2.3%	2.3%	2.3%	100.0%
US GoM OCS	41	42	0	11	25	5	7	3	2	136
	30.1%	30.9%	0.0%	8.1%	18.4%	3.7%	5.1%	2.2%	1.5%	100.0%
Total	48	64	3	14	30	6	8	4	3	180
	26.7%	35.6%	1.7%	7.8%	16.7%	3.3%	4.4%	2.2%	1.7%	100.0%

\* External causes are typical; storm, military activity, ship collision, fire and earthquake.

**Fig. 1.10** clearly shows the most blowouts occur during the initial drilling of the wells, the exploration and development phase with the single most incidents during the

exploration phase. **Table 1.1** is derived from the Foundation for Scientific and Industrial Research at the Norwegian Institute of Technology (SINTEF) blowout database. The SINTEF Group is a Norwegian R&D foundation which was hired by an industry group to study offshore blowouts. The resulting database is a proprietary database with limited results published. This database seems to be kept relatively up-to-date with the total number of offshore blowouts recorded at 487.<sup>5</sup> **Table 1.1** confirms the Skalle, et al. database findings. OCS blowouts had the highest rate of occurrence for development and exploration drilling followed by workover operations.

**Table 1.2 - Distribution of most frequent operation phase failures (Louisiana, Texas, OCS; 1960-96) shows majority of blowout causes are human error.<sup>4</sup>**

Primary Cause	Blowouts		Distribution of specific failed barrier					
	TX	OCS	Expl. drilling	Develop. drilling	Completion	Production	Workover	Wireline
Swabbing	217	31	77	96	9	-	75	5
Drilling break	73	14	52	32	-	-	2	-
Formation break down	58	6	38	16	3	3	4	-
Trapped/expanding gas	55	6	9	18	7	-	28	1
Gas cut mud	55	7	26	15	5	-	13	1
Too low mud weight	43	12	17	20	12	-	16	3
Wellhead failure	28	6	5	3	1	20	11	-
x-mas tree failure	23	5	-	-	1	25	6	-
While cement sets	21	10	5	5	23	-	2	-
<b>Secondary Cause</b>								
Failure to close BOP	152	7	66	56	6	2	38	3
BOP failed after closure	76	13	36	24	13	2	14	2
BOP not in place	60	10	9	11	20	-	39	1
Fracture at casing shoe	34	3	21	17	3	1	2	1
Failed to stab string valve	18	9	2	2	6	1	13	-
Casing leakage	30	6	10	6	2	17	6	1

**Table 1.2** breaks down **Fig. 1.10** into the causes of the blowouts within each operation phase. Concentrating on primary causes, several conclusions can be drawn. Overall, the majority of blowouts resulted from swabbed-in kicks. However, analyzing the results based on the type of operation in progress yields several interesting insights on causes other than swabbing. First, exploration drilling blowouts were more likely to be caused by unexpected obstacles and incomplete geological data than poor or sloppy

drilling practices. Drilling breaks, formation breakdown and gas cut mud problems were significantly higher in the exploration phase than in any other phase. All of these problems are ones that, when unexpected, can cause confusion on the drilling floor and lead to well control problems. Gas cut mud is a good example. When a drilling crew is expecting gas, they can increase mud logging frequency as well as put more emphasis on indicators such as slight pit gains which might otherwise be ignored.

In development drilling, **Table 1.2** shows that swabbing in kicks and having insufficient of mud weight were problems which occurred at rates higher than in other operation phases. Both problems are indicative of operators trying to speed up the drilling process. The operators are more likely to attempt to save time on development wells were they assume they know more about the potential challenges, than attempt to speed up the drilling of an exploration well through unknown challenges. Lowering mud weights increases the rate of penetration. Time taken to trip pipe out of the hole comprises a large amount of the time taken to drill a well. Therefore, operators try to reduce this time by pulling the pipe more quickly. Unfortunately, this causes a reduction in the pressure at the bottom of the wellbore and invites a kick. The most interesting finding in the available SINTEF data, the disparity between the North Sea and OCS in development well blowouts, touches on this problem. The North Sea had a much lower incidence rate of development well blowouts as highlighted in **Table 1.1**.

**Table 1.3 – Gulf of Mexico (GoM) development wells drilled twice as fast as Norwegian development wells.<sup>6</sup>**

	US GoM OCS		Norway	
	All Wells (days)	Wells With Duration <200 days (days)	All Wells (days)	Wells With Duration <200 days (days)
<b>Development Drilling</b>	36.6	32.6	102.4	66.9
<b>Exploration Drilling</b>	20.1	14.1	84.5	78.7

It is evident why the North Sea development well blowout rate was much less when taking into account **Table 1.3**. Development wells in the Norwegian sector of the North Sea took twice as long as development well in the Gulf of Mexico. The reasons behind this would easily supply the fodder for years of future research. However, suffice it to say that the rapid drilling of development wells obviously adversely affects the blowout rates in said wells.

Workover operations had the third highest number of blowouts. The cause which stands out in workover blowouts is trapped/expanding gas. This is most likely due to poor circulation techniques stemming from not enough complete circulations to rid the wellbore of gas after influxes, as well as poor handling of kicks, which allows unplanned expansion of gas.

It is important to remember that the data in **Fig. 1.7-1.10** the data is from onshore US and relatively shallow OCS wells. Ultradeep water wells will have similar well control issues but in an exaggerated manner. The increased pressures will cause influxes and blowouts to behave in different ways. Indicators and measurements of influxes such as pit gain and pressure values will be often deceptively benign until the situation has escalated to the point that control of problem will become a very complicated and dangerous task. The chief causes of blowouts shown in **Table 1.2** will probably not change statistically. Therefore a reasonable assumption would be that by concentrating on these principal causes and taking into account the exaggerated effects caused by the ultradeep water environment, a suitable suite of best practices may be compiled for ultradeep water drilling.

The compositions of the blowouts are not uniform. In fact, in the most comprehensive public database to date which was developed by Skalle, et al.<sup>4,7</sup> there are eleven categories for blowing fluid composition: gas, gas & oil, gas & water, gas & condensate, gas & oil & water, condensate, oil, oil & water, water, mud, and no data.

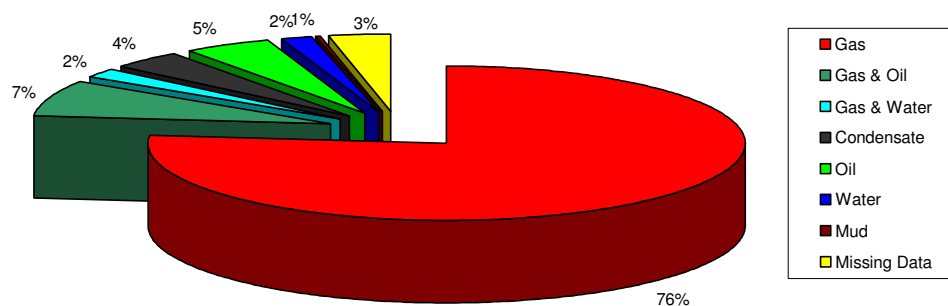


**Fig. 1.11 – Percentage of OCS blowouts having a certain fluid composition indicates majority of blowouts were gas.<sup>7</sup>**

Of the eleven possible fluid compositions, eight were observed in OCS blowouts from 1960 to 1996. **Fig. 1.11** shows the 74 percent of blowouts had gas as the blowing fluid.

In the Skalle, et al. database, kill methods were also studied. Eight primary kill methods were identified: collapse of open hole wellbore (bridging), closing BOP (BOP), pumping cement slurry (cement), capping, depletion of reservoir (depletion), installing equipment, pumping mud (mud), and drilling relief wells.

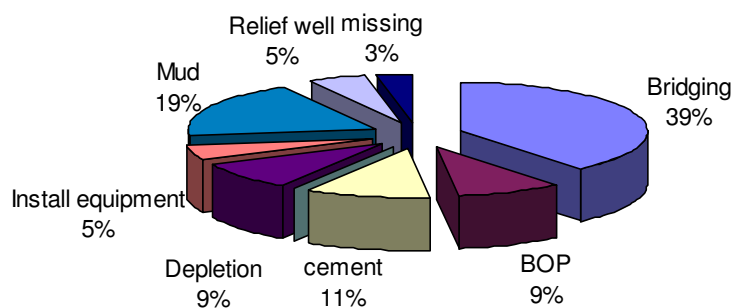


**Fig. 1.12 –Relative majority of OCS blowouts controlled by bridging.<sup>7</sup>**

Of these, seven were found to have been used to control OCS blowouts. Conspicuous in its absence was the technique of capping to actually stop the flow of

hydrocarbons. Of course, the majority of blowing wells will be capped once they are brought under control and decisions concerning the well's future are made. However, using capping as an initial control technique was not used in the OCS. This was most likely due to limited location size and the difficulty of maneuvering capping equipment around on the open water or on the seafloor.

**Fig. 1.12** reveals 48 percent of OCS blowouts were controlled by simply letting the blowout go. Thus bridging (39%) or depletion of the reservoir (9 %) occurred. The remaining kill methods employed were evenly distributed with pumping mud or bullheading being the next highest at 19 percent.

#### **1.4 Blowout Control Measures**

There are many different ways to control a blowout. Since each blowing well is a unique situation, new techniques are often made up on the spot. An example of this on-the-fly engineering was seen in Kuwait with the Hungarian MIG jet-engines or "Big Wind" machine which controlled the blowout's fire with a blast of jet-wash. However, there are several more conventional and accepted forms of blowout control which are divided into surface intervention methods and subsurface intervention or relief well methods.<sup>8</sup> The most common methods in these two classifications are:

Wellhead equipment installation/operation

- Capping
- Wellhead equipment installation/operation
- Cement/Gunk plug
- Bridging
- Depletion/flooding of reservoir
- Momentum kill/bullheading
- Dynamic kill

Capping operations occur when the blowout is controlled at the surface. Capping operations can be divided into three separate phases<sup>9</sup>:

- Extinguishing the fire
- Capping the well
- Killing the well

If the well is on fire, then the first phase of capping will be to extinguish it. Exceptions to this case occur if there is any chance of danger to the personnel on location from the blowing fluids. The best example of this is the presence of H<sub>2</sub>S or hydrogen sulfide. H<sub>2</sub>S is extremely toxic and is therefore flared to avoid problems. Extinguishing the fire may be done with any number of methods ranging from large amounts of water to dynamite.

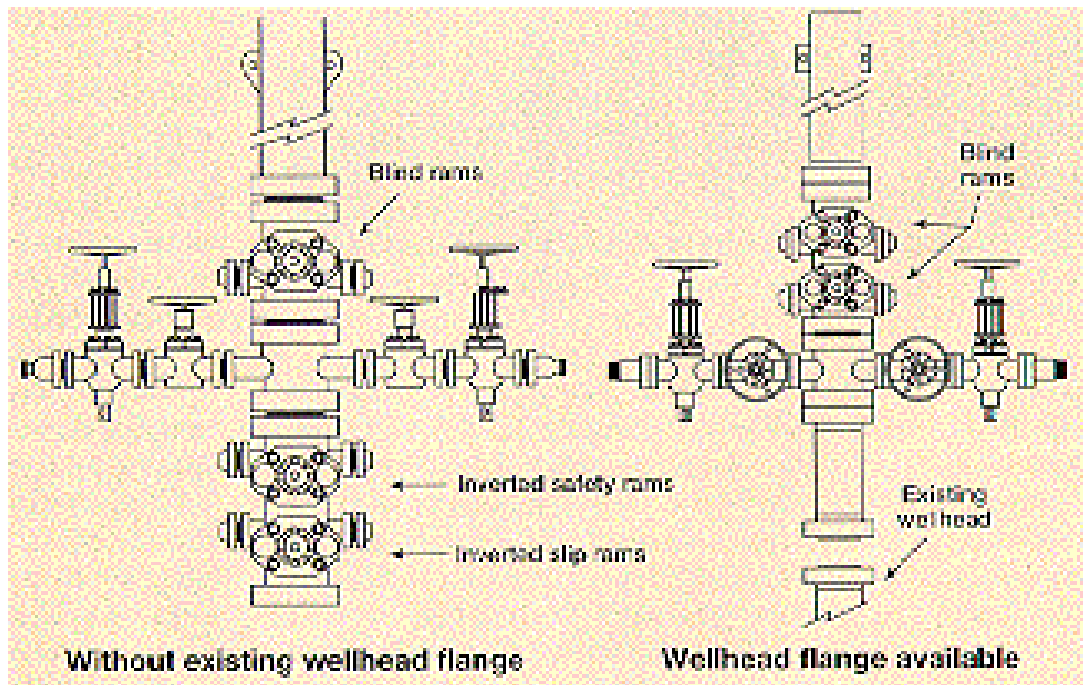


Fig. 1.13 – Typical capping stacks.<sup>8</sup>

Once the flare has been extinguished, the actual capping of the well is started. A capping stack is attached to the wellbore. The typical capping stack will consist of a bell nipple, several rams, a diverter spool and possibly a ball valve (**Fig. 1.13**).<sup>8</sup> Normally a flange of some type will still be on the wellbore. If there is no available flange for attachment, a flow cross-over prepared from an inverted pipe ram and a slip ram will be used to attach to bare pipe.<sup>8,9</sup> The capping stack is then maneuvered onto this flange or bare pipe. Once the capping stack is secured, flow will be diverted in a safe manner, either in a single vertical plume or through a diverter line. In situations where flow rates are high enough, the diverter line may be an emergency sale line.<sup>8</sup> This would reduce the economic loss caused by the blowout.

After the capping stack is successfully installed, the flow is diverted to a location some distance away from the wellhead using the rams and diverter spool in the capping stack.<sup>10</sup> The diversion of flow allows the well control operations to take place safely around the wellhead. The well control operations typically consist of pumping a heavy mud down the wellbore in an attempt to regain hydrostatic control of the well.<sup>9</sup> Capping is not applicable for use in ultra-deepwater situations because the blowing fluid must be coming to the surface. As will be discussed later in this report, the marine riser in ultra-deepwater situations has a good chance of failure in this event thus rendering capping useless.

Wellhead equipment installation and operation is a simple method that is usually employed in response to a very poorly handled blowout. To control a blowout through this method, blowout specialists will reenter the location or platform and operate or install the equipment necessary to shut-in the well safely. There are several instances in OCS files where rig personnel abandoned the rig before being able to operate the BOP. In these cases, the blowout was controlled by simply closing the BOP.<sup>11</sup> In cases of equipment failure, the blowout specialists need to remove the malfunctioning equipment and install new equipment. Once this is accomplished, the new equipment will be used to kill the blowout.

Fast-acting cement and gunk plugs are the least desirable of the blowout control alternatives. They are used in the event of an underground blowout to stem the flow of blowing fluids into the formation. Either compound is introduced into the wild wellbore from the wellhead, capping stack or, if necessary, from a relief well. Fast-acting cement is a cement compound mixed with an accelerant.<sup>12</sup> The hoped-for result is that the cement will set in the wild wellbore before exiting the said wellbore into the formation. This will stop the flow to the thief zone and allow the well to be effectively killed from the surface. Gunk and invert-Gunk are used with the same goal in mind. Gunk is mixture of cement, bentonite and diesel fuel. The mixture is stable until mixed with any type of water-based mud. Upon mixing with water, Gunk forms a thick gelatin plug.<sup>12</sup> Salt Gunk has guar and lost circulation material and reacts in the same way with saltwater.<sup>12</sup> Invert-Gunk is made with amine clay and water and reacts with oil-based muds. All of the Gunk products have a “bread-like” texture that is very drillable. However, long Gunk plugs are capable of handling large differential pressures.<sup>12</sup> The problem with Gunk and cement is an obvious one: they are permanent. If the plug is placed wrong, whether in the drillstring or above the thief zone, the damage is considered irreparable. A poorly spotted plug usually results in loss of the blowing wellbore and necessitates a relief well. Even a properly spotted plug can cause disastrous results. If the pressure behind the plug builds up high enough, a new thief zone may be created. However, because the plug is fairly permanent, wellbore or vertical intervention is not an option after a plug has been pumped. Thus, the more expensive and time-consuming option of a relief well must be used.

Bridging and depletion of the blowout are not active methods for blowout control. However, since they do account for the majority of kills, a mention is needed. Some studies have shown that blowouts likely to bridge will do so in 24 hours.<sup>13</sup> Once the 24 hours mark is reached, bridging will not occur unless triggered by another intervention method through active bridging.<sup>13</sup> The bridging will occur due to factors including near-wellbore pressure draw down, erosion of wellhead equipment, and formation failure due to high flow rates. The first simulator to be developed in the study this report is part of

deals exclusively with bridging and will cover this in much greater detail. Passive bridging is an always hoped-for solution because it does not require any work, and the only resulting economic losses are from the blowout itself. This being said, most blowout contingency plans require a planning and observation period after evacuation of the rig. During this period, the well is monitored for bridging. This negates a need to allow more time in a contingency plan for the wellbore to bridge.

Bullheading and momentum kills are very similar in process. Bullheading attempts to pump into the wellbore, push the blowing fluids back into the reservoir and finish with a wellbore full of kill-weight fluid.<sup>8</sup> Bullheading is the most common method of containing onshore blowouts, and ranks third in OCS blowouts.<sup>7</sup> The reason behind this statistic is the simplicity of the method and the ready availability of the necessary equipment on any drilling rig. The only problem with bullheading is the formation typically fractures during the process. If the mud thief zone is too shallow, not enough hydrostatic pressure will exist to control the blowout. Therefore, this method is best suited to deeper cased holes or blowouts with short open-hole intervals.<sup>8</sup> In ultra-deepwater situations, some leniency concerning the thief zone depth is given due to the hydrostatic pressures exerted by the seawater. This hydrostatic pressure may also save a bullheading operation that fractures a shallow formation.

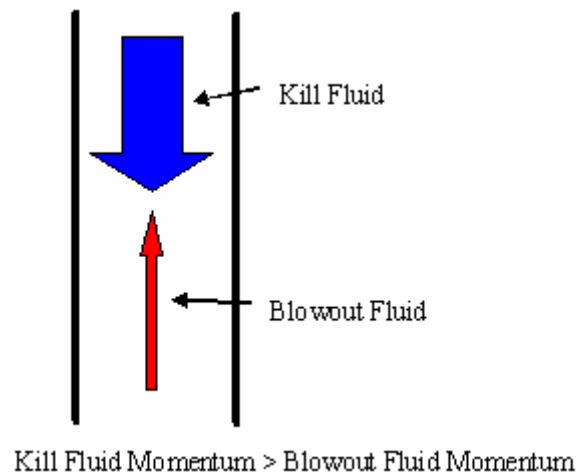


**Fig. 1.14 – Momentum kill theory.**<sup>8</sup>

Momentum kills are a compromise between dynamic kills and bullheading. In fact, many dynamic kill attempts mentioned in literature are actually momentum kills. Momentum kills are reserved for blowouts where the weight of a fluid alone can not force the fluid down the blowing wellbore. The purpose of the momentum kill is to force the kill fluid down the wellbore by creating a momentum overbalance. Using higher pumping rates in conjunction with high mud weights, the momentum of the blowing fluid can be overcome.<sup>8</sup> Of course, once the blowing fluid has been forced back into the reservoir, adequate hydrostatic head must be maintained to keep the blowing formation in check. Momentum kills can be difficult to model, as some simulators do not recognize that, even though the theoretical hydrostatic pressure of a column of kill mud may kill a well, the mud is unable to make it down the blowing wellbore based on weight alone. This report will not cover momentum kills for ultra-deepwater due the simulator's inability to model them and because the setup and planning for a momentum kill is essentially the same as a dynamic kill.

Relief wells can be drilled with several objectives in mind. The first objective is that they never be used. This is simply due to the time and cost involved in a relief well. Usually relief wells are spudded early on in a blowout when the possibility they might be

needed arises. While relief wells are being drilled, surface intervention techniques are still being attempted. If the surface intervention succeeds before the relief well total depth (TD) is reached, the relief well will often be drilled and completed as a producing well.<sup>14</sup> If the relief well is used to control the blowout, waterflooding, depletion, momentum kills, and dynamic kills are the methods used to kill the blowout.

If the relief well reaches TD it may be used for several purposes. All relief wells drilled before the late 1970's and some of the relief wells drilled after deal with the reservoir in two ways: flooding and depletion.

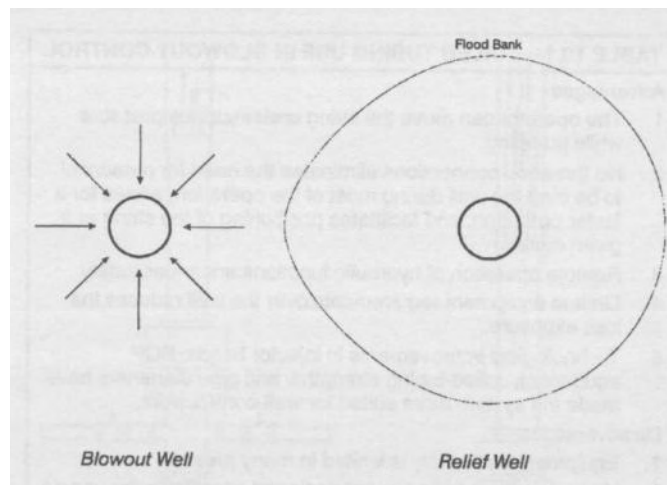


**Fig. 1.15 – Blowout control through flooding is a lengthy process.<sup>8</sup>**

Killing a blowout through flooding is a lengthy process. This was first accomplished in 1933 and was the standard use of relief wells until the 1970's.<sup>15</sup> The basic concept is to pump a volume of water into the reservoir that is significant enough to severely reduce the relative permeability of hydrocarbons to water.<sup>8</sup> **Fig. 1.15** shows the waterflood does not take as long as a normal waterflood to reach the blowing well. This phenomenon is due the high flow rate of the blowing well causing the waterflood to favor a flow path towards the blowing well.<sup>8</sup> This reduces the time needed to achieve

breakthrough. The waterflood needs to achieve breakthrough before the blowout can be killed. The bottomhole locations of the blowing wellbore and relief well are shown in **Fig. 1.16**. Three problems exist with implementing a waterflood kill. The first is obtaining an accurate reservoir model, which may not be possible with blowouts on exploration wells. The second concern is that the reservoir permeability must be high enough that the waterflood occurs in a reasonable amount of time and with a reasonable volume of water reaching breakthrough. Finally, the third problem is with pressures. If the fracture pressure is exceeded and a fracture begins to propagate, the waterflood will not be drawn towards the blowing well, but away from it along the fracture. On the other hand, the waterflood pressure must be high enough to overcome the static reservoir pressure in order to drive the waterflood.<sup>8</sup>

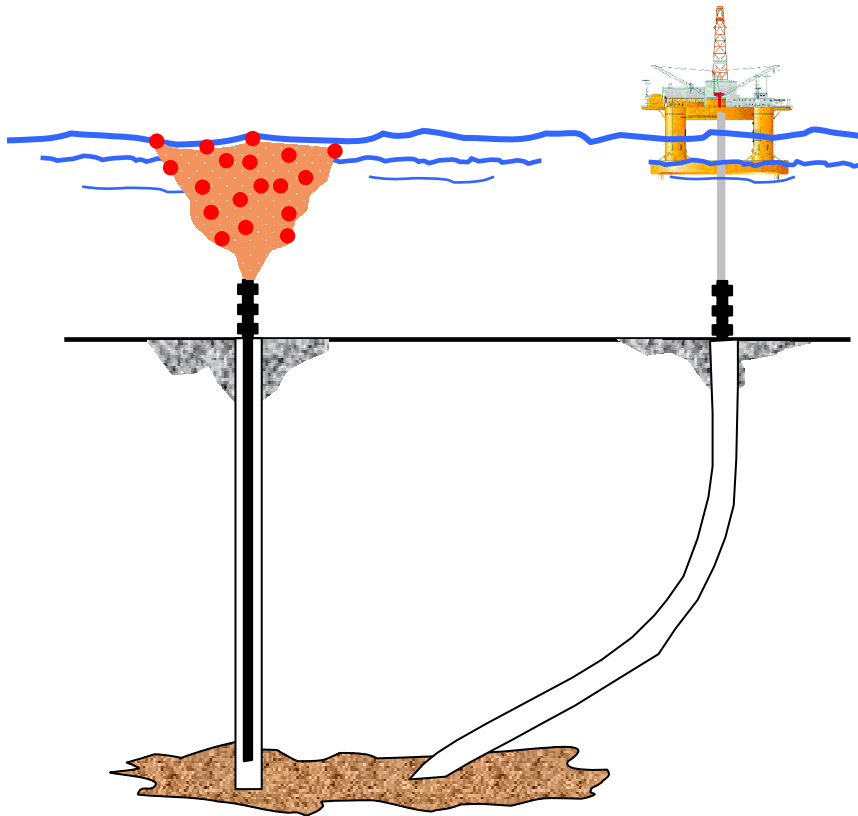


**Fig. 1.16 – Depletion kill or waterflood relief well bottomhole location.**

A depletion kill is a simple process entailing exactly what the name implies. For a depletion kill relief well, the relief well bottomhole locations are placed as close to possible to the blowing well open-hole section as seen in **Fig. 1.16**. The relief well is then turned into a producing well, with production rates as high as flaring or emergency sale lines can handle. The idea behind these actions is that the relief well production will deplete the reservoir around the blowing well and cause the blowout flow to subside or stop.<sup>8</sup> Surface intervention methods would then be applied to permanently kill the blowing well.

In 1978, Mobil Oil had a 400 MMscfd gas blowout of a well in Indonesia's Arun field. Instead of taking the expected one year or more to kill, the blowout was controlled in 89 days.<sup>16</sup> A new technique invented by Mobil Oil engineers was the reason for the quick kill: dynamic kill. The dynamic kill method is applied through a relief well which has intersected and entered the blowing wellbore as close as possible to the flowing zone as seen in **Fig. 1.17**. The dynamic kill method uses a kill fluid, typically salt water if offshore, which by itself does not have sufficient hydrostatic head to control the influx. However, when the kill fluid is pumped through the relief well and up the annulus of the blowing well, high pump rates create additional frictional pressure. This frictional pressure supplements the hydrostatic pressure of the kill fluid creating a pressure overbalance which stops the influx.<sup>8</sup>

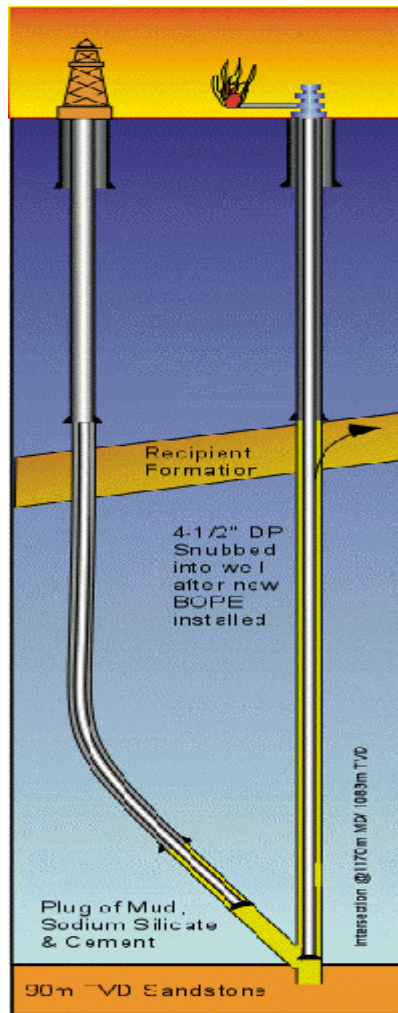


Fig. 1.17 – Relief intersection point allows maximum use of frictional pressure.<sup>17</sup>



**Fig. 1.18 – Control of large blowout completed using dynamic kill in approximately 12 minutes.**<sup>18</sup>

**Fig. 1.18** illustrates the dramatic kill sequence of blowout in Syria killed dynamically. The series of pictures in **Fig. 1.18** occurred over the span of twelve to fifteen minutes and shows graphically how several months of drilling a relief well culminates in a brief period of pumping kill fluid at high rates. Once control of a blowout has been gained with the light kill-fluid, a heavier mud is then pumped into the relief well. This mud should be capable of statically controlling the well with its hydrostatic pressure.

Dynamic kills are ideal for several situations. The first type of situation is one like the 1978 Arun field blowout. The key indicator for the suitability of a dynamic kill

was the high flowing rate. Some blowouts have even required multiple relief wells pumping simultaneously due to extreme blowout flow rates.<sup>19, 18</sup> In these wells, it is not possible to get the equipment in position for other kill methods such as bullheading, much less attempt to enact these other techniques. The dynamic kill method theoretically allows for multiple wells to control an infinitely large blowout. While in reality this is not practical due to pumping and other equipment requirements, the fact remains that the dynamic kill technique is often the best choice in high-flow rate or hard to access blowouts.

For other cases, the fracture gradient may be relatively low. Methods such as bullheading and momentum kills as well as surface intervention methods may raise wellbore pressures above the fracture pressure. This could lead to an underground blowout and complicate the blowout kill process. The dynamic kill method uses pump rates as the final push to overcome the wild well bottomhole pressure. Thus, the pump rates can be manipulated to stay within narrow pore pressure and fracture pressure differentials.<sup>8</sup> In fact, the dynamic kill itself typically causes minimal downhole damage. The subsequent static control method can be tailored to keep the wild well in production condition. In this manner, the operator can restart production either through the relief well or the wild well in a relatively short period of time.

The path for the flow of the kill fluid is down through the annulus of the relief well and out and up the wellbore of the wild well. Another possible path, particularly in deepwater is down a drillstring in the wild well, and back up the wild well annulus. This is because the dispersal of the blowing fluids is sufficient to allow well control vessel operation directly above the blowing well.<sup>20</sup> These paths are theoretical paths, as there is evidence fluid fallback occurs.<sup>21,22</sup> This is discussed further in the “Future Research” section of this thesis. However, the assumption that no fluid fallback occurs is a proven, valid assumption that merely overestimates the kill-rates required.<sup>21,22</sup>

### 1.5 - Kill Method Selection

Fighting blowouts is best left to specialists with years of experience. These specialists make decisions based not only on the parameters of the situation, but also on their personal experience. That being said, although there is an art to choosing a blowout method, there is a definite decision making process in selecting a blowout control method. **Figs. 1.19 (a-d)** show a kill method selection flowchart from Adams and Kuhlman<sup>9</sup> which shows the decision making process. Certainly the process is an exhaustive one which requires a lot of experience and knowledge.

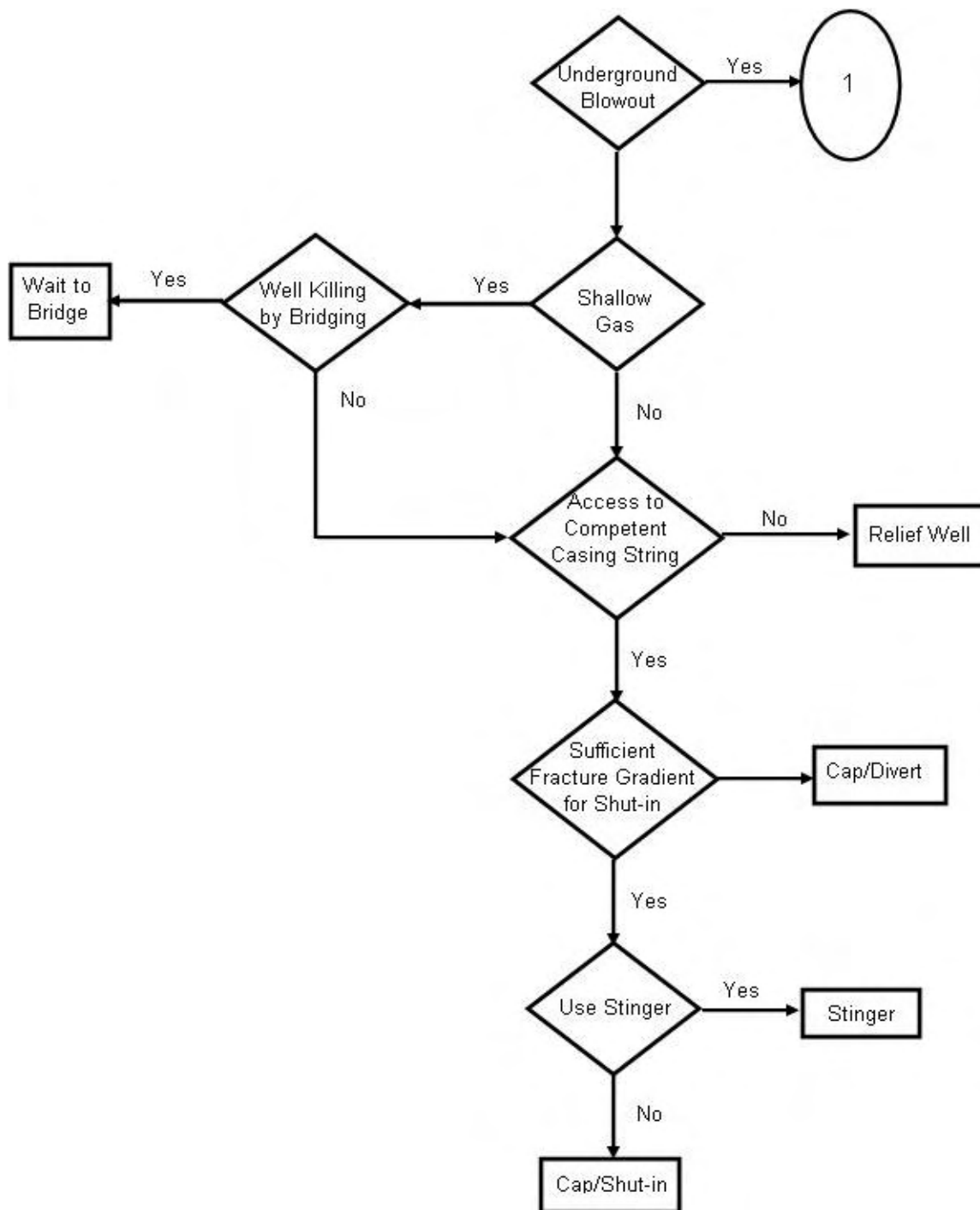


Fig. 1.19 (a) – Example kill method selection flowchart I.<sup>9</sup>

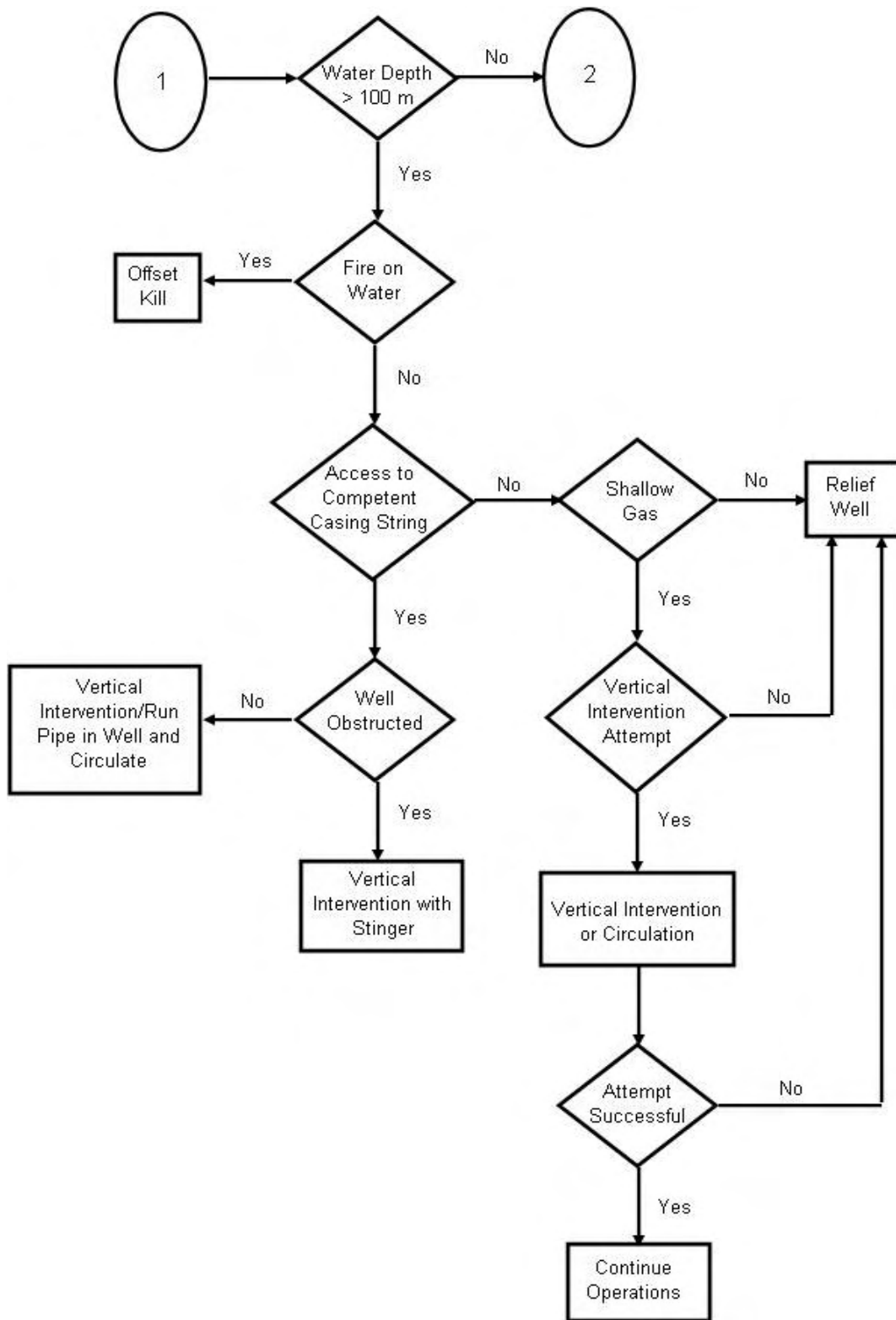
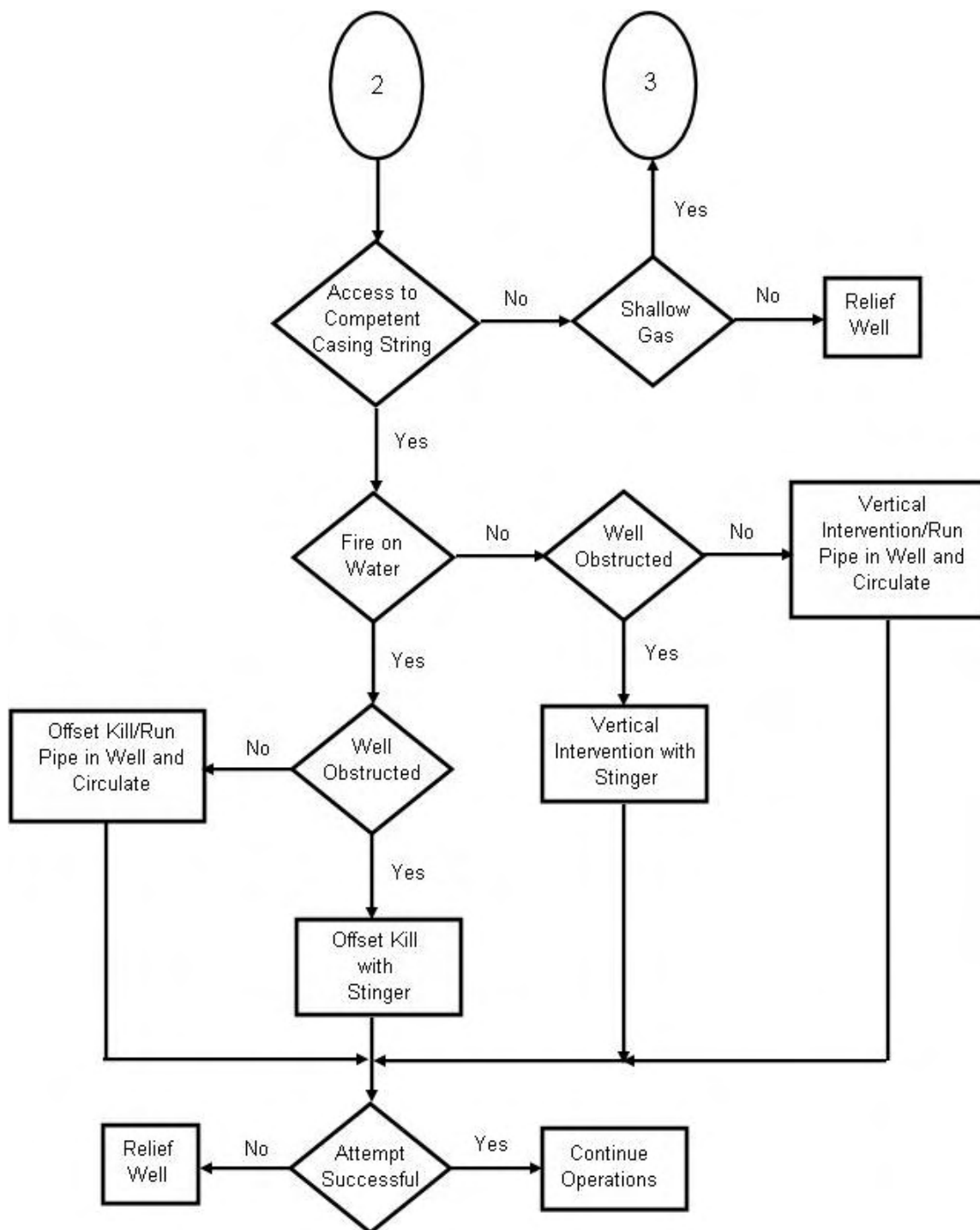
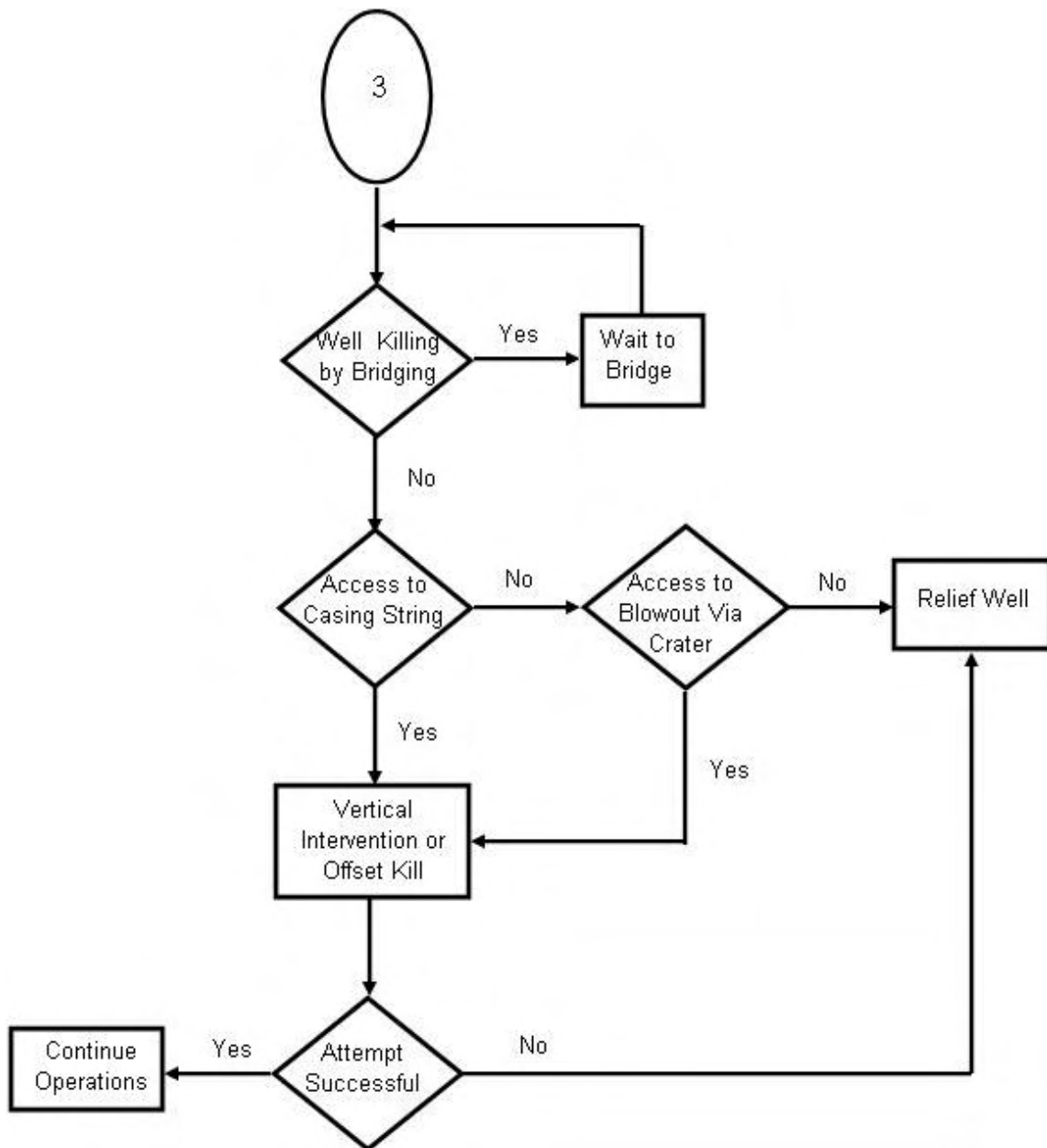


Fig. 1.19 (b) – Example kill method selection flowchart II.<sup>9</sup>



**Fig. 1.19 (c) – Example kill method selection flowchart III.<sup>9</sup>**



**Fig. 1.19 (d) – Example kill method selection flowchart IV.<sup>9</sup>**

## CHAPTER II

### RESEARCH BACKGROUND

#### 2.1 Proposal Background and Objectives

This study is part of a larger overall study originally submitted to the United States Minerals Management Service (MMS)<sup>23</sup> and later to the Research Partnership to Secure Energy for America<sup>24</sup> (RPSEA). The intent of the study was to develop up-to-date blowout prevention and control procedures for ultra-deepwater through modeling. The last major works in this area were publications such as *DEA-63: Floating Vessel Blowout Control* published by Neal Adams Firefighters in 1991.<sup>13</sup> These studies concentrated on water depths from 300 to 1500 feet with some slight consideration given to water depths greater than 1500 feet. At the time they were written, wells in water depths over 5000 feet were considered “one-off” wells that required years of planning and design. Publications covering this topic put forth the idea that a relief well for one of these “one-off” wells might not be realistic due to planning required and technology at the time of publishing.<sup>13</sup> However, in the past 13 years many advances in the deepwater drilling industry have been made and the limiting assumptions used in these studies are no longer valid. Since 1992, 1583 wells have been drilled in water depths exceeding 1500 feet and 328 wells were drilled in water depths greater than 5000 feet.<sup>25</sup> On January 7<sup>th</sup>, 2004, Chevron U.S.A., Inc. reached total depth on a Gulf of Mexico Well in 10,011 feet of water, a new world record.<sup>25</sup> Studies done in the early 1990’s also were not in a position to account for the many new drilling technology developments which have taken place over the last 13 years such as dual gradient drilling.<sup>26-28</sup> In short, studies to date are comprehensive concerning floating vessel blowout control and are still valid for the majority of offshore drilling and blowout situations. However, they do not cover all of the drilling and potential blowout scenarios possible today. Therefore, the purpose of this study was not to supplant these studies, but to supplement them and other industry blowout prevention and control best practices to cover the new drilling environments and technologies which exist today.

The proposed overall study was to begin the development of two simulators. The first simulator is concerned with the bridging tendencies of ultra-deepwater blowing wells. Deepwater Gulf of Mexico sediments are widely known to be unconsolidated. The prevailing theory is that the majority of blowouts in ultra-deepwater would therefore bridge and surface or subsurface intervention methods would not be necessary.<sup>24</sup>

The next simulator, COMASim, models the initial blowout conditions and the subsequent dynamic kill necessary to kill the wild well. The simulator is capable of modeling either a drillstring kill or relief wells to kill the blowout. A key feature of the simulator is that it is written in Java code which allows it to be easily accessed from the internet. The initial version of the simulator and a report were described by Oskarsen in 2004.<sup>29</sup>

The final portion of the study is to develop a series of best practices for ultra-deepwater drilling and blowouts. The initial intent was to develop the simulator first, then develop the best practices. However, due to longer than expected simulator development times as well as other time constraints, this part of the study began despite the simulators not being fully completed and debugged. The new intent of this project was to assist in the final development and debugging process of COMASim by running case histories and theoretical base cases as best practices were developed.

## **2.2 Thesis Objectives**

The objectives of this study were as follows:

- Validate the dynamic kill simulator through test cases and case histories
- Run test cases through dynamic kill simulator (COMASim)
- Using simulator results develop best practices recommendations for ultra-deepwater blowout prevention and control.

The validation of the simulator took place using two methods. The first involved running several case histories through the simulator. Attempts were made to match the simulator output with the real-life data. In the likely event the simulator output did not match the case history, differences were pinpointed. Then, the reasons for these

differences were identified. When using case histories, there always exists the distinct possibility that real-life data was recorded erroneously. When controlling a blowout, minimization of risk and loss is of utmost importance, while gathering data for future research is secondary. Therefore, if no case histories' results were able to be matched using the dynamic kill simulator, the study moved on to the next option for validation. This step involved using largely theoretical cases' results as comparison material. Although invented, these theoretical cases were realistic in wellbore and drillstring sizing and reservoir properties. However, some type of validation needed to occur, whether theoretical or case-history based in order for us to have any confidence in the later results.

The next steps in this portion of the study, running base cases, were a simple yet time consuming process. Base cases were chosen using a range of total vertical depth (TVD), water depth, wellbore size and drillstring size values. These base cases were then input into the dynamic kill simulator first to establish pressure profiles for the initial blowing conditions. Once the initial conditions had been established, the next step was to find a dynamic kill rate in COMASim based on several relief well or drillstring values. The last step in this phase of the study was to develop a set of ultra-deepwater best practices. These were conceptual best practices. This was because COMASim is a simple simulator with a relatively quick run time. The best practices dealt with new technologies such as dual-gradient drilling as well as new environments, specifically water depths from 5000 feet to 10000 feet deep. Wherever possible, the best practices were developed in such a way that the end-user could seamlessly integrate the new best practices with those already in place throughout the industry.

### **2.3 COMASim Background**

COMASim is a Java code based program simulating blowout initial conditions and dynamic kill requirements. The Java programming language was selected due to its versatility. Java is a language with platform independence. This gives potential COMASim users the capability to run COMASim from various platforms and operating

systems. Of particular interest to potential users is the fact that COMASim is capable of being run from a web-based application.<sup>29</sup>

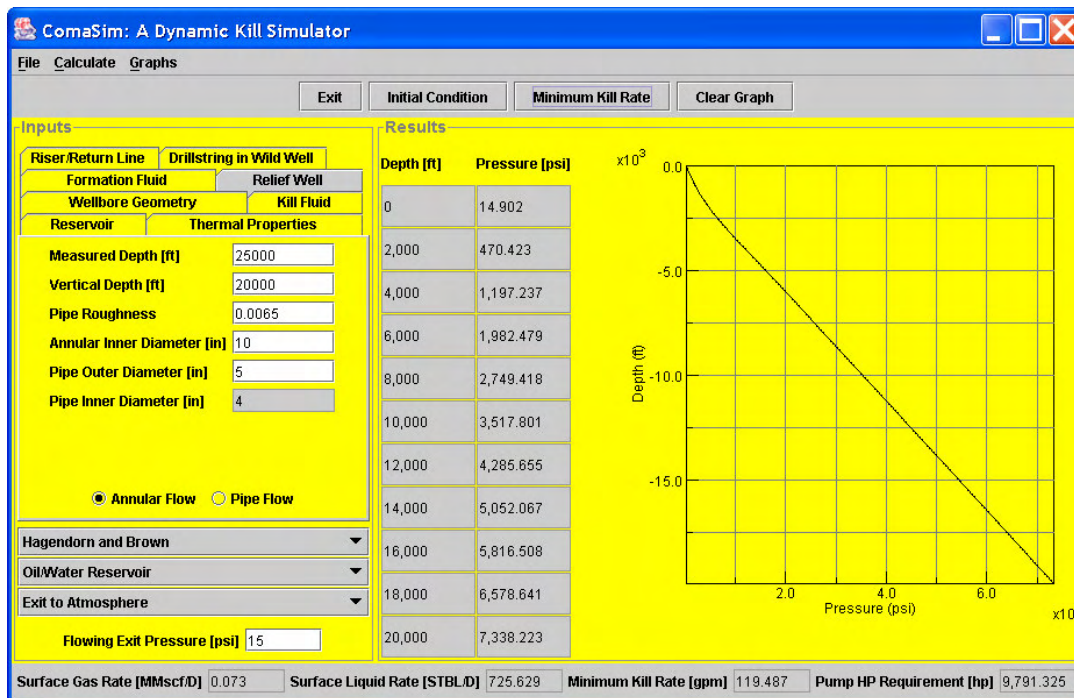


**Fig. 2.1 – Screen shot of COMASim interface shows simplicity of operation.**

COMASim's interface is designed for simple operation that would require a minimum of page refreshes during web operation.<sup>29</sup> **Fig. 2.1** illustrates the single page interface with both the input and output on the same page.

## 2.4 Simulator Calculations

COMASim calculates the initial conditions, then calculates the required flow rate of kill fluid for a dynamic kill. The initial conditions are based on multiphase calculations and use the concept of system or nodal analysis which is illustrated in **Fig. 2.2**. Once the IPR curve has been determined for a blowing wellbore, the kill rate can be determined. Successive iterations of a system curve encompassing the blowing wellbore

during the kill operation will converge to a final solution. This is shown graphically in **Fig. 2.3**. The initial inflow performance relationship curve or IPR curve is calculated using a multiphase model.

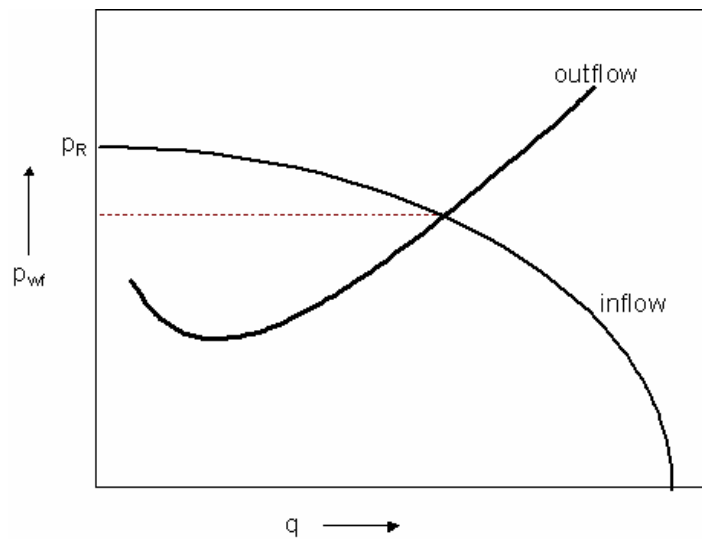


**Fig. 2.2** – Graphical example of general nodal analysis calculation.<sup>29</sup>

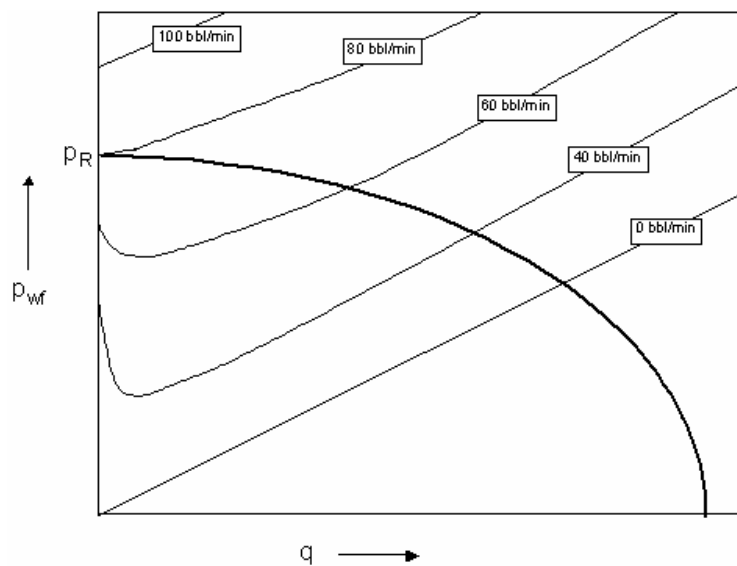


**Fig. 2.3** – Example of use of nodal analysis to find required dynamic kill rate.<sup>29</sup>

There are three possibilities for multiphase models, one of which is selected by the user:

- Hagendorn and Brown
- Beggs and Brill
- Duns and Ros

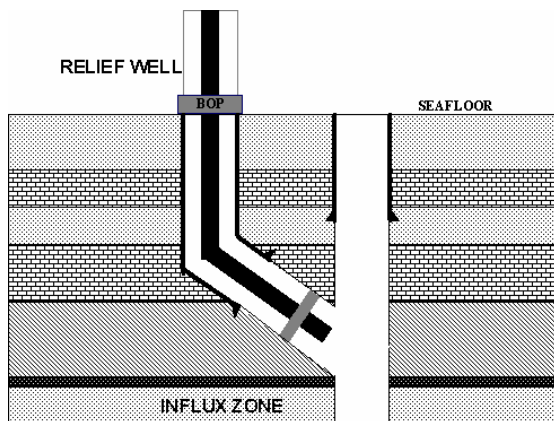


Fig. 2.4 – No drillstring in wild well.<sup>29</sup>

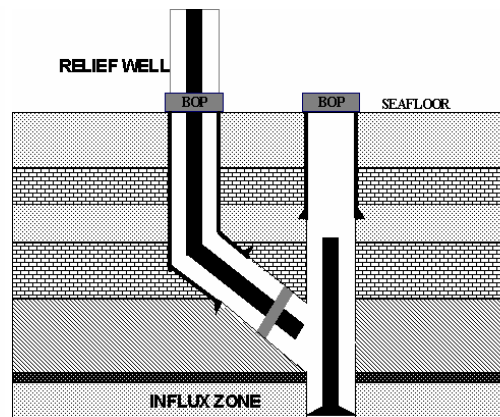


Fig. 2.5 – Drillstring dropped.<sup>29</sup>

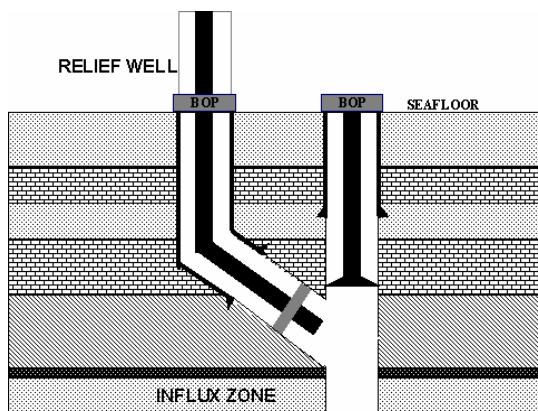


Fig. 2.6 – Drillstring hanging from BOP.<sup>29</sup>

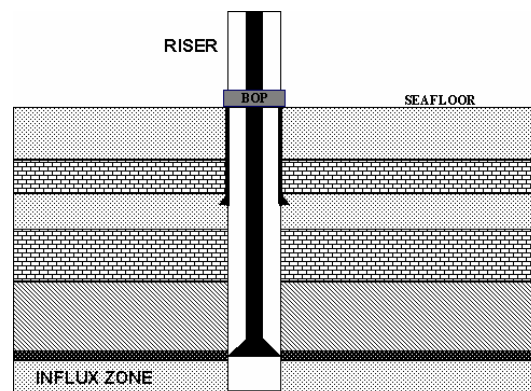


Fig. 2.7 Drillstring used to kill well.<sup>29</sup>

In addition to the multiphase model selection, the user also chooses between liquid or gas reservoir and the exit point, either to the mudline or to the surface. Drillstring options for the wild well cover all possibilities:

- No drillstring (**Fig. 2.4**)
- Drillstring fallen to bottom (any length possible) (**Fig. 2.5**)
- Drillstring hanging from BOP (any length possible) (**Fig. 2.6**)
- Drillstring snubbed in to attempt dynamic kill (any length possible) (**Fig. 2.7**)

**Table 2.1 – Input options for COMASim.**

<b>Marine Riser</b>	Riser OD	Riser ID	Heat transfer coefficient	Surface roughness				
<b>Riser Buoyancy Material</b>	Material OD	Depth of Material	Heat transfer coefficient					
<b>Wild Well Drillstring</b>	Drillpipe OD	Drillpipe ID	Drillpipe length	Drillpipe roughness	Drill collar ID	Drill collar OD	Drill collar length	
<b>Wild Well Drillstring Options</b>	No drillstring	Drillstring hanging from BOP	Drillstring dropped to bottom	Kill with drillstring				
<b>Wild Wellbore Geometry</b>	Total vertical depth	Casing depth from MSL	Water depth from MSL	Open hole ID	Open hole roughness	Casing ID	Casing roughness	
<b>Formation Fluid Options</b>	Gas and oil gravities	Bubble point pressure	H2S, CO2, N2 concentrations	Water gravity and salinity	Specific heat of formation liquid			
<b>Reservoir Properties</b>	Average reservoir pressure	Exit pressure	Permeability	Drainage area	Height of reservoir	Gas Oil ratio	Water cut	Flowing time of blowout
<b>Thermal Properties</b>	Thermal gradient	Exit temperature of fluid	Constant volume and pressure specific heats	Formation thermal conductivity	Formation thermal diffusivity	Heat transfer coefficient	Joule-Thompson coefficient	Straight-line or Newtonian fluid
<b>Kill Fluid</b>	Mud weight	Yield point	Plastic viscosity	Salinity	Surface temperature of kill fluid			

The term simple has been applied to COMASim in this section several times. It can certainly be seen from **Table 2.1** that this is a relative term. COMASim's available inputs are more than adequate to handle the large majority of case histories and test cases available. In fact, as with most simulators, using COMASim will require users to assume values for many parameters. A further investigation into the programming and theory behind COMASim are available in Oskarsen's 2004 report.<sup>29</sup>

## CHAPTER III

### COMASIM RESULTS AND ANALYSIS

#### 3.1 COMASim Simulation Input Values

The input values for COMASim were chosen after careful consideration. First, I chose a gas blowout as the default. As will be shown later on, COMASim was calibrated with a pseudo case history from Watson, et al.<sup>8</sup> Since I was unable to obtain a verification of COMASim from any other sources, I based the simulation run inputs on the Watson case that verified the simulator. This case was a gas blowout which allowed me to use the gas reservoir option. Since the ultimate goal of this study is to consider deepwater blowouts, I chose the “exit to mudline” rather than the “exit to atmosphere” exit point. In a deepwater blowout situation, the drillship will disconnect the riser and evacuate the area to avoid danger to equipment and personnel. The ratings and locations of BOPs and risers are the main reasons that drillships will move off the location in the event of a blowout.

BOPE (blowout preventer equipment) is normally located on the seafloor for floating drilling. This reduces the weight of drillstring requiring support as well as reducing the drillship’s weight. Risers are also not rated for high pressures. This allows the riser assembly to be lightweight, increasing the capacity of the drillship to store longer lengths of riser material.

I chose the formation fluid to be a pure gas with no H<sub>2</sub>S, CO<sub>2</sub>, or N<sub>2</sub> content and having a specific gas gravity of 0.6. These values were again chosen to coincide with the matching case history. In the Watson, et. al.<sup>8</sup> example, the pore pressure gradient is 0.624 psi/ft. I decided to round this gradient off to 0.6 psi/ft and use it for all of my cases. Thus, I have a constant pore pressure gradient regardless of the TVD or water depth. To match the initial blowing conditions of the Watson case history, I manipulated the permeability, drainage area and pay zone thickness and arrived at values of 10 md, 10,000 acres and 100 ft respectively. These are not typical values for Gulf of Mexico ultra-deep water reservoirs. A typical reservoir might have values of 100 md and only a

thousand acre drainage area. However, this was the only way to get the simulator to match up with the Watson example. Therefore I decided to keep the values the same as the only validating example I currently had. I kept the same values for the COMASim simulation runs with the exception of the reservoir height. The high cost of developing deepwater reservoirs currently means that only the larger reservoirs are being developed. I changed the reservoir height to 100 ft to more accurately depict a typical deepwater situation.

The blowing wellbore was setup to simulate drilling ahead after setting casing. During the drilling process, casing is often set before abnormally pressured zones are entered to protect other normally pressured zones. I assumed that a blowout while drilling ahead would be encountered in one of these abnormally pressured zones. I used a casing shoe depth of 500 feet less than the TVD to simulate this situation. I simulated three different casing sizes to account for different times in the drilling process. The first size I used was 8 5/8 inch OD, 44 lb/ft P-110 grade casing.<sup>30</sup> This size represents the production tubing in deepwater producing well. This casing size is slightly larger than is typically associated with production tubing, however deepwater wells will have multilateral construction and fairly high flow rates necessitating the larger casing sizes. The second size I used was 10 3/4 in OD, 60.7 lb/ft, P-110 grade casing.<sup>30</sup> This size would represent the liner or last string of intermediate casing in a large deepwater well. With an ID of 9.66 inches, bits and completion tools for multilateral construction could pass through leaving a small drift margin. The last casing size I used was 12 3/4 inch OD, 53 lb/ft. casing.<sup>31</sup> This is a non-typical size of casing, however I used it to keep the size difference fairly constant between the three casing sizes. This casing is a lighter weight casing suitable for lower pressured formations and could be used as surface casing in deeper holes due to its light overall weight. This light overall weight would guard against the parting of the casing string as it was lowered into the hole. The hole sizes were calculated from the Schlumberger Field Data Handbook to be 7.375 inches, 9 inches and 11 inches respectively.<sup>31</sup> The drillstring in this wellbore varied in length at 100%, 50%, and 25% of the TVD. I chose a 5 1/2 inch OD, 24.7 lb/ft drillpipe. The

slightly heavier 5 ½ in. drillpipe was chosen to account for increased downhole pressures as well as being able to support long drillstring lengths without parting.

The surface temperature was assumed to be 70 °F as stated in the Watson example. The geothermal gradient was 1.5 °F/100 ft. with an exit temperature of the flowing fluid of 120 °F. The kill fluid weight was assumed to 8.5 lb/gal. The kill fluid was assumed to be brackish water. Pure Gulf of Mexico seawater hydrostatic can be considered to be slightly higher in the area of 8.6 lb/gal. However, I chose a slightly lower weight to build a safety factor into my results. The higher weight of seawater would result in a lower kill rate. The characteristics of the relief well needed to deliver this fluid depended on the TVD of the blowing well. I assumed that the relief well always intersected at the TVD of the blowing well. From there, I used ratios of 1, 1.5 and 2 for the Measured Depth/TVD of the relief well. For each of these ratios, I calculated kill rates for Annular ID/ drill pipe (DP)<sub>relief well</sub> OD ratios of 2 and 1.5. I assumed a constant drillpipe OD of 5 inches, meaning the annular ID was either 10 inches or 7.5 inches. The 10 inch annular ID scenario is much more likely in a real life situation. The planning of the relief well would include attempting to get the largest possible casing size at the intersection of the relief well and blowing well. This would maximize the flow capability of the relief well and minimize the standpipe pressure on the relief well. However, I included the 7.5 inch annular ID because unforeseen problems in the drilling of the relief well might necessitate the use of an additional casing string, thus lowering the annular clearance in the relief well. After investigation, I decided against the use of a drillpipe flow path in the relief well.<sup>32,33</sup> The drillpipe flow path is typically only used when snubbing into the blowing wellbore and attempting a dynamic kill without the drilling of a relief well. The reduction in available flow caused by using a drillpipe flow path would make many relief wells insufficient to control the blowouts.

After completing several hundred simulations, I realized there was a need to allow multiple relief wells. After working with Oskarsen to improve COMASim, it was made capable of calculating kill parameters for multiple relief wells from 1 to 99. I

initially ran each simulation for a single relief well. If the standpipe pressure exceeded 15000 psi, then I continued adding relief wells until the 15000 psi threshold was met. After 10 relief wells, I stopped the simulations due to the high improbability that 10 or more relief wells would ever be drilled.

I used the straight line temperature model and Hagedorn and Brown multiphase flow model because these models gave the most consistent results over a broad range of situations.<sup>34</sup>

### **3.2 COMASim Simulation Procedure**

The simulation runs were completed using a Dell laptop running Windows XP. The COMASim initial condition simulations were completed according to **Appendix A**. The runs were first split into 190 series. These series were based on drillstring status, wild well TVD, water depth, casing size and casing length. The data gathered in these 190 series included flowing rates and a pressure profile for each set of parameters. The results are shown in **Appendix B** and **Appendix D**. Once the initial condition runs were completed, 777 different blowout and relief well scenarios were run through COMASim. These scenarios were based on the original 190 initial conditions. Each of the series blowouts' were killed with various types of relief wells. The relief well Annular ID to drillpipe OD ratio and measured depth to intersection point ratio were varied. The minimum kill rate, stand pipe pressure and horsepower were recorded in **Appendix C** and **Appendix E**.



**Fig. 3.1 – Typical 15000 psi fracturing vessel.**<sup>45</sup>

In the event that the stand pipe pressure exceeded 15000 psia, further simulations were run to determine the number of relief wells needed to bring the stand pipe pressure down to 15000 psia or less. If 10 relief wells or more were needed, the simulations were stopped. The 15000 psi threshold was determined after a search for large offshore pumping units. All of the major suppliers of offshore fracturing equipment have vessels similar to **Fig. 3.1** which are listed at a maximum of 15000 psi working pressure.<sup>35</sup>

### **3.3 Validation of COMASim**

An extensive blowout data collection effort was undertaken at the beginning of this study. Sources of data were MMS incident and investigation reports, Matthew Daniels blowout data, Larry Flak of Boots and Coots and the Skalle, et al. database courtesy of Dr. A.L. Podio. Unfortunately, in all the available blowout case histories, either COMASim was unable to match the results or the case histories were so lacking in data that no attempt at matching was possible. While this was a setback, it was not unexpected. For example, the case histories courtesy of Larry Flak were of extremely high blowout rates from unusually productive reservoirs.<sup>36</sup> COMASim was programmed initially based on theory. So, since no simultaneous validation and programming solutions work has been attempted, the unusual case histories that are available are not able to be simulated. Future validation efforts should be focused on blowout case histories instead of theoretical validation.

COMASim has been validated theoretically. The initial condition curves validated by replicating the Beggs and Brill pressure profiles in *Production Optimization Using NODAL<sup>tm</sup> Analysis*.<sup>29</sup> The initial condition flow rates and kill rates were validated using examples from *Advanced Well Control: SPE Textbook Series Vol. 10*.<sup>8</sup> The blowout data given is **Table 3.1**.

**Table 3.1 – Blowout information for COMASim validation problem.**<sup>8</sup>

<b>Wellbore Configuration</b>	
Vertical depth	1770 ft
Perforation midpoint depth	11500 ft
Casing description	7 in., 29.0 lbm/ft, P-110
Casing nominal ID	6.184 in.
Casing capacity	0.037 bbl/ft
Perforation quantity and number	50 X 0.45 in
<b>Blowout Data</b>	
Formation fluid	Single-Phase Gas
Specific gravity	0.6
Specific heat ratio	1.27
Gas temperature at exit point	120 °F
Static pore pressure	12 ppg equivalent
<b>Other Known or Assumed Information</b>	
Fracture initiation gradient at perms	0.82 psi/ft
Fraction propagation gradient	0.73 psi/ft
Geothermal wellbore temperature	70 °F + 1.5 °F/100 ft
<b>Standard Measurement Conditions</b>	
Pressure	14.65 psia
Temperature	60 °F

Example 10.3 in *Advanced Well Control: SPE Textbook Series Vol. 10* calculates the critical flow rate of gas be 23.6 MMscf/D. COMASim gives flow rate of 24.95 MMscf/Day when run with the data in **Table 3.1**. Example 10.6 deals with relief well pumping requirements. *Advanced Well Control: SPE Textbook Series Vol. 10* deals in hand calculations throughout all of its examples and Example 10.6 is no exception. The method used in the text is a simple hand calculation known with the final answer

obtained with a zero-derivative solution.<sup>8</sup> This type of calculation significantly over calculates the dynamic kill rate as shown in **Fig. 3.2**. A detailed discussion of this topic is available in Oskarsen (2004).<sup>29</sup>

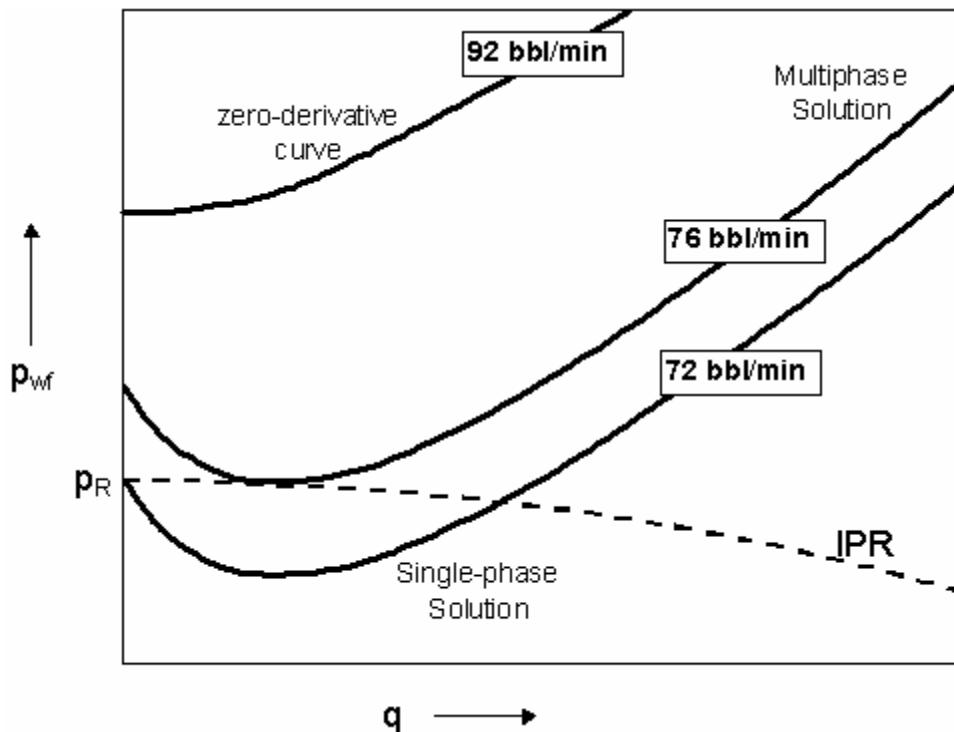


**Fig. 3.2 – Comparison of solution types shows zero-derivative curve grossly over calculates the dynamic kill solution.**<sup>29</sup>

COMASim calculated a dynamic kill rate of 78.5 bbl/min using a multiphase solution. Although Watson, et al. did not provide a multiphase solution to Example 10.6, the answer fits with the relationship between the zero-derivative answer provided and the multiphase solution COMASim calculated. Example 10.7 in *Advanced Well Control: SPE Textbook Series Vol. 10* provides a perfect match in with dynamic kill rates. The problem statement in Example 10.7 uses data in **Table 3.1** with several exceptions concerning the relief well. The measured depth (MD) of the relief well is changed to 11,950 feet and the annular ID and drill pipe OD are 8.535 inches and 3.5 inches respectively. Since Example 10.7 deals with simple hand pressure calculations, a kill

rate of 100 bbl/min is given in the problem statement as well. Apparently Watson, et al. used a multiphase model to make the problem more realistic. When COMASim ran the given data, it too came out with a dynamic kill rate of exactly 100 bbl/min. The agreement in values with Examples 10.3, 10.6 and 10.7 from *Advanced Well Control: SPE Textbook Series Vol. 10* indicates COMASim is theoretically sound. Therefore, the COMASim results discussed in this report can be viewed with a high degree of confidence.

### **3.4 COMASim Initial Condition Analyses**

COMASim was used to simulate 190 separate blowout situations. Each simulation resulted in a flowing rate and a pressure profile which are recorded in **Appendix B**. From these simulations several distinct trends were extracted. These trends can be predicted by anyone with a working knowledge of wellbores. By taking into account the frictional pressure losses and imposed pressures, the effect on a wellbore pressure profile can be predicted. However, while these trends are not ground-breaking, they do indicate COMASim is calculating the initial conditions of the blowout correctly.

COMASim's data output presented a significant problem during data collection. The graphing function for COMASim graphs a curve based on a large number of data points creating a smooth curve.

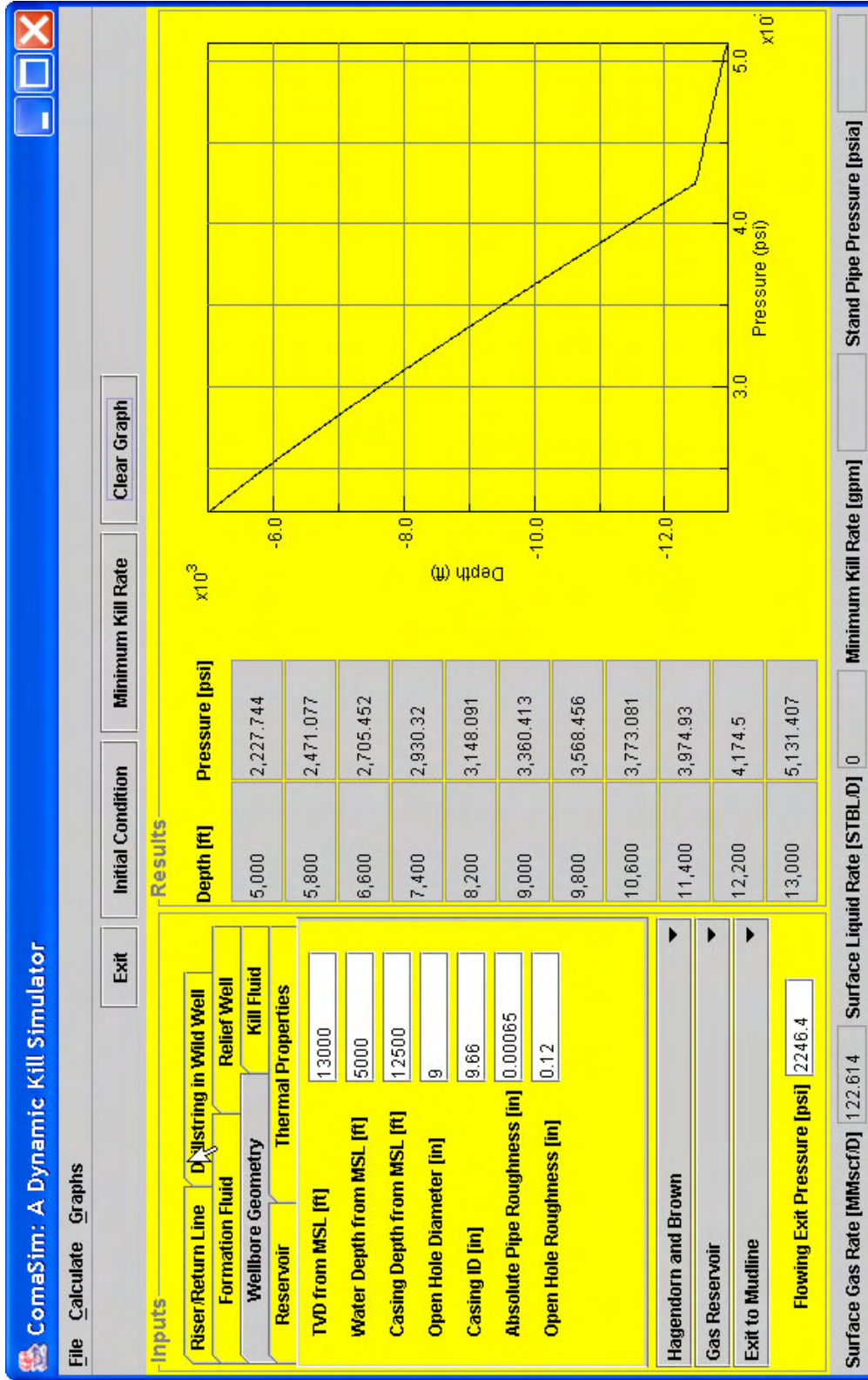
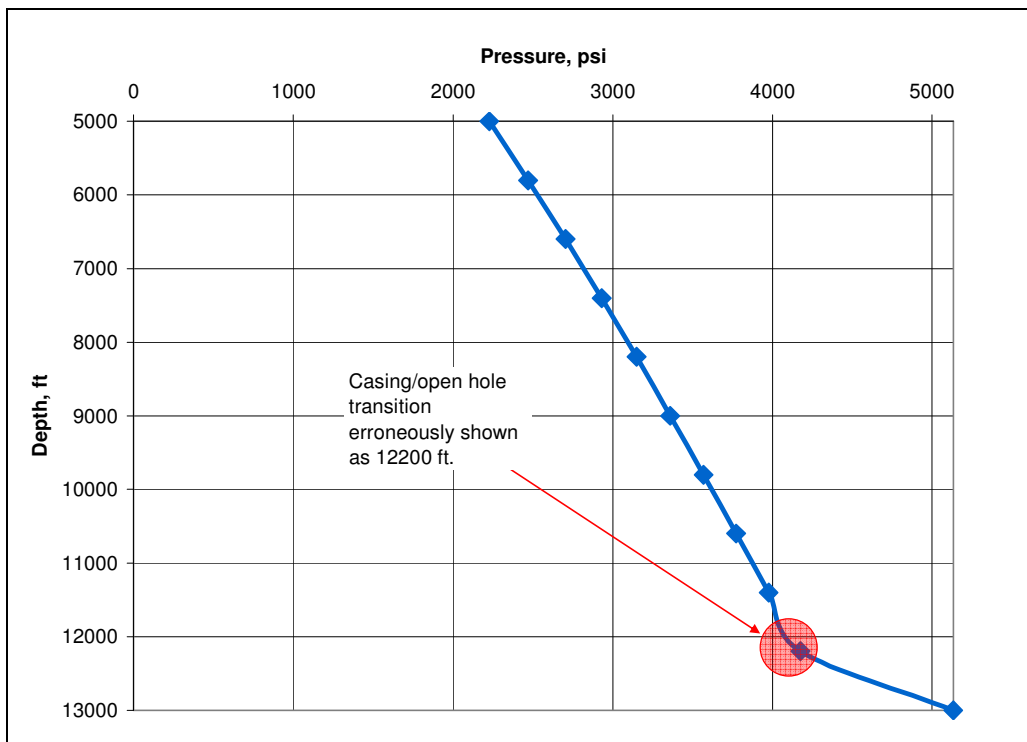
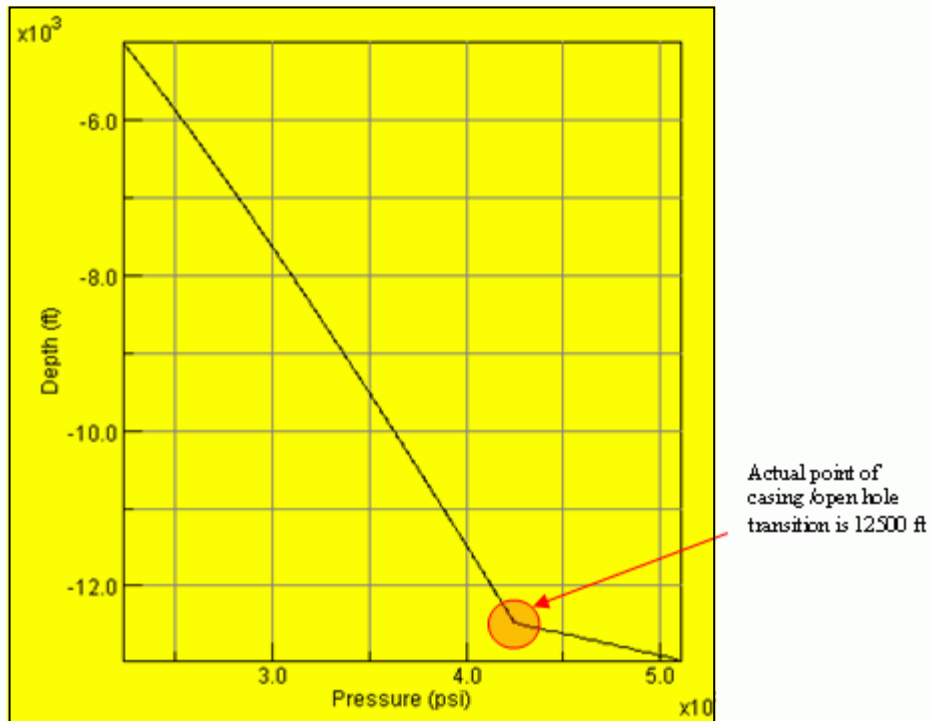


Fig. 3.3 – Numerical output of COMASim is limited to 10 equally spaced points

However, the table output to the left of the graph (**Fig. 3.3**) is limited to ten equally spaced data points. COMASim was not programmed to recognize important changes in the pressure profile or any other graphs. Therefore, when a significant change occurs, it most likely will not be recorded in the table unless it happens to occur exactly at one the ten depth values. For this simulation, this error meant that the change in pressure at the casing shoe was not output correctly in the table for the majority of the simulation runs.



**Fig. 3.4 – Numerical output for a hanging drillstring at 13000 ft TVD, 13000 ft drillstring, 5000 ft of water, 10 ¾ casing.**



**Fig. 3.5 – Close-up of graph from Fig. 3.3, a hanging drillstring at 13000 ft TVD, 13000 ft drillstring, 5000 ft of water, 10  $\frac{3}{4}$  inch casing.**

This can be seen by comparing **Fig. 3.5** and **Fig. 3.4**. In **Fig. 3.4** the casing shoe/open hole effect on the pressure profile is shown at 12,200 feet as opposed to the actual point at 12,500 feet shown in **Fig. 3.5** which is a close-up of the graph in **Fig. 3.3**. This deficiency in the simulator limits analysis to a trend based analysis as opposed to a numerical analysis or comparison concerning the pressure profile.

### 3.5 Effect of Casing Size and Drillstring Presence on Initial Conditions

Fig. 3.6 – 3.8 illustrate typical initial condition or flowing pressure profiles for hanging drillstring, dropped drillstring and no drillstring situations. In Fig. 3.6 -3.8 the drillstring length is 100% of TVD. This explains the similarity between a dropped drillstring and a hanging drillstring pressure profiles.

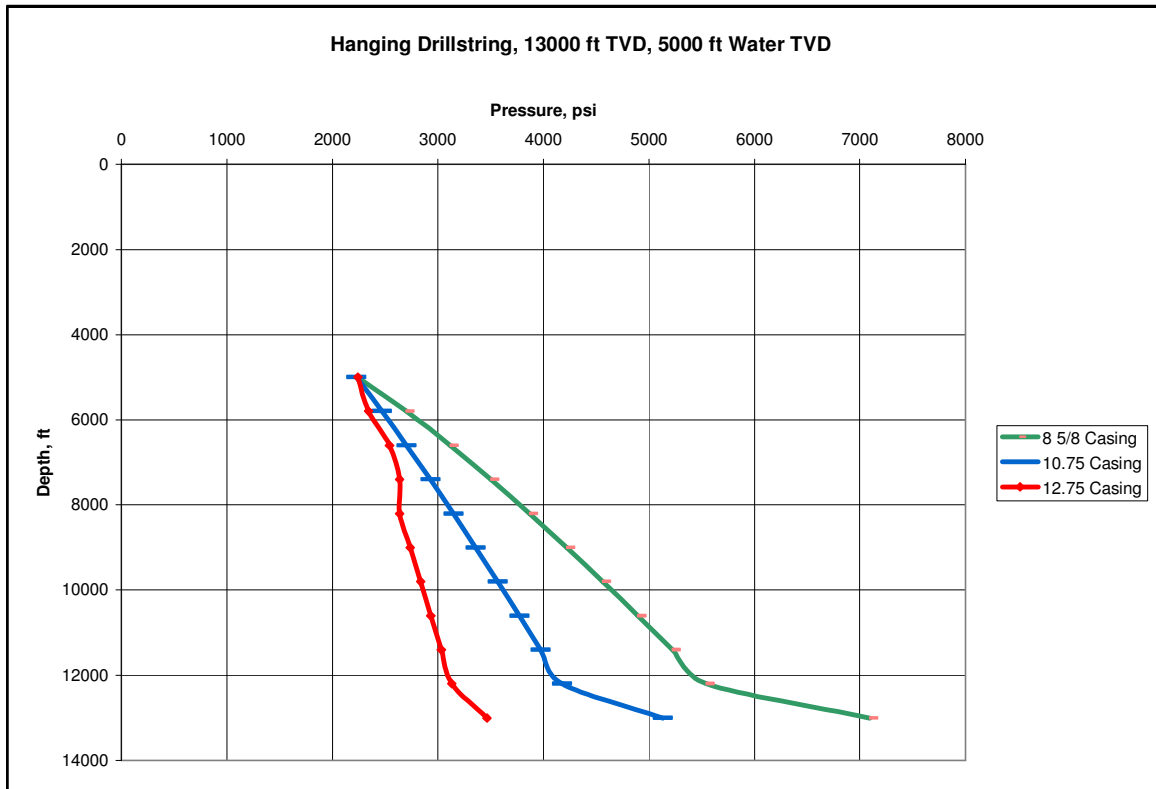
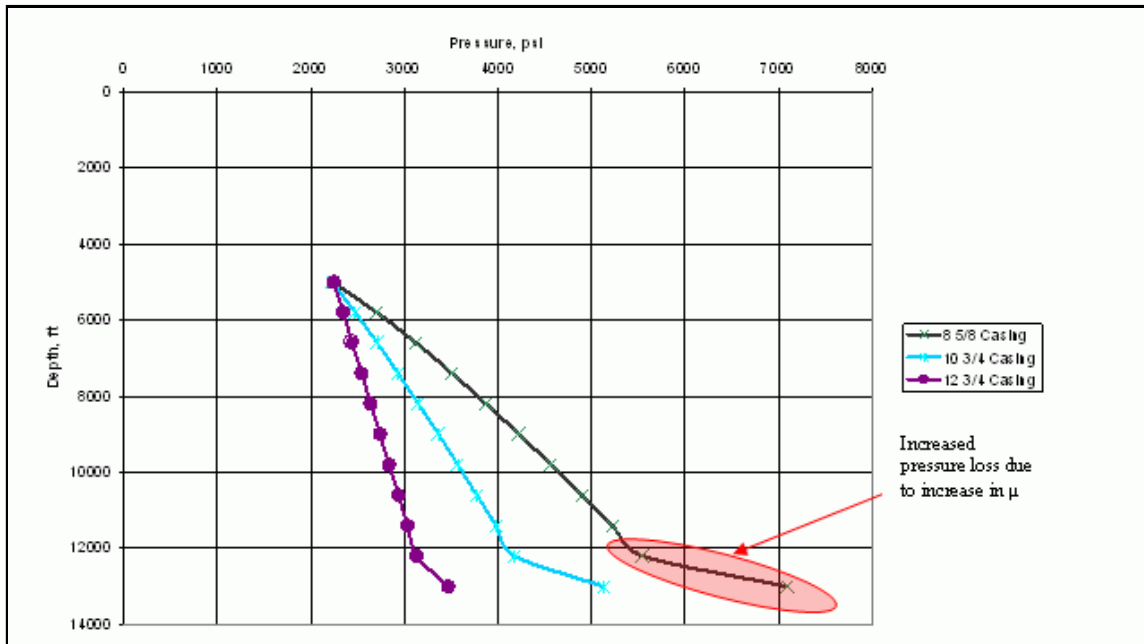
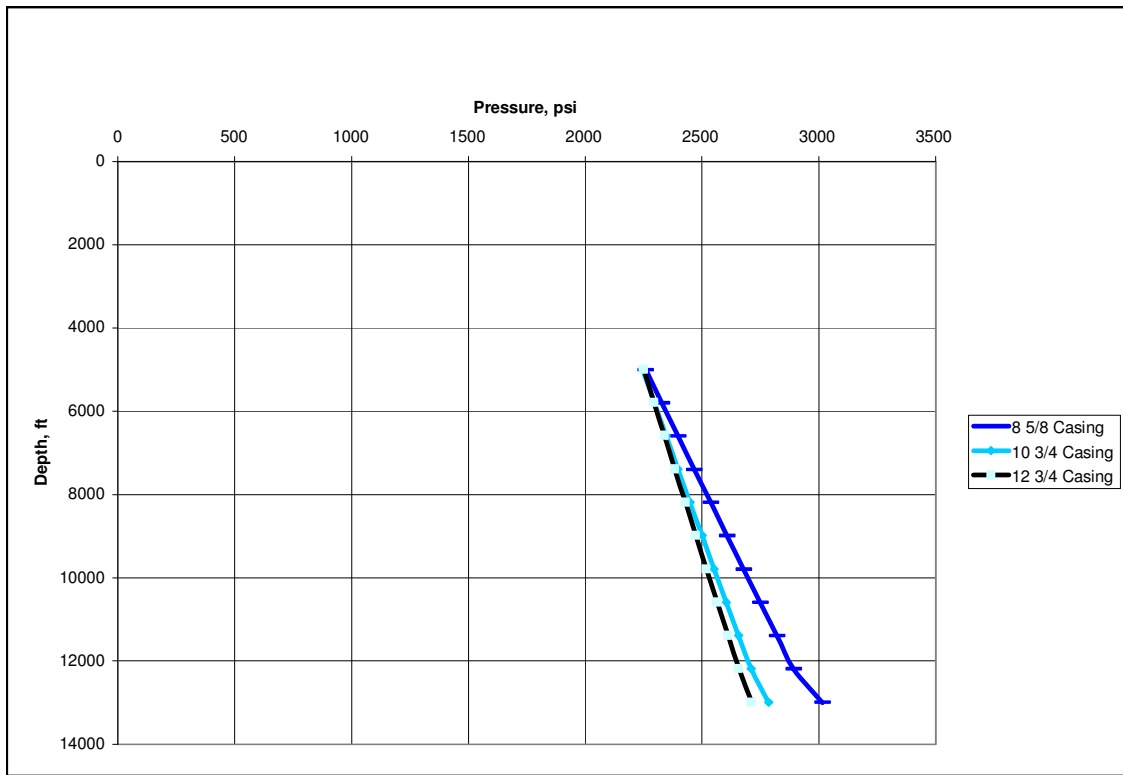


Fig. 3.6 – Hanging drillstring situations shows typical behavior for pressure profile.



**Fig. 3.7 – Dropped drillstring data matches hanging drillstring pressure profile.**



**Fig. 3.8 – No drillstring in hole reduces pressure value and variation.**

The values do differ slightly as evidenced by **Table 3.2**, however the difference is minute enough to ignore.

**Table 3.2 – Hanging and dropped drillstrings allow almost identical flow rates.**

Casing Size	Drillstring Status	$Q_g$
OD, inches		MMscf/d
8.625	Hanging	31.49
10.75	Hanging	122.61
12.75	Hanging	203.96
8.625	Dropped	31.47
10.75	Dropped	122.56
12.75	Dropped	203.92

While **Table 3.2** does illustrate that hanging and dropped full length drillstrings are essentially equal in flow rate values, the dropped drillstring flow rates were lower than the corresponding hanging drillstring flow rates in all three cases. **Fig. 3.6 – 3.7** show a sharp increase in pressure loss in the bottom 500 feet of the wellbore. The pressure loss is highlighted in **Fig. 3.7**. This increase is due to the coefficient of roughness,  $\mu$ , being almost 18,500 times larger for an open wellbore as opposed to a cased wellbore. The open hole  $\mu$  is 0.12 inches and the cased hole  $\mu$  is 0.00065 inches. This high  $\mu$  results in the dramatic increase in pressure loss experienced in the wellbore.

The decreasing absolute value of the slope in the pressure profile as the casing size decreases is related to a casing size's ability to accommodate blowout flow. As seen in **Table 3.2**, increasing sizes of casing causes a large increase in surface flow rate,  $Q_{g,surface}$ . Larger sizes of casing do not impose as much frictional pressure loss as smaller diameters of casing.

$$\left(\frac{dp}{dL}\right)_f = \frac{2f'\rho v^2}{g_c d} \dots\dots\dots \text{Eq. 3.1}$$

**Eq. 3.1** shows why the frictional pressure loss increases as diameter decreases. The decreasing diameter also results in a higher velocity, exacerbating the pressure loss due to friction. For example, the pressure differential from liquid entry to liquid exit in the wellbore for the case shown in **Fig. 3.6** is 4856 psi for 8 5/8 inch casing and 1221 psi for 12 3/4 inch casing. Since the exit pressure is kept constant for both casing sizes, this results in a smaller slope on the pressure profile graph for the 8 5/8 inch casing. This also results in an increase in  $Q_{g,surface}$  for the 12 3/4 inch casing due to a lower bottom hole pressure. The lower bottom hole pressure creates a larger negative pressure differential with respect the reservoir pressure causing an increased  $Q_{g,surface}$ .

The difference between the pressure profile shown in **Fig. 3.8** and **Fig. 3.6 -3.7** is also frictional pressure loss related. As previously discussed, smaller flow areas, i.e. the 8 5/8 inch casing, have larger differential pressures due to increased frictional pressure

loss. Continuing this concept to **Fig. 3.8** shows why its pressure drops are less than that of **Fig. 3.6-3.7**. With no drillstring in the wellbore, the frictional pressure drop is much less than that of wellbores with the added obstruction of a drillstring. The pressure differential for an 8 5/8 inch cased wellbore with no drillstring is 756.5 psi compared to a pressure differential of 4856 psi for an 8 5/8 inch cased wellbore with the drillstring present.

**Table 3.3 – Blowing wellbores with no drillstring have higher  $Q_{g,surface}$ .**

Casing Size OD, inches	Drillstring Status	$Q_g$ MMscf/d
8.625	Hanging	31.49
10.75	Hanging	122.61
12.75	Hanging	203.96
8.625	Dropped	31.47
10.75	Dropped	122.56
12.75	Dropped	203.92
8.625	No Drillstring	215.70
10.75	No Drillstring	230.61
12.75	No Drillstring	238.90

This low pressure loss in the drillstring-less wellbore also results in a much higher surface flow rate as shown in **Table 3.3**. Notice however, that as the pressure losses decrease, the increase in flow caused by larger casing sizes is less. This effect is most likely due to flow becoming primarily dependent on the pressure differential between the exit point and the pore pressure as opposed to being regulated by the frictional pressure drop. In the no drillstring case, frictional pressure losses do not affect the surface flow rate in the same manner as cases when a drillstring is present.

### 3.6 Effect of Drillstring Length

The previous discussion shows the effect of the presence of a drillstring that is 100 percent of the TVD. However, the majority of kicks, and resulting blowouts occur

during tripping operations.<sup>8</sup> Thus, the drillstring will not be on bottom. To simulate these conditions in COMASim, I varied the drillstring length for the various scenarios.

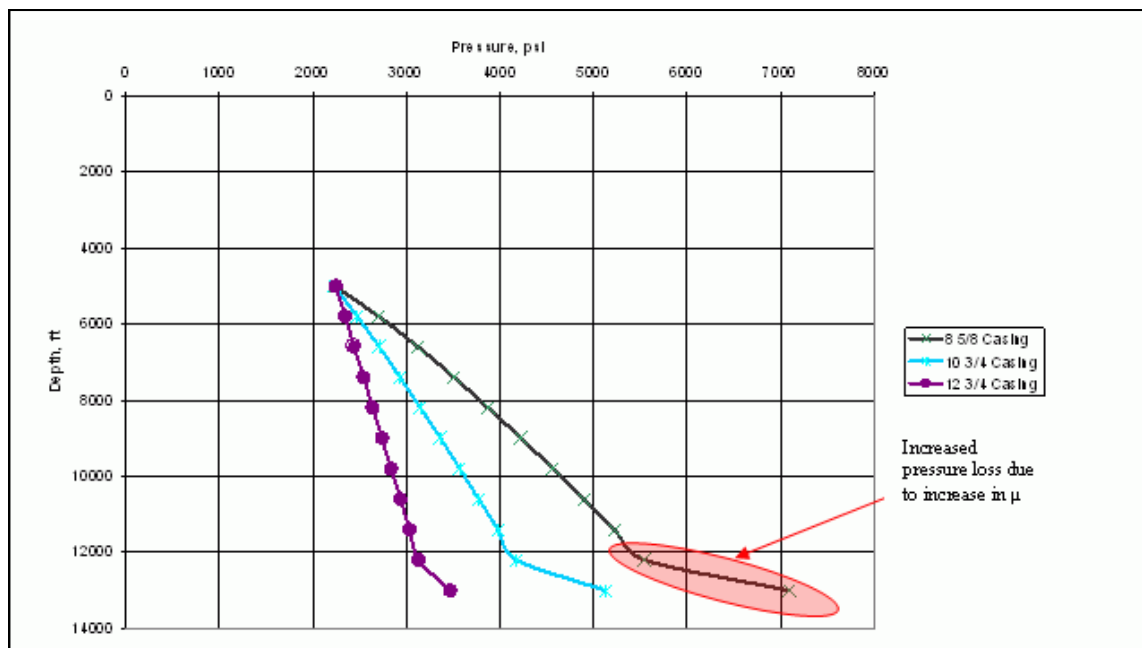


**Fig. 3.9 – Effect of drillstring length on hanging drillstring, 13000 ft TVD, 5000 ft water depth, 10 3/4 inch casing.**

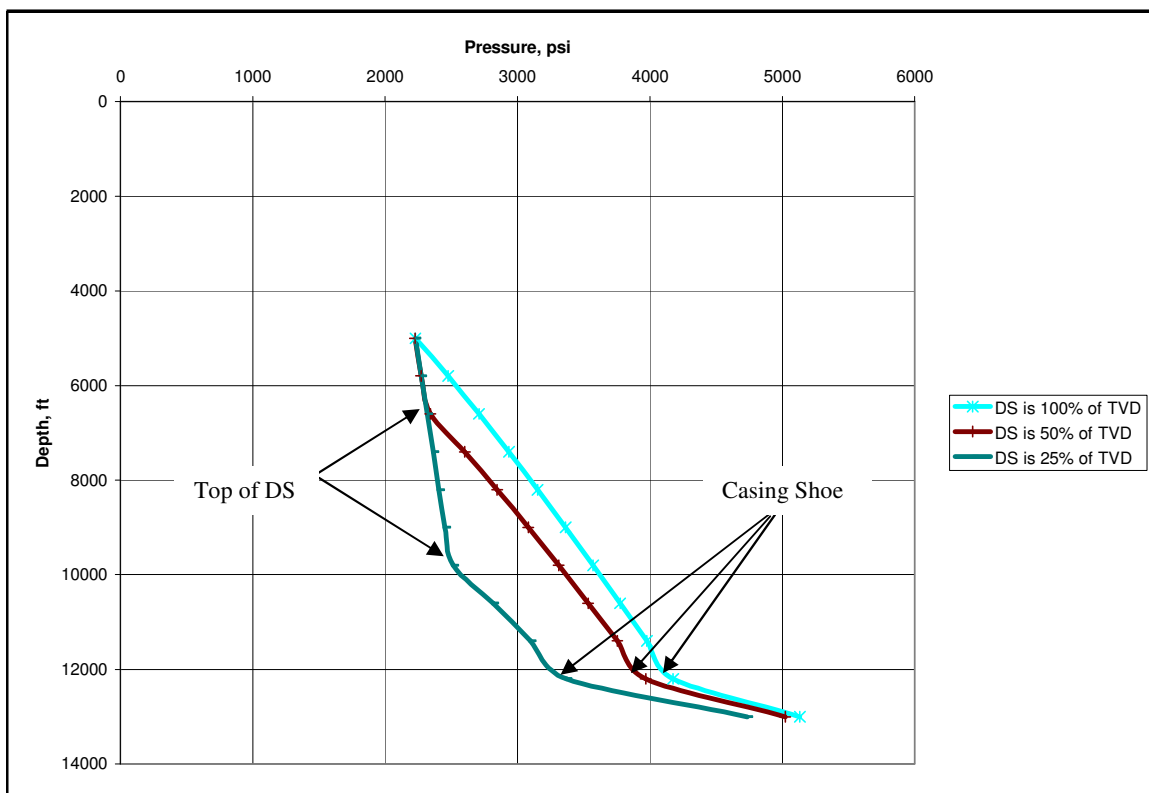


**Fig. 3.10 – Effect of drillstring length on dropped drillstring, 13000 ft. TVD, 5000 ft water depth, 10  $\frac{3}{4}$  inch casing.**

**Fig. 3.9 – 3.10** are typical of the trends that occurred when drillstring length was varied. Again, due to predetermined data points, the curves are not exactly correct. The points where the pressure profiles experience severe breaks may be off by several hundred feet.

The drillstring increases the frictional pressure drop calculated in **eq. 3.1** by decreasing the effective diameter and increasing the velocity of the fluid. As previously discussed, the drillstring causes the pressure profile to flatten out due to increased pressure drop. When hanging from a subsea BOP as shown in **Fig. 2.6**, the typical pressure profile resembles **Fig. 3.9**. As indicated on **Fig. 3.9** the drillstring caused increased pressure losses along its length. An interesting phenomenon was shown in **Fig. 3.9** as well. The curves for drillstring lengths of 25 percent and 50 percent of TVD show no increased pressure loss due to the open hole. Since there is no drillstring to increase

velocity in that section, the roughness increase due to an open wellbore does not have a significant effect. Only in situations such **Fig. 3.7** or **Fig. 3.10** where drillstring is located in the open hole section does the increase in roughness make a noticeable difference in the pressure profile.

**Fig. 3.10** displays a typical pressure profile for a dropped drillstring. From the bottom of the wellbore, the first break in the pressure profile is the casing shoe. This is the transition from the large roughness factor of the open hole to the small roughness factor of the casing. The second break is at the top of the dropped drillstring. Once the drillstring top is cleared, frictional pressure losses drop significantly.

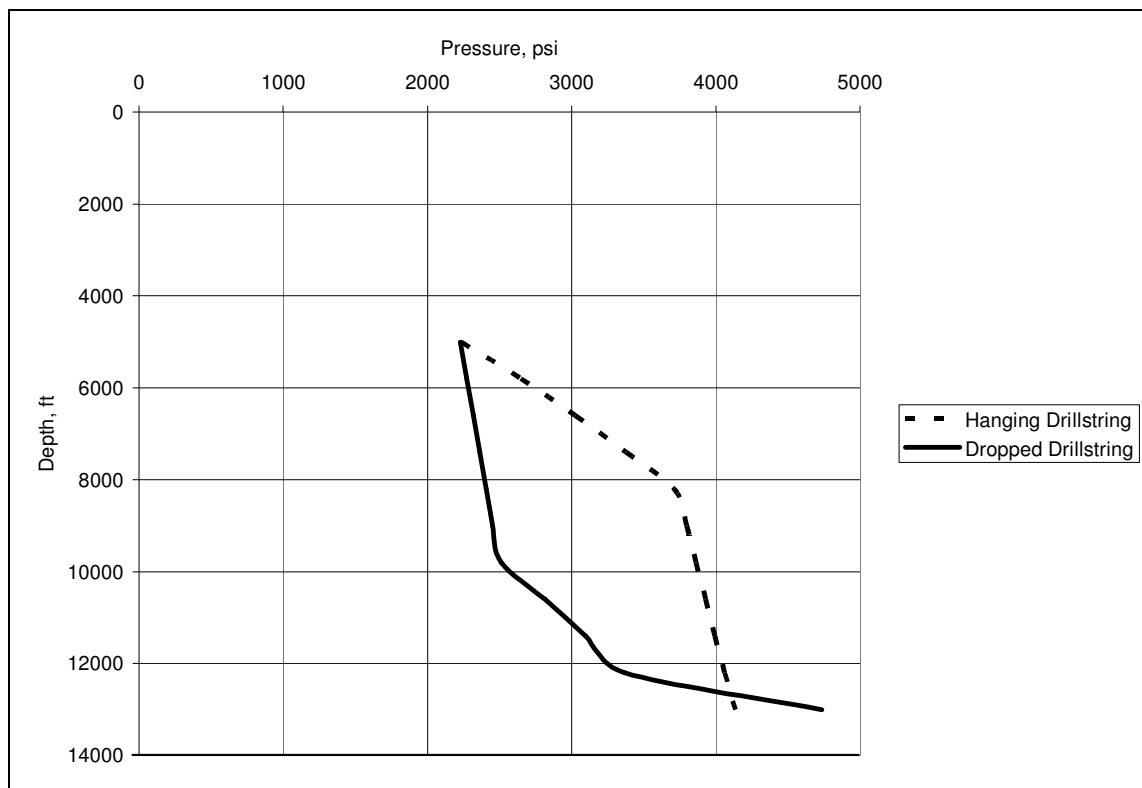


**Fig. 3.11 – Difference between 3250 ft. of drillstring in 13000 ft TVD in 5000 ft of water with 10 ¾ inch casing.**

**Fig. 3.11** is a graphical representation of the difference in pressure profiles for a hanging and dropped drillstring. Of particular interest in well control and blowout control are the ending points of both pressure profiles. According to **Fig. 3.11**, if the deepest formation was considered to be a weak formation, then hanging the drillstring off of the BOPs would be an advisable precaution in order to avoid the large bottomhole pressures exerted by a dropped drillstring. A dropped drillstring in the wrong conditions could cause the formation to fracture resulting in an underground blowout.

The increased pressure loss occurs due to the constriction between the wellbore and drillpipe. **Eq. 3.1** shows that while the diameter becomes smaller due to the drillpipe's presence, the resulting increasing velocity is the main cause of frictional pressure loss. Since both a smaller diameter and a larger velocity both increase the frictional pressure, there is an extreme difference between the frictional pressure loss in an empty wellbore and a wellbore with drillpipe present.

### **3.7 Kill with Drillstring Initial Conditions**

The discussion covering initial conditions for the "Kill With Drillstring" drillstring position options is separated out from the other three options due to two main differences. First, the "Kill With Drillstring" option is the only one which takes into account frictional pressure drop in the marine riser. A comparison of **Fig. 2.6** and **Fig. 2.7** yields a visual picture of the difference. Second, blowouts with the other three drillstring options selected require a separate relief well or wells to kill the blowout.

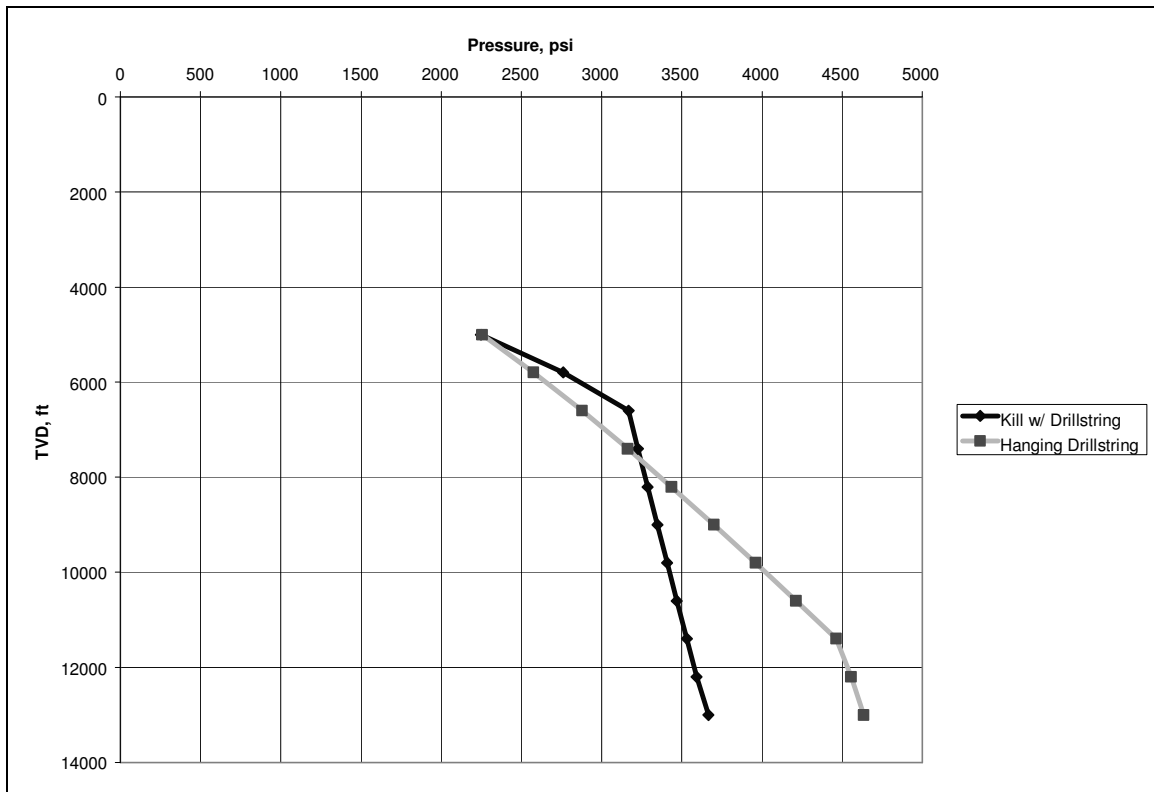


**Fig. 3.12 – 13000 ft TVD, 5000 ft water depth, 10 ¾ inch casing, drillstring is 75% of TVD.**

A kill with drillstring pressure profile is similar to a hanging drillstring pressure profile. The main difference is the drillstring effect is felt throughout the entire wellbore. Thus, a drillstring that is 75 percent of the TVD has less of an effect on the formation in a hanging drillstring situation. **Fig. 3.12** illustrates the difference between the two. The data composing **Fig. 3.12** as well as all of the other kill with drillstring initial condition runs can be found in **Appendix D**. The kill with drillstring curve shows a break at 75 percent of the total depth. Meanwhile, the break or bottom of the drillstring is at water depth plus 75 percent of total depth for the hanging drillstring. The “kill with drillstring” option exhibits a much steeper pressure profile but an overall lower pressure loss.

**Table 3.4 – Kill with drillstring configuration yields higher  $Q_{g,surface}$ .**

Drillstring Status	DS Length % of TVD	$Q_{g, surface}$ MMscf/d
Hanging	100	122.614
Hanging	75	122.614
Hanging	50	145.719
Kill w/ DS	100	122.562
Kill w/ DS	75	156.021
Kill w/ DS	50	190.456

This steeper pressure profile yields a higher surface flow rate as shown in **Table 3.4**. The previous discussion on flow rates covering **Table 3.2** and **Table 3.3** applies in this instance as well. The lower pressure loss exhibited in the kill with the drillstring configuration is the root cause of the higher flow rates.

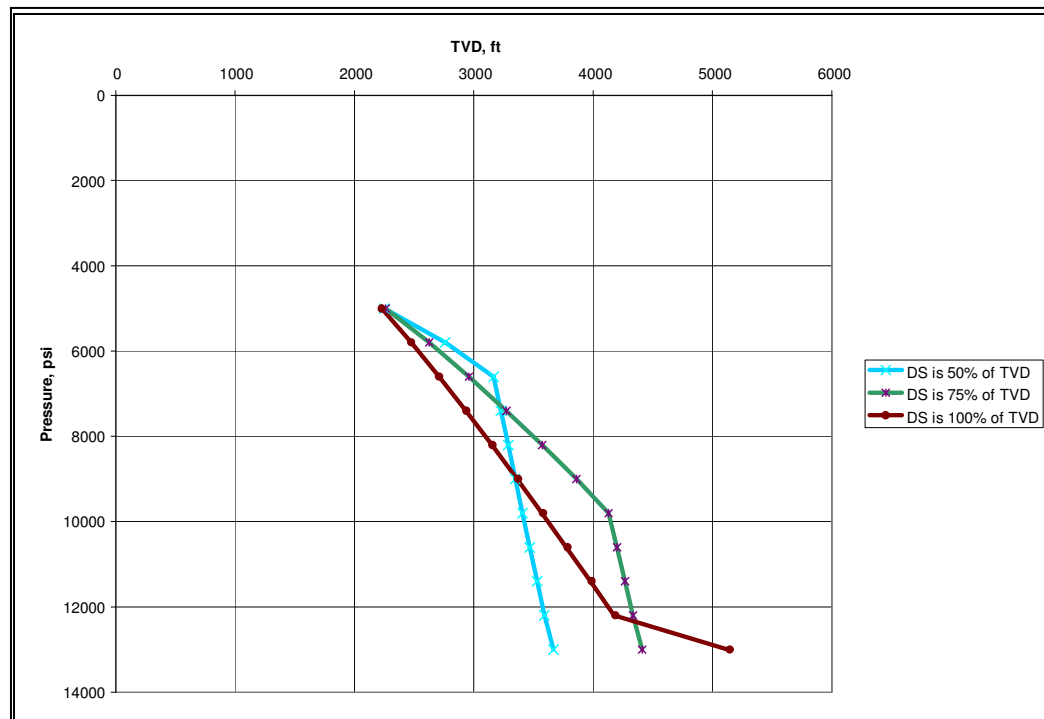


**Fig. 3.13 - Kill with drillstring, 13000 ft TVD, 5000 ft water depth, 10  $\frac{3}{4}$  inch casing shows decreasing bottom-hole pressures as drillstring length decreases.**

Drillstring length also causes differences in pressure profile and bottom-hole pressure. **Fig. 3.13** and **Table 3.5** show the effect of drillstring length on pressure profiles in a kill with drillstring setup. The shorter drillstring lengths result in a steeper pressure profile with less pressure loss in the wellbore. The lower pressure loss in the wellbore results in a higher flow rate. This effect is similar to that of varying the casing size.

**Table 3.5 – Kill with drillstring, 13000 ft TVD, 5000 ft water depth, 10 ¾ inch casing shows flow rate increases as drillstring length decreases.**

DS Length % of TVD	$Q_{g,surface}$ MMscf/d
100	122.562
75	156.02
50	190.465

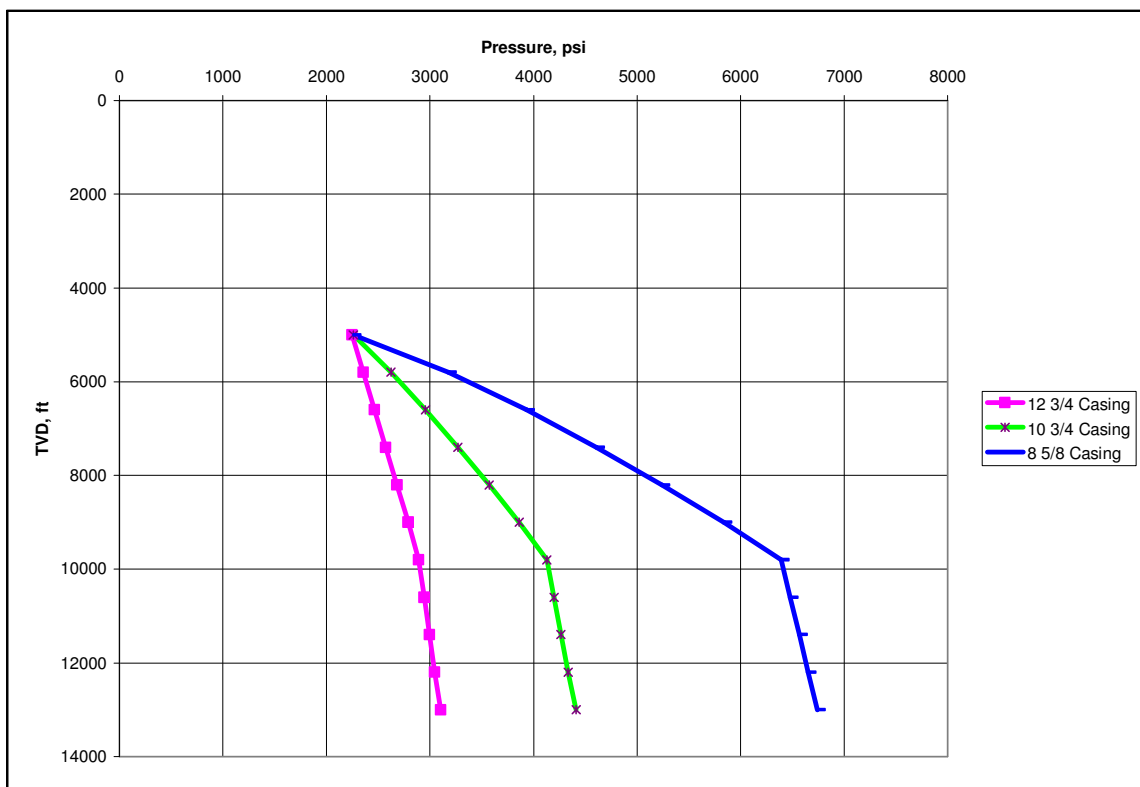


**Fig. 3.14- Kill with drillstring, 13000 ft TVD, 5000 ft water depth, drillstring length is 75% of TVD.**

**Fig. 3.14** shows the effect of varying the casing size in a kill with the drillstring situation is similar to that of any other drillstring option. The smaller casing decreases the flow area and increases the velocity. This in turn causes the frictional pressures to go up. The 8 5/8 inch casing curve depicted in **Fig. 3.14** shows a much larger pressure drop compared to the 12 3/4 inch casing due to smaller flow area.

### 3.8 Dynamic Kill Requirements for Relief Well Necessary Situations

Of the four COMASim drillstring options, the hanging drillstring, dropped drillstring and no drillstring all require relief wells to control the blowout. The kill with the drillstring option does not require a relief well as the name indicates. Therefore the latter option will be treated separately.

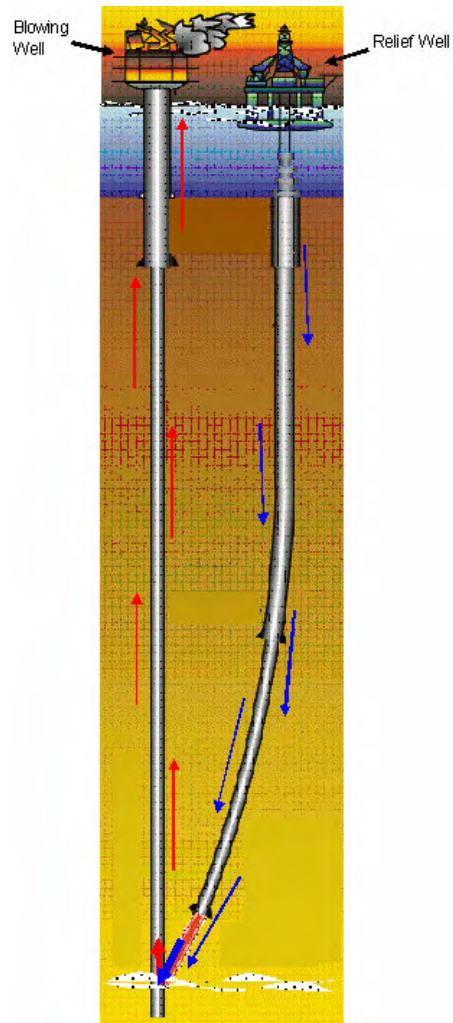


**Fig. 3.15 – Relief well flow path.**

For the remaining three drillstring options, the flow path for the kill fluid is shown in **Fig. 3.15**. For the three drillstring options requiring a relief well to quell the blowout, the dynamic kill parameters of standpipe pressure, number of relief wells, hydraulic horsepower and dynamic kill rate follow the same trends.

**Table 3.6 – 13000 ft TVD, 5000 ft water depth, kill rate increases with increasing casing size.**

Drillstring Status	Casing Size OD, inches	Kill Rate gal/min
Hanging DS	8 5/8	217.8
Hanging DS	10 3/4	1266.3
Hanging DS	12 3/4	4294.8
Dropped DS	8 5/8	218.6
Dropped DS	10 3/4	1270.4
Dropped DS	12 3/4	4307.7
No DS	8 5/8	7662.7
No DS	10 3/4	14093.4
No DS	12 3/4	24879.6

The first parameter taken into consideration is the dynamic kill rate. The dynamic kill rate is the rate at which the kill fluid must be pumped to create sufficient bottomhole pressure to control the blowout. COMASim does not account for fluid fallback, therefore these kill rates are slightly conservative. Fluid fallback is when the kill fluid flows against the blowout flow. For a blowout with a given rate, the kill fluid might overcome the momentum of the blowout fluid and begin to fall back down the wellbore in small quantities with the majority of it continuing up the wellbore. The fluid fallback creates an additional back pressure on the formation and begins to limit the blowout flow. This is a circular process that eventually leads to control of the blowout flow or a zero net liquid flow situation with regards to the kill fluid. Either way, fluid fallback helps reduce the necessary dynamic kill rate. Thus, ignoring fluid fallback simply builds in a safety factor to COMASim's calculations. **Table 3.6** shows a typical set of kill rates for a wellbore configuration. The dynamic kill rate increases as casing size increases for all of the drillstring positions. The increase in required kill rate is due to the increased flow rate and reduced wild well bore constriction. When **Table 3.6** is compared with **Table 3.3**, this trend is more apparent.

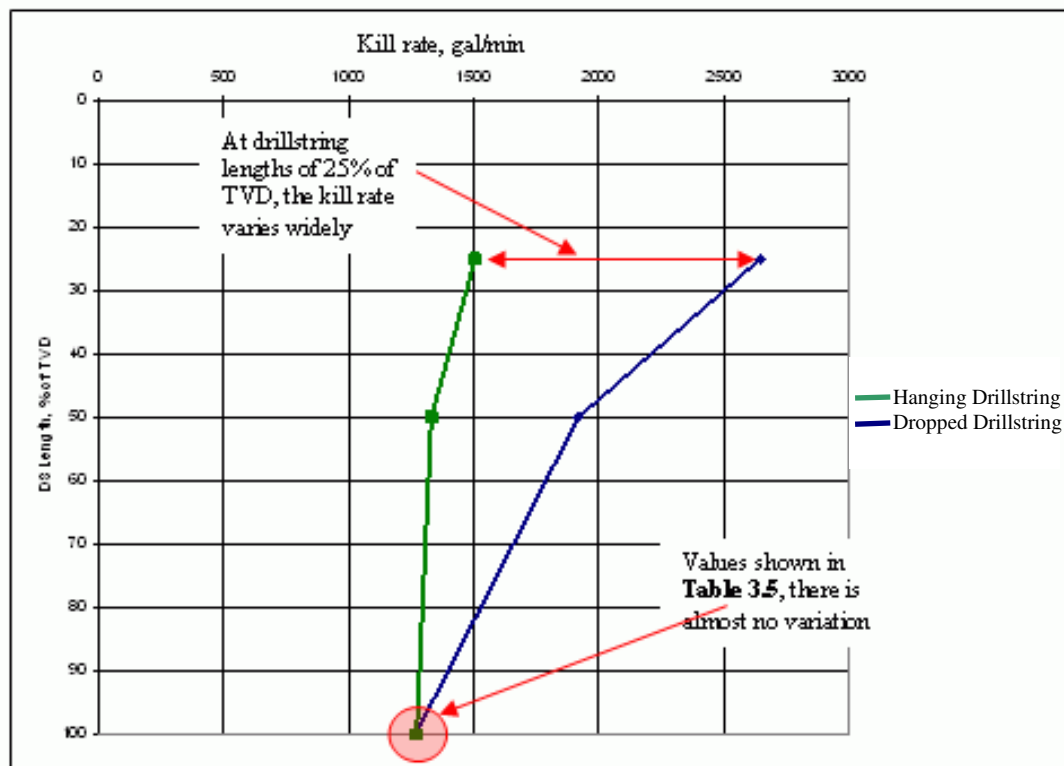


**Fig. 3.16 –Dynamic kill rates differ widely among drillstring statuses as drillstring length decreases.**

The drillstring length was kept constant at 100% of the TVD in **Table 3.6**. However if the drillstring length is varied as in **Fig. 3.16**, the dynamic kill rate begins to vary widely as shown. The dropped drillstring dynamic kill rate does not change as much. Since the drillstring is always on the bottom, and the relief well/blowing well intersection is also on the bottom, the drillstring always creates a high frictional pressure drop. Due to the high frictional pressure drop with all drillstring lengths, the dynamic kill rate will not vary as widely. For the hanging drillstring, the shortening of the drillstring pulls the bottom of the drillstring away from the relief well/blowing hole intersection thus opening up the wellbore and creating a no drillstring situation in a portion of the wellbore. **Table 3.6** shows that a no drillstring situation increases the dynamic kill rates. For that reason, the hanging drillstring dynamic kill rates begin to

increase dramatically as the drillstring length is reduced. **Fig. 3.16** shows a increase of over 1000 gal/min for the hanging drillstring length of 25 % of TVD. The hanging drillstring and dropped drillstring have nearly identical flow rates and therefore nearly identical dynamic kill rates. When there is no drillstring in the hole, the flow rates and therefore the dynamic kill rates increase. The reason for the increase in flow rates was previously discussed and shown to be a result of decreasing frictional pressure losses.

**Table 3.7 – Increasing relief well MD/TVD ratio increases relief well parameters.**

Casing Size	Relief well MD/TVD ratio	SPP for single Relief Well	# of Relief Wells	SPP/well	Pump hp per Relief Well
OD, inches		psi		psi	hp
8 5/8	1.0	3124.5	1	3124.5	397.
8 5/8	1.5	3159.5	1	3159.	401.4
8 5/8	2.0	3185.2	1	3185.2	404.7
10 3/4	1.0	5130.3	1	5130.3	3790.1
10 3/4	1.5	6255.7	1	6255.7	4621.5
10 3/4	2.0	7081.	1	7081.	5231.2
12 3/4	1.0	25318.1	2	8962.2	11228.5
12 3/4	1.5	36274.9	2	11741.	14710.
12 3/4	2.0	47231.7	2	14519.8	18191.5

Relief well parameters besides the dynamic kill rate also increase as the wild well casing size increases. The standpipe pressure for the relief well increases due to the increased kill rates. The number of relief wells was dependent of the 15000 psi standpipe pressure threshold discussed earlier. **Table 3.7**, taken from the hanging drillstring blowout shown in **Table 3.6**, shows the 12 3/4 inch casing needed a much higher dynamic kill rate, therefore two relief wells would be needed to accommodate the higher standpipe pressures. Even when the flow rate is split between two relief wells, the standpipe pressure per well is still higher for the 12 3/4 inch casing than for the 8 5/8 inch or 10 3/4 inch casing. The pump hydraulic horsepower exhibits the same trend as the

standpipe pressure. The values vary over a very wide range of measured depth to total vertical depth ratios or MD/TVD ratios, but the larger relief well MD/TVD ratios will not likely occur in practice. Thus for each casing size, the lower value for relief well parameters are the most realistic. This allows a dynamic kill to be considered in more situations due to increases capability and availability of drilling and pumping equipment. The reasons behind this are laid out in the best practices section of this thesis.

The hanging drillstring and dropped drillstring in the example case used throughout the thesis require two relief wells at most. However, when there is no drillstring in the blowing wellbore, the dynamic kill requirements increase significantly. The end result of the increased dynamic kill requirements is an increased number of relief wells.

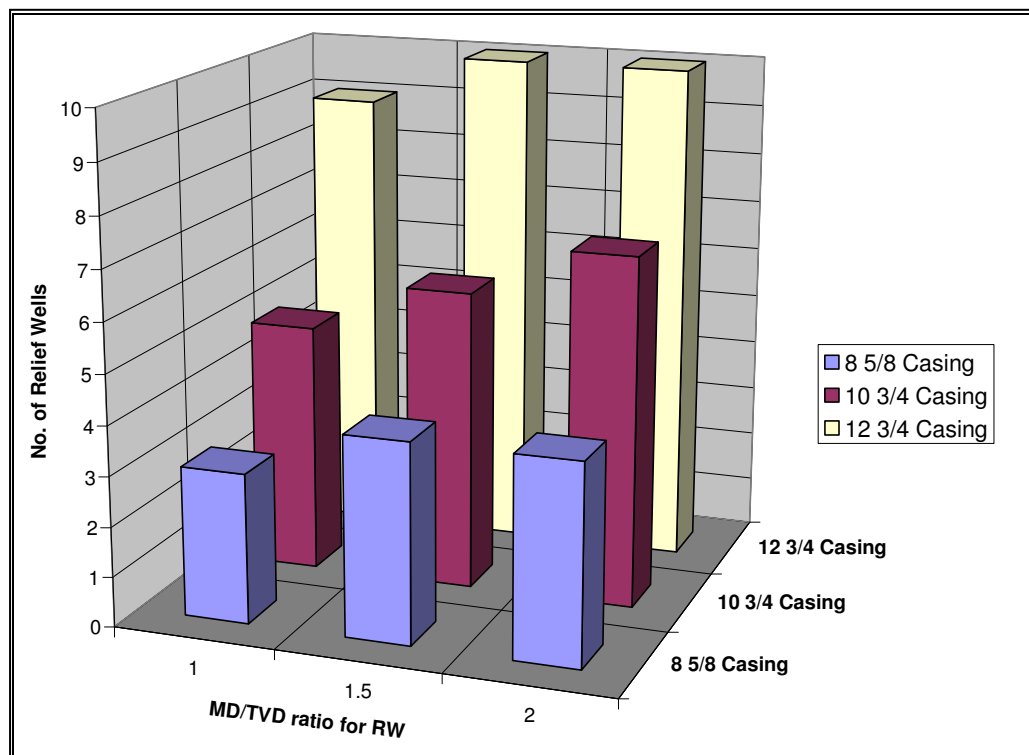


**Fig. 3.17 – Increasing casing size in with no drillstring present increases number of relief wells required.**

Using the 15000 psi standpipe pressure threshold, **Fig. 3.17** shows the sharp increase in the number of relief wells as the casing size increases. This factor is likely to be reduced in as slimhole drilling, casing drilling and dual gradient drilling become more common. These technologies reduce the size and number of casing used during various portions of the drilling program, thus reducing the flow rates of potential blowouts. **Fig. 3.17** also reinforces the need to keep the relief well MD/TVD ratio down, to reduce the number of relief wells required.

### 3.9 Dynamic Kill Requirement for Kill with the Drillstring Situation

Controlling a blowout with a drillstring in the blowing wellbore is an entirely different proposition from using a relief well. As will be discussed later in the best practices section the two methods may even be attempted concurrently. Therefore, the discussions of the two types of kill paths are separate. The results for the kill with the drillstring simulations are shown in **Appendix E**.

**Table 3.8 – Kill with drillstring kill rates similar to dropped drillstring.**

Drillstring Status	Casing Size OD, inches	Kill Rate gal/min
<b>Kill w/ DS</b>	<b>8 5/8</b>	<b>216</b>
<b>Kill w/ DS</b>	<b>10 3/4</b>	<b>1270.4</b>
<b>Kill w/ DS</b>	<b>12 3/4</b>	<b>4307.7</b>
Hanging DS	8 5/8	217.8
Hanging DS	10 3/4	1266.3
Hanging DS	12 3/4	4294.8
Dropped DS	8 5/8	218.6
Dropped DS	10 3/4	1270.4
Dropped DS	12 3/4	4307.7
No DS	8 5/8	7662.7
No DS	10 3/4	14093.4
No DS	12 3/4	24879.6

Controlling the blowout with the drillstring requires similar flow rates to the dropped drillstring and hanging drillstring situations as indicated in **Table 3.8**. The reasons for the kill rates being lower than that of a no drillstring situation are the same as previously discussed for the hanging and dropped drillstring.

**Table 3.9 – Decreasing drillstring length increases kill requirements.**

Casing Size OD, inches	DS Length % of TVD	Kill Rate gal/min	SPP psi	Horsepower hp
8.625	100	216	3156.2	402.5
8.625	75	508.6	6488.5	1925.4
8.625	50	1079.8	9246.8	5825.4
8.625	25	FRICTION FACTOR FAILED		
10.75	100	1270.4	5037.1	3733.4
10.75	75	3038.4	13959.8	24746.8
10.75	50	6606.7	31824.1	122667.8
10.75	25	FRICTION FACTOR FAILED		
12.75	100	4307.7	22903.8	57563.5
12.75	75	9908	81039.6	468461.8
12.75	50	21736.8	239274	3034446.9
12.75	25	FRICTION FACTOR FAILED		

If the drillstring length is decreased in a kill with the drillstring scenario, the relief well requirements rise significantly as indicated in **Table 3.9**. This increase in requirements is due to reduced wellbore constriction as the drillstring length shortens. The kill rate must increase to impart the same frictional pressure drop over a shorter length of constriction. The other kill requirements obviously follow the kill rate increase. During the simulations, COMASim crashed as drillstring lengths approached 25 percent of TVD. Error message stated that the friction factor failed. This failure was most likely due to the inability of the short wellbore constriction to provide enough frictional pressure loss to control the bottomhole pressure. However, this is only conjecture and I can not be sure of the reason. Whether or not the friction factor failure means it is

physically impossible to dynamically kill the well is unknown. Also, of interest are the large standpipe pressures starting with the 50 percent drillstring length in 10 3/4 inch casing. Because these pressures are above the 15000 psi working pressure threshold, a dynamic kill would not be possible through the drillstring.

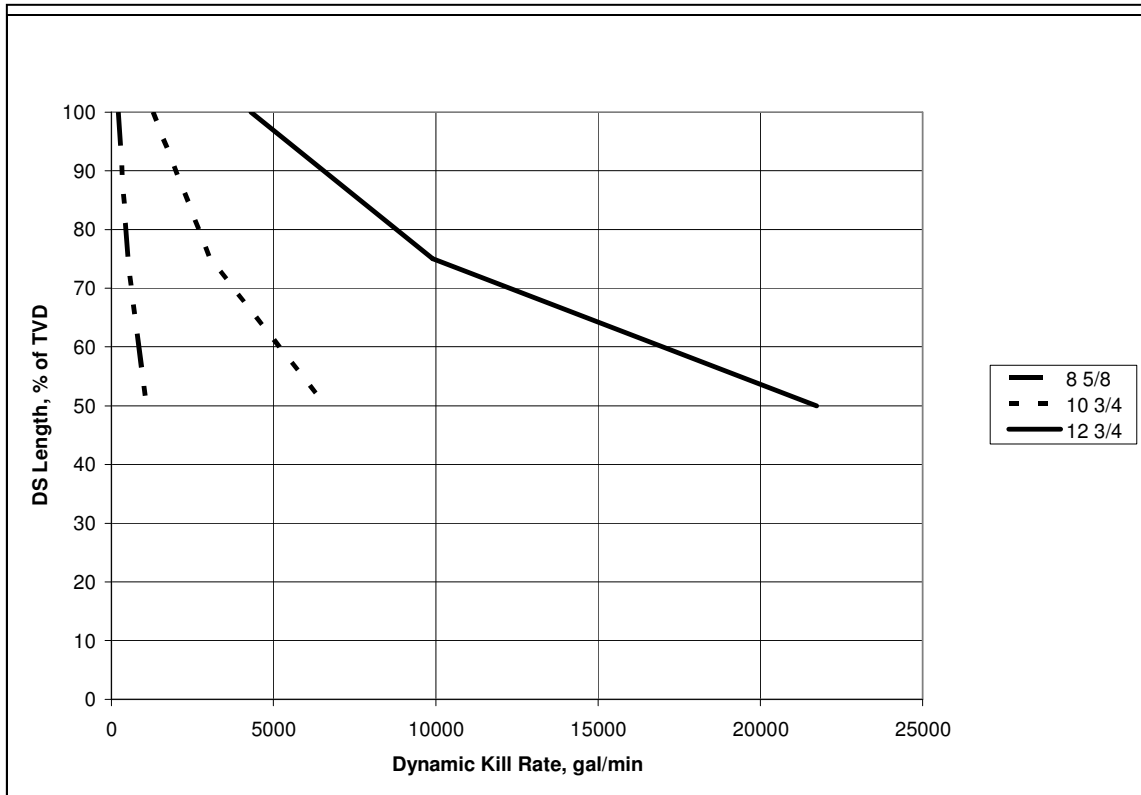


**Fig. 3.18 – Kill rates increase for larger casing sizes.**

The kill rate also increases as the blowing wellbore casing size increases. **Fig. 3.18** indicates a large difference in the required kill rates between 8 5/8 inch casing and 12 3/4 inch casing. This difference is due to the reduced constriction in the wellbore in the larger casing sizes. This reduced constriction requires a higher flow rate to kill the well. The 8 5/8 inch casing dynamic kill requirements do not vary nearly as much as those for the 12 3/4 inch casing. This also is due to the increased constriction imparted by the 8 5/8 inch casing.

## CHAPTER IV

# ULTRA-DEEP WATER BLOWOUT PREVENTION AND CONTROL

### 4.1 Ultra-deepwater Drilling Equipment

Ultra-deepwater drilling equipment and methods are selected due to a variety of reasons. The scope of this study does not include delving into a full set of ultra-deepwater equipment selection criteria. However, I will briefly explain how to select ultra-deepwater equipment with safety in mind.

The first piece of drilling equipment is the drilling rig itself. For ultra-deep water this will consist of a “floater” drilling rig.



**Fig. 4.1 – Example of drillship.**<sup>37</sup>

Floaters are either drillships (**Fig. 4.1**) or semi-submersibles (**Fig. 4.2**). These ships do not need to be touching the seafloor to drill as their name implies. However, they have a large problem in their storage capability. Since they need to be self-contained and do not have moored support vessels, storage space is limited. Therefore during the selection and outfitting of the floater, particular significance must be put on a floater’s ability to not only store well control equipment but also its ability to put that equipment into action.



**Fig. 4.2 – Example of semi-submersible.**<sup>37</sup>

As the deepwater frontier is exploited more and more each year, this problem is decreasing. Many of the leading drilling contractors now have significant numbers of the latest floaters in their fleets. For example, Transocean now has 12 operational fifth generation floaters in their fleet.<sup>37</sup> These fifth generation floaters are designed with water depths of up to 10,000 feet in mind, and thus have sufficient space for the storing and using of deepwater specific safety equipment.

The drillstrings used are typical drillstrings seen on any offshore drilling platform. The only design and safety consideration that changes is the drillstring's ability to support a long length. In ultra-deepwater, the drilled portion of the wellbore below the mudline could be just as deep as any land well. When this depth is coupled with the added length of drillstring to get down to the seafloor, the drillstring becomes heavy. Heavier walled pipe will be necessary toward the top of many ultra-deepwater drillstrings. Of more concern during ultra-deepwater operations is the drilling riser. The drilling or marine riser consists of a large diameter pipe with two smaller lines, the choke and kill lines, attached to it. In ultra-deepwater the riser would have buoyancy material attached to it to reduce the load on the floater. The marine riser is the connection between the floater and the equipment on the seafloor. It is not rated for high pressures as casing and drillpipe are. Risers are normally only designed to handle the

difference in pressure between the maximum weight drilling fluid and seawater. The riser will have issues with strength if it is unloaded and filled with gas. In this case, the riser will be subjected to high collapse pressures and would likely fail in ultra-deepwater situations. Problems such as this highlight the necessity of keeping the influx size to a minimum and reacting quickly to keep the influx out of the riser.

Alternative riser technologies are becoming commonplace in the deepwater drilling industry. Alternative materials such as the carbon fibers used in ABB Vetco Gray's Composite Marine Riser allow for increased riser storage and hanging capacity on floaters as shown in **Fig. 4.3**<sup>38</sup>

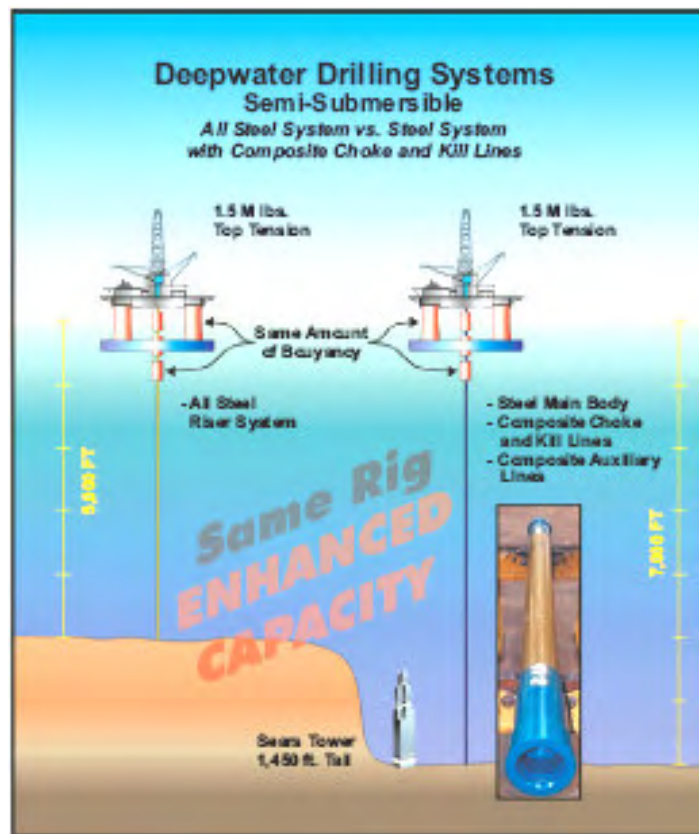


**Fig. 4.3 – ABB Vetco Gray composite material riser increases water depth capability of floaters.**<sup>38</sup>

Another new technology is riser fill valves.<sup>39</sup> Ultra-deepwater risers do not have to be completely unloaded to fail. Since they are rated only on the pressure differential between the drilling fluid and seawater, any amount of unloading begins to unduly stress the riser. In a typical emergency disconnect situation, drilling fluid will fall out of the riser and not be replaced with seawater until the riser is first completely evacuated of drilling fluid and filled with air. Consequently, the riser will fail before it can be filled with seawater to balance the internal and external pressures. To battle this, riser fill valves are now standard on newer riser strings. Riser fill valves are activated at the same time the emergency disconnect command is given. They close and prevent the riser from losing drilling fluid and collapsing.<sup>39</sup> Riser fill valves are also capable of preventing influxes into the riser.<sup>39</sup> This makes them another barrier to influxes breaching the deck of a floater.

Other equipment such as the lower marine riser package, wellhead, and BOPE should be rated for the extreme water depths and resulting pressure in ultra-deepwater drilling. The BOPE would ideally have several modifications for ultra-deepwater drilling. The first would be a large number of accumulator bottles. The deeper the accumulator bottles are situated, the lower the usable fluid volume is per accumulator bottle.<sup>8</sup> The only current solutions to reducing number of bottles is to replace them with larger bottles or accumulator bottles rated at higher pressures.<sup>8</sup> In addition to operator or regulatory guidelines on accumulator volume for safe well control an additional amount should be added. As will be shown later, shearing or dropping the drillstring may be necessary after control has been lost. In the event the BOP stack is still operational, enough accumulator volume must be available to complete this operation. In deepwater accumulator bottles could become prohibitory due to increased expense and floater capability to handle such large lower marine riser packages. An alternative method of operating the BOPE is placing the accumulators on the surface and delivering the power fluid down a steel line attached to the riser. This method is viable, but has one chief problem; the riser must be connected to the BOPE in order for the BOPE to operate. If a steel hydraulic fluid line is used, sufficient accumulator bottles must be placed on the

seafloor to close at least a blind ram and a shear ram in the event an emergency disconnect of the riser occurs.

If accumulator bottles are used, communication must be established with the lower marine riser package control pod which controls the accumulator bottles. The standard course is to use a small diameter line filled with hydraulic fluid to actuate the BOPE. The reaction time for a 3/16 control line in water follows a power law relationship. At 400 feet the reaction time is 1 second. In depths of 3000 feet, the reaction time is up to 10 seconds.<sup>8</sup> Thus, in ultra-deepwaters, the reaction time from the command to completion of the task for the BOPE may be disastrously slow. Three commercial alternatives exist to solve this problem. The first is the installation of a biased hydraulic control line. A biased line would be precharged to within several hundred psi of the activation pressure for the BOPE. Then, when a BOPE command is given, effects such as ballooning and compressibility would be reduced and the reaction time decreased.<sup>8</sup> Unfortunately, on long risers this could become expensive and prone to failure. The second method is an electrohydraulic system. As the name implies, an electronic signal activates the BOPE through a single line capable of coded transmissions or a multiplex system. The signal time is nearly instantaneous but the signal itself may be prone to electronic noise generated by the riser.<sup>8</sup> Another type of multiplex system is fiber optics. Fiber optics are not as common as electrohydraulic systems but are less susceptible to interference.<sup>8</sup>

The preceding communication techniques depend on the riser maintaining a connection to the BOPE. In an emergency disconnect or drive-off situation, the connection may be severed prior to the completion of the signal. In this event, two options for initiating BOPE operation exist, a remote operation vehicle (ROV) operated hotline system and an acoustic control system (**Fig. 4.4**).<sup>40</sup> These two systems will greatly assist in blowout control operations if necessary.



**Fig. 4.4 – Acoustic control system on lower marine riser package.**<sup>41</sup>

#### **4.2 Ultra-deepwater Blowout Control Equipment**

Once control of the well has been lost, blowout control equipment should begin to be staged. After the initial plans for control have been finalized among blowout personnel, the blowout control equipment should be deployed to the well site. For a dynamic kill, three areas of equipment are the most important. Bringing together the blowout control equipment should be easy for an operator. The MMS does not currently require relief well contingency plans but should in the face of growing ultra-deepwater exploration. An example is Norway which requires an operator to have a full relief contingency plan including spud locations, location of available kill equipment, and preliminary relief well plans.<sup>42</sup> Forcing operators to have relief well contingency plans in place results not only quicker drilling times, but a higher likelihood of success.

The first of the necessary equipment is the drilling rig or rigs used to kill the blowing well. In an ultra-deepwater situation, the original floating drilling rig would have likely completed an emergency disconnect and still be available for well control procedures. The original rig will most likely be involved in the vertical intervention

portion of blowout control. At least one other rig and possibly more need to be mobilized to the blowout location to begin drilling relief wells.

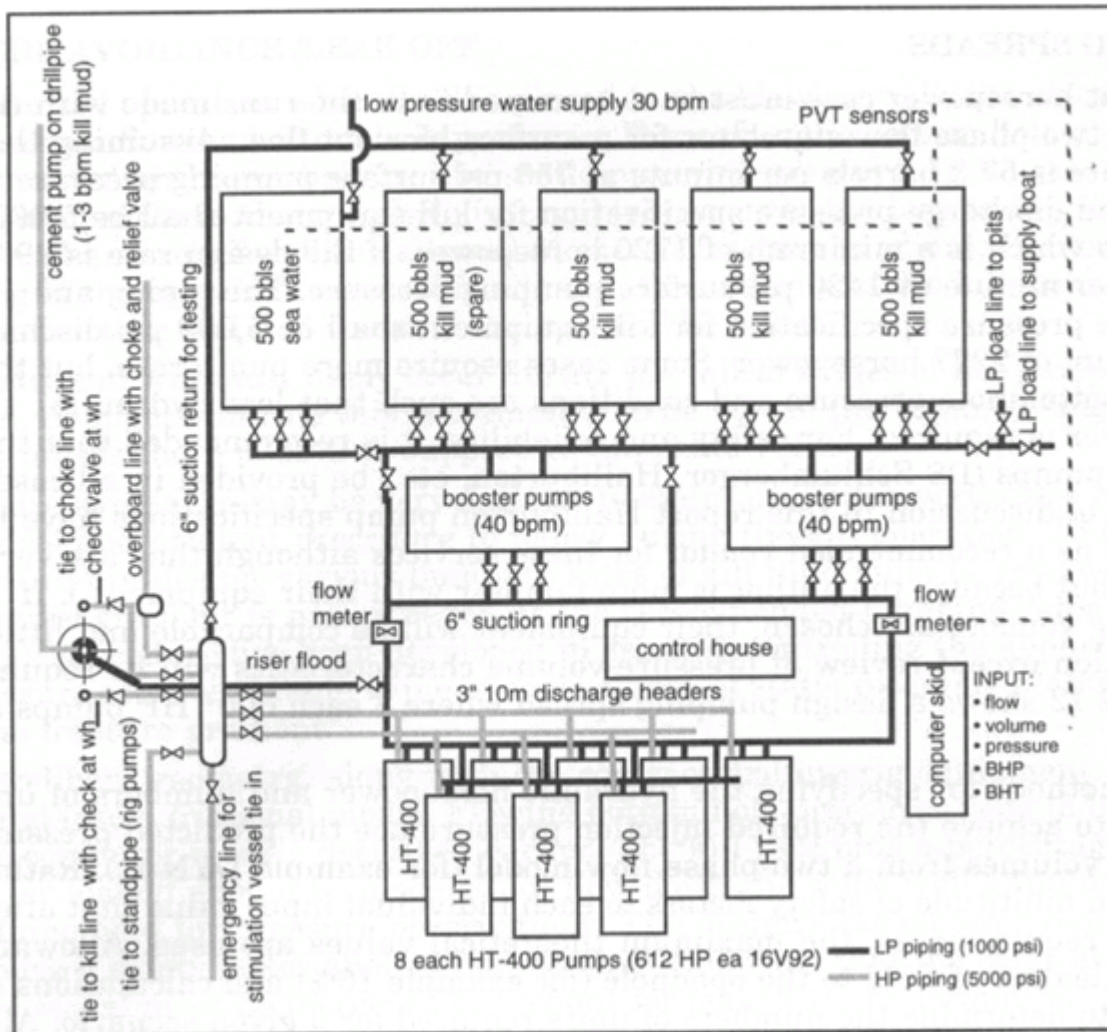


**Fig. 4.5 – Example of offshore dynamic kill pumping plant.**<sup>43</sup>

The pumping plant should be the next step for relief well planners. Running simulations on a model such as COMASim will give the planning team pumping requirements for a variety of scenarios in a brief time. The pumping plant then needs to be assembled. For ultra-deepwater this involves either the marshalling of multiple frac boats such as the one shown in **Fig. 3.1** or the building of a pumping plant on a floater

similar to that shown in **Fig. 4.5**. Of course a backup pumping plant should be available to pick up the slack in case the original plant goes down due to mechanical problems.

The third part of the blowout control equipment is the kill fluid. This report used seawater as the kill fluid in the simulations discussed. However, if the kill fluid is able to be weighted up this greatly reduces the kill requirements as evidenced by **Fig. 4.6**. The only requirement is that the kill fluid must be available in significant quantities. The dynamic kill planner should account for their kill fluid capabilities during the simulation phases.

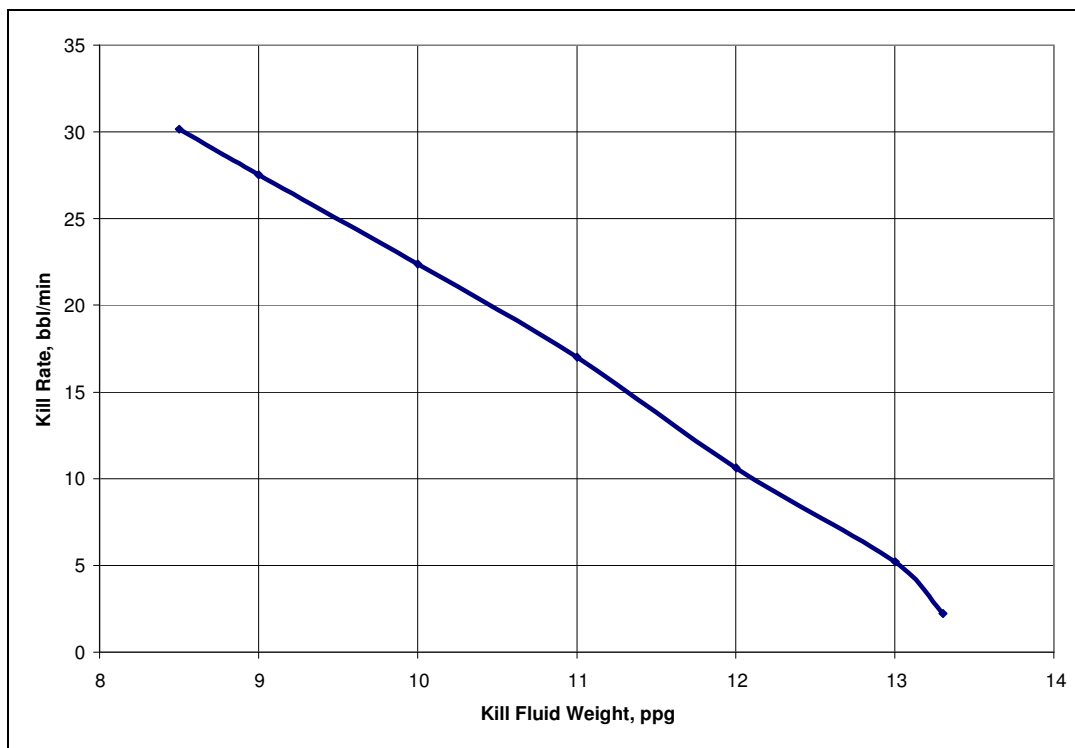


**Fig. 4.6 – Increasing kill fluid weight reduces the kill rate.**

Another important fluid to have on hand is acid. Due to uncertainties in targeting relief wells, the relief wellbore and wild wellbore may not directly intersect. In this case, acid is used to establish communication.<sup>16</sup> If the contingency plan is available and blowout control equipment listing is up-to-date, assembling the necessary equipment

could be done quickly and easily. Having the correct equipment on hand and on time will contribute to the overall smoothness and success of the blowout control operation.

### 4.3 Ultra-deepwater Kicks and Well Control

Several areas in the drilling operation are prone to human error and mishandled kicks. As shown in **Table 1.2**, the three most likely ways a blowout begins is through swabbing in, drilling breaks and formation breakdown.

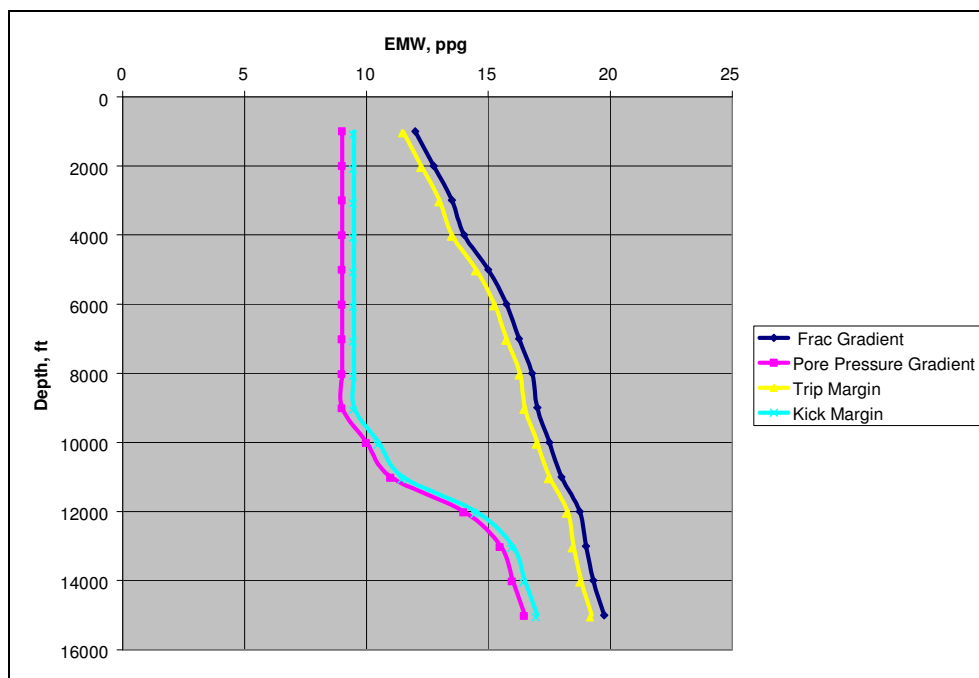


**Fig. 4.7a – Onshore gradients.**

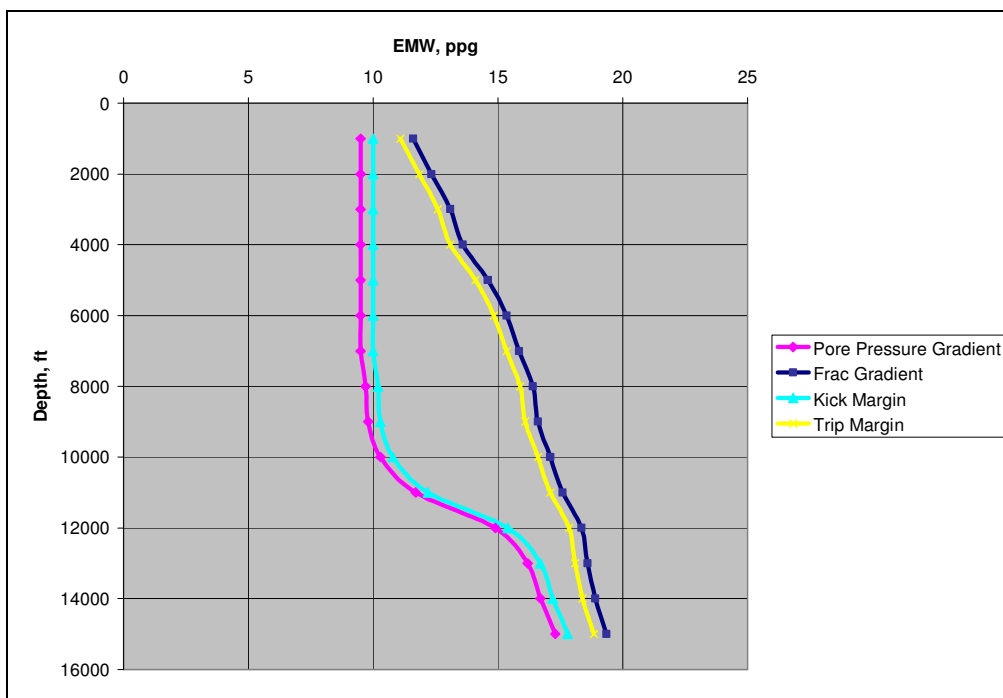


**Fig. 4.7b – Offshore gradients.**

Formation breakdown is avoidable although sometimes difficult to do as seen in **Fig. 4.7b**. **Fig. 4.7a** is what typical shallow water or onshore gradient curves would resemble. **Fig. 4.7b** is representative of deepwater gradients. The deepwater gradients are much closer together in value, particularly as the depth increases. This reduces the range of mud weights capable of avoiding formation fracture while at the same time controlling the pore pressure. This narrower window increases the chances that formation breakdown and subsequent lost circulation will occur. In ultra-deepwater drilling, the parties responsible for drilling fluids should be particularly careful to keep the mud weight within the bounds of the pore pressure and fracture gradients. Newer technologies such as dual gradient drilling may be solutions to this problem.

Drilling breaks indicate a sharp increase in drilling rate.<sup>8</sup> The drilling break could occur for several reasons. The break may be due to a change in formation. The more porous and permeable a formation is, the faster the penetration rate will be through it. Also drilling break may be caused by flowing formation fluids reducing pressure above the bit and cleaning the hole faster.<sup>8</sup> Either way, a drilling break indicates a

possible kick. The Skalle, et al. database<sup>9</sup> most likely had to use this general term because that was the notation on reports or other documents. The probable cause of a kick taken when a drilling break occurs is the unexpected encounter of a highly permeable, possibly overpressured hydrocarbon-bearing formation. This can lead to a large influx and blowout if it is not controlled. Drilling breaks are not avoidable, however they can be managed with no negative results. The first part of managing drilling breaks is through superior geological data. Armed with high-quality data, the operator can anticipate drilling breaks and be prepared. The second part is a constant vigilance by the driller. When a drilling break is noted, extra attention needs to be paid to kick indicators particularly in ultra-deepwater drilling. Since the influx may not stand out, the extra care and attention could prevent a disaster.

The largest cause of blowouts is the swabbing in of kicks that turn into blowouts. The reason so many kicks get swabbed in is because of the large amount of time associated with tripping pipe. Day rates were USD\$163,000 and USD\$149,500 for semi-submersibles and drillships respectively on August 13<sup>th</sup>, 2004.<sup>44</sup> The time spent tripping pipe is an area that drilling personnel see as having potential time savings. The result is increased tripping velocity, minimal wellbore fill-up and possible missed warning signs concerning influxes.

Swab pressure is created when the pipe is pulled from the wellbore. The resulting suction created by the acceleration of the pipe (**Eq. 4.1**) and initial movement of the pipe (**Eq 4.2**) is the swab pressure.

$$\Delta p_{ac} = -\frac{0.00162\rho_m a_s d_o^2 L}{d_h^2 - d_o^2} \dots\dots\dots \text{Eq. 4.1}^8$$

$$\Delta p_g = -\frac{\tau_g L}{300(d_h - d_o)} \dots\dots\dots \text{Eq. 4.2}^8$$

**Eq. 4.2** covers the pressure required to break the gel strength of the drilling fluid. This pressure always occurs and should be accounted for, but there is little an operator can to change this value due to the fact that all muds will have some gel strength. One small drilling trick is to reciprocate the drillstring several feet up and down during operations

that require letting the drilling fluid sit still. This reduces the amount of the gel strength the drilling fluid acquires by sitting still and reduces the value of Eq. 4.2. The value of Eq. 4.1 is directly dependent on the acceleration,  $a_s$ , of the tripping pipe. This in turn affects the swab pressure. When drilling personnel rush the tripping process, the swab pressure clearly would go up. However, this is not the main problem, it simply aggravates the influx intensity. During rushed trips, the fill-up procedures and kick detection measures become more casual, resulting in small, typical well control problems developing into near or full blown blowouts. The only way to avoid this problem is to trip pipe at or below recommended velocities. Also since even the recommended velocities may be too much at times, proper kick detection procedures such as a fill up log are instrumental in identifying kicks earlier.

Kick detection is difficult in ultra-deepwater drilling. Several problems will need to be addressed by operators in the area of initial kick detection. The first problem is with gas cut mud. Gas cut mud will be a significant problem in ultra-deep water well control for several reasons. First, gas cut mud in general “hides” the gas influx and does not cause a significant pit gain.<sup>8</sup> As the gas begins to expand and pit gains reach warning levels, the influx has migrated some distance up the wellbore. This reduces the amount of reaction time as well as possibly confounding any well control calculations which are dependent on the timing of the influx entry. This is significant in ultra-deep water because of the bubble point. The bubble point is defined as the point at which a hydrocarbon solution goes from being a liquid solution to a two-phase gas-liquid solution.<sup>45</sup> As the pressure is further reduced past the bubble point, higher fractions of gas are present.<sup>45</sup> There are implications for ultra-deep water drilling concerning bubble point pressure. The first is that the gas will stay in solution longer because the bubble point pressure will not be reached until the gas has migrated far up the wellbore. For example in a well in the Gulf of Mexico in 10,000 ft. of water the hydrostatic pressure at the seafloor would be approximately 4,650 psi. This pressure value could be near or even above the bubble point pressure for a hydrocarbon mixture. In this situation the gas would not come out of a liquid form and create a significant pit gain until it was past the

sea floor. This would mean that a kick would be in the riser, the weakest link in ultra-deep water drilling, before definite pit gain and pressure changes were noticed. Because an influx would be very difficult to handle in this event, a situation such as this could be catastrophic during ultra-deep water drilling operations.

#### **4.4 Ultra-deepwater Well Control**

When a deepwater influx is encountered, the well must first be shut in as in any typical well control operation. The problem with shutting in the well in ultra-deepwater operations is the amount of heave a floating rig experience. This heave reciprocates the drillstring through the BOPE. If the well is shut-in with a pipe ram, there is increased wear on the drill pipe and ram. There is also a risk of parting the string if a particularly large swell pulls the tool joint into the ram.<sup>8</sup> If the well is shut-in through the use of an annular preventer, then the heave experienced by the floater will cause undue wear on the annular preventer seals.<sup>8</sup> **Table 4.1** shows a typical procedure for safely hanging-off a drillstring from a floater. Wear will still occur in this case, but should be kept to minimum with the motion compensators on the floater.<sup>46</sup> Using this procedure will allow the driller to be confident that the drillstring not be parted by a tool joint/ram contact.

**Table 4.1 - Hang-off, shut-in, and flow-check procedure.<sup>8</sup>**

1.	Place the Drillstring in a predetermined position above the rotary table and shut off the pump
2.	Line up the flowline to the trip tank and observe for flow
3.	If the well is flowing close the upper annular preventer
4.	Open the necessary fail-safe valves on the BOP stack and close the choke. (Closing the choke is only applicable if the manifold has been arranged for a soft shut-in.
5.	Reduce the annular closing pressure to the minimum requirement.
6.	Determine the tool joint location and position the tool joint in the stack above the upper pipe ram.
7.	Close the upper pipe ram, slowly lower the string, and hang it off on the ram.
8.	Lock the upper pipe ram in position.
9.	Reduce the support pressure on the motion compensator and support the pipe weight above the rams with the compensator.
10.	Measure shut-in pressures and pit gain.

Once it has been determined that the well is flowing, and subsequently the well is shut-in and the drill pipe properly shut-in. The influx is circulated out of the wellbore. The two standard methods available for use are the Drillers method and the Engineers or Wait and Weight method. The Drillers method is the standard circulation kill technique used in deepwater drilling. This is most likely due to its ease of use.

**Table 4.2 – Driller method procedure for killing well.<sup>8</sup>**

1.	Take care of the well until the kill procedure can be started by maintaining a constant drillpipe pressure and allowing migrating gas to expand.
2.	Open the choke and slowly start the pump. Coordinate the choke setting with the pump speed so that the original SICP is maintained until the pump is brought up to the kill rate.
3.	Read the drillpipe pressure and compare to the computed ICP. Hold ICP constant by choke manipulation until the kick fluids are circulated from the hole and original mud weight is measured at the choke outlet.
4.	Reduce the pump speed while closing the choke so that a constant casing pressure is maintained. When the pump is barely running, shut off the pump and finish closing the choke.
5.	Observe pressure gauges and verify that both record the original SIDPP. If not, check for trapped pressure.
6.	Recalculate the kill mud weight and increase the density of the mud in the pits.
7.	Open the choke and slowly start the pump. Increase the pump speed to kill rate while maintaining constant casing pressure.
8.	Continue to hold casing pressure constant until KWM enters the annulus.
9.	Read the drillpipe pressure and hold constant until kill mud weight is measured at the choke outlet.
10.	Shut off the pump and close the well in.
11.	Open the choke and check for flow.
12.	Resume operations. Incorporate trip margin into the mud weight.

The Drillers method does not require complex calculations making it easy for all drilling personnel to understand. The Drillers method is also attractive pressure-wise and in many cases psychologically because it can be begun immediately. **Table 4.2** shows the Drillers method procedure for a surface stack.

**Table 4.3 – Wait and Weight method for killing well.**<sup>8</sup>

1.	Take care of the well until the kill procedure can be started by maintaining a constant drillpipe pressure and allowing migrating gas to expand.
2.	Calculate the kill mud weight and increase the weight of the mud in the suction pit. Determine the weight material addition rate needed for the pumping operation and generate the a drillpipe pressure-reduction chart
3.	Open the choke and slowly start the pump. Coordinate choke setting with pump speed so that the original SICP is maintained until the pump is brought up to the kill rate.
4.	Read the drillpipe pressure and compare to the computed ICP. Manipulate the choke so that the CDDP follows the pressure reduction schedule.
5.	Maintain drillpipe pressure constant at the FCP value until the kill mud density is measured at the choke outlet.
6.	Reduce the pump speed while closing the choke so that a constant casing pressure is maintained. When the pump is barely running, shut off the pump and finish closing the choke.
7.	Observe pressure gauges and verify that both read zero. If not, check for trapped pressure.
8.	Open the choke and check for flow.
9.	Resume operations incorporating trip margin density into the mud.

The Wait and Weight method shown in **Table 4.3** is more complicated but has advantages. It only requires one circulation to the Drillers method's two circulations. However, during the weighting up of the mud, the influx may migrate too far. This is particularly true for ultra-deepwater wells, where the influx may not be detected until a significant volume has entered the wellbore. **Table 4.3** shows a comparison of casing shoe pressures between the two methods. While the Drillers method does result in higher annular pressures, ultra-deepwater influx detection delays may negate that disadvantage. Since the influx will most likely be below its bubble point and expansion is limited, the influx may have already migrated to or past a deep casing shoe prior to detection. The Wait and Weight method also depends on a large supply of barite being

on hand to immediately mix the kill weight mud. On a floating rig, there may not be enough barite to complete the task immediately. This is another major advantage of the Drillers method in that it does not require any immediate mixing. The circulation is begun, the influx circulated out, and any barite shortfalls can be remedied by the time the second circulation is set to begin.

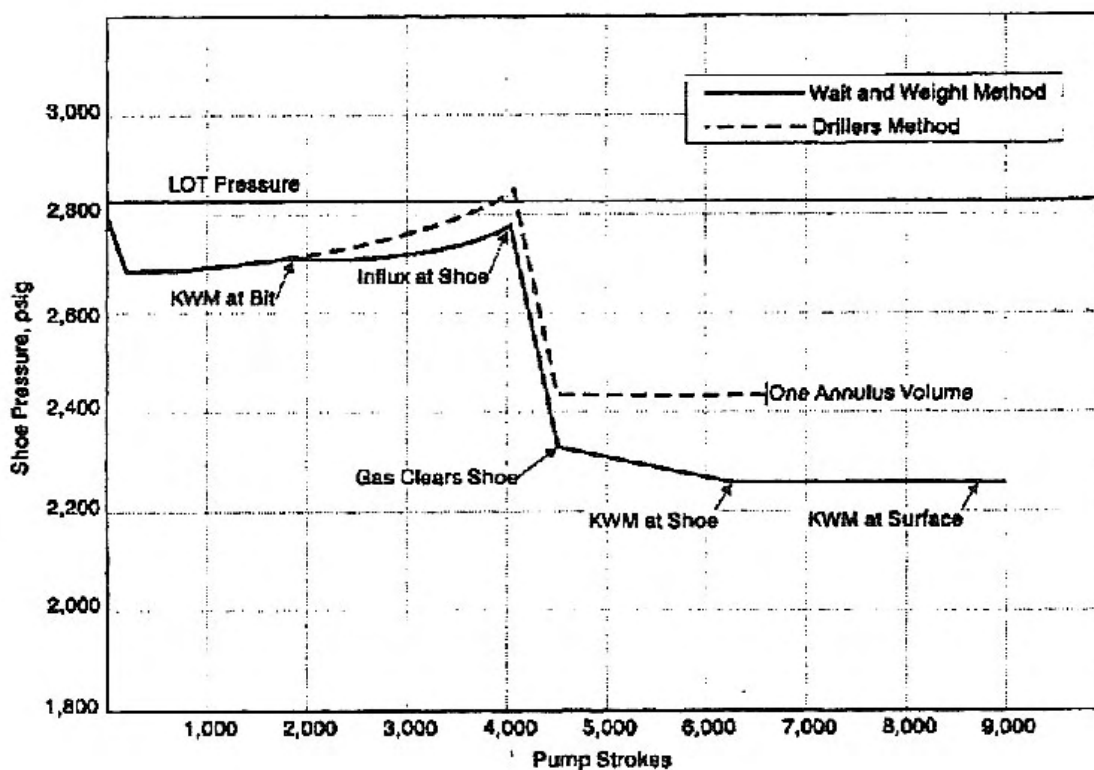


**Fig. 4.8 – Comparison of casing shoe pressures between Drillers method and Wait and Weight method shows Drillers method causes lost circulation.**<sup>8</sup>

The procedures shown in **Table 4.2** and **Table 4.3** are applicable for ultra-deepwater drilling until step 11 for the Drillers method and step 8 for the Wait and Weight method. Since ultra-deepwater deals with subsea BOP stacks, additional procedures need to be followed. The gas will be trapped at the BOP stack. This gas will have either not expanded much, or have expanded a tremendous amount in the last several hundred feet of circulation.<sup>46</sup> This means the influx is still under a tremendous

amount of pressure. For either circulation kill method, the following steps need to be followed to flush the gas from the top of the BOP stack.

Procedure for Flushing BOP stack:<sup>46</sup>

1. Close a set of rams below choke and kill line
2. To increase hydrostatic pressure on gas, circulate sea water down kill line and back up choke line.
3. Then allow gas to expand up choke line and vent appropriately.
4. Once gas has fully expanded, flush the choke line with sea water and proceed to killing the riser.

The gas will now have been circulated out of the wellbore. However, the riser still contains original weight mud (OWM). Bringing the riser and wellbore back into communication will result in a loss in hydrostatic head and another influx. Therefore, the following steps need to be followed to replace the OWM in the riser with kill weight mud (KWM).

Procedure for Killing the Riser:<sup>46</sup>

1. Flush BOP stack as shown above
2. Open the annular preventer while keeping lower rams closed.
3. Allow mud in riser to u-tube the sea water out of the choke and kill lines.
4. Put the rig pumps on the kill line and circulate KWM down the kill line and up the riser and choke line.
5. Once riser is full of KWM, open the lower rams and reestablish hydraulic communication with the wellbore.

According to some industry sources<sup>47</sup> “sandwiching” the influx is an acceptable method of influx control. Sandwiching a kick consists of concurrently displacing the drill pipe and annulus with heavy mud. This forces the kick into a lost circulation zone

created below the casing shoe. A secondary after effect is that young offshore formations will often bridge around the BHA and complete the kill.<sup>47</sup> While this would obviously be a successful method, the first choice should be a circulation method. These methods keep wellbore and formation damage to minimum as well as being methods drilling personnel are familiar with.

#### **4.5 Dynamic Kill Blowout Control**

There are many ways to control a blowout as previously mentioned in section 1. Many of the available publications cover these methods very ably.<sup>13</sup> While they did not account for the water depths drilled in today, with a few changes and considerations their discussion of these methods is sufficient. The first and foremost concern is the effect of increased water depth. The blowout control methods most affected are the surface intervention methods. To save the floater and reduce risk to personnel and equipment, the standard procedure for an influx that is not controllable is to close the BOP, disconnect the riser, and drive off of location. If for some unknown and extraordinary reason, the floater is left connected to the wellbore and the blowout is allowed to broach the surface, surface control techniques might be an option. However, this is not likely to ever occur due to the high cost of the floater and extreme danger associated with this action. Therefore, surface intervention is not considered an option.

Blowout control options are thus reduced to bridging or depletion, relief wells, or “vertical intervention”. Vertical intervention is a phrase coined by Adams to describe any kill attempts that involve wild wellbore re-entry.<sup>13</sup> For ultra-deepwater, this involves positioning a floater over the blowing well, and snubbing a drillstring or other equipment to control the well. This allows the operator to bypass the additional time and expense necessary drill a relief well. The extreme water depths may negate this option. 5000 to 10000 feet of drillpipe may be too long of a string to snub into a subsea BOP due to buckling concerns. Research in this area is non-existent, but it may be surmised that factors such as wellbore exit pressure, snubbed pipe strength and water depth would

determine if vertical intervention is possible. A solution to the buckling problem during vertical intervention may involve heavy wall drillpipe or high-grade casing.

Vertical intervention techniques include pumping gunk/cement plugs, bullheading, momentum kills, and dynamic kills down the blowing wellbore. Relief wells can be used to implement the same actions with the exception of bullheading. By the time a relief well is put into use, the other kill options are more attractive to the operator than bullheading because they do not carry the same risk of irreparable damage to the wellbore and formation.

This section of the report covers the use of relief wells and vertical intervention to deliver a dynamic kill to the blowing well. Best practices for the other kill options should be obtained from publications such as *DEA-63: Floating Vessel Blowout Control* or from blowout specialists.

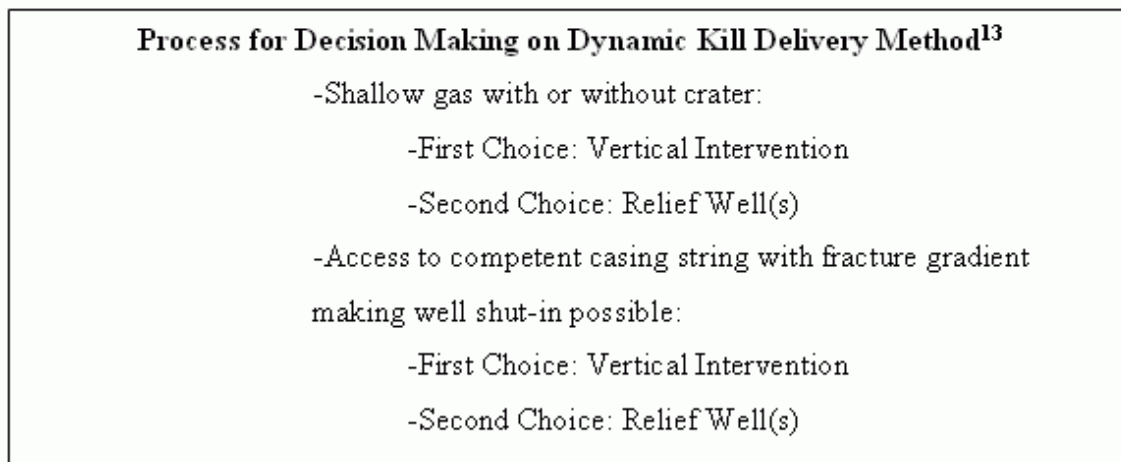


**Fig. 4.9 – Decision process for dynamic kill path.<sup>8</sup>**

The decision process for the dynamic kill delivery method is fairly simple as shown **Fig. 4.9**. This process is based on current environmental conditions as wellbore configuration, wild wellbore conditions and subsea equipment conditions. Vertical intervention is always preferable to a relief well for several reasons. The first is time necessary to complete the kill operation. Since vertical intervention uses the existing

wild wellbore as an access point to controlling the blowout, enormous amounts of time are saved. Relief wells require an entirely new wellbore that could take up to 50 or 60 days to drill depending on the environment and confidence in available geological information. Saving time through vertical intervention results in two main benefits for the operator.

The first is a reduction in the amount of hydrocarbons lost. This loss is not only economically disadvantageous but could cause with respect to environmental laws and public perception. The second benefit is a dramatic reduction in kill operation costs. At the time of this writing, day rates were USD\$163,000 and USD\$149,500 for semi-submersibles and drillships respectively.<sup>44</sup> This cost can be compounded attempting vertical intervention at the same time a relief well is being drilled. The cost of two floaters on location coupled with the cost of the hydrocarbon lost requires that the blowout be controlled as quickly as possible.

To quickly control the blowout, vertical intervention is recommended as long as it is possible. If the subsea equipment is damaged or the wellbore is damaged, vertical intervention may not be an option. If the wellhead or other subsea equipment is damaged or inoperable, repairs or replacement should be attempted. Typical methods to accomplish repairs or replacement involve the use of equipment such as ROVs and well-servicing rigs. However, the cost and time associated with these repairs is minimal in comparison with drilling a relief well. In shallow waters the use of vertical intervention is difficult to due to the loss of buoyancy resulting from the release of gas into the water directly over the wellbore. However, in ultra-deepwaters, the loss of buoyancy is approximately five percent as shown in **Fig. 4.10**.<sup>20</sup>

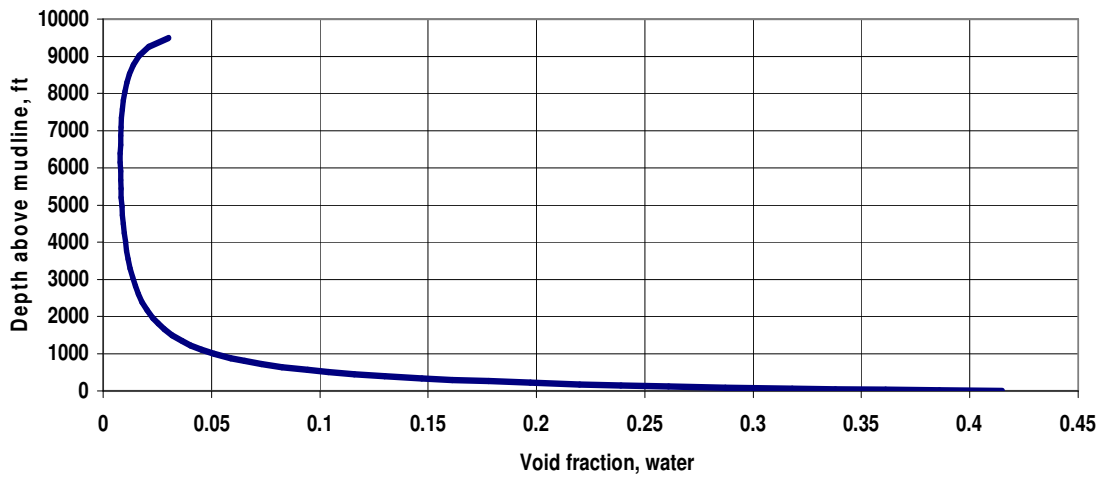


**Fig. 4.10 – Data from Adams et al. shows minimal loss of buoyancy from blowout plume.**<sup>20</sup>

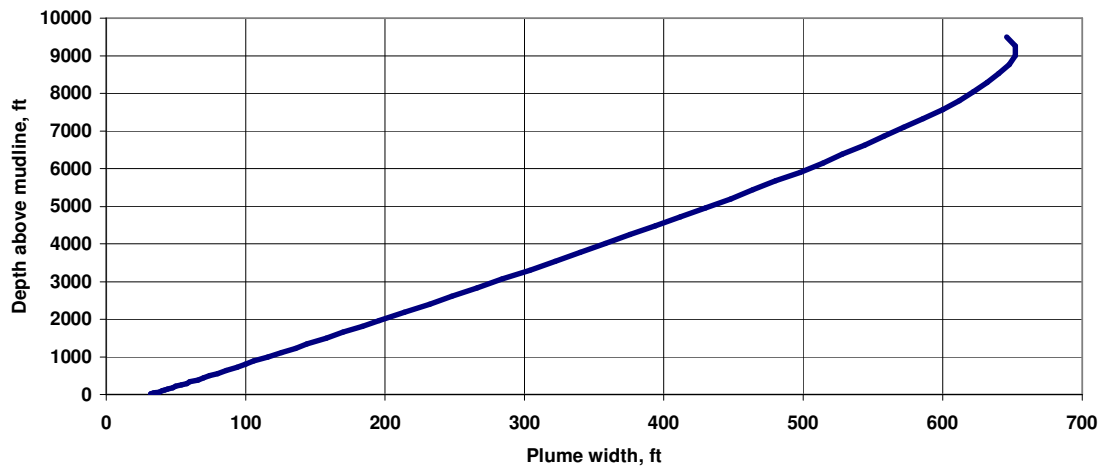


**Fig. 4.11– Data from Adams et al. shows wide plume at surface for blowout in 10000 feet of water.**<sup>20</sup>

This minimal loss of buoyancy would not limit any vertical intervention attempts. The data shown is for 10,000 feet of water. At the lower end of the ultra-deepwater range at approximately 5,000 feet of water, the loss of buoyancy is the same five percent. In the unlikely event a drillship was affected by this loss of buoyancy, a semi-submersible could be used if the flotation tanks were not filled with as much water as normal. This could allow vertical intervention in instances where buoyancy loss exceeded the calculations by Adams, et al.<sup>20</sup> Although, a floater would be able to float above the blowout, it would still have to contend with the surface conditions created by the blowout plume.<sup>20</sup> **Fig. 4.11** shows the width of the plume would be approximately 650 feet in 10,000 feet of water. The same data shows a plume width of approximately 350 feet in 5,000 feet of water. These values indicate that the floater would be surrounded by the blowout plume. This could cause adverse water surface conditions and air quality conditions. This discussion assumes a worst case scenario of water with no currents. Since any ultra-deepwater location will have some currents present, the plume will be dispersed. The extent to which the plume is dispersed is dependent on the strength, number and direction of the currents.<sup>20</sup> The presence of these conditions would need to be evaluated on a case-by-case basis to account for currents and wind conditions which may or may not take the plume and gas out of the way. The negligible loss of buoyancy also affects relief well MD/TVD ratios. Higher MD/TVD ratios are seen for land blowouts due to the need to distance blowout control personnel from the blowing fluids and related dangers. However, the land relief well MD/TVD ratios are not high for even the worst blowouts. For a 400 MMscfd/60,000 bopd blowout in the El Isba field in Syria, the relief wells were only 750 meters away from the blowing well. In this extreme case the MD/TVD ratio was less than 1.2. The relief well MD/TVD ratio will be even less for ultra-deepwater blowouts. Since buoyancy will be adequate for floaters to operate, the limiting factor in this case will be maintaining a safe separation of the blowout control vessels.

Whether or not it is established that vertical intervention is possible, relief well planning should be undertaken as well. The kill rates and pumping requirements will be

discussed in a later section of this report. The drilling and targeting requirements are ably discussed in many of the available blowout control texts.<sup>42,13,1,8,9,10,39</sup> Ultra-deepwater does little to change planning during the drilling and target operations. The large water depth induces the same changes in relief well planning as it does in normal ultra-deepwater directional wells. The rig selection, riser selection and seafloor equipment selection are most affected due to longer drillstrings and longer riser requirements. The targeting tools and principals remain the same, however the calculations may be slightly more complicated.

Timing of the relief well or wells is a critical concept that is the same regardless of the water depth. However, because the ultra-deepwater drilling equipment is expensive and not as readily available, timing becomes especially important. The order of operations for blowouts capable of being killed with one relief well is vertical intervention first, followed by spudding of the first relief well. The vertical intervention should be attempted for several days in order to allow for the well to bridge as well as to reduce cost associated with the mobilization of relief well drilling equipment in the event the well is killed quickly. If after several days, the vertical intervention process is not successful, the relief well may be begun. If backup relief wells are deemed necessary, the first relief well should be spudded as before. The operator should then wait several days to a week before beginning the backup relief wells. This lag time gives the blowout specialists time to plan the backup well after more important tasks have been taken care of, as well as saving the operator a significant amount of money.

Whether a blowout is initially considered as capable of being controlled through vertical intervention or relief wells is based on calculations from simulators such as COMASim in conjunction with the personal experience of the (hopefully) very experienced blowout specialists the operator saw fit to retain before the blowing well was even spudded. This report will base its recommendations mainly on COMASim simulation runs discussed earlier as well as blowout specialists advice from literature.

An important decision to be made prior to running simulations or calculations is the drillstring status. As **Table 1.2** indicated, the majority of blowouts stem from

improperly controlled influxes that occurred due to swabbing during tripping operations. This fact indicates that in these blowouts, the drillstring would not be at the bottom of the hole. One of the first calculations that should be made is whether or not the drillstring should be sheared or dropped to the bottom. As **Table 3.3** shows, the drillstring status has little to do with the blowout flow rate. However, **Fig. 3.16** indicates it has a dramatic effect on the kill rate. Although dropping the drillstring may seem to be a necessity in most dynamic kills, there can be a major problem with that action. **Fig. 3.11** shows that the bottomhole pressure for a dropped drillstring is almost 500 psi higher than that of a hanging drillstring. If the fracture and pore pressure gradients are similar to the lower portion of **Fig. 4.7b**, the operator may have already been close to fracturing the formation. The act of dropping the drillstring might cause the formation to fracture through the physical impact, which could bring about an underground blowout. The effect of surge pressure because of a falling drillstring would be minimal. The size of this effect is due to the wellbore having a large upward force in the form of the blowing fluid. Also, this fluid is most likely to be gas, therefore the lower density of the gas will not respond to the falling pipe. If the formation will hold, the pressure profile calculated with COMASim should then be used to check the expected casing shoe pressures. Again, excess pressure could cause an underground blowout. An underground blowout would change the blowout flow and possibly ruin the wellhead and BOPE. Understandably, the operator needs to keep as much of the wellbore and related equipment operational in order to retain some semblance of control over the situation. An underground blowout further complicates the control operation. If the formation will not be fractured by the pressure increase caused by the dropped drillstring, then dropping the drillstring, particularly a shorter one, will lower the kill requirements appreciably as illustrated in **Fig. 3.16**.

An untested idea is to use the drillstring kill option in conjunction with the relief well option to reduce drilling costs and time. More study needs to be completed on this topic, however it could provide a means to carry out dynamic kills of wells that would be unable to be controlled otherwise due to higher numbers of required relief wells. The

following discussion of pumping requirements illustrates the potential for high-rate, large wellbore blowouts to resist being controlled through dynamic means. These wells require multiple relief wells and the operator would benefit from considering this unorthodox approach to controlling the blowing well through less cost and in less time.

Once the wild well drillstring status during the dynamic kill has been determined, the pressure profile is calculated through use of a simulator such as COMASim. This pressure profile shows the pressure within the wellbore prior to pumping the dynamic kill.

The pumping requirements are also obtained through simulation. The basic trends concerning the pumping requirements are simple in nature and are discussed in detail in earlier sections. Higher blowout flow rates require higher kill rates. Larger wild wellbores require higher kill rates as well. Larger relief wellbores lower the pumping equipment requirements. A basic offshore pumping plant is shown in **Fig. 4.5**. This pumping plant requires clearing a large portion of a floater. However, it may be easier to put this style of pumping plant together than to contend with the linking of frac vessels such as the one shown in **Fig. 3.1**. Whatever the design for the pumping plant may be, it will be tailored to each blowout and should be reasonably developed in the contingency plan. This will allow the operator to quickly mobilize, and if necessary build, the pumping plant. Pumping requirements will also change with changing blowout flow rates. As previously discussed, blowouts have a tendency to bridge during the time range from 0 to 24 hours. While a blowout might not bridge in this period, vertical intervention methods can cause partial bridging to occur. This could change the pumping plant requirements and should be accounted for with new simulations.

## CHAPTER V

### CONCLUSIONS AND RECOMMENDED FUTURE RESEARCH

#### 5.1 Ultradeep Water Blowout Control Conclusions

- Blowouts are and have been a problem for the oil and gas industry. Even as technology has advanced, the incident rate for blowouts has remained constant.
- Causes for blowouts vary widely, however there is a constant. The majority of blowouts can be attributed to complacent, careless drilling practices.
- The COMASim simulator is an excellent simple simulator for calculating the requirements for a dynamic kill. Its ease of use makes COMASim a likely candidate for a preliminary or rough analysis in ultradeep water blowout situations.
- The pressure loss for the open hole section of the wild wellbore is dramatically higher due to a higher coefficient of friction.
- Without the added constriction of a drillstring in the wellbore, there is much less variation in pressure profiles and bottomhole pressures.
- Since surface gas flow rates depend on bottomhole pressures, two conclusions may be drawn. First, shorter drillstring lengths result in higher surface gas flow rates. Also, dropping the drillstring reduces the surface flow rate when compared to hanging drillstring situations.
- Relief well requirements increase with larger casing sizes due to increased blowout flow rate.
- Dynamic kill rates begin to vary widely between drillstring statuses as the drillstring length begins to decrease.
- Relief well measured depth to total vertical depth ratio should be as close to one as possible to keep the dynamic kill requirements to a minimum.
- Relief well annular ID to drillpipe OD ratio should be as large as possible to reduce the pumping requirements for the dynamic kill.

- Dropping the drillstring in the wild wellbore reduces your dynamic kill requirements.
- Dropping the drillstring in the wild wellbore increases the bottomhole pressure.
- Ultradeep water drilling and blowout control equipment needs to be designed specifically with the harsh ultradeep water environment in mind.
- Increasing the kill fluid reduces the required kill rate and pumping requirements.
- The Driller's Method is the industry recommended offshore well control procedure for most situations and will remain as such for ultradeep water drilling. This is due to its simplicity and ability to begin immediately circulating out the influx as opposed to allowing pressure to build up.
- During blowout control operations, there will be minimal loss of buoyancy. This means the rig administering the dynamic kill can position itself as close to the plume as necessary without worrying about buoyancy loss.
- If the drillstring can handle the buckling forces, attempts to vertically intervene should be made in conjunction with relief well operations. Time and monetary savings mean vertical intervention will pay off if it is successful.

Several areas exist that need to be improved on in order for COMASim to be more complete industry and research tool. These improvements will in turn allow more accurate best practices recommendations to be made in the area of ultra-deepwater blowout prevention and control.

## **5.2 Simple COMASim User Tasks and Extended Analysis Capability**

Perhaps the most important task to accomplish is to create, in COMASim, an effective tool that can be used for industry dynamic kill calculations as well as research into blowouts and dynamic kills. The first step needs to be creating a more detailed simulator capable of basic program functions. The basic functions would include the ability to save the input data as the default data, as well as export the input data in order to save it. The ability to recognize important points of change in the pressure profile is

also important for the end user. This would mean that the data output of the pressure profile to the left of the graphical output would be based on large changes in the pressure profile, not ten evenly spaced data points. The problem can be seen in **Fig. 3.4** and **Fig. 3.3**. Extending the analysis capability would include the ability to export the simulation output as a “.dat” file and/or to Microsoft Excel. This capability would increase the number of runs possible and accuracy of collected data leading to better analysis.

### **5.3 Multilateral Capability**

As previously discussed, the majority of wells in ultra-deepwater will not be the rigid vertical wells currently modeled by COMASim. Ultra-deepwater wells will not only have deviated main wellbores but also have several laterals. COMASim needs to have the capability to model the deviated wellbores as well as multilaterals. The calculations for this wellbore geometry and its effect on the friction factor are fairly simple. The calculations for multilateral situations would also be relatively simple if each lateral was kept identical to the others. I suggest this is the first type of multilateral calculation made available. Once this calculation is working, if the multilaterals need to be unique, then investigator should attempt to implement those calculations. Either way, the addition of multilateral and directional wellbore capability will allow COMASim to simulate more realistic situations.

### **5.4 Fluid Fallback**

Fluid fallback or counterflow has been considered for some time in dynamic kill literature but is not currently a part of COMASim calculations.<sup>21,22</sup> It is often ignored in practice because doing so simply makes the dynamic kill calculations more conservative. The COMASim results that show that ultradeep water, high-flow blowouts may require three or more relief wells necessitate the investigation of the safety factor given to dynamic kill calculations which ignore fluid fallback. An option given to the user of whether or not to include fluid fallback in the calculations could change the number of relief wells and pumping requirements in high flow rate blowouts.

### **5.5 Underground Blowout Capability**

Many blowouts become underground blowouts due to weak exposed formations, weak casing or cement, or poor well or blowout control practices. Modeling an underground blowout is currently possible in COMASim by manipulating the simulator using the exit pressure to mimic the thief zone pressure. However this is an imperfect solution that is often confusing to the user and likely to yield suspect results. The capability to model underground blowouts would extend the usefulness of COMASim into an entirely new type of blowout thereby giving it added research and industry value.

### **5.6 Linking to Dr. Jongguen Choe's Simulator**

A simulator developed by Dr. Jongguen Choe, with a significant amount of help from several of the committee members for thesis, simulates well control for many aspects of drilling including multilaterals and tripping.<sup>48</sup> Both of these situations will be factors in many blowouts making Choe's simulator an important tool in the analysis of ultra-deepwater blowouts. There is currently no link between COMASim and Choe's simulator. An ideal situation would exist in which Choe's simulator output a data file when a blowout occurred during a simulation due to a poorly handled influx. This data file would be compatible with COMASim. After COMASim reads the data file, it could calculate the blowout initial conditions as well as the dynamic kill requirements. Adding this capability would increase the usefulness to industry personnel as well as researchers for both simulators.

### **5.7 Simulator Validation**

An important part of the initial planning of this study included validation of COMASim using field cases. Unfortunately, the only data that resulted in a match was an example from Watson, et al.<sup>8</sup> Other blowout case histories obtained from the MMS and Larry Flak of Boots and Coots caused the simulator to fail. An in-depth study needs to be done to rectify the situation. To complete this, an investigator proficient in Java code needs to be found. The problems relating to the case histories should be identified

and solutions to COMASim's inability to simulate these case histories would be found. The study would need to obtain access to several databases such as the Neal Adams/Matthew Daniels blowout database, the Wellflow Dynamics blowout database and SINTEF's blowout database. Successful access to these databases could yield several more standard case histories that are closer to COMASim's capabilities than the extraordinary cases in literature. This validation process would focus on real-life situations and COMASim's ability to handle these situations. With validation of COMASim would come an increased confidence in its results.

### **5.8 Combination Vertical Intervention and Relief Well Dynamic Kill Operations**

A brief discussion in the best practices section covered the possibility of using a combination kill operation in which kill fluid flow paths simultaneously included relief well(s) and vertical intervention. This is a complex operation hydraulically, but it is certainly possible. This type of operation could reduce the drilling requirements for blowouts requiring multiple relief wells to a point where a dynamic kill was possible. The addition of this option would create interesting research and discussion opportunities as well as possibly improve the capability of the industry to handle blowouts dynamically.

## NOMENCLATURE

$a$	= acceleration
BOP	= Blowout preventer
BOPE	= Blowout preventer equipment
COMASim	= Cherokee Offshore, MMS, Texas A&M Simulator
$d$	= pipe diameter, L
DP	= drill pipe
$f'$	= Fanning friction factor
$g$	= acceleration of gravity, L/t <sup>2</sup>
GOM	= Gulf of Mexico
IPR	= inflow performance relationship
$L$	= length, L
md	= millidarcy
MMscfd	= million cubic feet per day
MMS	= Mineral Management Service
OCS	= Outer Continental Shelf
$P$	= pressure, m/L <sup>2</sup>
psi	= pounds per square inch
ROV	= Remote operated vehicle
RPSEA	= Research Partnership to Secure Energy for America
SINTEF	= Foundation for Scientific and Industrial Research at the Norwegian Institute of Technology
TD	= Total Depth
TVD	= Total Vertical Depth
$v$	= velocity, L/t
$\mu$	= viscosity, m/Lt
$\mu$	= coefficient of friction
$\rho$	= density, m/L <sup>3</sup>
$\tau$	= shear stress, m/Lt <sup>2</sup>

## Subscripts

<i>ac</i>	=	acceleration
<i>c</i>	=	conversion constant
<i>f</i>	=	fluid
<i>g</i>	=	gas
<i>h</i>	=	hydrostatic
<i>m</i>	=	mixture
<i>o</i>	=	outer
<i>s</i>	=	superficial

## REFERENCES

1. Goins, W.C., Jr. and Sheffield, R.: *Blowout Prevention*, Gulf Publishing Company, Houston, Texas (1983).
2. "History of Spindletop Oil Discovery," <http://www.priweb.org/ed/pgws/history/spindletop/spindletop.html>; Accessed June 2004.
3. "Cooper-Cameron Profile," [http://www.businessnewsonline.com/%20Web%20Site%20Files/Feature\\_Business/Cameron.html](http://www.businessnewsonline.com/%20Web%20Site%20Files/Feature_Business/Cameron.html); Accessed June 2004.
4. Skalle, P. and Podio, A.L.: "Trends Extracted from 1200 Gulf Coast Blowouts During 1960-1996," paper SPE 39354 presented at the 1998 IADC/SPE Drilling Conference, Dallas, TX, 3-6 March.
5. "SINTEF Overview," <http://www.sintef.no/>; Accessed July 2004.
6. Holand, P.: *Offshore Blowout: Causes and Control*, Gulf Publishing Company, Houston, TX (1997).
7. Skalle, P., Trondheim, J.H. and Podio A.L.: "Killing Methods and Consequences of 1120 Gulf Coast Blowouts During 1960-1996," paper SPE 53974 presented at the 1999 IADC/SPE Drilling Conference, Dallas, TX, 3-6 March.
8. Watson, D., Brittenham, T. and Moore, P.L.: *Advanced Well Control: SPE Textbook Series Vol. 10*, Society of Petroleum Engineers, Richardson, TX (2003).
9. Adams, N. and Kuhlman, L.: *Kicks and Blowout Control*. 2<sup>nd</sup> Edition, Pennwell Books, Tulsa, OK (1994).
10. Grace, R.D.: *Advanced Blowout & Well Control*, Gulf Publishing Company, Houston, TX (1994).
11. Confidential Minerals Management Service (MMS) well control incident reports obtained April 2004 from MMS.
12. Tarr, B.A. and Flak, L.: "Part 6 – Underground Blowouts," John Wright Company, Houston, TX, [www.jwco.com](http://www.jwco.com), Accessed July 2004.
13. Neal Adams Firefighters, Inc.: "Joint Industry Program for Floating Vessel Blowout Control (DEA-63)," Neal Adams Firefighters, Inc., Houston, TX (1991).

14. "Summary of 1986 Lake Maracaibo Blowout," [http://www.jwco.com/case-histories/lake\\_maracaibo\\_venezuela\\_1986/lake\\_maracaibo\\_venezuela\\_1986.htm](http://www.jwco.com/case-histories/lake_maracaibo_venezuela_1986/lake_maracaibo_venezuela_1986.htm), Accessed July 2004.
15. Wright, J.W. and Flak, L.: "Part 11-Relief wells: Advancements in Technology and Application Engineering Make the Relief Well a more Practical Blowout Control Option," John Wright Company, Houston, TX, [www.jwco.com](http://www.jwco.com), Accessed July 2004.
16. Blount, E.M. and Soeimah, E.: "Dynamic Kill Controlling Wild Wells a New Way", *World Oil* (Oct. 1981) 109-116.
17. "Summary of 1994 Patagonia, Argentina Blowout," [http://www.jwco.com/case-histories/patagonia\\_argentina\\_1994/patagonia\\_argentina\\_1994.htm](http://www.jwco.com/case-histories/patagonia_argentina_1994/patagonia_argentina_1994.htm), Accessed July 2004.
18. "Relief Well Overview," [http://www.jwco.com/is\\_relief\\_well.htm](http://www.jwco.com/is_relief_well.htm), Accessed July 2004.
19. "Summary of 1995 Syrian Blowout," [http://www.jwco.com/case-histories/syria\\_1995/syria\\_1995.htm](http://www.jwco.com/case-histories/syria_1995/syria_1995.htm), Accessed July 2004.
20. Adams, N. and Economides, M.J.: "Characterization of Blowout Behavior in Deepwater Environments," paper SPE 79879 presented 2003 SPE/IADC Drilling Conference, Amsterdam, The Netherlands, 19-21 February.
21. Flores-Avila, F.S., Smith, J.R., Bourgoyne, A.T. Jr.: "New Dynamic Kill Procedure for Off-Bottom Blowout Wells Considering Counter-Current Flow of Kill Fluid," paper SPE 85292 presented 2003 SPE/IADC Middle East Drilling Technology Conference & Exhibition, Abu Dhabi, UAE, 20-22 October.
22. Flores-Avila, F.S., Smith, J. R., Bourgoyne, A.T., Bourgoyne, D.A.: "Experimental Evaluation of Control Fluid Fallback During Off-Bottom Well Control: Effect of Deviation Angle," paper IADC/SPE 74568 presented 2002 IADC/SPE Drilling Conference, Dallas, TX, 26-28 February.
23. Schubert, J.J. and Weddle, C.E. III: "Development of a Blowout Intervention Method and Dynamic Kill Simulator for Blowouts Occurring in Ultra-Deepwater," JIP Proposal available from Mineral Management Service, Houston, TX (October 2000).

24. Schubert, J.J.: "Development of a Blowout Intervention Method and Dynamic Kill Simulator for Blowouts Occurring in Ultra-Deepwater," JIP Proposal available from Research Project to Secure Energy for America, Sugar Land, TX (2003).
25. "Gulf of Mexico Borehole History," <http://www.gomr.mms.gov/homepg/fastfacts/borehole/borelist.asp>, Accessed July 2004.
26. Choe, J. and Juvkam-Wold, H.C.: "Riserless Drilling: Concepts, Applications, Advantages, and Limitations," paper CADE/CAODC 97-140 presented 1997 CADE/CAODC Spring Drilling Conference, Calgary, 8-10 April.
27. Choe, J. and Juvkam-Wold, H.C.: "Riserless Drilling and Well Control for Deep Water Applications," *Proc. 1997 IADC International Deep Water Well Control Conference and Exhibition*, Houston, 15-16 September.
28. Gault, A.D.: "Riserless Drilling: Circumventing the Size/Cost Cycle in Deepwater," *Offshore* (1996) 56, No. 5, 49-54.
29. Oskarsen, R.T.: "Development of a Dynamic Kill Simulator for Ultradeep Water," PhD Dissertation, Texas A&M University, College Station, TX (2004).
30. Halliburton Cementing Tables, Halliburton Company, Houston, TX (2001).
31. Schlumberger Field Data Handbook. Schlumberger, Houston, TX (2001).
32. Personal communication with Ray T. Oskarsen, Texas A&M University, College Station, TX, 4/15/04.
33. Personal communication with Larry Flak, Boots and Coots, Houston, TX 5/4/04.
34. Personal communication with Dr. Ray T. Oskarsen, John Wright Co., Houston, TX 7/25/04.
35. "BJ Services Deepwater Stimulation Vessels," [http://www.bjservices.com/website/ps.nsf/0/634FE8289F16FB9086256DC600621609/\\$file/Deepwater+Stimulation+Vessels-Gulf+of+Mexico.pdf](http://www.bjservices.com/website/ps.nsf/0/634FE8289F16FB9086256DC600621609/$file/Deepwater+Stimulation+Vessels-Gulf+of+Mexico.pdf), Accessed August 2004.
36. Flak, L.: "Blowout Case Histories," presentations available upon request from Larry Flak, Boots & Coots, Houston, TX.

37. "Offshore Rig Fleet Information," <http://www.deepwater.com/FleetInformation.cfm>, Accessed August 2004.
38. "ABB Vetco Grey Product Flier for Deepwater Riser," <http://www.abb.com/global/abbzh/abbzh251.nsf!OpenDatabase&db=/global/noofs/noofs187.nsf&v=F216&e=us&m=9F2&c=4D91C6E88ACCE11A85256C67006BF951>, Accessed August 2004.
39. Vigeant, S.P.: "How Well Control Equipment Is Advancing to Meet Deepwater Needs - Part 2," *World Oil* (July 1998) 54-56.
40. "Kingdom Drilling Practices Manuel," <http://www.kingdomdrilling.co.uk/drillops/equipment/DWSS01.pdf>, 3. Accessed August 2004.
41. "Sonardyne BOP Product Brochure," [http://www.sonardyne.co.uk/Downloads/brochures/bop\\_brochure.pdf](http://www.sonardyne.co.uk/Downloads/brochures/bop_brochure.pdf), Accessed August 2004.
42. "Norwegian Drilling Standards," [http://www.standard.no/pronorm-3/data/f/0/01/30/1\\_10704\\_0/D-010.pdf](http://www.standard.no/pronorm-3/data/f/0/01/30/1_10704_0/D-010.pdf), Accessed August 2004.
43. Abel, L.W., Bowden, J.R., and Campbell, P.J.: *Firefighting and Blowout Control*, Wild Well Control, Inc., Spring, TX (1994).
44. "Dayrates for Gulf of Mexico for August 13<sup>th</sup>, 2004," <http://www.rigzone.com/data/dayrates/>, Accessed August 2004.
45. Dake, L.P.: *Fundamentals of Reservoir Engineering*, Elsevier Scientific Publishing Company, Amsterdam (1978).
46. Schubert, J.J.: "Well Control," M. Eng report, Texas A&M University, College Station, TX (1995).
47. Grace, R.D., *Blowout and Well Control Handbook*, Gulf Professional Publishing, New York (2003).
48. Choe, J, Schubert, J.J., Juvkam-Wold, H.C.: "Well Control Analyses on Extended Reach and Multilateral Trajectories," paper OTC presented at 2004 Offshore Technology Conference, Houston, TX, 3-6 May.

## APPENDIX A

### SIMULATION RUN MATRIX

#### Relief Well Run Matrix

RUN #	TVD	WATER	DS	PARAMETER	PARAMETER	MD/TVD	ANN ID/
	BML	DEPTH	STATUS	VARIED	VALUE	RATIO	OD RATIO
1	3000	0	Hanging from BOP	Casing OD	7	1	2
3	3000	0	Hanging from BOP	Casing OD	7	1	1.5
5	3000	0	Hanging from BOP	Casing OD	7	1.5	2
7	3000	0	Hanging from BOP	Casing OD	7	1.5	1.5
9	3000	0	Hanging from BOP	Casing OD	7	2	2
11	3000	0	Hanging from BOP	Casing OD	7	2	1.5
13	3000	0	Hanging from BOP	Casing OD	10.75	1	2
15	3000	0	Hanging from BOP	Casing OD	10.75	1	1.5
17	3000	0	Hanging from BOP	Casing OD	10.75	1.5	2
19	3000	0	Hanging from BOP	Casing OD	10.75	1.5	1.5
21	3000	0	Hanging from BOP	Casing OD	10.75	2	2
23	3000	0	Hanging from BOP	Casing OD	10.75	2	1.5
25	3000	0	Hanging from BOP	Casing OD	12.75	1	2
27	3000	0	Hanging from BOP	Casing OD	12.75	1	1.5
29	3000	0	Hanging from BOP	Casing OD	12.75	1.5	2
31	3000	0	Hanging from BOP	Casing OD	12.75	1.5	1.5
33	3000	0	Hanging from BOP	Casing OD	12.75	2	2
35	3000	0	Hanging from BOP	Casing OD	12.75	2	1.5
37	3000	0	Hanging from BOP	DS Length	50%	1	2
39	3000	0	Hanging from BOP	DS Length	50%	1	1.5
41	3000	0	Hanging from BOP	DS Length	50%	1.5	2
43	3000	0	Hanging from BOP	DS Length	50%	1.5	1.5
45	3000	0	Hanging from BOP	DS Length	50%	2	2
47	3000	0	Hanging from BOP	DS Length	50%	2	1.5
49	3000	0	Hanging from BOP	DS Length	25%	1	2
51	3000	0	Hanging from BOP	DS Length	25%	1	1.5
53	3000	0	Hanging from BOP	DS Length	25%	1.5	2
55	3000	0	Hanging from BOP	DS Length	25%	1.5	1.5
57	3000	0	Hanging from BOP	DS Length	25%	2	2
59	3000	0	Hanging from BOP	DS Length	25%	2	1.5
61	3000	0	Dropped DS	Casing OD	7	1	2
63	3000	0	Dropped DS	Casing OD	7	1	1.5
65	3000	0	Dropped DS	Casing OD	7	1.5	2
67	3000	0	Dropped DS	Casing OD	7	1.5	1.5
69	3000	0	Dropped DS	Casing OD	7	2	2
71	3000	0	Dropped DS	Casing OD	7	2	1.5
73	3000	0	Dropped DS	Casing OD	10.75	1	2
75	3000	0	Dropped DS	Casing OD	10.75	1	1.5

77	3000	0	Dropped DS	Casing OD	10.75	1.5	2
79	3000	0	Dropped DS	Casing OD	10.75	1.5	1.5
81	3000	0	Dropped DS	Casing OD	10.75	2	2
83	3000	0	Dropped DS	Casing OD	10.75	2	1.5
85	3000	0	Dropped DS	Casing OD	12.75	1	2
87	3000	0	Dropped DS	Casing OD	12.75	1	1.5
89	3000	0	Dropped DS	Casing OD	12.75	1.5	2
91	3000	0	Dropped DS	Casing OD	12.75	1.5	1.5
93	3000	0	Dropped DS	Casing OD	12.75	2	2
95	3000	0	Dropped DS	Casing OD	12.75	2	1.5
97	3000	0	Dropped DS	DS Length	50%	1	2
99	3000	0	Dropped DS	DS Length	50%	1	1.5
101	3000	0	Dropped DS	DS Length	50%	1.5	2
103	3000	0	Dropped DS	DS Length	50%	1.5	1.5
105	3000	0	Dropped DS	DS Length	50%	2	2
107	3000	0	Dropped DS	DS Length	50%	2	1.5
109	3000	0	Dropped DS	DS Length	25%	1	2
111	3000	0	Dropped DS	DS Length	25%	1	1.5
113	3000	0	Dropped DS	DS Length	25%	1.5	2
115	3000	0	Dropped DS	DS Length	25%	1.5	1.5
117	3000	0	Dropped DS	DS Length	25%	2	2
119	3000	0	Dropped DS	DS Length	25%	2	1.5
121	3000	0	No DS	Casing OD	7	1	2
123	3000	0	No DS	Casing OD	7	1	1.5
125	3000	0	No DS	Casing OD	7	1.5	2
127	3000	0	No DS	Casing OD	7	1.5	1.5
129	3000	0	No DS	Casing OD	7	2	2
131	3000	0	No DS	Casing OD	7	2	1.5
133	3000	0	No DS	Casing OD	10.75	1	2
135	3000	0	No DS	Casing OD	10.75	1	1.5
137	3000	0	No DS	Casing OD	10.75	1.5	2
139	3000	0	No DS	Casing OD	10.75	1.5	1.5
141	3000	0	No DS	Casing OD	10.75	2	2
143	3000	0	No DS	Casing OD	10.75	2	1.5
145	3000	0	No DS	Casing OD	12.75	1	2
147	3000	0	No DS	Casing OD	12.75	1	1.5
149	3000	0	No DS	Casing OD	12.75	1.5	2
151	3000	0	No DS	Casing OD	12.75	1.5	1.5
153	3000	0	No DS	Casing OD	12.75	2	2
155	3000	0	No DS	Casing OD	12.75	2	1.5
160	3000	5000	Hanging from BOP	Casing OD	7	1	2
162	3000	5000	Hanging from BOP	Casing OD	7	1	1.5
164	3000	5000	Hanging from BOP	Casing OD	7	1.5	2
166	3000	5000	Hanging from BOP	Casing OD	7	1.5	1.5
168	3000	5000	Hanging from BOP	Casing OD	7	2	2
170	3000	5000	Hanging from BOP	Casing OD	7	2	1.5
172	3000	5000	Hanging from BOP	Casing OD	10.75	1	2
174	3000	5000	Hanging from BOP	Casing OD	10.75	1	1.5

176	3000	5000	Hanging from BOP	Casing OD	10.75	1.5	2
178	3000	5000	Hanging from BOP	Casing OD	10.75	1.5	1.5
180	3000	5000	Hanging from BOP	Casing OD	10.75	2	2
182	3000	5000	Hanging from BOP	Casing OD	10.75	2	1.5
184	3000	5000	Hanging from BOP	Casing OD	12.75	1	2
186	3000	5000	Hanging from BOP	Casing OD	12.75	1	1.5
188	3000	5000	Hanging from BOP	Casing OD	12.75	1.5	2
190	3000	5000	Hanging from BOP	Casing OD	12.75	1.5	1.5
192	3000	5000	Hanging from BOP	Casing OD	12.75	2	2
194	3000	5000	Hanging from BOP	Casing OD	12.75	2	1.5
196	3000	5000	Hanging from BOP	DS Length	50%	1	2
198	3000	5000	Hanging from BOP	DS Length	50%	1	1.5
200	3000	5000	Hanging from BOP	DS Length	50%	1.5	2
202	3000	5000	Hanging from BOP	DS Length	50%	1.5	1.5
204	3000	5000	Hanging from BOP	DS Length	50%	2	2
206	3000	5000	Hanging from BOP	DS Length	50%	2	1.5
208	3000	5000	Hanging from BOP	DS Length	25%	1	2
210	3000	5000	Hanging from BOP	DS Length	25%	1	1.5
212	3000	5000	Hanging from BOP	DS Length	25%	1.5	2
214	3000	5000	Hanging from BOP	DS Length	25%	1.5	1.5
216	3000	5000	Hanging from BOP	DS Length	25%	2	2
218	3000	5000	Hanging from BOP	DS Length	25%	2	1.5
220	3000	5000	Dropped DS	Casing OD	7	1	2
222	3000	5000	Dropped DS	Casing OD	7	1	1.5
224	3000	5000	Dropped DS	Casing OD	7	1.5	2
226	3000	5000	Dropped DS	Casing OD	7	1.5	1.5
228	3000	5000	Dropped DS	Casing OD	7	2	2
230	3000	5000	Dropped DS	Casing OD	7	2	1.5
232	3000	5000	Dropped DS	Casing OD	10.75	1	2
234	3000	5000	Dropped DS	Casing OD	10.75	1	1.5
236	3000	5000	Dropped DS	Casing OD	10.75	1.5	2
238	3000	5000	Dropped DS	Casing OD	10.75	1.5	1.5
240	3000	5000	Dropped DS	Casing OD	10.75	2	2
242	3000	5000	Dropped DS	Casing OD	10.75	2	1.5
244	3000	5000	Dropped DS	Casing OD	12.75	1	2
246	3000	5000	Dropped DS	Casing OD	12.75	1	1.5
248	3000	5000	Dropped DS	Casing OD	12.75	1.5	2
250	3000	5000	Dropped DS	Casing OD	12.75	1.5	1.5
252	3000	5000	Dropped DS	Casing OD	12.75	2	2
254	3000	5000	Dropped DS	Casing OD	12.75	2	1.5
256	3000	5000	Dropped DS	DS Length	50%	1	2
258	3000	5000	Dropped DS	DS Length	50%	1	1.5
260	3000	5000	Dropped DS	DS Length	50%	1.5	2
262	3000	5000	Dropped DS	DS Length	50%	1.5	1.5
264	3000	5000	Dropped DS	DS Length	50%	2	2
266	3000	5000	Dropped DS	DS Length	50%	2	1.5
268	3000	5000	Dropped DS	DS Length	25%	1	2
270	3000	5000	Dropped DS	DS Length	25%	1	1.5

272	3000	5000	Dropped DS	DS Length	25%	1.5	2
274	3000	5000	Dropped DS	DS Length	25%	1.5	1.5
276	3000	5000	Dropped DS	DS Length	25%	2	2
278	3000	5000	Dropped DS	DS Length	25%	2	1.5
280	3000	5000	No DS	Casing OD	7	1	2
282	3000	5000	No DS	Casing OD	7	1	1.5
284	3000	5000	No DS	Casing OD	7	1.5	2
286	3000	5000	No DS	Casing OD	7	1.5	1.5
288	3000	5000	No DS	Casing OD	7	2	2
290	3000	5000	No DS	Casing OD	7	2	1.5
292	3000	5000	No DS	Casing OD	10.75	1	2
294	3000	5000	No DS	Casing OD	10.75	1	1.5
296	3000	5000	No DS	Casing OD	10.75	1.5	2
298	3000	5000	No DS	Casing OD	10.75	1.5	1.5
300	3000	5000	No DS	Casing OD	10.75	2	2
302	3000	5000	No DS	Casing OD	10.75	2	1.5
304	3000	5000	No DS	Casing OD	12.75	1	2
306	3000	5000	No DS	Casing OD	12.75	1	1.5
308	3000	5000	No DS	Casing OD	12.75	1.5	2
310	3000	5000	No DS	Casing OD	12.75	1.5	1.5
312	3000	5000	No DS	Casing OD	12.75	2	2
314	3000	5000	No DS	Casing OD	12.75	2	1.5
322	3000	10000	Hanging from BOP	Casing OD	7	1	2
324	3000	10000	Hanging from BOP	Casing OD	7	1	1.5
326	3000	10000	Hanging from BOP	Casing OD	7	1.5	2
328	3000	10000	Hanging from BOP	Casing OD	7	1.5	1.5
330	3000	10000	Hanging from BOP	Casing OD	7	2	2
332	3000	10000	Hanging from BOP	Casing OD	7	2	1.5
334	3000	10000	Hanging from BOP	Casing OD	10.75	1	2
336	3000	10000	Hanging from BOP	Casing OD	10.75	1	1.5
338	3000	10000	Hanging from BOP	Casing OD	10.75	1.5	2
340	3000	10000	Hanging from BOP	Casing OD	10.75	1.5	1.5
342	3000	10000	Hanging from BOP	Casing OD	10.75	2	2
344	3000	10000	Hanging from BOP	Casing OD	10.75	2	1.5
346	3000	10000	Hanging from BOP	Casing OD	12.75	1	2
348	3000	10000	Hanging from BOP	Casing OD	12.75	1	1.5
350	3000	10000	Hanging from BOP	Casing OD	12.75	1.5	2
352	3000	10000	Hanging from BOP	Casing OD	12.75	1.5	1.5
354	3000	10000	Hanging from BOP	Casing OD	12.75	2	2
356	3000	10000	Hanging from BOP	Casing OD	12.75	2	1.5
358	3000	10000	Hanging from BOP	DS Length	50%	1	2
360	3000	10000	Hanging from BOP	DS Length	50%	1	1.5
362	3000	10000	Hanging from BOP	DS Length	50%	1.5	2
364	3000	10000	Hanging from BOP	DS Length	50%	1.5	1.5
366	3000	10000	Hanging from BOP	DS Length	50%	2	2
368	3000	10000	Hanging from BOP	DS Length	50%	2	1.5
370	3000	10000	Hanging from BOP	DS Length	25%	1	2
372	3000	10000	Hanging from BOP	DS Length	25%	1	1.5

374	3000	10000	Hanging from BOP	DS Length	25%	1.5	2
376	3000	10000	Hanging from BOP	DS Length	25%	1.5	1.5
378	3000	10000	Hanging from BOP	DS Length	25%	2	2
380	3000	10000	Hanging from BOP	DS Length	25%	2	1.5
382	3000	10000	Dropped DS	Casing OD	7	1	2
384	3000	10000	Dropped DS	Casing OD	7	1	1.5
386	3000	10000	Dropped DS	Casing OD	7	1.5	2
388	3000	10000	Dropped DS	Casing OD	7	1.5	1.5
390	3000	10000	Dropped DS	Casing OD	7	2	2
392	3000	10000	Dropped DS	Casing OD	7	2	1.5
394	3000	10000	Dropped DS	Casing OD	10.75	1	2
396	3000	10000	Dropped DS	Casing OD	10.75	1	1.5
398	3000	10000	Dropped DS	Casing OD	10.75	1.5	2
400	3000	10000	Dropped DS	Casing OD	10.75	1.5	1.5
402	3000	10000	Dropped DS	Casing OD	10.75	2	2
404	3000	10000	Dropped DS	Casing OD	10.75	2	1.5
406	3000	10000	Dropped DS	Casing OD	12.75	1	2
408	3000	10000	Dropped DS	Casing OD	12.75	1	1.5
410	3000	10000	Dropped DS	Casing OD	12.75	1.5	2
412	3000	10000	Dropped DS	Casing OD	12.75	1.5	1.5
414	3000	10000	Dropped DS	Casing OD	12.75	2	2
416	3000	10000	Dropped DS	Casing OD	12.75	2	1.5
418	3000	10000	Dropped DS	DS Length	50%	1	2
420	3000	10000	Dropped DS	DS Length	50%	1	1.5
422	3000	10000	Dropped DS	DS Length	50%	1.5	2
424	3000	10000	Dropped DS	DS Length	50%	1.5	1.5
426	3000	10000	Dropped DS	DS Length	50%	2	2
428	3000	10000	Dropped DS	DS Length	50%	2	1.5
430	3000	10000	Dropped DS	DS Length	25%	1	2
432	3000	10000	Dropped DS	DS Length	25%	1	1.5
434	3000	10000	Dropped DS	DS Length	25%	1.5	2
436	3000	10000	Dropped DS	DS Length	25%	1.5	1.5
438	3000	10000	Dropped DS	DS Length	25%	2	2
440	3000	10000	Dropped DS	DS Length	25%	2	1.5
442	3000	10000	No DS	Casing OD	7	1	2
444	3000	10000	No DS	Casing OD	7	1	1.5
446	3000	10000	No DS	Casing OD	7	1.5	2
448	3000	10000	No DS	Casing OD	7	1.5	1.5
450	3000	10000	No DS	Casing OD	7	2	2
452	3000	10000	No DS	Casing OD	7	2	1.5
454	3000	10000	No DS	Casing OD	10.75	1	2
456	3000	10000	No DS	Casing OD	10.75	1	1.5
458	3000	10000	No DS	Casing OD	10.75	1.5	2
460	3000	10000	No DS	Casing OD	10.75	1.5	1.5
462	3000	10000	No DS	Casing OD	10.75	2	2
464	3000	10000	No DS	Casing OD	10.75	2	1.5
466	3000	10000	No DS	Casing OD	12.75	1	2
468	3000	10000	No DS	Casing OD	12.75	1	1.5

470	3000	10000	No DS	Casing OD	12.75	1.5	2
472	3000	10000	No DS	Casing OD	12.75	1.5	1.5
474	3000	10000	No DS	Casing OD	12.75	2	2
476	3000	10000	No DS	Casing OD	12.75	2	1.5
484	8000	0	Hanging from BOP	Casing OD	7	1	2
486	8000	0	Hanging from BOP	Casing OD	7	1	1.5
488	8000	0	Hanging from BOP	Casing OD	7	1.5	2
490	8000	0	Hanging from BOP	Casing OD	7	1.5	1.5
492	8000	0	Hanging from BOP	Casing OD	7	2	2
494	8000	0	Hanging from BOP	Casing OD	7	2	1.5
496	8000	0	Hanging from BOP	Casing OD	10.75	1	2
498	8000	0	Hanging from BOP	Casing OD	10.75	1	1.5
500	8000	0	Hanging from BOP	Casing OD	10.75	1.5	2
502	8000	0	Hanging from BOP	Casing OD	10.75	1.5	1.5
504	8000	0	Hanging from BOP	Casing OD	10.75	2	2
506	8000	0	Hanging from BOP	Casing OD	10.75	2	1.5
508	8000	0	Hanging from BOP	Casing OD	12.75	1	2
510	8000	0	Hanging from BOP	Casing OD	12.75	1	1.5
512	8000	0	Hanging from BOP	Casing OD	12.75	1.5	2
514	8000	0	Hanging from BOP	Casing OD	12.75	1.5	1.5
516	8000	0	Hanging from BOP	Casing OD	12.75	2	2
518	8000	0	Hanging from BOP	Casing OD	12.75	2	1.5
520	8000	0	Hanging from BOP	DS Length	50%	1	2
522	8000	0	Hanging from BOP	DS Length	50%	1	1.5
524	8000	0	Hanging from BOP	DS Length	50%	1.5	2
526	8000	0	Hanging from BOP	DS Length	50%	1.5	1.5
528	8000	0	Hanging from BOP	DS Length	50%	2	2
530	8000	0	Hanging from BOP	DS Length	50%	2	1.5
532	8000	0	Hanging from BOP	DS Length	25%	1	2
534	8000	0	Hanging from BOP	DS Length	25%	1	1.5
536	8000	0	Hanging from BOP	DS Length	25%	1.5	2
538	8000	0	Hanging from BOP	DS Length	25%	1.5	1.5
540	8000	0	Hanging from BOP	DS Length	25%	2	2
542	8000	0	Hanging from BOP	DS Length	25%	2	1.5
544	8000	0	Dropped DS	Casing OD	7	1	2
546	8000	0	Dropped DS	Casing OD	7	1	1.5
548	8000	0	Dropped DS	Casing OD	7	1.5	2
550	8000	0	Dropped DS	Casing OD	7	1.5	1.5
552	8000	0	Dropped DS	Casing OD	7	2	2
554	8000	0	Dropped DS	Casing OD	7	2	1.5
556	8000	0	Dropped DS	Casing OD	10.75	1	2
558	8000	0	Dropped DS	Casing OD	10.75	1	1.5
560	8000	0	Dropped DS	Casing OD	10.75	1.5	2
562	8000	0	Dropped DS	Casing OD	10.75	1.5	1.5
564	8000	0	Dropped DS	Casing OD	10.75	2	2
566	8000	0	Dropped DS	Casing OD	10.75	2	1.5
568	8000	0	Dropped DS	Casing OD	12.75	1	2
570	8000	0	Dropped DS	Casing OD	12.75	1	1.5

572	8000	0	Dropped DS	Casing OD	12.75	1.5	2
574	8000	0	Dropped DS	Casing OD	12.75	1.5	1.5
576	8000	0	Dropped DS	Casing OD	12.75	2	2
578	8000	0	Dropped DS	Casing OD	12.75	2	1.5
580	8000	0	Dropped DS	DS Length	50%	1	2
582	8000	0	Dropped DS	DS Length	50%	1	1.5
584	8000	0	Dropped DS	DS Length	50%	1.5	2
586	8000	0	Dropped DS	DS Length	50%	1.5	1.5
588	8000	0	Dropped DS	DS Length	50%	2	2
590	8000	0	Dropped DS	DS Length	50%	2	1.5
592	8000	0	Dropped DS	DS Length	25%	1	2
594	8000	0	Dropped DS	DS Length	25%	1	1.5
596	8000	0	Dropped DS	DS Length	25%	1.5	2
598	8000	0	Dropped DS	DS Length	25%	1.5	1.5
600	8000	0	Dropped DS	DS Length	25%	2	2
602	8000	0	Dropped DS	DS Length	25%	2	1.5
604	8000	0	No DS	Casing OD	7	1	2
606	8000	0	No DS	Casing OD	7	1	1.5
608	8000	0	No DS	Casing OD	7	1.5	2
610	8000	0	No DS	Casing OD	7	1.5	1.5
612	8000	0	No DS	Casing OD	7	2	2
614	8000	0	No DS	Casing OD	7	2	1.5
616	8000	0	No DS	Casing OD	10.75	1	2
618	8000	0	No DS	Casing OD	10.75	1	1.5
620	8000	0	No DS	Casing OD	10.75	1.5	2
622	8000	0	No DS	Casing OD	10.75	1.5	1.5
624	8000	0	No DS	Casing OD	10.75	2	2
626	8000	0	No DS	Casing OD	10.75	2	1.5
628	8000	0	No DS	Casing OD	12.75	1	2
630	8000	0	No DS	Casing OD	12.75	1	1.5
632	8000	0	No DS	Casing OD	12.75	1.5	2
634	8000	0	No DS	Casing OD	12.75	1.5	1.5
636	8000	0	No DS	Casing OD	12.75	2	2
638	8000	0	No DS	Casing OD	12.75	2	1.5
646	8000	5000	Hanging from BOP	Casing OD	7	1	2
648	8000	5000	Hanging from BOP	Casing OD	7	1	1.5
650	8000	5000	Hanging from BOP	Casing OD	7	1.5	2
652	8000	5000	Hanging from BOP	Casing OD	7	1.5	1.5
654	8000	5000	Hanging from BOP	Casing OD	7	2	2
656	8000	5000	Hanging from BOP	Casing OD	7	2	1.5
658	8000	5000	Hanging from BOP	Casing OD	10.75	1	2
660	8000	5000	Hanging from BOP	Casing OD	10.75	1	1.5
662	8000	5000	Hanging from BOP	Casing OD	10.75	1.5	2
664	8000	5000	Hanging from BOP	Casing OD	10.75	1.5	1.5
666	8000	5000	Hanging from BOP	Casing OD	10.75	2	2
668	8000	5000	Hanging from BOP	Casing OD	10.75	2	1.5
670	8000	5000	Hanging from BOP	Casing OD	12.75	1	2
672	8000	5000	Hanging from BOP	Casing OD	12.75	1	1.5

674	8000	5000	Hanging from BOP	Casing OD	12.75	1.5	2
676	8000	5000	Hanging from BOP	Casing OD	12.75	1.5	1.5
678	8000	5000	Hanging from BOP	Casing OD	12.75	2	2
680	8000	5000	Hanging from BOP	Casing OD	12.75	2	1.5
682	8000	5000	Hanging from BOP	DS Length	50%	1	2
684	8000	5000	Hanging from BOP	DS Length	50%	1	1.5
686	8000	5000	Hanging from BOP	DS Length	50%	1.5	2
688	8000	5000	Hanging from BOP	DS Length	50%	1.5	1.5
690	8000	5000	Hanging from BOP	DS Length	50%	2	2
692	8000	5000	Hanging from BOP	DS Length	50%	2	1.5
694	8000	5000	Hanging from BOP	DS Length	25%	1	2
696	8000	5000	Hanging from BOP	DS Length	25%	1	1.5
698	8000	5000	Hanging from BOP	DS Length	25%	1.5	2
700	8000	5000	Hanging from BOP	DS Length	25%	1.5	1.5
702	8000	5000	Hanging from BOP	DS Length	25%	2	2
704	8000	5000	Hanging from BOP	DS Length	25%	2	1.5
706	8000	5000	Dropped DS	Casing OD	7	1	2
708	8000	5000	Dropped DS	Casing OD	7	1	1.5
710	8000	5000	Dropped DS	Casing OD	7	1.5	2
712	8000	5000	Dropped DS	Casing OD	7	1.5	1.5
714	8000	5000	Dropped DS	Casing OD	7	2	2
716	8000	5000	Dropped DS	Casing OD	7	2	1.5
718	8000	5000	Dropped DS	Casing OD	10.75	1	2
720	8000	5000	Dropped DS	Casing OD	10.75	1	1.5
722	8000	5000	Dropped DS	Casing OD	10.75	1.5	2
724	8000	5000	Dropped DS	Casing OD	10.75	1.5	1.5
726	8000	5000	Dropped DS	Casing OD	10.75	2	2
728	8000	5000	Dropped DS	Casing OD	10.75	2	1.5
730	8000	5000	Dropped DS	Casing OD	12.75	1	2
732	8000	5000	Dropped DS	Casing OD	12.75	1	1.5
734	8000	5000	Dropped DS	Casing OD	12.75	1.5	2
736	8000	5000	Dropped DS	Casing OD	12.75	1.5	1.5
738	8000	5000	Dropped DS	Casing OD	12.75	2	2
740	8000	5000	Dropped DS	Casing OD	12.75	2	1.5
742	8000	5000	Dropped DS	DS Length	50%	1	2
744	8000	5000	Dropped DS	DS Length	50%	1	1.5
746	8000	5000	Dropped DS	DS Length	50%	1.5	2
748	8000	5000	Dropped DS	DS Length	50%	1.5	1.5
750	8000	5000	Dropped DS	DS Length	50%	2	2
752	8000	5000	Dropped DS	DS Length	50%	2	1.5
754	8000	5000	Dropped DS	DS Length	25%	1	2
756	8000	5000	Dropped DS	DS Length	25%	1	1.5
758	8000	5000	Dropped DS	DS Length	25%	1.5	2
760	8000	5000	Dropped DS	DS Length	25%	1.5	1.5
762	8000	5000	Dropped DS	DS Length	25%	2	2
764	8000	5000	Dropped DS	DS Length	25%	2	1.5
766	8000	5000	No DS	Casing OD	7	1	2
768	8000	5000	No DS	Casing OD	7	1	1.5

770	8000	5000	No DS	Casing OD	7	1.5	2
772	8000	5000	No DS	Casing OD	7	1.5	1.5
774	8000	5000	No DS	Casing OD	7	2	2
776	8000	5000	No DS	Casing OD	7	2	1.5
778	8000	5000	No DS	Casing OD	10.75	1	2
780	8000	5000	No DS	Casing OD	10.75	1	1.5
782	8000	5000	No DS	Casing OD	10.75	1.5	2
784	8000	5000	No DS	Casing OD	10.75	1.5	1.5
786	8000	5000	No DS	Casing OD	10.75	2	2
788	8000	5000	No DS	Casing OD	10.75	2	1.5
790	8000	5000	No DS	Casing OD	12.75	1	2
792	8000	5000	No DS	Casing OD	12.75	1	1.5
794	8000	5000	No DS	Casing OD	12.75	1.5	2
796	8000	5000	No DS	Casing OD	12.75	1.5	1.5
798	8000	5000	No DS	Casing OD	12.75	2	2
800	8000	5000	No DS	Casing OD	12.75	2	1.5
808	8000	10000	Hanging from BOP	Casing OD	7	1	2
810	8000	10000	Hanging from BOP	Casing OD	7	1	1.5
812	8000	10000	Hanging from BOP	Casing OD	7	1.5	2
814	8000	10000	Hanging from BOP	Casing OD	7	1.5	1.5
816	8000	10000	Hanging from BOP	Casing OD	7	2	2
818	8000	10000	Hanging from BOP	Casing OD	7	2	1.5
820	8000	10000	Hanging from BOP	Casing OD	10.75	1	2
822	8000	10000	Hanging from BOP	Casing OD	10.75	1	1.5
824	8000	10000	Hanging from BOP	Casing OD	10.75	1.5	2
826	8000	10000	Hanging from BOP	Casing OD	10.75	1.5	1.5
828	8000	10000	Hanging from BOP	Casing OD	10.75	2	2
830	8000	10000	Hanging from BOP	Casing OD	10.75	2	1.5
832	8000	10000	Hanging from BOP	Casing OD	12.75	1	2
834	8000	10000	Hanging from BOP	Casing OD	12.75	1	1.5
836	8000	10000	Hanging from BOP	Casing OD	12.75	1.5	2
838	8000	10000	Hanging from BOP	Casing OD	12.75	1.5	1.5
840	8000	10000	Hanging from BOP	Casing OD	12.75	2	2
842	8000	10000	Hanging from BOP	Casing OD	12.75	2	1.5
844	8000	10000	Hanging from BOP	DS Length	50%	1	2
846	8000	10000	Hanging from BOP	DS Length	50%	1	1.5
848	8000	10000	Hanging from BOP	DS Length	50%	1.5	2
850	8000	10000	Hanging from BOP	DS Length	50%	1.5	1.5
852	8000	10000	Hanging from BOP	DS Length	50%	2	2
854	8000	10000	Hanging from BOP	DS Length	50%	2	1.5
856	8000	10000	Hanging from BOP	DS Length	25%	1	2
858	8000	10000	Hanging from BOP	DS Length	25%	1	1.5
860	8000	10000	Hanging from BOP	DS Length	25%	1.5	2
862	8000	10000	Hanging from BOP	DS Length	25%	1.5	1.5
864	8000	10000	Hanging from BOP	DS Length	25%	2	2
866	8000	10000	Hanging from BOP	DS Length	25%	2	1.5
868	8000	10000	Dropped DS	Casing OD	7	1	2
870	8000	10000	Dropped DS	Casing OD	7	1	1.5

872	8000	10000	Dropped DS	Casing OD	7	1.5	2
874	8000	10000	Dropped DS	Casing OD	7	1.5	1.5
876	8000	10000	Dropped DS	Casing OD	7	2	2
878	8000	10000	Dropped DS	Casing OD	7	2	1.5
880	8000	10000	Dropped DS	Casing OD	10.75	1	2
882	8000	10000	Dropped DS	Casing OD	10.75	1	1.5
884	8000	10000	Dropped DS	Casing OD	10.75	1.5	2
886	8000	10000	Dropped DS	Casing OD	10.75	1.5	1.5
888	8000	10000	Dropped DS	Casing OD	10.75	2	2
890	8000	10000	Dropped DS	Casing OD	10.75	2	1.5
892	8000	10000	Dropped DS	Casing OD	12.75	1	2
894	8000	10000	Dropped DS	Casing OD	12.75	1	1.5
896	8000	10000	Dropped DS	Casing OD	12.75	1.5	2
898	8000	10000	Dropped DS	Casing OD	12.75	1.5	1.5
900	8000	10000	Dropped DS	Casing OD	12.75	2	2
902	8000	10000	Dropped DS	Casing OD	12.75	2	1.5
904	8000	10000	Dropped DS	DS Length	50%	1	2
906	8000	10000	Dropped DS	DS Length	50%	1	1.5
908	8000	10000	Dropped DS	DS Length	50%	1.5	2
910	8000	10000	Dropped DS	DS Length	50%	1.5	1.5
912	8000	10000	Dropped DS	DS Length	50%	2	2
914	8000	10000	Dropped DS	DS Length	50%	2	1.5
916	8000	10000	Dropped DS	DS Length	25%	1	2
918	8000	10000	Dropped DS	DS Length	25%	1	1.5
920	8000	10000	Dropped DS	DS Length	25%	1.5	2
922	8000	10000	Dropped DS	DS Length	25%	1.5	1.5
924	8000	10000	Dropped DS	DS Length	25%	2	2
926	8000	10000	Dropped DS	DS Length	25%	2	1.5
928	8000	10000	No DS	Casing OD	7	1	2
930	8000	10000	No DS	Casing OD	7	1	1.5
932	8000	10000	No DS	Casing OD	7	1.5	2
934	8000	10000	No DS	Casing OD	7	1.5	1.5
936	8000	10000	No DS	Casing OD	7	2	2
938	8000	10000	No DS	Casing OD	7	2	1.5
940	8000	10000	No DS	Casing OD	10.75	1	2
942	8000	10000	No DS	Casing OD	10.75	1	1.5
944	8000	10000	No DS	Casing OD	10.75	1.5	2
946	8000	10000	No DS	Casing OD	10.75	1.5	1.5
948	8000	10000	No DS	Casing OD	10.75	2	2
950	8000	10000	No DS	Casing OD	10.75	2	1.5
952	8000	10000	No DS	Casing OD	12.75	1	2
954	8000	10000	No DS	Casing OD	12.75	1	1.5
956	8000	10000	No DS	Casing OD	12.75	1.5	2
958	8000	10000	No DS	Casing OD	12.75	1.5	1.5
960	8000	10000	No DS	Casing OD	12.75	2	2
962	8000	10000	No DS	Casing OD	12.75	2	1.5
970	12000	0	Hanging from BOP	Casing OD	7	1	2
972	12000	0	Hanging from BOP	Casing OD	7	1	1.5

974	12000	0	Hanging from BOP	Casing OD	7	1.5	2
976	12000	0	Hanging from BOP	Casing OD	7	1.5	1.5
978	12000	0	Hanging from BOP	Casing OD	7	2	2
980	12000	0	Hanging from BOP	Casing OD	7	2	1.5
982	12000	0	Hanging from BOP	Casing OD	10.75	1	2
984	12000	0	Hanging from BOP	Casing OD	10.75	1	1.5
986	12000	0	Hanging from BOP	Casing OD	10.75	1.5	2
988	12000	0	Hanging from BOP	Casing OD	10.75	1.5	1.5
990	12000	0	Hanging from BOP	Casing OD	10.75	2	2
992	12000	0	Hanging from BOP	Casing OD	10.75	2	1.5
994	12000	0	Hanging from BOP	Casing OD	12.75	1	2
996	12000	0	Hanging from BOP	Casing OD	12.75	1	1.5
998	12000	0	Hanging from BOP	Casing OD	12.75	1.5	2
1000	12000	0	Hanging from BOP	Casing OD	12.75	1.5	1.5
1002	12000	0	Hanging from BOP	Casing OD	12.75	2	2
1004	12000	0	Hanging from BOP	Casing OD	12.75	2	1.5
1006	12000	0	Hanging from BOP	DS Length	50%	1	2
1008	12000	0	Hanging from BOP	DS Length	50%	1	1.5
1010	12000	0	Hanging from BOP	DS Length	50%	1.5	2
1012	12000	0	Hanging from BOP	DS Length	50%	1.5	1.5
1014	12000	0	Hanging from BOP	DS Length	50%	2	2
1016	12000	0	Hanging from BOP	DS Length	50%	2	1.5
1018	12000	0	Hanging from BOP	DS Length	25%	1	2
1020	12000	0	Hanging from BOP	DS Length	25%	1	1.5
1022	12000	0	Hanging from BOP	DS Length	25%	1.5	2
1024	12000	0	Hanging from BOP	DS Length	25%	1.5	1.5
1026	12000	0	Hanging from BOP	DS Length	25%	2	2
1028	12000	0	Hanging from BOP	DS Length	25%	2	1.5
1030	12000	0	Dropped DS	Casing OD	7	1	2
1032	12000	0	Dropped DS	Casing OD	7	1	1.5
1034	12000	0	Dropped DS	Casing OD	7	1.5	2
1036	12000	0	Dropped DS	Casing OD	7	1.5	1.5
1038	12000	0	Dropped DS	Casing OD	7	2	2
1040	12000	0	Dropped DS	Casing OD	7	2	1.5
1042	12000	0	Dropped DS	Casing OD	10.75	1	2
1044	12000	0	Dropped DS	Casing OD	10.75	1	1.5
1046	12000	0	Dropped DS	Casing OD	10.75	1.5	2
1048	12000	0	Dropped DS	Casing OD	10.75	1.5	1.5
1050	12000	0	Dropped DS	Casing OD	10.75	2	2
1052	12000	0	Dropped DS	Casing OD	10.75	2	1.5
1054	12000	0	Dropped DS	Casing OD	12.75	1	2
1056	12000	0	Dropped DS	Casing OD	12.75	1	1.5
1058	12000	0	Dropped DS	Casing OD	12.75	1.5	2
1060	12000	0	Dropped DS	Casing OD	12.75	1.5	1.5
1062	12000	0	Dropped DS	Casing OD	12.75	2	2
1064	12000	0	Dropped DS	Casing OD	12.75	2	1.5
1066	12000	0	Dropped DS	DS Length	50%	1	2
1068	12000	0	Dropped DS	DS Length	50%	1	1.5

1070	12000	0	Dropped DS	DS Length	50%	1.5	2
1072	12000	0	Dropped DS	DS Length	50%	1.5	1.5
1074	12000	0	Dropped DS	DS Length	50%	2	2
1076	12000	0	Dropped DS	DS Length	50%	2	1.5
1078	12000	0	Dropped DS	DS Length	25%	1	2
1080	12000	0	Dropped DS	DS Length	25%	1	1.5
1082	12000	0	Dropped DS	DS Length	25%	1.5	2
1084	12000	0	Dropped DS	DS Length	25%	1.5	1.5
1086	12000	0	Dropped DS	DS Length	25%	2	2
1088	12000	0	Dropped DS	DS Length	25%	2	1.5
1090	12000	0	No DS	Casing OD	7	1	2
1092	12000	0	No DS	Casing OD	7	1	1.5
1094	12000	0	No DS	Casing OD	7	1.5	2
1096	12000	0	No DS	Casing OD	7	1.5	1.5
1098	12000	0	No DS	Casing OD	7	2	2
1100	12000	0	No DS	Casing OD	7	2	1.5
1102	12000	0	No DS	Casing OD	10.75	1	2
1104	12000	0	No DS	Casing OD	10.75	1	1.5
1106	12000	0	No DS	Casing OD	10.75	1.5	2
1108	12000	0	No DS	Casing OD	10.75	1.5	1.5
1110	12000	0	No DS	Casing OD	10.75	2	2
1112	12000	0	No DS	Casing OD	10.75	2	1.5
1114	12000	0	No DS	Casing OD	12.75	1	2
1116	12000	0	No DS	Casing OD	12.75	1	1.5
1118	12000	0	No DS	Casing OD	12.75	1.5	2
1120	12000	0	No DS	Casing OD	12.75	1.5	1.5
1122	12000	0	No DS	Casing OD	12.75	2	2
1124	12000	0	No DS	Casing OD	12.75	2	1.5
1132	12000	5000	Hanging from BOP	Casing OD	7	1	2
1134	12000	5000	Hanging from BOP	Casing OD	7	1	1.5
1136	12000	5000	Hanging from BOP	Casing OD	7	1.5	2
1138	12000	5000	Hanging from BOP	Casing OD	7	1.5	1.5
1140	12000	5000	Hanging from BOP	Casing OD	7	2	2
1142	12000	5000	Hanging from BOP	Casing OD	7	2	1.5
1144	12000	5000	Hanging from BOP	Casing OD	10.75	1	2
1146	12000	5000	Hanging from BOP	Casing OD	10.75	1	1.5
1148	12000	5000	Hanging from BOP	Casing OD	10.75	1.5	2
1150	12000	5000	Hanging from BOP	Casing OD	10.75	1.5	1.5
1152	12000	5000	Hanging from BOP	Casing OD	10.75	2	2
1154	12000	5000	Hanging from BOP	Casing OD	10.75	2	1.5
1156	12000	5000	Hanging from BOP	Casing OD	12.75	1	2
1158	12000	5000	Hanging from BOP	Casing OD	12.75	1	1.5
1160	12000	5000	Hanging from BOP	Casing OD	12.75	1.5	2
1162	12000	5000	Hanging from BOP	Casing OD	12.75	1.5	1.5
1164	12000	5000	Hanging from BOP	Casing OD	12.75	2	2
1166	12000	5000	Hanging from BOP	Casing OD	12.75	2	1.5
1168	12000	5000	Hanging from BOP	DS Length	50%	1	2
1170	12000	5000	Hanging from BOP	DS Length	50%	1	1.5

1172	12000	5000	Hanging from BOP	DS Length	50%	1.5	2
1174	12000	5000	Hanging from BOP	DS Length	50%	1.5	1.5
1176	12000	5000	Hanging from BOP	DS Length	50%	2	2
1178	12000	5000	Hanging from BOP	DS Length	50%	2	1.5
1180	12000	5000	Hanging from BOP	DS Length	25%	1	2
1182	12000	5000	Hanging from BOP	DS Length	25%	1	1.5
1184	12000	5000	Hanging from BOP	DS Length	25%	1.5	2
1186	12000	5000	Hanging from BOP	DS Length	25%	1.5	1.5
1188	12000	5000	Hanging from BOP	DS Length	25%	2	2
1190	12000	5000	Hanging from BOP	DS Length	25%	2	1.5
1192	12000	5000	Dropped DS	Casing OD	7	1	2
1194	12000	5000	Dropped DS	Casing OD	7	1	1.5
1196	12000	5000	Dropped DS	Casing OD	7	1.5	2
1198	12000	5000	Dropped DS	Casing OD	7	1.5	1.5
1200	12000	5000	Dropped DS	Casing OD	7	2	2
1202	12000	5000	Dropped DS	Casing OD	7	2	1.5
1204	12000	5000	Dropped DS	Casing OD	10.75	1	2
1206	12000	5000	Dropped DS	Casing OD	10.75	1	1.5
1208	12000	5000	Dropped DS	Casing OD	10.75	1.5	2
1210	12000	5000	Dropped DS	Casing OD	10.75	1.5	1.5
1212	12000	5000	Dropped DS	Casing OD	10.75	2	2
1214	12000	5000	Dropped DS	Casing OD	10.75	2	1.5
1216	12000	5000	Dropped DS	Casing OD	12.75	1	2
1218	12000	5000	Dropped DS	Casing OD	12.75	1	1.5
1220	12000	5000	Dropped DS	Casing OD	12.75	1.5	2
1222	12000	5000	Dropped DS	Casing OD	12.75	1.5	1.5
1224	12000	5000	Dropped DS	Casing OD	12.75	2	2
1226	12000	5000	Dropped DS	Casing OD	12.75	2	1.5
1228	12000	5000	Dropped DS	DS Length	50%	1	2
1230	12000	5000	Dropped DS	DS Length	50%	1	1.5
1232	12000	5000	Dropped DS	DS Length	50%	1.5	2
1234	12000	5000	Dropped DS	DS Length	50%	1.5	1.5
1236	12000	5000	Dropped DS	DS Length	50%	2	2
1238	12000	5000	Dropped DS	DS Length	50%	2	1.5
1240	12000	5000	Dropped DS	DS Length	25%	1	2
1242	12000	5000	Dropped DS	DS Length	25%	1	1.5
1244	12000	5000	Dropped DS	DS Length	25%	1.5	2
1246	12000	5000	Dropped DS	DS Length	25%	1.5	1.5
1248	12000	5000	Dropped DS	DS Length	25%	2	2
1250	12000	5000	Dropped DS	DS Length	25%	2	1.5
1252	12000	5000	No DS	Casing OD	7	1	2
1254	12000	5000	No DS	Casing OD	7	1	1.5
1256	12000	5000	No DS	Casing OD	7	1.5	2
1258	12000	5000	No DS	Casing OD	7	1.5	1.5
1260	12000	5000	No DS	Casing OD	7	2	2
1262	12000	5000	No DS	Casing OD	7	2	1.5
1264	12000	5000	No DS	Casing OD	10.75	1	2
1266	12000	5000	No DS	Casing OD	10.75	1	1.5

1268	12000	5000	No DS	Casing OD	10.75	1.5	2
1270	12000	5000	No DS	Casing OD	10.75	1.5	1.5
1272	12000	5000	No DS	Casing OD	10.75	2	2
1274	12000	5000	No DS	Casing OD	10.75	2	1.5
1276	12000	5000	No DS	Casing OD	12.75	1	2
1278	12000	5000	No DS	Casing OD	12.75	1	1.5
1280	12000	5000	No DS	Casing OD	12.75	1.5	2
1282	12000	5000	No DS	Casing OD	12.75	1.5	1.5
1284	12000	5000	No DS	Casing OD	12.75	2	2
1286	12000	5000	No DS	Casing OD	12.75	2	1.5
1294	12000	10000	Hanging from BOP	Casing OD	7	1	2
1296	12000	10000	Hanging from BOP	Casing OD	7	1	1.5
1298	12000	10000	Hanging from BOP	Casing OD	7	1.5	2
1300	12000	10000	Hanging from BOP	Casing OD	7	1.5	1.5
1302	12000	10000	Hanging from BOP	Casing OD	7	2	2
1304	12000	10000	Hanging from BOP	Casing OD	7	2	1.5
1306	12000	10000	Hanging from BOP	Casing OD	10.75	1	2
1308	12000	10000	Hanging from BOP	Casing OD	10.75	1	1.5
1310	12000	10000	Hanging from BOP	Casing OD	10.75	1.5	2
1312	12000	10000	Hanging from BOP	Casing OD	10.75	1.5	1.5
1314	12000	10000	Hanging from BOP	Casing OD	10.75	2	2
1316	12000	10000	Hanging from BOP	Casing OD	10.75	2	1.5
1318	12000	10000	Hanging from BOP	Casing OD	12.75	1	2
1320	12000	10000	Hanging from BOP	Casing OD	12.75	1	1.5
1322	12000	10000	Hanging from BOP	Casing OD	12.75	1.5	2
1324	12000	10000	Hanging from BOP	Casing OD	12.75	1.5	1.5
1326	12000	10000	Hanging from BOP	Casing OD	12.75	2	2
1328	12000	10000	Hanging from BOP	Casing OD	12.75	2	1.5
1330	12000	10000	Hanging from BOP	DS Length	50%	1	2
1332	12000	10000	Hanging from BOP	DS Length	50%	1	1.5
1334	12000	10000	Hanging from BOP	DS Length	50%	1.5	2
1336	12000	10000	Hanging from BOP	DS Length	50%	1.5	1.5
1338	12000	10000	Hanging from BOP	DS Length	50%	2	2
1340	12000	10000	Hanging from BOP	DS Length	50%	2	1.5
1342	12000	10000	Hanging from BOP	DS Length	25%	1	2
1344	12000	10000	Hanging from BOP	DS Length	25%	1	1.5
1346	12000	10000	Hanging from BOP	DS Length	25%	1.5	2
1348	12000	10000	Hanging from BOP	DS Length	25%	1.5	1.5
1350	12000	10000	Hanging from BOP	DS Length	25%	2	2
1352	12000	10000	Hanging from BOP	DS Length	25%	2	1.5
1354	12000	10000	Dropped DS	Casing OD	7	1	2
1356	12000	10000	Dropped DS	Casing OD	7	1	1.5
1358	12000	10000	Dropped DS	Casing OD	7	1.5	2
1360	12000	10000	Dropped DS	Casing OD	7	1.5	1.5
1362	12000	10000	Dropped DS	Casing OD	7	2	2
1364	12000	10000	Dropped DS	Casing OD	7	2	1.5
1366	12000	10000	Dropped DS	Casing OD	10.75	1	2
1368	12000	10000	Dropped DS	Casing OD	10.75	1	1.5

1370	12000	10000	Dropped DS	Casing OD	10.75	1.5	2
1372	12000	10000	Dropped DS	Casing OD	10.75	1.5	1.5
1374	12000	10000	Dropped DS	Casing OD	10.75	2	2
1376	12000	10000	Dropped DS	Casing OD	10.75	2	1.5
1378	12000	10000	Dropped DS	Casing OD	12.75	1	2
1380	12000	10000	Dropped DS	Casing OD	12.75	1	1.5
1382	12000	10000	Dropped DS	Casing OD	12.75	1.5	2
1384	12000	10000	Dropped DS	Casing OD	12.75	1.5	1.5
1386	12000	10000	Dropped DS	Casing OD	12.75	2	2
1388	12000	10000	Dropped DS	Casing OD	12.75	2	1.5
1390	12000	10000	Dropped DS	DS Length	50%	1	2
1392	12000	10000	Dropped DS	DS Length	50%	1	1.5
1394	12000	10000	Dropped DS	DS Length	50%	1.5	2
1396	12000	10000	Dropped DS	DS Length	50%	1.5	1.5
1398	12000	10000	Dropped DS	DS Length	50%	2	2
1400	12000	10000	Dropped DS	DS Length	50%	2	1.5
1402	12000	10000	Dropped DS	DS Length	25%	1	2
1404	12000	10000	Dropped DS	DS Length	25%	1	1.5
1406	12000	10000	Dropped DS	DS Length	25%	1.5	2
1408	12000	10000	Dropped DS	DS Length	25%	1.5	1.5
1410	12000	10000	Dropped DS	DS Length	25%	2	2
1412	12000	10000	Dropped DS	DS Length	25%	2	1.5
1414	12000	10000	No DS	Casing OD	7	1	2
1416	12000	10000	No DS	Casing OD	7	1	1.5
1418	12000	10000	No DS	Casing OD	7	1.5	2
1420	12000	10000	No DS	Casing OD	7	1.5	1.5
1422	12000	10000	No DS	Casing OD	7	2	2
1424	12000	10000	No DS	Casing OD	7	2	1.5
1426	12000	10000	No DS	Casing OD	10.75	1	2
1428	12000	10000	No DS	Casing OD	10.75	1	1.5
1430	12000	10000	No DS	Casing OD	10.75	1.5	2
1432	12000	10000	No DS	Casing OD	10.75	1.5	1.5
1434	12000	10000	No DS	Casing OD	10.75	2	2
1436	12000	10000	No DS	Casing OD	10.75	2	1.5
1438	12000	10000	No DS	Casing OD	12.75	1	2
1440	12000	10000	No DS	Casing OD	12.75	1	1.5
1442	12000	10000	No DS	Casing OD	12.75	1.5	2
1444	12000	10000	No DS	Casing OD	12.75	1.5	1.5
1446	12000	10000	No DS	Casing OD	12.75	2	2
1448	12000	10000	No DS	Casing OD	12.75	2	1.5
1450	12000	10000	No DS	DS Length	25%	2	1.5

### Kill With Drillstring Run Matrix

DS #	TVD	WATER	DS	PARAMETER	PARAMETER	DS
	BML	DEPTH	STATUS	VARIED	VALUE	LENGTH
1	8000	0	Kill w/ DS	Casing OD	8.63	1
2	8000	0	Kill w/ DS	Casing OD	8.63	0.75
3	8000	0	Kill w/ DS	Casing OD	8.63	0.5
4	8000	0	Kill w/ DS	Casing OD	8.63	0.25
5	8000	0	Kill w/ DS	Casing OD	10.75	1
6	8000	0	Kill w/ DS	Casing OD	10.75	0.75
7	8000	0	Kill w/ DS	Casing OD	10.75	0.5
8	8000	0	Kill w/ DS	Casing OD	10.75	0.25
9	8000	0	Kill w/ DS	Casing OD	12.75	1
10	8000	0	Kill w/ DS	Casing OD	12.75	0.75
11	8000	0	Kill w/ DS	Casing OD	12.75	0.5
12	8000	0	Kill w/ DS	Casing OD	12.75	0.25
13	8000	5000	Kill w/ DS	Casing OD	8.63	1
14	8000	5000	Kill w/ DS	Casing OD	8.63	0.75
15	8000	5000	Kill w/ DS	Casing OD	8.63	0.5
16	8000	5000	Kill w/ DS	Casing OD	8.63	0.25
17	8000	5000	Kill w/ DS	Casing OD	10.75	1
18	8000	5000	Kill w/ DS	Casing OD	10.75	0.75
19	8000	5000	Kill w/ DS	Casing OD	10.75	0.5
20	8000	5000	Kill w/ DS	Casing OD	10.75	0.25
21	8000	5000	Kill w/ DS	Casing OD	12.75	1
22	8000	5000	Kill w/ DS	Casing OD	12.75	0.75
23	8000	5000	Kill w/ DS	Casing OD	12.75	0.5
24	8000	5000	Kill w/ DS	Casing OD	12.75	0.25
25	8000	10000	Kill w/ DS	Casing OD	8.63	1
26	8000	10000	Kill w/ DS	Casing OD	8.63	0.75
27	8000	10000	Kill w/ DS	Casing OD	8.63	0.5
28	8000	10000	Kill w/ DS	Casing OD	8.63	0.25
29	8000	10000	Kill w/ DS	Casing OD	10.75	1
30	8000	10000	Kill w/ DS	Casing OD	10.75	0.75
31	8000	10000	Kill w/ DS	Casing OD	10.75	0.5
32	8000	10000	Kill w/ DS	Casing OD	10.75	0.25
33	8000	10000	Kill w/ DS	Casing OD	12.75	1
34	8000	10000	Kill w/ DS	Casing OD	12.75	0.75
35	8000	10000	Kill w/ DS	Casing OD	12.75	0.5
36	8000	10000	Kill w/ DS	Casing OD	12.75	0.25
37	12000	0	Kill w/ DS	Casing OD	8.63	1
38	12000	0	Kill w/ DS	Casing OD	8.63	0.75
39	12000	0	Kill w/ DS	Casing OD	8.63	0.5
40	12000	0	Kill w/ DS	Casing OD	8.63	0.25
41	12000	0	Kill w/ DS	Casing OD	10.75	1
42	12000	0	Kill w/ DS	Casing OD	10.75	0.75
43	12000	0	Kill w/ DS	Casing OD	10.75	0.5

44	12000	0	Kill w/ DS	Casing OD	10.75	0.25	
45	12000	0	Kill w/ DS	Casing OD	12.75	1	
46	12000	0	Kill w/ DS	Casing OD	12.75	0.75	
47	12000	0	Kill w/ DS	Casing OD	12.75	0.5	
48	12000	0	Kill w/ DS	Casing OD	12.75	0.25	
49	12000	5000	Kill w/ DS	Casing OD	8.63	1	
50	12000	5000	Kill w/ DS	Casing OD	8.63	0.75	
51	12000	5000	Kill w/ DS	Casing OD	8.63	0.5	
52	12000	5000	Kill w/ DS	Casing OD	8.63	0.25	
53	12000	5000	Kill w/ DS	Casing OD	10.75	1	
54	12000	5000	Kill w/ DS	Casing OD	10.75	0.75	
55	12000	5000	Kill w/ DS	Casing OD	10.75	0.5	
56	12000	5000	Kill w/ DS	Casing OD	10.75	0.25	
57	12000	5000	Kill w/ DS	Casing OD	12.75	1	
58	12000	5000	Kill w/ DS	Casing OD	12.75	0.75	
59	12000	5000	Kill w/ DS	Casing OD	12.75	0.5	
60	12000	5000	Kill w/ DS	Casing OD	12.75	0.25	
61	12000	10000	Kill w/ DS	Casing OD	8.63	1	
62	12000	10000	Kill w/ DS	Casing OD	8.63	0.75	
63	12000	10000	Kill w/ DS	Casing OD	8.63	0.5	
64	12000	10000	Kill w/ DS	Casing OD	8.63	0.25	
65	12000	10000	Kill w/ DS	Casing OD	10.75	1	
66	12000	10000	Kill w/ DS	Casing OD	10.75	0.75	
67	12000	10000	Kill w/ DS	Casing OD	10.75	0.5	
68	12000	10000	Kill w/ DS	Casing OD	10.75	0.25	
69	12000	10000	Kill w/ DS	Casing OD	12.75	1	
70	12000	10000	Kill w/ DS	Casing OD	12.75	0.75	
71	12000	10000	Kill w/ DS	Casing OD	12.75	0.5	
72	12000	10000	Kill w/ DS	Casing OD	12.75	0.25	

## APPENDIX B

### RELIEF WELL INITIAL CONDITION RUNS

SERIES	TVD	WATER	CASING	DS	DS	GAS	TVD
	BML	DEPTH	SIZE	STATUS	LEN %	RATE	MSL
1	3000	0	8.625	hanging	100	10.05	3000
2	3000	0	10.75	hanging	100	27.30	3000
3	3000	0	12.75	hanging	100	33.47	3000
4	3000	0	10.75	hanging	50	31.68	3000
5	3000	0	10.75	hanging	25	151.33	3000
6	3000	0	8.625	dropped	100	10.05	3000
7	3000	0	10.75	dropped	100	27.30	3000
8	3000	0	12.75	dropped	100	33.47	3000
9	3000	0	10.75	dropped	50	28.18	3000
10	3000	0	10.75	dropped	25	28.62	3000
11	3000	0	8.625	no DS	0	32.86	3000
12	3000	0	10.75	no DS	0	33.78	3000
13	3000	0	12.75	no DS	0	34.60	3000
14	3000	5000	8.625	hanging	100	25.27	8000
15	3000	5000	10.75	hanging	100	80.56	8000
16	3000	5000	12.75	hanging	100	109.49	8000
17	3000	5000	10.75	hanging	50	80.56	8000
18	3000	5000	10.75	hanging	25	98.34	8000
19	3000	5000	8.625	dropped	100	25.26	8000
20	3000	5000	10.75	dropped	100	80.55	8000
21	3000	5000	12.75	dropped	100	109.48	8000
22	3000	5000	10.75	dropped	50	80.55	8000
23	3000	5000	10.75	dropped	25	83.13	8000
24	3000	5000	8.625	no DS	0	109.82	8000
25	3000	5000	10.75	no DS	0	112.41	8000
26	3000	5000	12.75	no DS	0	114.92	8000
27	3000	10000	8.625	hanging	100	33.74	13000
28	3000	10000	10.75	hanging	100	103.58	13000
29	3000	10000	12.75	hanging	100	135.15	13000
30	3000	10000	10.75	hanging	50	103.58	13000
31	3000	10000	10.75	hanging	25	103.58	13000
32	3000	10000	8.625	dropped	100	33.72	13000
33	3000	10000	10.75	dropped	100	103.57	13000
34	3000	10000	12.75	dropped	100	135.15	13000
35	3000	10000	10.75	dropped	50	103.57	13000
36	3000	10000	10.75	dropped	25	103.57	13000
37	3000	10000	8.625	no DS	100	133.85	13000
38	3000	10000	10.75	no DS	100	137.02	13000
39	3000	10000	12.75	no DS	100	140.08	13000
40	8000	0	8.625	hanging	100	20.95	8000
41	8000	0	10.75	hanging	100	79.67	8000
42	8000	0	12.75	hanging	100	131.02	8000
43	8000	0	10.75	hanging	50	104.15	8000
44	8000	0	10.75	hanging	25	117.06	8000
45	8000	0	8.625	dropped	100	20.95	8000

46	8000	0	10.75	dropped	100	79.67	8000
47	8000	0	12.75	dropped	100	131.02	8000
48	8000	0	10.75	dropped	50	89.03	8000
49	8000	0	10.75	dropped	25	95.04	8000
50	8000	0	8.625	no DS	0	139.95	8000
51	8000	0	10.75	no DS	0	151.25	8000
52	8000	0	12.75	no DS	0	158.74	8000
53	8000	5000	8.625	hanging	100	31.49	13000
54	8000	5000	10.75	hanging	100	122.61	13000
55	8000	5000	12.75	hanging	100	203.96	13000
56	8000	5000	10.75	hanging	50	145.72	13000
57	8000	5000	10.75	hanging	25	168.82	13000
58	8000	5000	8.625	dropped	100		13000
59	8000	5000	10.75	dropped	100	122.56	13000
60	8000	5000	12.75	dropped	100	203.92	13000
61	8000	5000	10.75	dropped	50	127.68	13000
62	8000	5000	10.75	dropped	25	140.99	13000
63	8000	5000	8.625	no DS	0	215.70	13000
64	8000	5000	10.75	no DS	0	230.61	13000
65	8000	5000	12.75	no DS	0	238.90	13000
66	8000	10000	8.625	hanging	100	23.84	18000
67	8000	10000	10.75	hanging	100	143.39	18000
68	8000	10000	12.75	hanging	100	227.66	18000
69	8000	10000	10.75	hanging	50	143.39	18000
70	8000	10000	10.75	hanging	25	183.67	18000
71	8000	10000	8.625	dropped	100	37.65	18000
72	8000	10000	10.75	dropped	100	143.34	18000
73	8000	10000	12.75	dropped	100	227.63	18000
74	8000	10000	10.75	dropped	50	143.34	18000
75	8000	10000	10.75	dropped	25	157.55	18000
76	8000	10000	8.625	no DS	0	235.55	18000
77	8000	10000	10.75	no DS	0	245.87	18000
78	8000	10000	12.75	no DS	0	255.41	18000
79	12000	0	8.625	hanging	100	28.05	12000
80	12000	0	10.75	hanging	100	106.10	12000
81	12000	0	12.75	hanging	100	191.51	12000
82	12000	0	10.75	hanging	50	140.46	12000
83	12000	0	10.75	hanging	25	163.12	12000
84	12000	0	8.625	dropped	75	28.44	12000
85	12000	0	10.75	dropped	100	106.10	12000
86	12000	0	12.75	dropped	100	191.51	12000
87	12000	0	10.75	dropped	50	123.09	12000
88	12000	0	10.75	dropped	25	135.36	12000
89	12000	0	8.625	no DS	0	212.19	12000
90	12000	0	10.75	no DS	0	237.41	12000
91	12000	0	12.75	no DS	0	254.09	12000
92	12000	5000	8.625	hanging	95	39.95	17000
93	12000	5000	10.75	hanging	100	142.88	17000
94	12000	5000	12.75	hanging	100	259.48	17000
95	12000	5000	10.75	hanging	50	174.17	17000
96	12000	5000	10.75	hanging	25	206.78	17000
97	12000	5000	8.625	dropped	100	38.42	17000
98	12000	5000	10.75	dropped	100	142.81	17000

99	12000	5000	12.75	dropped	100	259.42	17000
100	12000	5000	10.75	dropped	50	154.72	17000
101	12000	5000	10.75	dropped	25	174.58	17000
102	12000	5000	8.625	no DS	100	284.44	17000
103	12000	5000	10.75	no DS	100	312.87	17000
104	12000	5000	12.75	no DS	100	327.85	17000
105	12000	10000	8.625	hanging	40	49.69	22000
106	12000	10000	10.75	hanging	100	162.10	22000
107	12000	10000	12.75	hanging	100	283.96	22000
108	12000	10000	10.75	hanging	50	183.99	22000
109	12000	10000	10.75	hanging	25	220.16	22000
110	12000	10000	8.625	dropped	30	43.99	22000
111	12000	10000	10.75	dropped	100	162.02	22000
112	12000	10000	12.75	dropped	100	283.89	22000
113	12000	10000	10.75	dropped	50	165.37	22000
114	12000	10000	10.75	dropped	25	188.76	22000
115	12000	10000	8.625	no DS	0	304.26	22000
116	12000	10000	10.75	no DS	0	325.96	22000
117	12000	10000	12.75	no DS	0	340.98	22000
Series							
1	Run #	1-12					
	<b>Intitial Conditions</b>						
	Surface Gas Rate		10.046	MMscf/D	<b>Wellbore</b>		units
					TVD BML	3000	ft
	<b>Depth, ft</b>	<b>Pressure, psia</b>			Water TVD	0	ft
	0	62.421			DS Status	hanging	n/a
	300	323.79			Parameter	csg	n/a
	600	444.9			Par. Value	8.625	in
	900	538.847					
	1200	618.705					
	1500	689.593					
	1800	754.152					
	2100	813.958					
	2400	870.04					
	2700	1160.139					
	3000	1475.988					
2	Run #	13-24					
	<b>Intitial Conditions</b>						
	Surface Gas Rate		27.297	MMscf/D	<b>Wellbore</b>		units
					TVD BML	3000	ft
	<b>Depth, ft</b>	<b>Pressure, psia</b>			Water TVD	0	ft
	0	44.834			DS Status	hanging	n/a
	300	164.204			Parameter	csg	n/a
	600	221.02			Par. Value	10.75	
	900	265.483					
	1200	303.484					
	1500	337.346					
	1800	368.275					
	2100	396.99					
	2400	423.966					
	2700	575.3					
	3000	739.253					

3	Run #	25-36					
	<b>Intitial Conditions</b>						
	Surface Gas Rate		33.473	MMscf/D	<b>Wellbore</b>		units
					TVD BML	3000	ft
	<b>Depth, ft</b>	<b>Pressure, psia</b>			Water TVD	0	ft
	0	24.46			DS Status	hanging	n/a
	300	68.567			Parameter	csg	n/a
	600	90.578			Par. Value	12.75	
	900	107.913					
	1200	122.788					
	1500	136.082					
	1800	148.252					
	2100	159.572					
	2400	170.222					
	2700	222.929					
	3000	281.335					
4	Run #	37-48					
	<b>Intitial Conditions</b>						
	Surface Gas Rate		31.678	MMscf/D	<b>Wellbore</b>		units
					TVD BML	3000	ft
	<b>Depth, ft</b>	<b>Pressure, psia</b>			Water TVD	0	ft
	0	55.867			DS Status	hanging	n/a
	300	190.426			Parameter	ds length	n/a
	600	256.099			Par. Value	50	%
	900	307.492					
	1200	351.409					
	1500	390.536					
	1800	394.064					
	2100	396.064					
	2400	399.793					
	2700	403.85					
	3000	408.515					
5	Run #	49-60					
	<b>Intitial Conditions</b>						
	Surface Gas Rate		151.336	MMscf/D	<b>Wellbore</b>		units
					TVD BML	3000	ft
	<b>Depth, ft</b>	<b>Pressure, psia</b>			Water TVD	0	ft
	0	57.048			DS Status	hanging	n/a
	300	195.429			Parameter	ds length	n/a
	600	262.826			Par. Value	25	
	900	292.624					
	1200	295.035					
	1500	297.457					
	1800	299.889					
	2100	302.333					
	2400	304.787					
	2700	308.881					
	3000	313.797					
6	Run #	61-72					

	<b>Intitial Conditions</b>					
	Surface Gas Rate		10.046	MMscf/D	<b>Wellbore</b>	units
					TVD BML	3000 ft
	<b>Depth, ft</b>	<b>Pressure, psia</b>			Water TVD	0 ft
	0	62.421			DS Status	dropped n/a
	300	323.79			Parameter	csg n/a
	600	444.9			Par. Value	8.625
	900	538.847				
	1200	618.705				
	1500	689.593				
	1800	754.152				
	2100	813.958				
	2400	870.04				
	2700	1160.139				
	3000	1475.988				
7	<b>Run #</b>	<b>73-84</b>				
	<b>Intitial Conditions</b>					
	Surface Gas Rate		27.297	MMscf/D	<b>Wellbore</b>	units
					TVD BML	3000 ft
	<b>Depth, ft</b>	<b>Pressure, psia</b>			Water TVD	0 ft
	0	44.834			DS Status	dropped n/a
	300	164.204			Parameter	csg n/a
	600	221.02			Par. Value	10.75
	900	265.483				
	1200	303.484				
	1500	337.346				
	1800	368.275				
	2100	396.99				
	2400	423.966				
	2700	575.3				
	3000	739.253				
8	<b>Run #</b>	<b>85-96</b>				
	<b>Intitial Conditions</b>					
	Surface Gas Rate		33.473	MMscf/D	<b>Wellbore</b>	units
					TVD BML	3000 ft
	<b>Depth, ft</b>	<b>Pressure, psia</b>			Water TVD	0 ft
	0	24.46			DS Status	dropped n/a
	300	68.567			Parameter	csg n/a
	600	90.578			Par. Value	12.75
	900	107.913				
	1200	122.788				
	1500	136.082				
	1800	148.252				
	2100	159.572				
	2400	170.222				
	2700	222.929				
	3000	281.335				
9	<b>Run #</b>	<b>97-108</b>				
	<b>Intitial Conditions</b>					
	Surface Gas Rate		28.175	MMscf/D	<b>Wellbore</b>	units

					TVD BML	3000	ft
	<b>Depth, ft</b>	<b>Pressure, psia</b>			Water TVD	0	ft
	0	28.635			DS Status	dropped	n/a
	300	33.877			Parameter	ds length	n/a
	600	38.38			Par. Value	50	
	900	42.41					
	1200	46.103					
	1500	49.541					
	1800	169.223					
	2100	227.645					
	2400	273.377					
	2700	487.878					
	3000	684.279					
10	<b>Run #</b>	<b>109-120</b>					
	<b>Intitial Conditions</b>						
	Surface Gas Rate		28.622	MMscf/D	<b>Wellbore</b>		units
					TVD BML	3000	ft
	<b>Depth, ft</b>	<b>Pressure, psia</b>			Water TVD	0	ft
	0	17.898			DS Status	dropped	n/a
	300	26.09			Parameter	ds length	n/a
	600	31.955			Par. Value	25	
	900	36.835					
	1200	41.131					
	1500	45.029					
	1800	48.634					
	2100	52.011					
	2400	131.215					
	2700	436.448					
	3000	654.768					
11	<b>Run #</b>	<b>121-132</b>					
	<b>Intitial Conditions</b>						
	Surface Gas Rate		32.857	MMscf/D	<b>Wellbore</b>		units
					TVD BML	3000	ft
	<b>Depth, ft</b>	<b>Pressure, psia</b>			Water TVD	0	ft
	0	18.334			DS Status	no DS	n/a
	300	45.804			Parameter	csg	n/a
	600	59.79			Par. Value	8.625	
	900	70.866					
	1200	80.396					
	1500	88.929					
	1800	96.749					
	2100	104.03					
	2400	110.886					
	2700	129.42					
	3000	150.84					
12	<b>Run #</b>	<b>133-144</b>					
	<b>Intitial Conditions</b>						
	Surface Gas Rate		33.779	MMscf/D	<b>Wellbore</b>		units
					TVD BML	3000	ft
	<b>Depth, ft</b>	<b>Pressure, psia</b>			Water TVD	0	ft

	0	15.154			DS Status	no DS	n/a
	300	27.727			Parameter	csg	n/a
	600	35.273			Par. Value	10.75	
	900	41.341					
	1200	46.598					
	1500	51.325					
	1800	55.67					
	2100	59.724					
	2400	63.547					
	2700	75.165					
	3000	88.6					
13	Run #	145-156					
	<b>Intitial Conditions</b>						
	Surface Gas Rate		34.6	MMscf/D	<b>Wellbore</b>		units
					TVD BML	3000	ft
	<b>Depth, ft</b>	<b>Pressure, psia</b>			Water TVD	0	ft
	0	15.292			DS Status	no DS	n/a
	300	20.229			Parameter	csg	n/a
	600	24.028			Par. Value	12.75	
	900	27.266					
	1200	30.152					
	1500	32.79					
	1800	35.243					
	2100	37.55					
	2400	39.739					
	2700	46.505					
	3000	54.403					
14	Run #	160-171					
	<b>Intitial Conditions</b>						
	Surface Gas Rate		25.273	MMscf/D	<b>Wellbore</b>		units
					TVD BML	3000	ft
	<b>Depth, ft</b>	<b>Pressure, psia</b>			Water TVD	5000	ft
	5000	2233.582			DS Status	hanging	n/a
	5300	2356.182			Parameter	csg	n/a
	5600	2475.372			Par. Value	8.625	
	5900	2589.797					
	6200	2700.167					
	6500	2807.053					
	6800	2910.923					
	7100	3012.167					
	7400	3111.114					
	7700	3617.699					
	8000	4257.778					
15	Run #	172-183					
	<b>Intitial Conditions</b>						
	Surface Gas Rate		80.56	MMscf/D	<b>Wellbore</b>		units
					TVD BML	3000	ft
	<b>Depth, ft</b>	<b>Pressure, psia</b>			Water TVD	5000	ft
	5000	2238.115			DS Status	hanging	n/a
	5300	2286.941			Parameter	csg	n/a

	5600	2335.866			Par. Value	10.75	
	5900	2384.268					
	6200	2432.205					
	6500	2479.731					
	6800	2526.897					
	7100	2573.751					
	7400	2620.337					
	7700	2834.752					
	8000	3114.34					
16	Run #	184-195					
	<b>Intitial Conditions</b>						
	Surface Gas Rate		109.488	MMscf/D	<b>Wellbore</b>		units
					TVD BML	3000	ft
	<b>Depth, ft</b>	<b>Pressure, psia</b>			Water TVD	5000	ft
	5000	2253.064			DS Status	hanging	n/a
	5300	2274.704			Parameter	csg	n/a
	5600	2296.656			Par. Value	12.75	
	5900	2318.806					
	6200	2341.167					
	6500	2363.749					
	6800	2386.563					
	7100	2409.623					
	7400	2432.941					
	7700	2485.826					
	8000	2552.877					
17	Run #	196-207					
	<b>Intitial Conditions</b>						
	Surface Gas Rate		80.56	MMscf/D	<b>Wellbore</b>		units
					TVD BML	3000	ft
	<b>Depth, ft</b>	<b>Pressure, psia</b>			Water TVD	5000	ft
	5000	2238.115			DS Status	hanging	n/a
	5300	2286.941			Parameter	ds length	n/a
	5600	2335.866			Par. Value	50	
	5900	2384.268					
	6200	2432.205					
	6500	2479.731					
	6800	2526.897					
	7100	2573.751					
	7400	2620.337					
	7700	2834.752					
	8000	3114.34					
18	Run #	208-219					
	<b>Intitial Conditions</b>						
	Surface Gas Rate		98.399	MMscf/D	<b>Wellbore</b>		units
					TVD BML	3000	ft
	<b>Depth, ft</b>	<b>Pressure, psia</b>			Water TVD	5000	ft
	5000	2249.385			DS Status	hanging	n/a
	5300	2314.357			Parameter	ds length	n/a
	5600	2379.017			Par. Value	25	
	5900	2442.491					

	6200	2504.905					
	6500	2566.372					
	6800	2626.996					
	7100	2674.169					
	7400	2694.353					
	7700	2716.288					
	8000	2739.291					
19	<b>Run #</b>	220-231					
	<b>Intitial Conditions</b>						
	Surface Gas Rate		25.259	MMscf/D	<b>Wellbore</b>		units
					TVD BML	3000	ft
	<b>Depth, ft</b>	<b>Pressure, psia</b>			Water TVD	5000	ft
	5000	2234.204			DS Status	dropped	n/a
	5300	2358.83			Parameter	csg	n/a
	5600	2477.823			Par. Value	8.625	
	5900	2592.075					
	6200	2702.29					
	6500	2809.038					
	6800	2912.782					
	7100	3013.912					
	7400	3112.752					
	7700	3618.688					
	8000	4258.06					
20	<b>Run #</b>	232-243					
	<b>Intitial Conditions</b>						
	Surface Gas Rate		80.545	MMscf/D	<b>Wellbore</b>		units
					TVD BML	3000	ft
	<b>Depth, ft</b>	<b>Pressure, psia</b>			Water TVD	5000	ft
	5000	2238.087			DS Status	dropped	n/a
	5300	2287.579			Parameter	csg	n/a
	5600	2336.488			Par. Value	10.75	
	5900	2384.874					
	6200	2432.796					
	6500	2480.308					
	6800	2527.46					
	7100	2574.301					
	7400	2620.876					
	7700	2835.189					
	8000	3114.654					
21	<b>Run #</b>	244-255					
	<b>Intitial Conditions</b>						
	Surface Gas Rate		109.482	MMscf/D	<b>Wellbore</b>		units
					TVD BML	3000	ft
	<b>Depth, ft</b>	<b>Pressure, psia</b>			Water TVD	5000	ft
	5000	2253.079			DS Status	dropped	n/a
	5300	2274.843			Parameter	csg	n/a
	5600	2296.794			Par. Value	12.75	
	5900	2318.945					
	6200	2341.305					
	6500	2363.887					

	6800	2386.702					
	7100	2409.762					
	7400	2433.079					
	7700	2485.959					
	8000	2553.003					
22	<b>Run #</b>	<b>256-267</b>					
	<b>Intitial Conditions</b>						
	Surface Gas Rate		80.545	MMscf/D	<b>Wellbore</b>		units
					TVD BML	3000	ft
	<b>Depth, ft</b>	<b>Pressure, psia</b>			Water TVD	5000	ft
	5000	2238.087			DS Status	dropped	n/a
	5300	2287.579			Parameter	ds length	n/a
	5600	2336.488			Par. Value	50	
	5900	2384.874					
	6200	2432.796					
	6500	2480.308					
	6800	2527.46					
	7100	2574.301					
	7400	2620.876					
	7700	2835.189					
	8000	3114.654					
23	<b>Run #</b>	<b>268-279</b>					
	<b>Intitial Conditions</b>						
	Surface Gas Rate		83.126	MMscf/D	<b>Wellbore</b>		units
					TVD BML	3000	ft
	<b>Depth, ft</b>	<b>Pressure, psia</b>			Water TVD	5000	ft
	5000	2241.826			DS Status	dropped	n/a
	5300	2257.575			Parameter	ds length	n/a
	5600	2273.59			Par. Value	25	
	5900	2289.879					
	6200	2328.884					
	6500	2379.018					
	6800	2428.636					
	7100	2477.799					
	7400	2526.563					
	7700	2759.283					
	8000	3060.6					
24	<b>Run #</b>	<b>280-291</b>					
	<b>Intitial Conditions</b>						
	Surface Gas Rate		109.823	MMscf/D	<b>Wellbore</b>		units
					TVD BML	3000	ft
	<b>Depth, ft</b>	<b>Pressure, psia</b>			Water TVD	5000	ft
	5000	2241.814			DS Status	no DS	n/a
	5300	2259.869			Parameter	csg	n/a
	5600	2278.163			Par. Value	8.625	
	5900	2296.704					
	6200	2315.504					
	6500	2334.571					
	6800	2353.916					
	7100	2373.551					

	7400	2393.485					
	7700	2419.14					
	8000	2447.788					
25	Run #	292-303					
	<b>Intitial Conditions</b>						
	Surface Gas Rate		112.41	MMscf/D	<b>Wellbore</b>		units
					TVD BML	3000	ft
	<b>Depth, ft</b>	<b>Pressure, psia</b>			Water TVD	5000	ft
	5000	2260.774			DS Status	no DS	n/a
	5300	2277.035			Parameter	csg	n/a
	5600	2293.559			Par. Value	10.75	
	5900	2310.357					
	6200	2327.436					
	6500	2344.806					
	6800	2362.479					
	7100	2380.464					
	7400	2398.772					
	7700	2419.438					
	8000	2441.458					
26	Run #	304-315					
	<b>Intitial Conditions</b>						
	Surface Gas Rate		114.919	MMscf/D	<b>Wellbore</b>		units
					TVD BML	3000	ft
	<b>Depth, ft</b>	<b>Pressure, psia</b>			Water TVD	5000	ft
	5000	2266.841			DS Status	no DS	n/a
	5300	2282.584			Parameter	csg	n/a
	5600	2298.599			Par. Value	12.75	
	5900	2314.892					
	6200	2331.474					
	6500	2348.542					
	6800	2365.542					
	7100	2383.049					
	7400	2400.885					
	7700	2419.789					
	8000	2439.409					
27	Run #	322-333					
	<b>Intitial Conditions</b>						
	Surface Gas Rate		33.737	MMscf/D	<b>Wellbore</b>		units
					TVD BML	3000	ft
	<b>Depth, ft</b>	<b>Pressure, psia</b>			Water TVD	10000	ft
	10000	4493.958			DS Status	hanging	n/a
	10300	4627.924			Parameter	csg	n/a
	10600	4761.889			Par. Value	8.625	
	10900	4893.88					
	11200	5024.092					
	11500	5152.691					
	11800	5279.827					
	12100	5405.631					
	12400	5530.221					
	12700	6167.483					

	13000	7021.6					
28	Run #	334-345					
	<b>Intitial Conditions</b>						
	Surface Gas Rate		103.584	MMscf/D	<b>Wellbore</b>		units
					TVD BML	3000	ft
	<b>Depth, ft</b>	<b>Pressure, psia</b>			Water TVD	10000	ft
	10000	4484.997			DS Status	hanging	n/a
	10300	4543.363			Parameter	csg	n/a
	10600	4602.303			Par. Value	10.75	
	10900	4661.216					
	11200	4720.12					
	11500	4779.034					
	11800	4837.972					
	12100	4896.952					
	12400	4955.988					
	12700	5189.871					
	13000	5505.081					
29	Run #	346-357					
	<b>Intitial Conditions</b>						
	Surface Gas Rate		135.15	MMscf/D	<b>Wellbore</b>		units
					TVD BML	3000	ft
	<b>Depth, ft</b>	<b>Pressure, psia</b>			Water TVD	10000	ft
	10000	4480.23			DS Status	hanging	n/a
	10300	4513.294			Parameter	csg	n/a
	10600	4546.784			Par. Value	12.75	
	10900	4580.602					
	11200	4614.753					
	11500	4649.244					
	11800	4684.079					
	12100	4719.264					
	12400	4754.803					
	12700	4816.928					
	13000	4892.431					
30	Run #	358-369					
	<b>Intitial Conditions</b>						
	Surface Gas Rate		103.584	MMscf/D	<b>Wellbore</b>		units
					TVD BML	3000	ft
	<b>Depth, ft</b>	<b>Pressure, psia</b>			Water TVD	10000	ft
	10000	4484.997			DS Status	hanging	n/a
	10300	4543.363			Parameter	ds length	n/a
	10600	4602.303			Par. Value	50	
	10900	4661.216					
	11200	4720.12					
	11500	4779.034					
	11800	4837.972					
	12100	4896.952					
	12400	4955.988					
	12700	5189.871					
	13000	5505.081					

31	Run #	370-381	same as previous			
	<b>Intitial Conditions</b>					
	Surface Gas Rate		103.584	MMscf/D	<b>Wellbore</b>	units
					TVD BML	3000 ft
	<b>Depth, ft</b>	<b>Pressure, psia</b>			Water TVD	10000 ft
	10000	4484.997			DS Status	hanging n/a
	10300	4543.363			Parameter	ds length n/a
	10600	4602.303			Par. Value	25
	10900	4661.216				
	11200	4720.12				
	11500	4779.034				
	11800	4837.972				
	12100	4896.952				
	12400	4955.988				
	12700	5189.871				
	13000	5505.081				
32	Run #	382-393				
	<b>Intitial Conditions</b>					
	Surface Gas Rate		33.723	MMscf/D	<b>Wellbore</b>	units
					TVD BML	3000 ft
	<b>Depth, ft</b>	<b>Pressure, psia</b>			Water TVD	10000 ft
	10000	4494.075			DS Status	dropped n/a
	10300	4630.119			Parameter	csg n/a
	10600	4763.977			Par. Value	8.625
	10900	4895.868				
	11200	5025.983				
	11500	5154.491				
	11800	5281.538				
	12100	5407.258				
	12400	5531.766				
	12700	6168.484				
	13000	7021.91				
33	Run #	394-405				
	<b>Intitial Conditions</b>					
	Surface Gas Rate		103.566	MMscf/D	<b>Wellbore</b>	units
					TVD BML	3000 ft
	<b>Depth, ft</b>	<b>Pressure, psia</b>			Water TVD	10000 ft
	10000	4485.011			DS Status	dropped n/a
	10300	4543.986			Parameter	csg n/a
	10600	4602.916			Par. Value	10.75
	10900	4661.819				
	11200	4720.713				
	11500	4779.617				
	11800	4838.546				
	12100	4897.517				
	12400	4956.543				
	12700	5190.35				
	13000	5505.454				
34	Run #	406-417				
	<b>Intitial Conditions</b>					

	Surface Gas Rate		135.145	MMscf/D	<b>Wellbore</b>		units
					TVD BML	3000	ft
	<b>Depth, ft</b>	<b>Pressure, psia</b>			Water TVD	10000	ft
	10000	4480.235			DS Status	dropped	n/a
	10300	4513.403			Parameter	csg	n/a
	10600	4546.893			Par. Value	12.75	
	10900	4580.711					
	11200	4614.862					
	11500	4649.353					
	11800	4684.188					
	12100	4719.372					
	12400	4754.912					
	12700	4817.034					
	13000	4892.534					
35	<b>Run #</b>	<b>418-429</b>					
	<b>Intitial Conditions</b>						
	Surface Gas Rate		103.566	MMscf/D	<b>Wellbore</b>		units
					TVD BML	3000	ft
	<b>Depth, ft</b>	<b>Pressure, psia</b>			Water TVD	10000	ft
	10000	4485.011			DS Status	dropped	n/a
	10300	4543.986			Parameter	ds length	n/a
	10600	4602.916			Par. Value	50	
	10900	4661.819					
	11200	4720.713					
	11500	4779.617					
	11800	4838.546					
	12100	4897.517					
	12400	4956.543					
	12700	5190.35					
	13000	5505.454					
36	<b>Run #</b>	<b>430-441</b>					
	<b>Intitial Conditions</b>						
	Surface Gas Rate		103.566	MMscf/D	<b>Wellbore</b>		units
					TVD BML	3000	ft
	<b>Depth, ft</b>	<b>Pressure, psia</b>			Water TVD	10000	ft
	10000	4485.011			DS Status	dropped	n/a
	10300	4543.986			Parameter	ds length	n/a
	10600	4602.916			Par. Value	25	
	10900	4661.819					
	11200	4720.713					
	11500	4779.617					
	11800	4838.546					
	12100	4897.517					
	12400	4956.543					
	12700	5190.35					
	13000	5505.454					
37	<b>Run #</b>	<b>442-453</b>					
	<b>Intitial Conditions</b>						
	Surface Gas Rate		133.849	MMscf/D	<b>Wellbore</b>		units
					TVD BML	3000	ft

	<b>Depth, ft</b>	<b>Pressure, psia</b>		Water TVD	10000	ft
	10000	4472.865		DS Status	no DS	n/a
	10300	4502.871		Parameter	csg	n/a
	10600	4533.23		Par. Value	8.625	
	10900	4563.949				
	11200	4595.032				
	11500	4626.485				
	11800	4658.312				
	12100	4690.519				
	12400	4723.11				
	12700	4760.728				
	13000	4801.065				
38	<b>Run #</b>	<b>454-465</b>				
	<b>Intitial Conditions</b>					
	Surface Gas Rate		137.015	MMscf/D	<b>Wellbore</b>	units
					TVD BML	3000 ft
	<b>Depth, ft</b>	<b>Pressure, psia</b>		Water TVD	10000	ft
	10000	4486.709		DS Status	no DS	n/a
	10300	4515.198		Parameter	csg	n/a
	10600	4544.055		Par. Value	10.75	
	10900	4573.286				
	11200	4602.896				
	11500	4632.889				
	11800	4663.271				
	12100	4694.047				
	12400	4725.22				
	12700	4758.532				
	13000	4793.124				
39	<b>Run #</b>	<b>466-477</b>				
	<b>Intitial Conditions</b>					
	Surface Gas Rate		140.076	MMscf/D	<b>Wellbore</b>	units
					TVD BML	3000 ft
	<b>Depth, ft</b>	<b>Pressure, psia</b>		Water TVD	10000	ft
	10000	4491.171		DS Status	no DS	n/a
	10300	4519.217		Parameter	csg	n/a
	10600	4547.635		Par. Value	12.75	
	10900	4576.431				
	11200	4605.61				
	11500	4635.177				
	11800	4665.136				
	12100	4695.492				
	12400	4726.25				
	12700	4758.038				
	13000	4790.549				
40	<b>Run #</b>	<b>484-495</b>				
	<b>Intitial Conditions</b>					
	Surface Gas Rate		20.951	MMscf/D	<b>Wellbore</b>	units
					TVD BML	8000 ft
	<b>Depth, ft</b>	<b>Pressure, psia</b>		Water TVD	0	ft
	0	137.103		DS Status	hanging	n/a

	800	1040.893			Parameter	csg	n/a
	1600	1459.201			Par. Value	8.625	
	2400	1790.575					
	3200	2079.94					
	4000	2344.313					
	4800	2592.166					
	5600	2828.359					
	6400	3055.937					
	7200	3276.931					
	8000	4312.821					
41	Run #	496-507					
	<b>Intitial Conditions</b>						
	Surface Gas Rate		79.665	MMscf/D	<b>Wellbore</b>		units
					TVD BML	8000	ft
	<b>Depth, ft</b>	<b>Pressure, psia</b>			Water TVD	0	ft
	0	125.333			DS Status	hanging	n/a
	800	718.351			Parameter	csg	n/a
	1600	996.037			Par. Value	10.75	
	2400	1216.467					
	3200	1408.56					
	4000	1583.455					
	4800	1746.793					
	5600	1901.871					
	6400	2050.788					
	7200	2194.969					
	8000	2904.993					
42	Run #	508-519					
	<b>Intitial Conditions</b>						
	Surface Gas Rate		131.021	MMscf/D	<b>Wellbore</b>		units
					TVD BML	8000	ft
	<b>Depth, ft</b>	<b>Pressure, psia</b>			Water TVD	0	ft
	0	106.359			DS Status	hanging	n/a
	800	393.703			Parameter	csg	n/a
	1600	539.679			Par. Value	12.75	
	2400	656.224					
	3200	757.929					
	4000	850.48					
	4800	936.787					
	5600	1018.567					
	6400	1096.927					
	7200	1172.627					
	8000	1500.847					
43	Run #	520-531					
	<b>Intitial Conditions</b>						
	Surface Gas Rate		104.145	MMscf/D	<b>Wellbore</b>		units
					TVD BML	8000	ft
	<b>Depth, ft</b>	<b>Pressure, psia</b>			Water TVD	0	ft
	0	177.747			DS Status	hanging	n/a
	800	933.05			Parameter	ds length	n/a
	1600	1291.933			Par. Value	50	

	2400	1577.177					
	3200	1826.33					
	4000	2053.789					
	4800	2093.496					
	5600	2129.557					
	6400	2165.634					
	7200	2201.729					
	8000	2244.026					
44	<b>Run #</b>	532-543					
	<b>Intitial Conditions</b>						
	Surface Gas Rate		117.058	MMscf/D	<b>Wellbore</b>		units
					TVD BML	8000	ft
	<b>Depth, ft</b>	<b>Pressure, psia</b>			Water TVD	0	ft
	0	176.751			DS Status	hanging	n/a
	800	1044.685			Parameter	ds length	n/a
	1600	1446.212			Par. Value	25	
	2400	1633.788					
	3200	1664.885					
	4000	1696.046					
	4800	1727.268					
	5600	1758.55					
	6400	1789.893					
	7200	1821.293					
	8000	1862.221					
45	<b>Run #</b>	544-555					
	<b>Intitial Conditions</b>						
	Surface Gas Rate		20.951	MMscf/D	<b>Wellbore</b>		units
					TVD BML	8000	ft
	<b>Depth, ft</b>	<b>Pressure, psia</b>			Water TVD	0	ft
	0	137.103			DS Status	dropped	n/a
	800	1040.893			Parameter	csg	n/a
	1600	1459.201			Par. Value	8.625	
	2400	1790.575					
	3200	2079.94					
	4000	2344.313					
	4800	2592.166					
	5600	2828.359					
	6400	3055.937					
	7200	3276.931					
	8000	4312.821					
46	<b>Run #</b>	556-567					
	<b>Intitial Conditions</b>						
	Surface Gas Rate		79.665	MMscf/D	<b>Wellbore</b>		units
					TVD BML	8000	ft
	<b>Depth, ft</b>	<b>Pressure, psia</b>			Water TVD	0	ft
	0	125.333			DS Status	dropped	n/a
	800	718.351			Parameter	csg	n/a
	1600	996.037			Par. Value	10.75	
	2400	1216.467					
	3200	1408.56					

	4000	1583.455					
	4800	1746.793					
	5600	1901.871					
	6400	2050.788					
	7200	2194.969					
	8000	2904.993					
47	<b>Run #</b>	<b>568-579</b>					
	<b>Intitial Conditions</b>						
	Surface Gas Rate		131.021	MMscf/D	<b>Wellbore</b>		units
					TVD BML	8000	ft
	<b>Depth, ft</b>	<b>Pressure, psia</b>			Water TVD	0	ft
	0	106.359			DS Status	dropped	n/a
	800	393.703			Parameter	csg	n/a
	1600	539.679			Par. Value	12.75	
	2400	656.224					
	3200	757.929					
	4000	850.48					
	4800	936.787					
	5600	1018.567					
	6400	1096.927					
	7200	1172.627					
	8000	1500.847					
48	<b>Run #</b>	<b>580-591</b>					
	<b>Intitial Conditions</b>						
	Surface Gas Rate		89.025	MMscf/D	<b>Wellbore</b>		units
					TVD BML	8000	ft
	<b>Depth, ft</b>	<b>Pressure, psia</b>			Water TVD	0	ft
	0	45.458			DS Status	dropped	n/a
	800	104.253			Parameter	ds length	n/a
	1600	138.869			Par. Value	50	
	2400	167.03					
	3200	191.807					
	4000	214.451					
	4800	833.376					
	5600	1151.897					
	6400	1405.292					
	7200	1626.217					
	8000	2659.759					
49	<b>Run #</b>	<b>592-603</b>					
	<b>Intitial Conditions</b>						
	Surface Gas Rate		95.037	MMscf/D	<b>Wellbore</b>		units
					TVD BML	8000	ft
	<b>Depth, ft</b>	<b>Pressure, psia</b>			Water TVD	0	ft
	0	33.529			DS Status	dropped	n/a
	800	107.819			Parameter	ds length	n/a
	1600	145.579			Par. Value	25	
	2400	175.995					
	3200	202.645					
	4000	226.944					
	4800	249.621					

	5600	271.111					
	6400	678.937					
	7200	1095.767					
	8000	2497.731					
50	Run #	604-615					
	<b>Intitial Conditions</b>						
	Surface Gas Rate		139.948	MMscf/D	<b>Wellbore</b>		units
					TVD BML	8000	ft
	<b>Depth, ft</b>	<b>Pressure, psia</b>			Water TVD	0	ft
	0	61.574			DS Status	no DS	n/a
	800	281.568			Parameter	csg	n/a
	1600	383.392			Par. Value	8.625	
	2400	465.003					
	3200	536.34					
	4000	601.304					
	4800	661.899					
	5600	719.311					
	6400	774.309					
	7200	827.419					
	8000	958.436					
51	Run #	616-627					
	<b>Intitial Conditions</b>						
	Surface Gas Rate		151.253	MMscf/D	<b>Wellbore</b>		units
					TVD BML	8000	ft
	<b>Depth, ft</b>	<b>Pressure, psia</b>			Water TVD	0	ft
	0	52.978			DS Status	no DS	n/a
	800	170.585			Parameter	csg	n/a
	1600	230.174			Par. Value	10.75	
	2400	278.137					
	3200	320.152					
	4000	358.456					
	4800	394.205					
	5600	428.085					
	6400	460.542					
	7200	491.881					
	8000	578.959					
52	Run #	628-639					
	<b>Intitial Conditions</b>						
	Surface Gas Rate		158.738	MMscf/D	<b>Wellbore</b>		units
					TVD BML	8000	ft
	<b>Depth, ft</b>	<b>Pressure, psia</b>			Water TVD	0	ft
	0	31.29			DS Status	no DS	n/a
	800	105.687			Parameter	csg	n/a
	1600	141.672			Par. Value	12.75	
	2400	170.683					
	3200	196.124					
	4000	219.335					
	4800	241.008					
	5600	261.554					
	6400	281.238					

	7200	300.247					
	8000	354.41					
53	Run #	646-657					
	<b>Intitial Conditions</b>						
	Surface Gas Rate		31.489	MMscf/D	<b>Wellbore</b>		units
					TVD BML	8000	ft
	<b>Depth, ft</b>	<b>Pressure, psia</b>			Water TVD	5000	ft
	5000	2236.96			DS Status	hanging	n/a
	5800	2698.03			Parameter	csg	n/a
	6600	3116.629			Par. Value	8.625	
	7400	3504.173					
	8200	3871.145					
	9000	4223.528					
	9800	4565.061					
	10600	4898.228					
	11400	5224.762					
	12200	5545.917					
	13000	7093.155					
54	Run #	658-669					
	<b>Intitial Conditions</b>						
	Surface Gas Rate		122.614	MMscf/D	<b>Wellbore</b>		units
					TVD BML	8000	ft
	<b>Depth, ft</b>	<b>Pressure, psia</b>			Water TVD	5000	ft
	5000	2227.744			DS Status	hanging	n/a
	5800	2471.077			Parameter	csg	n/a
	6600	2705.452			Par. Value	10.75	
	7400	2930.32					
	8200	3148.091					
	9000	3360.413					
	9800	3568.456					
	10600	3773.081					
	11400	3974.93					
	12200	4174.5					
	13000	5131.407					
55	Run #	670-681					
	<b>Intitial Conditions</b>						
	Surface Gas Rate		203.959	MMscf/D	<b>Wellbore</b>		units
					TVD BML	8000	ft
	<b>Depth, ft</b>	<b>Pressure, psia</b>			Water TVD	5000	ft
	5000	2244.637			DS Status	hanging	n/a
	5800	2343.308			Parameter	csg	n/a
	6600	2541.534			Par. Value	12.75	
	7400	2640.176					
	8200	2640.176					
	9000	2738.623					
	9800	2836.945					
	10600	2935.199					
	11400	3033.433					
	12200	3131.687					
	13000	3466.186					

56	Run #	682-693					
	<b>Intitial Conditions</b>						
	Surface Gas Rate		145.719	MMscf/D	<b>Wellbore</b>		units
					TVD BML	8000	ft
	<b>Depth, ft</b>	<b>Pressure, psia</b>			Water TVD	5000	ft
	5000	2255.656			DS Status	hanging	n/a
	5800	2575.694			Parameter	ds length	n/a
	6600	2877.34			Par. Value	50	
	7400	3162.629					
	8200	3436.26					
	9000	3701.221					
	9800	3959.525					
	10600	4212.586					
	11400	4461.431					
	12200	4556.784					
	13000	4633.58					
57	Run #	694-705					
	<b>Intitial Conditions</b>						
	Surface Gas Rate		168.821	MMscf/D	<b>Wellbore</b>		units
					TVD BML	8000	ft
	<b>Depth, ft</b>	<b>Pressure, psia</b>			Water TVD	5000	ft
	5000	2233.611			DS Status	hanging	n/a
	5800	2645.884			Parameter	ds length	n/a
	6600	3024.136			Par. Value	25	
	7400	3376.327					
	8200	3710.88					
	9000	3797.084					
	9800	3862.551					
	10600	3929.23					
	11400	3994.116					
	12200	4060.204					
	13000	4135.202					
58	Run #	706-717					
	<b>Intitial Conditions</b>						
	Surface Gas Rate		31.473	MMscf/D	<b>Wellbore</b>		units
					TVD BML	8000	ft
	<b>Depth, ft</b>	<b>Pressure, psia</b>			Water TVD	5000	ft
	5000	2235.089			DS Status	dropped	n/a
	5800	2704.047			Parameter	csg	n/a
	6600	3121.677			Par. Value	8.625	
	7400	3508.542					
	8200	3874.979					
	9000	4226.916					
	9800	4568.06					
	10600	4900.88					
	11400	5227.096					
	12200	5547.957					
	13000	7093.52					
59	Run #	718-729					

	<b>Intitial Conditions</b>					
	Surface Gas Rate		122.562	MMscf/D	<b>Wellbore</b>	units
					TVD BML	8000 ft
	<b>Depth, ft</b>	<b>Pressure, psia</b>			Water TVD	5000 ft
	5000	2227.765			DS Status	dropped n/a
	5800	2474.895			Parameter	csg n/a
	6600	2708.915			Par. Value	10.75
	7400	2933.494				
	8200	3151.022				
	9000	3363.133				
	9800	3570.99				
	10600	3775.445				
	11400	3977.139				
	12200	4176.565				
	13000	5132.52				
60	<b>Run #</b>	<b>730-741</b>				
	<b>Intitial Conditions</b>					
	Surface Gas Rate		203.923	MMscf/D	<b>Wellbore</b>	units
					TVD BML	8000 ft
	<b>Depth, ft</b>	<b>Pressure, psia</b>			Water TVD	5000 ft
	5000	2244.619			DS Status	dropped n/a
	5800	2344.404			Parameter	csg n/a
	6600	2443.682			Par. Value	12.75
	7400	2542.579				
	8200	2641.198				
	9000	2739.624				
	9800	2837.926				
	10600	2936.162				
	11400	3034.378				
	12200	3132.615				
	13000	3466.962				
61	<b>Run #</b>	<b>742-753</b>				
	<b>Intitial Conditions</b>					
	Surface Gas Rate		127.678	MMscf/D	<b>Wellbore</b>	units
					TVD BML	8000 ft
	<b>Depth, ft</b>	<b>Pressure, psia</b>			Water TVD	5000 ft
	5000	2226.367			DS Status	dropped n/a
	5800	2269.618			Parameter	ds length n/a
	6600	2340.299			Par. Value	50
	7400	2600.158				
	8200	2846.26				
	9000	3082.427				
	9800	3311.15				
	10600	3534.131				
	11400	3752.586				
	12200	3967.404				
	13000	5022.291				
62	<b>Run #</b>	<b>754-765</b>				
	<b>Intitial Conditions</b>					
	Surface Gas Rate		140.986	MMscf/D	<b>Wellbore</b>	units

					TVD BML	8000	ft
	<b>Depth, ft</b>	<b>Pressure, psia</b>			Water TVD	5000	ft
	5000	2228.571			DS Status	dropped	n/a
	5800	2272.512			Parameter	ds length	n/a
	6600	2316.763			Par. Value	25	%
	7400	2361.319					
	8200	2406.178					
	9000	2451.333					
	9800	2512.82					
	10600	2813.668					
	11400	3096.877					
	12200	3367.504					
	13000	4735.571					
63	<b>Run #</b>	<b>766-777</b>					
	<b>Intitial Conditions</b>						
	Surface Gas Rate		215.701	MMscf/D	<b>Wellbore</b>		units
					TVD BML	8000	ft
	<b>Depth, ft</b>	<b>Pressure, psia</b>			Water TVD	5000	ft
	5000	2259.415			DS Status	no DS	n/a
	5800	2328.567			Parameter	csg	n/a
	6600	2397.975			Par. Value	8.625	
	7400	2467.651					
	8200	2537.601					
	9000	2607.834					
	9800	2678.3521					
	10600	2749.16					
	11400	2820.26					
	12200	2891.653					
	13000	3015.863					
64	<b>Run #</b>	<b>778-789</b>					
	<b>Intitial Conditions</b>						
	Surface Gas Rate		230.605	MMscf/D	<b>Wellbore</b>		units
					TVD BML	8000	ft
	<b>Depth, ft</b>	<b>Pressure, psia</b>			Water TVD	5000	ft
	5000	2246.037			DS Status	no DS	n/a
	5800	2296.268			Parameter	csg	n/a
	6600	2346.843			Par. Value	10.75	
	7400	2397.756					
	8200	2449.004					
	9000	2500.582					
	9800	2552.485					
	10600	2604.708					
	11400	2657.247					
	12200	2710.097					
	13000	2786.278					
65	<b>Run #</b>	<b>790-801</b>					
	<b>Intitial Conditions</b>						
	Surface Gas Rate		238.9	MMscf/D	<b>Wellbore</b>		units
					TVD BML	8000	ft
	<b>Depth, ft</b>	<b>Pressure, psia</b>			Water TVD	5000	ft

	5000	2250.742			DS Status	no DS	n/a
	5800	2294.852			Parameter	csg	n/a
	6600	2339.271			Par. Value	12.75	
	7400	2383.995					
	8200	2429.018					
	9000	2474.336					
	9800	2519.945					
	10600	2665.841					
	11400	2612.02					
	12200	2658.476					
	13000	2713.907					
66	Run #	808-819					
	<b>Intitial Conditions</b>						
	Surface Gas Rate		37.672	MMscf/D	<b>Wellbore</b>		units
					TVD BML	8000	ft
	<b>Depth, ft</b>	<b>Pressure, psia</b>			Water TVD	10000	ft
	10000	4466.947			DS Status	hanging	n/a
	10800	4891.65			Parameter	csg	n/a
	11600	5310.98			Par. Value	8.625	
	12400	5720.545					
	13200	6122.354					
	14000	6517.848					
	14800	6908.096					
	15600	7293.915					
	16400	7675.94					
	17200	8054.677					
	18000	9913.932					
67	Run #	820-831					
	<b>Intitial Conditions</b>						
	Surface Gas Rate		143.39	MMscf/D	<b>Wellbore</b>		units
					TVD BML	8000	ft
	<b>Depth, ft</b>	<b>Pressure, psia</b>			Water TVD	10000	ft
	10000	4485.524			DS Status	hanging	n/a
	10800	4715.199			Parameter	csg	n/a
	11600	4946.139			Par. Value	10.75	
	12400	5175.481					
	13200	5403.464					
	14000	5630.283					
	14800	5856.097					
	15600	6081.038					
	16400	6305.217					
	17200	6528.725					
	18000	7559.168					
68	Run #	832-843					
	<b>Intitial Conditions</b>						
	Surface Gas Rate		227.661	MMscf/D	<b>Wellbore</b>		units
					TVD BML	8000	ft
	<b>Depth, ft</b>	<b>Pressure, psia</b>			Water TVD	10000	ft
	10000	4479.167			DS Status	hanging	n/a
	10800	4592.945			Parameter	csg	n/a

	11600	4707.769			Par. Value	12.75	
	12400	4822.848					
	13200	4938.177					
	14000	5053.75					
	14800	5169.561					
	15600	5285.605					
	16400	5401.876					
	17200	5518.369					
	18000	5831.296					
69	Run #	844-855					
	<b>Intitial Conditions</b>						
	Surface Gas Rate		143.39	MMscf/D	<b>Wellbore</b>		units
					TVD BML	8000	ft
	<b>Depth, ft</b>	<b>Pressure, psia</b>			Water TVD	10000	ft
	10000	4485.524			DS Status	hanging	n/a
	10800	4715.199			Parameter	ds length	n/a
	11600	4946.139			Par. Value	50	
	12400	5175.481					
	13200	5403.464					
	14000	5630.283					
	14800	5856.097					
	15600	6081.038					
	16400	6305.217					
	17200	6528.725					
	18000	7559.168					
70	Run #	856-867					
	<b>Intitial Conditions</b>						
	Surface Gas Rate		183.667	MMscf/D	<b>Wellbore</b>		units
					TVD BML	8000	ft
	<b>Depth, ft</b>	<b>Pressure, psia</b>			Water TVD	10000	ft
	10000	4474.247			DS Status	hanging	n/a
	10800	4802.322			Parameter	ds length	n/a
	11600	5129.216			Par. Value	25	
	12400	5450.965					
	13200	5768.483					
	14000	6082.465					
	14800	6313.879					
	15600	6402.992					
	16400	6492.153					
	17200	6581.363					
	18000	6678.123					
71	Run #	868-879					
	<b>Intitial Conditions</b>						
	Surface Gas Rate		37.65	MMscf/D	<b>Wellbore</b>		units
					TVD BML	8000	ft
	<b>Depth, ft</b>	<b>Pressure, psia</b>			Water TVD	10000	ft
	10000	4466.368			DS Status	dropped	n/a
	10800	4897.727			Parameter	csg	n/a
	11600	5316.491			Par. Value	8.625	
	12400	5725.551					

	13200	6126.899					
	14000	6521.965					
	14800	6911.812					
	15600	7297.249					
	16400	7678.909					
	17200	8057.296					
	18000	9914.43					
72	Run #	880-891					
	<b>Intitial Conditions</b>						
	Surface Gas Rate		143.336	MMscf/D	<b>Wellbore</b>		units
					TVD BML	8000	ft
	<b>Depth, ft</b>	<b>Pressure, psia</b>			Water TVD	10000	ft
	10000	4485.53			DS Status	dropped	n/a
	10800	4718.213			Parameter	csg	n/a
	11600	4949.007			Par. Value	10.75	
	12400	5178.209					
	13200	5406.059					
	14000	5632.751					
	14800	5858.443					
	15600	6083.265					
	16400	6307.328					
	17200	6530.723					
	18000	7560.357					
73	Run #	892-903					
	<b>Intitial Conditions</b>						
	Surface Gas Rate		227.63	MMscf/D	<b>Wellbore</b>		units
					TVD BML	8000	ft
	<b>Depth, ft</b>	<b>Pressure, psia</b>			Water TVD	10000	ft
	10000	4479.174			DS Status	dropped	n/a
	10800	4593.728			Parameter	csg	n/a
	11600	4708.545			Par. Value	12.75	
	12400	4823.617					
	13200	4938.938					
	14000	5054.504					
	14800	5170.308					
	15600	5286.345					
	16400	5402.609					
	17200	5519.095					
	18000	5831.946					
74	Run #	904-915					
	<b>Intitial Conditions</b>						
	Surface Gas Rate		143.336	MMscf/D	<b>Wellbore</b>		units
					TVD BML	8000	ft
	<b>Depth, ft</b>	<b>Pressure, psia</b>			Water TVD	10000	ft
	10000	4485.53			DS Status	dropped	n/a
	10800	4718.213			Parameter	ds length	n/a
	11600	1919.007			Par. Value	50	
	12400	5178.209					
	13200	5406.059					
	14000	5632.751					

	14800	5858.443					
	15600	6083.265					
	16400	6307.328					
	17200	6530.723					
	18000	7560.357					
75	Run #	916-927					
	<b>Intitial Conditions</b>						
	Surface Gas Rate		157.553	MMscf/D	<b>Wellbore</b>		units
					TVD BML	8000	ft
	<b>Depth, ft</b>	<b>Pressure, psia</b>			Water TVD	10000	ft
	10000	4450.23			DS Status	dropped	n/a
	10800	4526.02			Parameter	ds length	n/a
	11600	4601.975			Par. Value	25	%
	12400	4678.091					
	13200	4754.363					
	14000	4947.983					
	14800	5211.061					
	15600	5471.591					
	16400	5729.96					
	17200	5986.476					
	18000	7248					
76	Run #	928-939					
	<b>Intitial Conditions</b>						
	Surface Gas Rate		235.551	MMscf/D	<b>Wellbore</b>		units
					TVD BML	8000	ft
	<b>Depth, ft</b>	<b>Pressure, psia</b>			Water TVD	10000	ft
	10000	4480.381			DS Status	no DS	n/a
	10800	4572.782			Parameter	csg	n/a
	11600	4665.439			Par. Value	8.625	
	12400	4758.344					
	13200	4851.491					
	14000	4944.872					
	14800	5038.482					
	15600	5132.313					
	16400	5226.361					
	17200	5320.619					
	18000	5454.079					
77	Run #	940-951					
	<b>Intitial Conditions</b>						
	Surface Gas Rate		245.872	MMscf/D	<b>Wellbore</b>		units
					TVD BML	8000	ft
	<b>Depth, ft</b>	<b>Pressure, psia</b>			Water TVD	10000	ft
	10000	4515.594			DS Status	no DS	n/a
	10800	4595.608			Parameter	csg	n/a
	11600	4675.807			Par. Value	10.75	
	12400	4756.187					
	13200	4836.742					
	14000	4917.469					
	14800	4998.363					
	15600	5079.419					

	16400	5160.633					
	17200	5242.002					
	18000	5338.905					
78	Run #	952-963					
	<b>Intitial Conditions</b>						
	Surface Gas Rate		255.41	MMscf/D	<b>Wellbore</b>		units
					TVD BML	8000	ft
	<b>Depth, ft</b>	<b>Pressure, psia</b>			Water TVD	10000	ft
	10000	4479.977			DS Status	no DS	n/a
	10800	4555.745			Parameter	csg	n/a
	11600	4631.673			Par. Value	12.75	
	12400	4707.757					
	13200	4783.991					
	14000	4860.374					
	14800	4936.9					
	15600	5013.567					
	16400	5090.37					
	17200	5167.308					
	18000	5250.147					
79	Run #	970-981			The drillstring could not be any longer than 11700 ft		
	<b>Intitial Conditions</b>						
	Surface Gas Rate		28.049	MMscf/D	<b>Wellbore</b>		units
					TVD BML	12000	ft
	<b>Depth, ft</b>	<b>Pressure, psia</b>			Water TVD	0	ft
	0	178.698			DS Status	hanging	n/a
	1200	1675.161			Parameter	csg	n/a
	2400	2378.249			Par. Value	8.625	
	3600	2954.465			<b>DS Length</b>	11700	
	4800	3473.274					
	6000	3959.453					
	7200	4424.707					
	8400	4875.471					
	9600	5315.645					
	10800	5747.766					
	12000	6543.663					
80	Run #	982-993					
	<b>Intitial Conditions</b>						
	Surface Gas Rate		106.096	MMscf/D	<b>Wellbore</b>		units
					TVD BML	12000	ft
	<b>Depth, ft</b>	<b>Pressure, psia</b>			Water TVD	0	ft
	0	165.567			DS Status	hanging	n/a
	1200	114.113			Parameter	csg	n/a
	2400	1606.949			Par. Value	10.75	
	3600	1982.571					
	4800	2317.358					
	6000	2628.552					
	7200	2924.553					
	8400	3210.076					
	9600	3488.014					
	10800	3760.258					

	12000	4727.526					
81	Run #	994-1005					
	<b>Intitial Conditions</b>						
	Surface Gas Rate		191.509	MMscf/D	Wellbore		units
					TVD BML	12000	ft
	Depth, ft	Pressure, psia			Water TVD	0	ft
	0	120.125			DS Status	hanging	n/a
	1200	681.875			Parameter	csg	n/a
	2400	950.021			Par. Value	12.75	
	3600	1167.223					
	4800	1359.839					
	6000	1537.902					
	7200	1706.427					
	8400	1868.295					
	9600	2025.318					
	10800	2178.704					
	12000	2652.204					
82	Run #	1006-1017					
	<b>Intitial Conditions</b>						
	Surface Gas Rate		140.464	MMscf/D	Wellbore		units
					TVD BML	12000	ft
	Depth, ft	Pressure, psia			Water TVD	0	ft
	0	185.764			DS Status	hanging	n/a
	1200	1500.82			Parameter	ds length	n/a
	2400	2108.681			Par. Value	50	
	3600	2605.855					
	4800	3052.184					
	6000	3469.432					
	7200	3557.314					
	8400	3638.077					
	9600	3718.254					
	10800	3797.88					
	12000	3884.374					
83	Run #	1018-1029					
	<b>Intitial Conditions</b>						
	Surface Gas Rate		163.122	MMscf/D	Wellbore		units
					TVD BML	12000	ft
	Depth, ft	Pressure, psia			Water TVD	0	ft
	0	260.305			DS Status	hanging	n/a
	1200	1734.345			Parameter	ds length	n/a
	2400	2438.992			Par. Value	25	%
	3600	2785.737					
	4800	2859.509					
	6000	2932.847					
	7200	3005.781					
	8400	3078.337					
	9600	3150.538					
	10800	3222.407					
	12000	3305.461					

84	Run #	1030-1041	DS length caused surface pressure to not converge			
	Intitial Conditions		had to reduce DS length to 9000 ft.			
	Surface Gas Rate		28.441	MMscf/D	Wellbore	units
					TVD BML	12000 ft
	Depth, ft	Pressure, psia			Water TVD	0 ft
	0	154.134			DS Status	dropped n/a
	1200	170.348			Parameter	csg n/a
	2400	185.981			Par. Value	8.625
	3600	1254.654			DS length	9000 ft
	4800	2154.34				
	6000	2812.067				
	7200	3381.752				
	8400	3905.131				
	9600	4400.004				
	10800	4875.626				
	12000	6534.454				
85	Run #	1042-1053				
	Intitial Conditions					
	Surface Gas Rate		106.096	MMscf/D	Wellbore	units
					TVD BML	12000 ft
	Depth, ft	Pressure, psia			Water TVD	0 ft
	0	165.567			DS Status	dropped n/a
	1200	1144.113			Parameter	csg n/a
	2400	1606.949			Par. Value	10.75
	3600	1982.571				
	4800	2317.358				
	6000	2628.552				
	7200	2924.553				
	8400	3210.076				
	9600	3488.014				
	10800	3760.258				
	12000	4727.526				
86	Run #	1054-1065				
	Intitial Conditions					
	Surface Gas Rate		191.509	MMscf/D	Wellbore	units
					TVD BML	12000 ft
	Depth, ft	Pressure, psia			Water TVD	0 ft
	0	120.125			DS Status	dropped n/a
	1200	681.875			Parameter	csg n/a
	2400	950.021			Par. Value	12.75
	3600	1167.223				
	4800	1359.839				
	6000	1537.902				
	7200	1706.427				
	8400	1868.295				
	9600	2025.318				
	10800	2178.704				
	12000	2652.204				
87	Run #	1066-1077				
	Intitial Conditions					

	Surface Gas Rate		123.09	MMscf/D	<b>Wellbore</b>		units
					TVD BML	12000	ft
	<b>Depth, ft</b>	<b>Pressure, psia</b>			Water TVD	0	ft
	0	57.533			DS Status	dropped	n/a
	1200	167.783			Parameter	ds length	n/a
	2400	229.247			Par. Value	50	
	3600	279.615					
	4800	324.404					
	6000	365.788					
	7200	1424.254					
	8400	1991.911					
	9600	2454.005					
	10800	2865.555					
	12000	4314.891					
88	<b>Run #</b>	<b>1078-1088</b>					
	<b>Intitial Conditions</b>						
	Surface Gas Rate		135.363	MMscf/D	<b>Wellbore</b>		units
					TVD BML	12000	ft
	<b>Depth, ft</b>	<b>Pressure, psia</b>			Water TVD	0	ft
	0	68.522			DS Status	dropped	n/a
	1200	185.619			Parameter	ds length	n/a
	2400	252.751			Par. Value	25	
	3600	307.884					
	4800	356.956					
	6000	402.322					
	7200	445.195					
	8400	486.287					
	9600	1204.675					
	10800	1970.222					
	12000	4011.798					
89	<b>Run #</b>	<b>1090-1101</b>					
	<b>Intitial Conditions</b>						
	Surface Gas Rate		212.186	MMscf/D	<b>Wellbore</b>		units
					TVD BML	12000	ft
	<b>Depth, ft</b>	<b>Pressure, psia</b>			Water TVD	0	ft
	0	115.132			DS Status	no DS	n/a
	1200	507.452			Parameter	csg	n/a
	2400	701.292			Par. Value	8.625	
	3600	858.953					
	4800	998.86					
	6000	1128.131					
	7200	1250.361					
	8400	1367.637					
	9600	1481.283					
	10800	1592.19					
	12000	1802.077					
90	<b>Run #</b>	<b>1102-1113</b>					
	<b>Intitial Conditions</b>						
	Surface Gas Rate		237.405	MMscf/D	<b>Wellbore</b>		units
					TVD BML	12000	ft

	<b>Depth, ft</b>	<b>Pressure, psia</b>		Water TVD	0	ft
	0	69.17		DS Status	no DS	n/a
	1200	315.518		Parameter	csg	n/a
	2400	433.812		Par. Value	10.75	
	3600	530.201				
	4800	615.749				
	6000	694.748				
	7200	769.376				
	8400	840.903				
	9600	910.143				
	10800	977.646				
	12000	1118.184				
91	<b>Run #</b>	<b>1114-1125</b>				
	<b>Intitial Conditions</b>					
	Surface Gas Rate		254.085	MMscf/D	<b>Wellbore</b>	units
					TVD BML	12000
	<b>Depth, ft</b>	<b>Pressure, psia</b>		Water TVD	0	ft
	0	48.827		DS Status	no DS	n/a
	1200	199.015		Parameter	csg	n/a
	2400	271.892		Par. Value	12.75	
	3600	331.415				
	4800	384.292				
	6000	433.133				
	7200	479.268				
	8400	523.474				
	9600	566.251				
	10800	607.937				
	12000	696.632				
92	<b>Run #</b>	<b>1132-1143</b>	DS length caused surface pressure to not converge			
	<b>Intitial Conditions</b>		had to reduce DS length to 11500 ft.			
	Surface Gas Rate		39.948	MMscf/D	<b>Wellbore</b>	units
					TVD BML	12000
	<b>Depth, ft</b>	<b>Pressure, psia</b>		Water TVD	5000	ft
	5000	2233.037		DS Status	hanging	n/a
	6200	3228.878		Parameter	csg	n/a
	7400	4067.113		Par. Value	8.625	
	8600	4827.977		<b>DS Length</b>	11500	ft
	9800	5545.367				
	11000	6234.752				
	12200	6904.512				
	13400	7559.703				
	14600	8203.62				
	15800	8838.531				
	17000	9272.727				
93	<b>Run #</b>	<b>1144-1155</b>				
	<b>Intitial Conditions</b>					
	Surface Gas Rate		142.881	MMscf/D	<b>Wellbore</b>	units
					TVD BML	12000
	<b>Depth, ft</b>	<b>Pressure, psia</b>		Water TVD	5000	ft
	5000	2225.023		DS Status	hanging	n/a

	6200	2686.583			Parameter	csg	n/a
	7400	3114.88			Par. Value	10.75	
	8600	3518.58					
	9800	3906.309					
	11000	4282.943					
	12200	4651.481					
	13400	5013.892					
	14600	5371.528					
	15800	5725.353					
	17000	6981.855					
94	Run #	1156-1167					
	<b>Intitial Conditions</b>						
	Surface Gas Rate		259.481	MMscf/D	<b>Wellbore</b>		units
					TVD BML	12000	ft
	<b>Depth, ft</b>	<b>Pressure, psia</b>			Water TVD	5000	ft
	5000	2231.141			DS Status	hanging	n/a
	6200	2431.956			Parameter	csg	n/a
	7400	2631.477			Par. Value	12.75	
	8600	2828.034					
	9800	3022.396					
	11000	3215.108					
	12200	3406.562					
	13400	3597.05					
	14600	3786.789					
	15800	3975.946					
	17000	4504.613					
95	Run #	1168-1179					
	<b>Intitial Conditions</b>						
	Surface Gas Rate		174.174	MMscf/D	<b>Wellbore</b>		units
					TVD BML	12000	ft
	<b>Depth, ft</b>	<b>Pressure, psia</b>			Water TVD	5000	ft
	5000	2251.437			DS Status	hanging	n/a
	6200	2884.577			Parameter	ds length	n/a
	7400	3451.11			Par. Value	50	%
	8600	3976.176					
	9800	4475.905					
	11000	4958.624					
	12200	5429.174					
	13400	5890.608					
	14600	6042.772					
	15800	6160.471					
	17000	6285.125					
96	Run #	1180-1191					
	<b>Intitial Conditions</b>						
	Surface Gas Rate		206.778	MMscf/D	<b>Wellbore</b>		units
					TVD BML	12000	ft
	<b>Depth, ft</b>	<b>Pressure, psia</b>			Water TVD	5000	ft
	5000	2248.118			DS Status	hanging	n/a
	6200	3088.794			Parameter	ds length	n/a
	7400	3812.441			Par. Value	25	

	8600	4473.625					
	9800	4877.035					
	11000	4990.087					
	12200	5102.619					
	13400	5214.657					
	14600	5326.225					
	15800	5437.343					
	17000	5559.545					
97	<b>Run #</b>	<b>1192-1203</b>	<b>DS length caused surface pressure to not converge</b>				
	<b>Intitial Conditions</b>		had to reduce DS length to 8500 ft.				
	Surface Gas Rate		38.418 MMscf/D	<b>Wellbore</b>		units	
				TVD BML	12000	ft	
	<b>Depth, ft</b>	<b>Pressure, psia</b>		Water TVD	50000	ft	
	5000	2244.629		DS Status	dropped	n/a	
	6200	2306.673		Parameter	csg	n/a	
	7400	2368.675		Par. Value	8.625		
	8600	2512.553					
	9800	3453.615					
	11000	4253.232					
	12200	4984.885					
	13400	5676.284					
	14600	6340.959					
	15800	6986.547					
	17000	9308.083					
98	<b>Run #</b>	<b>1204-1215</b>					
	<b>Intitial Conditions</b>						
	Surface Gas Rate		142.806 MMscf/D	<b>Wellbore</b>		units	
				TVD BML	12000	ft	
	<b>Depth, ft</b>	<b>Pressure, psia</b>		Water TVD	5000	ft	
	5000	2225.189		DS Status	dropped	n/a	
	6200	2693.896		Parameter	csg	n/a	
	7400	3121.207		Par. Value	10.75		
	8600	3524.19					
	9800	3911.353					
	11000	4287.513					
	12200	4655.638					
	13400	5017.679					
	14600	5374.975					
	15800	5728.485					
	17000	6983.535					
99	<b>Run #</b>	<b>1216-1227</b>					
	<b>Intitial Conditions</b>						
	Surface Gas Rate		259.416 MMscf/D	<b>Wellbore</b>		units	
				TVD BML	12000	ft	
	<b>Depth, ft</b>	<b>Pressure, psia</b>		Water TVD	5000	ft	
	5000	2230.967		DS Status	dropped	n/a	
	6200	2434.418		Parameter	csg	n/a	
	7400	2633.808		Par. Value	12.75		
	8600	2830.253					
	9800	3024.519					

	11000	3217.144					
	12200	3408.519					
	13400	3598.935					
	14600	3788.606					
	15800	3977.7					
	17000	4506.038					
100	<b>Run #</b>	<b>1228-1239</b>					
	<b>Intitial Conditions</b>						
	Surface Gas Rate		154.717	MMscf/D	<b>Wellbore</b>		units
					TVD BML	12000	ft
	<b>Depth, ft</b>	<b>Pressure, psia</b>			Water TVD	5000	ft
	5000	2248.266			DS Status	dropped	n/a
	6200	2315.583			Parameter	ds length	n/a
	7400	2382.979			Par. Value	50	
	8600	2409.311					
	9800	3017.497					
	11000	3497.437					
	12200	3949.219					
	13400	4382.436					
	14600	4802.569					
	15800	5213.032					
	17000	6718.187					
101	<b>Run #</b>	<b>1240-1251</b>					
	<b>Intitial Conditions</b>						
	Surface Gas Rate		174.581	MMscf/D	<b>Wellbore</b>		units
					TVD BML	12000	ft
	<b>Depth, ft</b>	<b>Pressure, psia</b>			Water TVD	5000	ft
	5000	2253.842			DS Status	dropped	n/a
	6200	2323.072			Parameter	ds length	n/a
	7400	2392.417			Par. Value	25	
	8600	2461.872					
	9800	2531.435					
	11000	2601.1					
	12200	2670.866					
	13400	3065.38					
	14600	3673.698					
	15800	4232.331					
	17000	6276.075					
102	<b>Run #</b>	<b>1252-1263</b>					
	<b>Intitial Conditions</b>						
	Surface Gas Rate		284.44	MMscf/D	<b>Wellbore</b>		units
					TVD BML	12000	ft
	<b>Depth, ft</b>	<b>Pressure, psia</b>			Water TVD	5000	ft
	5000	2254.147			DS Status	no DS	n/a
	6200	2388.826			Parameter	csg	n/a
	7400	2523.24			Par. Value	8.625	
	8600	2657.512					
	9800	2791.729					
	11000	2925.958					
	12200	3060.247					

	13400	3194.632						
	14600	3329.139						
	15800	3463.786						
	17000	3683.365						
103	Run #	1264-1275						
	<b>Intitial Conditions</b>							
	Surface Gas Rate		312.868	MMscf/D	<b>Wellbore</b>		units	
					TVD BML	12000	ft	
	<b>Depth, ft</b>	<b>Pressure, psia</b>			Water TVD	5000	ft	
	5000	2242.426			DS Status	no DS	n/a	
	6200	2329.658			Parameter	csg	n/a	
	7400	2417.236			Par. Value	10.75		
	8600	2505.146						
	9800	2593.372						
	11000	2681.9						
	12200	2770.719						
	13400	2859.814						
	14600	2949.175						
	15800	3038.791						
	17000	3170.387						
104	Run #	1276-1287						
	<b>Intitial Conditions</b>							
	Surface Gas Rate		327.848	MMscf/D	<b>Wellbore</b>		units	
					TVD BML	12000	ft	
	<b>Depth, ft</b>	<b>Pressure, psia</b>			Water TVD	5000	ft	
	5000	2256.46			DS Status	no DS	n/a	
	6200	2327.072			Parameter	csg	n/a	
	7400	2397.823			Par. Value	12.75		
	8600	2468.708						
	9800	2539.722						
	11000	2610.859						
	12200	2682.116						
	13400	2753.488						
	14600	2824.97						
	15800	2896.559						
	17000	2984.868						
105	Run #	1294-1306	DS length caused surface pressure to not converge					
	<b>Intitial Conditions</b>		had to reduce DS length to 11500 ft.					
	Surface Gas Rate		46.045	MMscf/D	<b>Wellbore</b>		units	
					TVD BML	12000	ft	
	<b>Depth, ft</b>	<b>Pressure, psia</b>			Water TVD	10000	ft	
	10000	4469.968			DS Status	hanging	n/a	
	11200	5350.204			Parameter	csg	n/a	
	12400	6197.633			Par. Value	8.625		
	13600	7013.631						
	14800	7807.605						
	16000	8585.175						
	17200	9349.979						
	18400	10104.523						
	19600	10850.609						

	20800	11589.582					
	22000	12094.059					
106	<b>Run #</b>	<b>1306-1317</b>					
	<b>Intitial Conditions</b>						
	Surface Gas Rate		162.096	MMscf/D	<b>Wellbore</b>		units
					TVD BML	12000	ft
	<b>Depth, ft</b>	<b>Pressure, psia</b>			Water TVD	10000	ft
	10000	4498.425			DS Status	hanging	n/a
	11200	4906.203			Parameter	csg	n/a
	12400	5314.213			Par. Value	10.75	
	13600	5717.712					
	14800	6117.623					
	16000	6514.616					
	17200	6909.193					
	18400	7301.74					
	19600	7692.557					
	20800	8081.886					
	22000	9446.124					
107	<b>Run #</b>	<b>1318-1329</b>					
	<b>Intitial Conditions</b>						
	Surface Gas Rate		283.957	MMscf/D	<b>Wellbore</b>		units
					TVD BML	12000	ft
	<b>Depth, ft</b>	<b>Pressure, psia</b>			Water TVD	10000	ft
	10000	4496.458			DS Status	hanging	n/a
	11200	4700.333			Parameter	csg	n/a
	12400	4906.133			Par. Value	12.75	
	13600	5112.035					
	14800	5318.036					
	16000	5524.133					
	17200	5730.324					
	18400	5936.604					
	19600	6142.972					
	20800	6349.422					
	22000	6854.937					
108	<b>Run #</b>	<b>1330-1341</b>					
	<b>Intitial Conditions</b>						
	Surface Gas Rate		183.994	MMscf/D	<b>Wellbore</b>		units
					TVD BML	12000	ft
	<b>Depth, ft</b>	<b>Pressure, psia</b>			Water TVD	10000	ft
	10000	4503.164			DS Status	hanging	n/a
	11200	4994.398			Parameter	ds length	n/a
	12400	5482.607			Par. Value	50	
	13600	5962.739					
	14800	6436.613					
	16000	6905.499					
	17200	7370.315					
	18400	7831.7545					
	19600	8290.317					
	20800	8746.442					
	22000	8951.26					

109	Run #	1342-1353						
	<b>Intitial Conditions</b>							
	Surface Gas Rate		220.159	MMscf/D	<b>Wellbore</b>		units	
					TVD BML	12000	ft	
	<b>Depth, ft</b>	<b>Pressure, psia</b>			Water TVD	10000	ft	
	10000	4501.931			DS Status	hanging	n/a	
	11200	5152.195			Parameter	ds length	n/a	
	12400	5789.802			Par. Value	25		
	13600	6410.782						
	14800	7019.464						
	16000	7436.231						
	17200	7576.311						
	18400	7715.625						
	19600	7854.201						
	20800	7992.068						
	22000	8139.586						
110	Run #	1354-1365	DS length caused surface pressure to not converge					
	<b>Intitial Conditions</b>		had to reduce DS length to 8500 ft.					
	Surface Gas Rate		43.992	MMscf/D	<b>Wellbore</b>		units	
					TVD BML	12000	ft	
	<b>Depth, ft</b>	<b>Pressure, psia</b>			Water TVD	10000	ft	
	10000	4475.112			DS Status	dropped	n/a	
	11200	4585.983			Parameter	csg	n/a	
	12400	4696.126			Par. Value	8.625		
	13600	4866.224						
	14800	5703.971						
	16000	6501.774						
	17200	7272.643						
	18400	8024.002						
	19600	8760.505						
	20800	9486.271						
	22000	12143.047						
111	Run #	1366-1377						
	<b>Intitial Conditions</b>							
	Surface Gas Rate		162.019	MMscf/D	<b>Wellbore</b>		units	
					TVD BML	12000	ft	
	<b>Depth, ft</b>	<b>Pressure, psia</b>			Water TVD	10000	ft	
	10000	4498.437			DS Status	dropped	n/a	
	11200	4911.828			Parameter	csg	n/a	
	12400	5319.442			Par. Value	10.75		
	13600	5722.58						
	14800	6122.155						
	16000	6518.831						
	17200	6913.107						
	18400	7305.363						
	19600	7695.901						
	20800	8084.958						
	22000	9447.875						
112	Run #	1379-1390						

	<b>Intitial Conditions</b>					
	Surface Gas Rate		283.893	MMscf/D	<b>Wellbore</b>	units
					TVD BML	12000 ft
	<b>Depth, ft</b>	<b>Pressure, psia</b>			Water TVD	10000 ft
	10000	4496.573			DS Status	dropped n/a
	11200	4702.231			Parameter	csg n/a
	12400	4907.993			Par. Value	12.75
	13600	5113.857				
	14800	5319.821				
	16000	5525.881				
	17200	5732.034				
	18400	5938.278				
	19600	6144.608				
	20800	6351.021				
	22000	6856.324				
113	<b>Run #</b>	<b>1390-1401</b>				
	<b>Intitial Conditions</b>					
	Surface Gas Rate		165.37	MMscf/D	<b>Wellbore</b>	units
					TVD BML	12000 ft
	<b>Depth, ft</b>	<b>Pressure, psia</b>			Water TVD	10000 ft
	10000	4497.941			DS Status	dropped n/a
	11200	4662.878			Parameter	ds length n/a
	12400	5088.627			Par. Value	50
	13600	5508.192				
	14800	5922.944				
	16000	6333.849				
	17200	6741.615				
	18400	7146.774				
	19600	7549.733				
	20800	7950.816				
	22000	9371.963				
114	<b>Run #</b>	<b>1402-1503</b>				
	<b>Intitial Conditions</b>					
	Surface Gas Rate		188.757	MMscf/D	<b>Wellbore</b>	units
					TVD BML	12000 ft
	<b>Depth, ft</b>	<b>Pressure, psia</b>			Water TVD	10000 ft
	10000	4495.571			DS Status	dropped n/a
	11200	4611.152			Parameter	ds length n/a
	12400	4726.094			Par. Value	25
	13600	4840.434				
	14800	4954.2				
	16000	5067.423				
	17200	5422.988				
	18400	5943.862				
	19600	6454.308				
	20800	6956.624				
	22000	8843.969				
115	<b>Run #</b>	<b>1414-1425</b>				
	<b>Intitial Conditions</b>					
	Surface Gas Rate		304.261	MMscf/D	<b>Wellbore</b>	units

					TVD BML	12000	ft
	<b>Depth, ft</b>	<b>Pressure, psia</b>			Water TVD	10000	ft
	10000	4497.873			DS Status	no DS	n/a
	11200	4655.111			Parameter	csg	n/a
	12400	4812.334			Par. Value	8.625	
	13600	4969.542					
	14800	5126.735					
	16000	5283.913					
	17200	5441.078					
	18400	5598.229					
	19600	5755.367					
	20800	5912.492					
	22000	6134.996					
116	<b>Run #</b>	<b>1426-1437</b>					
	<b>Intitial Conditions</b>						
	Surface Gas Rate		325.962	MMscf/D	<b>Wellbore</b>		units
					TVD BML	12000	ft
	<b>Depth, ft</b>	<b>Pressure, psia</b>			Water TVD	10000	ft
	10000	4522.838			DS Status	no Ds	n/a
	11200	4649.351			Parameter	csg	n/a
	12400	4775.423			Par. Value	10.75	
	13600	4901.079					
	14800	5026.343					
	16000	5151.234					
	17200	5275.773					
	18400	5399.977					
	19600	5523.862					
	20800	5647.444					
	22000	5798.533					
117	<b>Run #</b>	<b>1438-1449</b>					
	<b>Intitial Conditions</b>						
	Surface Gas Rate		340.982	MMscf/D	<b>Wellbore</b>		units
					TVD BML	12000	ft
	<b>Depth, ft</b>	<b>Pressure, psia</b>			Water TVD	10000	ft
	10000	4483.238			DS Status	no Ds	n/a
	11200	4599.012			Parameter	csg	n/a
	12400	4714.159			Par. Value	12.75	
	13600	4828.714					
	14800	4942.706					
	16000	5056.163					
	17200	5169.113					
	18400	5281.578					
	19600	5393.58					
	20800	5505.141					
	22000	5626.952					

## APPENDIX C

### RELIEF WELL KILL REQUIREMENTS

Run #	TVD BML	WATER DEPTH	DRILLSTRING STATUS	PAR. VARIED	PAR. VALUE	MD/TVD Ratio	ANN ID/ DS OD	KILL RATE	SPP	RELIEF WELLS	SPP/WELL	PUMP HP
487	8000	0	Hanging from BOP	Casing OD	8.625	1	1.5	177.3	2950.6	1	2950.6	305.2
491	8000	0	Hanging from BOP	Casing OD	8.625	1.5	1.5	177.3	3405.6	1	3405.6	352.2
495	8000	0	Hanging from BOP	Casing OD	8.625	2	1.5	177.3	3860.6	1	3860.6	399.3
499	8000	0	Hanging from BOP	Casing OD	10.75	1	1.5	1017.2	31423.1	2	9416.7	2807.6
503	8000	0	Hanging from BOP	Casing OD	10.75	1.5	1.5	1017.2	46103.5	2	13161.5	3905.5
507	8000	0	Hanging from BOP	Casing OD	10.75	2	1.5	1017.2	60784.0	2	8666.1	1714.4
511	8000	0	Hanging from BOP	Casing OD	12.75	1	1.5	3430.8	328184.0	6	11527.4	3845.6
515	8000	0	Hanging from BOP	Casing OD	12.75	1.5	1.5	3430.8	491183.0	7	12496.7	3573.4
519	8000	0	Hanging from BOP	Casing OD	12.75	2	1.5	3430.8	654181.9	8	12725.5	3183.9
523	8000	0	Hanging from BOP	DS Length	50%	1	1.5	1944.3	108466.3	3	14349.3	5425.7
527	8000	0	Hanging from BOP	DS Length	50%	1.5	1.5	1944.3	161516.9	4	12507	3546.8
531	8000	0	Hanging from BOP	DS Length	50%	2	1.5	1944.3	214567.5	5	11038.7	2504.3
535	8000	0	Hanging from BOP	DS Length	25%	1	1.5	2684.1	203073.7	5	10527.1	3297.1
539	8000	0	Hanging from BOP	DS Length	25%	1.5	1.5	2684.1	303466.4	5	14646.5	4587.2

543	8000	0	Hanging from BOP	DS Length	25%	2	1.5	2684.1	403859.1	6	13752	3589.2
547	8000	0	Dropped DS	Casing OD	8.625	1	1.5	177.3	2950.6	1	2950.6	305.2
551	8000	0	Dropped DS	Casing OD	8.625	1.5	1.5	177.3	3405.6	1	3405.6	352.2
555	8000	0	Dropped DS	Casing OD	8.625	2	1.5	177.3	3860.6	1	3860.6	399.3
559	8000	0	Dropped DS	Casing OD	10.75	1	1.5	1017.2	31423.1	2	9461.7	2807.6
563	8000	0	Dropped DS	Casing OD	10.75	1.5	1.5	1017.2	46103.5	2	13161.5	3905.5
567	8000	0	Dropped DS	Casing OD	10.75	2	1.5	1017.2	60784.0	3	8666.1	1714.4
571	8000	0	Dropped DS	Casing OD	12.75	1	1.5	3430.8	328184.0	6	11527.4	3845.6
575	8000	0	Dropped DS	Casing OD	12.75	1.5	1.5	3430.8	491183.0	7	12496.7	3573.4
579	8000	0	Dropped DS	Casing OD	12.75	2	1.5	3430.8	654181.9	8	12725.5	3183.9
583	8000	0	Dropped DS	DS Length	50%	1	1.5	1158.4	39824.6	2	11402.1	3853
587	8000	0	Dropped DS	DS Length	50%	1.5	1.5	1158.4	58827.5	3	8233.7	1854.9
591	8000	0	Dropped DS	DS Length	50%	2	1.5	1158.4	77830.4	3	10372	2336.6
595	8000	0	Dropped DS	DS Length	25%	1	1.5	1247.2	45625.8	2	12719.9	4627.8
599	8000	0	Dropped DS	DS Length	25%	1.5	1.5	1247.2	67628.9	3	9050.3	2195.1
603	8000	0	Dropped DS	DS Length	25%	2	1.5	1247.2	89635.0	3	11527.2	2795.9
607	8000	0	No DS	Casing OD	8.625	1	1.5	6127.3	1023995.1	10	13091	4679.8
611	8000	0	No DS	Casing OD	8.625	1.5	1.5	6127.3	1534806.6	10+		
615	8000	0	No DS	Casing OD	8.625	2	1.5	6127.3	1611428.3	10+		
619	8000	0	No DS	Casing OD	10.75	1	1.5	11231.4	3356966.5	10+		

623	8000	0	No DS	Casing OD	10.75	1.5	1.5	11231.4	5034252.0	10+		
627	8000	0	No DS	Casing OD	10.75	2	1.5	11231.4	6711537.7	10+		
631	8000	0	No DS	Casing OD	12.75	1	1.5	19778.7	10143065.6	10+		
635	8000	0	No DS	Casing OD	12.75	1.5	1.5	19778.7	15213380.9	10+		
639	8000	0	No DS	Casing OD	12.75	2	1.5	19778.7	20283696.1	10+		
649	8000	5000	Hanging from BOP	Casing OD	8.625	1	1.5	217.8	5288.2	1	5288.2	671.9
653	8000	5000	Hanging from BOP	Casing OD	8.625	1.5	1.5	217.8	6571.5	1	6571.5	834.9
657	8000	5000	Hanging from BOP	Casing OD	8.625	2	1.5	217.8	7512.6	1	7512.6	954.5
661	8000	5000	Hanging from BOP	Casing OD	10.75	1	1.5	1266.3	76875.4	3	11476.2	2826.1
665	8000	5000	Hanging from BOP	Casing OD	10.75	1.5	1.5	1266.3	119392.3	4	10560.2	1950.4
669	8000	5000	Hanging from BOP	Casing OD	10.75	2	1.5	1266.3	150571.3	4	12540.4	2316.1
673	8000	5000	Hanging from BOP	Casing OD	12.75	1	1.5	4294.8	828349.5	9	13996.8	3896.9
677	8000	5000	Hanging from BOP	Casing OD	12.75	1.5	1.5	4294.8	1240822.0	10+		
681	8000	5000	Hanging from BOP	Casing OD	12.75	2	1.5	4294.8	1653294.4	10+		
685	8000	5000	Hanging from BOP	DS Length	50%	1	1.5	1919.1	171739.8	4	14419.1	4036.1
689	8000	5000	Hanging from BOP	DS Length	50%	1.5	1.5	1919.1	255753.1	5	14013.6	3138.1
693	8000	5000	Hanging from BOP	DS Length	50%	2	1.5	1919.1	339766.5	6	13268.2	2476
697	8000	5000	Hanging from BOP	DS Length	25%	1	1.5	2644.9	320459.8	6	12582.8	3236.1
701	8000	5000	Hanging from BOP	DS Length	25%	1.5	1.5	2644.9	478921.0	7	13521	2980.6
705	8000	5000	Hanging from BOP	DS Length	25%	2	1.5	2644.9	637382.1	8	13742.7	2650.8

709	8000	5000	Dropped DS	Casing OD	8.625	1	1.5	218.6	5330.4	1	5330.4	679.7
713	8000	5000	Dropped DS	Casing OD	8.625	1.5	1.5	218.6	6450.8	1	6450.8	822.6
717	8000	5000	Dropped DS	Casing OD	8.625	2	1.5	218.6	7571.2	1	7571.2	965.5
721	8000	5000	Dropped DS	Casing OD	10.75	1	1.5	1270.4	77376.0	3	11554.1	2854.6
725	8000	5000	Dropped DS	Casing OD	10.75	1.5	1.5	1270.4	114463.4	4	10269.8	1902.9
729	8000	5000	Dropped DS	Casing OD	10.75	2	1.5	1270.4	151550.0	4	12625.2	2339.4
733	8000	5000	Dropped DS	Casing OD	12.75	1	1.5	4307.7	833259.2	9	14084.2	3933
737	8000	5000	Dropped DS	Casing OD	12.75	1.5	1.5	4307.7	1248174.0	10+		
741	8000	5000	Dropped DS	Casing OD	12.75	2	1.5	4307.7	1663089.7	10+		
745	8000	5000	Dropped DS	DS Length	50%	1	1.5	1329.8	84300.8	3	12235.1	3164.1
749	8000	5000	Dropped DS	DS Length	50%	1.5	1.5	1329.8	124906.4	4	10828.4	2100.2
753	8000	5000	Dropped DS	DS Length	50%	2	1.5	1329.8	165512.0	4	13407.9	2600.6
757	8000	5000	Dropped DS	DS Length	25%	1	1.5	1504.7	106574.4	3	14498.6	4242.8
761	8000	5000	Dropped DS	DS Length	25%	1.5	1.5	1504.7	158460.3	4	12699.3	2787.2
765	8000	5000	Dropped DS	DS Length	25%	2	1.5	1504.7	210346.2	5	11267.2	1978.3
769	8000	5000	No DS	Casing OD	8.625	1	1.5	7662.7	2579528.2	10+		
773	8000	5000	No DS	Casing OD	8.625	1.5	1.5	7662.7	3867451.0	10+		
777	8000	5000	No DS	Casing OD	8.625	2	1.5	7662.7	5155375.0	10+		
781	8000	5000	No DS	Casing OD	10.75	1	1.5	14093.4	8503352.5	10+		
785	8000	5000	No DS	Casing OD	10.75	1.5	1.5	14093.4	10E6+	10+		

789	8000	5000	No DS	Casing OD	10.75	2	1.5	14093.4	10E6+	10+		
793	8000	5000	No DS	Casing OD	12.75	1	1.5	24879.6	10E6+	10+		
797	8000	5000	No DS	Casing OD	12.75	1.5	1.5	24879.6	10E6+	10+		
801	8000	5000	No DS	Casing OD	12.75	2	1.5	24879.6	10E6+	10+		
811	8000	10000	Hanging from BOP	Casing OD	8.625	1	1.5	254.9	8391.3	1	8391.3	1248.1
815	8000	10000	Hanging from BOP	Casing OD	8.625	1.5	1.5	254.9	10497.9	1	10497.9	1561.5
819	8000	10000	Hanging from BOP	Casing OD	8.625	2	1.5	254.9	12604.5	1	12604.5	1874.8
823	8000	10000	Hanging from BOP	Casing OD	10.75	1	1.5	1494.5	146153.8	4	13417.6	2924.8
827	8000	10000	Hanging from BOP	Casing OD	10.75	1.5	1.5	1494.5	217027.8	5	13077.1	2280.4
831	8000	10000	Hanging from BOP	Casing OD	10.75	2	1.5	1494.5	287901.8	6	12451.3	1809.4
835	8000	10000	Hanging from BOP	Casing OD	12.75	1	1.5	5078.4	1593548.9	10+		
839	8000	10000	Hanging from BOP	Casing OD	12.75	1.5	1.5	5078.4	2387957.8	10+		
843	8000	10000	Hanging from BOP	Casing OD	12.75	2	1.5	5078.4	3182366.6	10+		
847	8000	10000	Hanging from BOP	DS Length	50%	1	1.5	1494.5	146153.8	4	13417.6	2924.8
851	8000	10000	Hanging from BOP	DS Length	50%	1.5	1.5	1494.5	217027.8	5	13077.1	2280.4
855	8000	10000	Hanging from BOP	DS Length	50%	2	1.5	1494.5	287901.8	6	12451.3	1809.4
859	8000	10000	Hanging from BOP	DS Length	25%	1	1.5	2647.5	444522.2	7	14093.2	3109.8
863	8000	10000	Hanging from BOP	DS Length	25%	1.5	1.5	2647.5	664353.4	9	13260	2275.7
867	8000	10000	Hanging from BOP	DS Length	25%	2	1.5	2647.5	884184.7	10+		
871	8000	10000	Dropped DS	Casing OD	8.625	1	1.5	255.9	8457.3	1	8457.3	1262.6

875	8000	10000	Dropped DS	Casing OD	8.625	1.5	1.5	255.9	10579.4	1	10579.4	1579.4
879	8000	10000	Dropped DS	Casing OD	8.625	2	1.5	255.9	12701.5	1	12701.5	1896.2
883	8000	10000	Dropped DS	Casing OD	10.75	1	1.5	1499.2	147083.2	4	13507.4	2953.7
887	8000	10000	Dropped DS	Casing OD	10.75	1.5	1.5	1499.2	218405.7	5	13164.7	2303
891	8000	10000	Dropped DS	Casing OD	10.75	2	1.5	1499.2	289728.1	6	12534.9	1827.4
895	8000	10000	Dropped DS	Casing OD	12.75	1	1.5	5093.2	1602741.2	10+		
899	8000	10000	Dropped DS	Casing OD	12.75	1.5	1.5	5093.2	2401729.8	10+		
903	8000	10000	Dropped DS	Casing OD	12.75	2	1.5	5093.2	3200718.5	10+		
907	8000	10000	Dropped DS	DS Length	50%	1	1.5	1499.2	147083.2	4	13507.4	2953.7
911	8000	10000	Dropped DS	DS Length	50%	1.5	1.5	1499.2	218405.7	5	13164.7	2303
915	8000	10000	Dropped DS	DS Length	50%	2	1.5	1499.2	289728.1	6	12534.9	1827.4
919	8000	10000	Dropped DS	DS Length	25%	1	1.5	1706.9	188617.3	5	11686.9	2327.7
923	8000	10000	Dropped DS	DS Length	25%	1.5	1.5	1706.9	280847.7	6	12015.8	1994.3
927	8000	10000	Dropped DS	DS Length	25%	2	1.5	1706.9	373078.1	6	14635.6	2429.1
931	8000	10000	No DS	Casing OD	8.625	1	1.5	9033.9	4931328.8	10+		
935	8000	10000	No DS	Casing OD	8.625	1.5	1.5	9033.9	7394452.7	10+		
939	8000	10000	No DS	Casing OD	8.625	2	1.5	9033.9	8857576.6	10+		
943	8000	10000	No DS	Casing OD	10.75	1	1.5	16646	6299319.7	10+		
947	8000	10000	No DS	Casing OD	10.75	1.5	1.5	16646	10E6+	10+		
951	8000	10000	No DS	Casing OD	10.75	2	1.5	16646	10E6+	10+		

955	8000	10000	No DS	Casing OD	12.75	1	1.5	29415.6	9466214.6	10+		
959	8000	10000	No DS	Casing OD	12.75	1.5	1.5	29415.6	10E6+	10+		
963	8000	10000	No DS	Casing OD	12.75	2	1.5	29415.6	10E6+	10+		
973	12000	0	Hanging from BOP	Casing OD	8.625	1	1.5	223.2	5684.8	1	5684.8	740.2
977	12000	0	Hanging from BOP	Casing OD	8.625	1.5	1.5	223.2	6762.8	1	6762.8	880.6
981	12000	0	Hanging from BOP	Casing OD	8.625	2	1.5	223.2	7840.8	1	7840.8	1020.9
985	12000	0	Hanging from BOP	Casing OD	10.75	1	1.5	1090.6	53657.2	3	8774.4	1860.9
989	12000	0	Hanging from BOP	Casing OD	10.75	1.5	1.5	1090.6	78943.1	3	11618.9	2464.2
993	12000	0	Hanging from BOP	Casing OD	10.75	2	1.5	1090.6	104229.0	3	14463.3	3067.5
997	12000	0	Hanging from BOP	Casing OD	12.75	1	1.5	3637.6	552106.7	7	14828	4495.6
1001	12000	0	Hanging from BOP	Casing OD	12.75	1.5	1.5	3637.6	826538.3	9	13781.7	3249.9
1005	12000	0	Hanging from BOP	Casing OD	12.75	2	1.5	3637.6	1100969.0	10+		
1009	12000	0	Hanging from BOP	DS Length	50%	1	1.5	1895	154634.3	4	12999.5	3593.1
1013	12000	0	Hanging from BOP	DS Length	50%	1.5	1.5	1895	230270.3	5	12634.5	2793.8
1017	12000	0	Hanging from BOP	DS Length	50%	2	1.5	1895	305906.3	6	11963.6	2204.5
1021	12000	0	Hanging from BOP	DS Length	25%	1	1.5	2612.7	288785.1	5	14949.8	4557.7
1025	12000	0	Hanging from BOP	DS Length	25%	1.5	1.5	2612.7	431559.1	7	12230.9	2663.4
1029	12000	0	Hanging from BOP	DS Length	25%	2	1.5	2612.7	574333.0	8	12430.7	2368.6
1033	12000	0	Dropped DS	Casing OD	8.625	1	1.5	204.2	4683.4	1	4683.4	557.9
1037	12000	0	Dropped DS	Casing OD	8.625	1.5	1.5	204.2	5586.8	1	5586.8	665.5

1041	12000	0	Dropped DS	Casing OD	8.625	2	1.5	204.2	6490.1	1	6490.1	773.1
1045	12000	0	Dropped DS	Casing OD	10.75	1	1.5	1090.6	53657.2	3	8774.4	1860.9
1049	12000	0	Dropped DS	Casing OD	10.75	1.5	1.5	1090.6	78943.1	3	11618.9	2464.2
1053	12000	0	Dropped DS	Casing OD	10.75	2	1.5	1090.6	104229.0	3	14463.3	3067.5
1057	12000	0	Dropped DS	Casing OD	12.75	1	1.5	3637.6	552106.7	7	14828	4495.6
1061	12000	0	Dropped DS	Casing OD	12.75	1.5	1.5	3637.6	826538.3	9	13781.7	3249.9
1065	12000	0	Dropped DS	Casing OD	12.75	2	1.5	3637.6	1100696.9	10+		
1069	12000	0	Dropped DS	DS Length	50%	1	1.5	1292.1	73548.0	3	10713.2	2692
1073	12000	0	Dropped DS	DS Length	50%	1.5	1.5	1292.1	97150.4	3	13370.6	3359.8
1077	12000	0	Dropped DS	DS Length	50%	2	1.5	1292.1	144355.2	4	11735.6	2211.7
1081	12000	0	Dropped DS	DS Length	25%	1	1.5	1741.4	131487.1	4	11676.1	2965.8
1085	12000	0	Dropped DS	DS Length	25%	1.5	1.5	1741.4	195465.2	5	11367.7	2309.9
1089	12000	0	Dropped DS	DS Length	25%	2	1.5	1741.4	259443.3	5	13980	2840.8
1093	12000	0	No DS	Casing OD	8.625	1	1.5	6273	1608410.8	10+		
1097	12000	0	No DS	Casing OD	8.625	1.5	1.5	6273	2410869.8	10+		
1101	12000	0	No DS	Casing OD	8.625	2	1.5	6273	3213328.7	10+		
1105	12000	0	No DS	Casing OD	10.75	1	1.5	11571	8004591.0	10+		
1109	12000	0	No DS	Casing OD	10.75	1.5	1.5	11571	8004591.2	10+		
1113	12000	0	No DS	Casing OD	10.75	2	1.5	11571	10E6+	10+		
1117	12000	0	No DS	Casing OD	12.75	1	1.5	20406.3	6170659.5	10+		

1121	12000	0	No DS	Casing OD	12.75	1.5	1.5	20406.3	10E6+	10+		
1125	12000	0	No DS	Casing OD	12.75	2	1.5	20406.3	10E6+	10+		
1135	12000	5000	Hanging from BOP	Casing OD	8.625	1	1.5	280.8	9618.6	1	9618.6	1575.9
1139	12000	5000	Hanging from BOP	Casing OD	8.625	1.5	1.5	280.8	12030.1	1	12030.1	1971
1143	12000	5000	Hanging from BOP	Casing OD	8.625	2	1.5	280.8	14441.5	1	14441.5	2366.1
1147	12000	5000	Hanging from BOP	Casing OD	10.75	1	1.5	1265.6	100407.8	3	14979.4	3686.8
1151	12000	5000	Hanging from BOP	Casing OD	10.75	1.5	1.5	1265.6	148540.8	4	13312.6	2457.4
1155	12000	5000	Hanging from BOP	Casing OD	10.75	2	1.5	1265.6	196673.8	5	11986.9	1770.1
1159	12000	5000	Hanging from BOP	Casing OD	12.75	1	1.5	4239.8	1056094.1	10+		
1163	12000	5000	Hanging from BOP	Casing OD	12.75	1.5	1.5	4239.8	1581946.5	10+		
1167	12000	5000	Hanging from BOP	Casing OD	12.75	2	1.5	4239.8	2107799.0	10+		
1171	12000	5000	Hanging from BOP	DS Length	50%	1	1.5	1858.8	210839.7	5	12990.8	2817.7
1175	12000	5000	Hanging from BOP	DS Length	50%	1.5	1.5	1858.8	313977.9	6	13358.3	2414.5
1179	12000	5000	Hanging from BOP	DS Length	50%	2	1.5	1858.8	417116.1	7	13193.4	2044.1
1183	12000	5000	Hanging from BOP	DS Length	25%	1	1.5	2543.7	387991.0	7	12347.1	2617.8
1187	12000	5000	Hanging from BOP	DS Length	25%	1.5	1.5	2543.7	579839.9	8	13555.2	2514.7
1191	12000	5000	Hanging from BOP	DS Length	25%	2	1.5	2543.7	771688.7	9	14063	2319
1195	12000	5000	Dropped DS	Casing OD	8.625	1	1.5	239.1	7289.5	1	7289.5	1016.9
1199	12000	5000	Dropped DS	Casing OD	8.625	1.5	1.5	239.1	9040.9	1	9040.9	1261.2
1203	12000	5000	Dropped DS	Casing OD	8.625	2	1.5	239.1	10792.3	1	10792.3	1505.5

1207	12000	5000	Dropped DS	Casing OD	10.75	1	1.5	1270.3	101159.2	4	10337.1	1915.3
1211	12000	5000	Dropped DS	Casing OD	10.75	1.5	1.5	1270.3	149649.9	4	13416.8	2485.9
1215	12000	5000	Dropped DS	Casing OD	10.75	2	1.5	1270.3	198140.6	5	12081.2	1790.7
1219	12000	5000	Dropped DS	Casing OD	12.75	1	1.5	4254.4	1063280.3	10+		
1223	12000	5000	Dropped DS	Casing OD	12.75	1.5	1.5	4254.4	1592708.1	10+		
1227	12000	5000	Dropped DS	Casing OD	12.75	2	1.5	4254.4	2122135.9	10+		
1231	12000	5000	Dropped DS	DS Length	50%	1	1.5	1397.7	121204.4	4	11424.1	2329
1235	12000	5000	Dropped DS	DS Length	50%	1.5	1.5	1397.7	179819.3	5	11143	1817.3
1239	12000	5000	Dropped DS	DS Length	50%	2	1.5	1397.7	238434.2	5	13532.5	2207.1
1243	12000	5000	Dropped DS	DS Length	25%	1	1.5	1620.7	160811.7	4	13601.4	3215.2
1247	12000	5000	Dropped DS	DS Length	25%	1.5	1.5	1620.7	239417.6	5	13222.9	2500.6
1251	12000	5000	Dropped DS	DS Length	25%	2	1.5	1620.7	318023.4	6	12527.7	1974.3
1255	12000	5000	No DS	Casing OD	8.625	1	1.5	7304.2	3070682.1	10+		
1259	12000	5000	No DS	Casing OD	8.625	1.5	1.5	7304.2	4603666.8	10+		
1263	12000	5000	No DS	Casing OD	8.625	2	1.5	7304.2	6136651.4	10+		
1267	12000	5000	No DS	Casing OD	10.75	1	1.5	13509.7	10E6+	10+		
1271	12000	5000	No DS	Casing OD	10.75	1.5	1.5	13509.7	10E6+	10+		
1275	12000	5000	No DS	Casing OD	10.75	2	1.5	13509.7	10E6+	10+		
1279	12000	5000	No DS	Casing OD	12.75	1	1.5	23872	10E6+	10+		
1283	12000	5000	No DS	Casing OD	12.75	1.5	1.5	23872	10E6+	10+		

1287	12000	5000	No DS	Casing OD	12.75	2	1.5	23872	10E6+	10+		
1297	12000	10000	Hanging from BOP	Casing OD	8.625	1	1.5	313.2	13688.3	1	13688.3	2501.1
1301	12000	10000	Hanging from BOP	Casing OD	8.625	1.5	1.5	313.2	17564.9	2	8869.7	810.3
1305	12000	10000	Hanging from BOP	Casing OD	8.625	2	1.5	313.2	21441.6	2	9848	899.7
1309	12000	10000	Hanging from BOP	Casing OD	10.75	1	1.5	1434.2	164966.7	5	11809	1976.3
1313	12000	10000	Hanging from BOP	Casing OD	10.75	1.5	1.5	1434.2	244800.6	6	12094.6	1686.7
1317	12000	10000	Hanging from BOP	Casing OD	10.75	2	1.5	1434.2	324634.4	6	14359.8	2002.6
1321	12000	10000	Hanging from BOP	Casing OD	12.75	1	1.5	4813.7	1753315.0	10+		
1325	12000	10000	Hanging from BOP	Casing OD	12.75	1.5	1.5	4813.7	2627156.8	10+		
1329	12000	10000	Hanging from BOP	Casing OD	12.75	2	1.5	4813.7	3500997.9	10+		
1333	12000	10000	Hanging from BOP	DS Length	50%	1	1.5	1866.1	274953.5	6	13578.4	2463.9
1337	12000	10000	Hanging from BOP	DS Length	50%	1.5	1.5	1866.1	409464.7	7	14373	2235.5
1341	12000	10000	Hanging from BOP	DS Length	50%	2	1.5	1866.1	543975.8	8	14562.7	1981.9
1345	12000	10000	Hanging from BOP	DS Length	25%	1	1.5	2516.2	491373.2	8	13217.8	2425.5
1349	12000	10000	Hanging from BOP	DS Length	25%	1.5	1.5	2516.2	734360.3	9	14677.7	2394.1
1353	12000	10000	Hanging from BOP	DS Length	25%	2	1.5	2516.2	977348.0	10+		
1357	12000	10000	Dropped DS	Casing OD	8.625	1	1.5	271.5	10703.9	1	10703.9	1695.6
1361	12000	10000	Dropped DS	Casing OD	8.625	1.5	1.5	271.5	13622.3	1	13622.3	2158
1365	12000	10000	Dropped DS	Casing OD	8.625	2	1.5	271.5	16540.7	2	7816.5	619.1
1369	12000	10000	Dropped DS	Casing OD	10.75	1	1.5	1439.5	166189.3	5	11902.6	1999.3

1373	12000	10000	Dropped DS	Casing OD	10.75	1.5	1.5	1439.5	246611.8	6	12190.3	1706.4
1377	12000	10000	Dropped DS	Casing OD	10.75	2	1.5	1439.5	327034.2	6	14472.2	2025.8
1381	12000	10000	Dropped DS	Casing OD	12.75	1	1.5	4830.1	1765106.1	10+		
1385	12000	10000	Dropped DS	Casing OD	12.75	1.5	1.5	4830.1	2644819.9	10+		
1389	12000	10000	Dropped DS	Casing OD	12.75	2	1.5	4830.1	3524533.0	10+		
1393	12000	10000	Dropped DS	DS Length	50%	1	1.5	1475.7	174238.0	5	12161.4	2094.2
1397	12000	10000	Dropped DS	DS Length	50%	1.5	1.5	1475.7	258721.5	6	12463.4	1788.5
1401	12000	10000	Dropped DS	DS Length	50%	2	1.5	1475.7	343205.0	6	14860.8	2132.5
1405	12000	10000	Dropped DS	DS Length	25%	1	1.5	1781.8	250430.5	5	14977.2	3113.9
1409	12000	10000	Dropped DS	DS Length	25%	1.5	1.5	1781.8	373169.7	7	12652.2	1879
1413	12000	10000	Dropped DS	DS Length	25%	2	1.5	1781.8	495908.9	8	12825.6	1666.6
1417	12000	10000	No DS	Casing OD	8.625	1	1.5	8270	5069017.6	10+		
1421	12000	10000	No DS	Casing OD	8.625	1.5	1.5	8270	7600520.0	10+		
1425	12000	10000	No DS	Casing OD	8.625	2	1.5	8270	10E6+	10+		
1429	12000	10000	No DS	Casing OD	10.75	1	1.5	15323.5	6946833.0	10+		
1433	12000	10000	No DS	Casing OD	10.75	1.5	1.5	15323.5	10E6+	10+		
1437	12000	10000	No DS	Casing OD	10.75	2	1.5	15323.5	10E6+	10+		
1441	12000	10000	No DS	Casing OD	12.75	1	1.5	27104.5	10E6+	10+		
1445	12000	10000	No DS	Casing OD	12.75	1.5	1.5	27104.5	10E6+	10+		
1449	12000	10000	No DS	Casing OD	12.75	2	1.5	27104.5	10E6+	10+		

## APPENDIX D

### KILL WITH DRILLSTRING INITIAL CONDITIONS

**Run #**      **DS1**

**Initial Conditions**

Surface Gas Rate		20.938 MMscf/D	<b>Wellbore</b>	units
<b>Depth, ft</b>	<b>Pressure, psia</b>		TVD BML	8000 ft
	0	126.193	Water TVD	0 ft
	800	1049.791	DS Status	1 n/a
	1600	1465.164	Parameter	csg n/a
	2400	1795.191	Par. Value	8.625
	3200	2083.724		
	4000	2347.506		
	4800	2594.901		
	5600	2830.717		
	6400	3057.974		
7200	3278.685			
8000	4313.13			

**Run #**      **DS2**

**Initial Conditions**

Surface Gas Rate		28.335 MMscf/D	<b>Wellbore</b>	units
<b>Depth, ft</b>	<b>Pressure, psia</b>		TVD BML	8000 ft
	0	164.682	Water TVD	0 ft
	800	1406.603	DS Status	0.75 n/a
	1600	1962.283	Parameter	CSG n/a
	2400	2406.842	Par. Value	8.625
	3200	2798.486		
	4000	3159.017		
	4800	3499.122		
	5600	3824.842		
	6400	4018.567		
7200	4078.264			
8000	4138.461			

**Run # DS3**

**Initial Conditions**

Surface Gas Rate	33.345 MMscf/D	<b>Wellbore</b>	units
<b>Depth, ft</b>	<b>Pressure, psia</b>	TVD BML	8000 ft
0	205.358	Water TVD	0 ft
800	1645.894	DS Status	0.5 n/a
1600	2297.404	Parameter	csg n/a
2400	2822.193	Par. Value	8.625
3200	3287.36		
4000	3717.66		
4800	3783.938		
5600	3842.827		
6400	3901.497		
7200	3959.954		
8000	4019.229		

**Run # DS4**

**Initial Conditions**

Surface Gas Rate	43.472 MMscf/D	<b>Wellbore</b>	units
<b>Depth, ft</b>	<b>Pressure, psia</b>	TVD BML	8000 ft
0	216.1	Water TVD	0 ft
800	2125.579	DS Status	0.25 n/a
1600	2977.565	Parameter	csg n/a
2400	3379.629	Par. Value	8.625
3200	3436.495		
4000	3493.154		
4800	3549.614		
5600	3605.883		
6400	3661.968		
7200	3717.874		
8000	3775.447		

**Run # DS5**

**Initial Conditions**

Surface Gas Rate		79.633 MMscf/D	<b>Wellbore</b>	units
<b>Depth, ft</b>	<b>Pressure, psia</b>		TVD BML	8000 ft
	0	117.527	Water TVD	0 ft
	800	724.449	DS Status	1 n/a
	1600	1000.264	Parameter	CSG n/a
	2400	1219.84	Par. Value	10.75
	3200	1411.413		
	4000	1585.945		
	4800	1749.01		
	5600	1903.869		
	6400	2052.605		
7200	2196.632			
8000	2905.814			

**Run # DS6**

**Initial Conditions**

Surface Gas Rate		95.837 MMscf/D	<b>Wellbore</b>	units
<b>Depth, ft</b>	<b>Pressure, psia</b>		TVD BML	8000 ft
	0	165.571	Water TVD	0 ft
	800	868.323	DS Status	0.75 n/a
	1600	1197.592	Parameter	CSG n/a
	2400	1459.932	Par. Value	10.75
	3200	1689.147		
	4000	1898.328		
	4800	2094.106		
	5600	2280.338		
	6400	2393.013		
7200	2432.08			
8000	2475.881			

**Run # DS7**

**Initial Conditions**

Surface Gas Rate	104.061 MMscf/D	<b>Wellbore</b>	units
<b>Depth, ft</b>	<b>Pressure, psia</b>	TVD BML	8000 ft
0	158.454	Water TVD	0 ft
800	940.208	DS Status	0.5 n/a
1600	1296.631	Parameter	CSG n/a
2400	1580.708	Par. Value	10.75
3200	1829.122		
4000	2056.043		
4800	2095.771		
5600	2131.862		
6400	2167.97		
7200	2204.095		
8000	2246.406		

**Run # DS8**

**Initial Conditions**

Surface Gas Rate	116.914 MMscf/D	<b>Wellbore</b>	units
<b>Depth, ft</b>	<b>Pressure, psia</b>	TVD BML	8000 ft
0	72.14	Water TVD	0 ft
800	1052.635	DS Status	0.25 n/a
1600	1451.144	Parameter	CSG n/a
2400	1637.885	Par. Value	10.75
3200	1669.036		
4000	1700.25		
4800	1731.526		
5600	1762.861		
6400	1794.225		
7200	1825.708		
8000	1866.641		

**Run # DS9**

**Initial Conditions**

Surface Gas Rate	130.997 MMscf/D	<b>Wellbore</b>	units
<b>Depth, ft</b>	<b>Pressure, psia</b>	TVD BML	8000 ft
0	105.627	Water TVD	0 ft
800	396.879	DS Status	1 n/a
1600	541.958	Parameter	CSG n/a
2400	658.096	Par. Value	12.75
3200	759.556		
4000	851.94		
4800	938.122		
5600	1019.805		
6400	1098.087		
7200	1173.723		
8000	1501.619		

**Run # DS10**

**Initial Conditions**

Surface Gas Rate	139.977 MMscf/D	<b>Wellbore</b>	units
<b>Depth, ft</b>	<b>Pressure, psia</b>	TVD BML	8000 ft
0	83.312	Water TVD	0 ft
800	422.255	DS Status	0.75 n/a
1600	577.351	Parameter	CSG n/a
2400	701.361	Par. Value	12.75
3200	809.652		
4000	908.239		
4800	1000.207		
5600	1087.377		
6400	1140.839		
7200	1160.932		
8000	1188.539		

**Run # DS11**

**Initial Conditions**

Surface Gas Rate		144.002 MMscf/D	<b>Wellbore</b>	units
<b>Depth, ft</b>	<b>Pressure, psia</b>		TVD BML	8000 ft
0	103.607		Water TVD	0 ft
800	434.601		DS Status	0.5 n/a
1600	593.912		Parameter	CSG n/a
2400	721.325		Par. Value	12.75
3200	832.601			
4000	933.917			
4800	953.639			
5600	971.84			
6400	990.106			
7200	1008.436			
8000	1035.954			

**Run # DS12**

**Initial Conditions**

Surface Gas Rate		149.281 MMscf/D	<b>Wellbore</b>	units
<b>Depth, ft</b>	<b>Pressure, psia</b>		TVD BML	8000 ft
0	81.422		Water TVD	0 ft
800	449.811		DS Status	0.25 n/a
1600	614.903		Parameter	CSG n/a
2400	693.88		Par. Value	12.75
3200	709.846			
4000	725.873			
4800	741.961			
5600	758.109			
6400	774.317			
7200	790.584			
8000	819.489			

**Run # DS13**

**Initial Conditions**

Surface Gas Rate	31.473 MMscf/D	<b>Wellbore</b>	units
<b>Depth, ft</b>	<b>Pressure, psia</b>	TVD BML	8000 ft
5000	2235.089	Water TVD	5000 ft
5800	2704.047	DS Status	1 n/a
6600	3121.677	Parameter	CSG n/a
7400	3508.542	Par. Value	8.625
8200	3874.979		
9000	4226.916		
9800	4568.06		
10600	4900.88		
11400	5227.096		
12200	5547.957		
13000	7093.52		

**Run # DS14**

**Initial Conditions**

Surface Gas Rate	47.176 MMscf/D	<b>Wellbore</b>	units
<b>Depth, ft</b>	<b>Pressure, psia</b>	TVD BML	8000 ft
5000	2254.505	Water TVD	5000 ft
5800	3177.214	DS Status	0.75 n/a
6600	3931.308	Parameter	csg n/a
7400	4608.069	Par. Value	8.625
8200	5239.728		
9000	5841.584		
9800	6393.038		
10600	6480.274		
11400	6567.509		
12200	6654.744		
13000	6743.342		

**Run #** DS15

**Initial Conditions**

Surface Gas Rate	74.205 MMscf/D	<b>Wellbore</b>	units
<b>Depth, ft</b>	<b>Pressure, psia</b>	TVD BML	8000 ft
5000	2244.051	Water TVD	5000 ft
5800	4183.142	DS Status	0.5 n/a
6600	5469.953	Parameter	csg n/a
7400	5553.565	Par. Value	8.625
8200	5637.224		
9000	5720.927		
9800	5804.673		
10600	5888.462		
11400	5972.292		
12200	6056.161		
13000	6143.647		

**Run #** DS17

**Initial Conditions**

Surface Gas Rate	122.562 MMscf/D	<b>Wellbore</b>	units
<b>Depth, ft</b>	<b>Pressure, psia</b>	TVD BML	8000 ft
5000	2227.765	Water TVD	5000 ft
5800	2474.895	DS Status	1 n/a
6600	2708.915	Parameter	csg n/a
7400	2933.494	Par. Value	10.75
8200	3151.022		
9000	3363.133		
9800	3570.99		
10600	3775.445		
11400	3977.139		
12200	4176.565		
13000	5132.52		

**Run # DS18**

**Initial Conditions**

Surface Gas Rate	156.02 MMscf/D	<b>Wellbore</b>	units
<b>Depth, ft</b>	<b>Pressure, psia</b>	TVD BML	8000 ft
5000	2260.831	Water TVD	5000 ft
5800	2624.979	DS Status	0.75 n/a
6600	2958.494	Parameter	csg n/a
7400	3272.059	Par. Value	10.75
8200	3571.685		
9000	3861.085		
9800	4130.086		
10600	4198.412		
11400	4266.917		
12200	4335.596		
13000	4411.525		

**Run # DS19**

**Initial Conditions**

Surface Gas Rate	190.465 MMscf/D	<b>Wellbore</b>	units
<b>Depth, ft</b>	<b>Pressure, psia</b>	TVD BML	8000 ft
5000	2248.771	Water TVD	5000 ft
5800	2760.952	DS Status	0.5 n/a
6600	3167.274	Parameter	csg n/a
7400	3227.204	Par. Value	10.75
8200	3287.413		
9000	3347.894		
9800	3408.64		
10600	3469.646		
11400	3530.907		
12200	3592.416		
13000	3666.403		

**Run # DS21**

**Initial Conditions**

Surface Gas Rate	203.923 MMscf/D	<b>Wellbore</b>	units
<b>Depth, ft</b>	<b>Pressure, psia</b>	TVD BML	8000 ft
5000	2244.619	Water TVD	5000 ft
5800	2344.404	DS Status	1 n/a
6600	2443.682	Parameter	csg n/a
7400	2542.579	Par. Value	12.75
8200	2641.198		
9000	2739.624		
9800	2837.926		
10600	2936.162		
11400	3034.378		
12200	3132.615		
13000	3466.962		

**Run # DS22**

**Initial Conditions**

Surface Gas Rate	220.816 MMscf/D	<b>Wellbore</b>	units
<b>Depth, ft</b>	<b>Pressure, psia</b>	TVD BML	8000 ft
5000	2247.438	Water TVD	5000 ft
5800	2357.243	DS Status	0.75 n/a
6600	2466.143	Parameter	csg n/a
7400	2574.334	Par. Value	12.75
8200	2681.976		
9000	2789.195		
9800	2892.744		
10600	2943.811		
11400	2995.143		
12200	3046.737		
13000	3105.133		

**Run #** DS23

**Intitial Conditions**

Surface Gas Rate		231.313 MMscf/D	<b>Wellbore</b>	units
<b>Depth, ft</b>	<b>Pressure, psia</b>		TVD BML	8000 ft
5000	2264.392		Water TVD	5000 ft
5800	2380.569		DS Status	0.5 n/a
6600	2487.448		Parameter	csg n/a
7400	2534.379		Par. Value	12.75
8200	2581.605			
9000	2629.122			
9800	2676.926			
10600	2725.011			
11400	2773.374			
12200	2822.009			
13000	2878.62			

## APPENDIX E

### KILL WITH DRILLSTRING KILL REQUIREMENTS

RUN	TVD	WATER	DS	PAR.	PAR.	DS	KILL	SPP	PUMP
	BML	DEPTH	STATUS	VARIED	VALUE	LEN.	RATE	/WELL	HP
DS1	8000	0	Kill w/ DS	Casing OD	8.625	1	177.9	2084.9	216.4
DS2	8000	0	Kill w/ DS	Casing OD	8.625	0.75	361.9	4142.2	874.5
DS3	8000	0	Kill w/ DS	Casing OD	8.625	0.5	518.1	5535.6	1673.3
DS4	8000	0	Kill w/ DS	Casing OD	8.625	0.25	825.8	6868.8	3309.4
DS5	8000	0	Kill w/ DS	Casing OD	10.75	1	1020.4	2819.1	1678.3
DS6	8000	0	Kill w/ DS	Casing OD	10.75	0.75	2128	6415.8	7965.5
DS7	8000	0	Kill w/ DS	Casing OD	10.75	0.5	3097.2	8860.8	16011.4
DS8	8000	0	Kill w/ DS	Casing OD	10.75	0.25	5022.3	11362.4	33293.7
DS9	8000	0	Kill w/ DS	Casing OD	12.75	1	3440.7	9940.4	19954.8
DS10	8000	0	Kill w/ DS	Casing OD	12.75	0.75	6888.1	26706.2	107.3251
DS11	8000	0	Kill w/ DS	Casing OD	12.75	0.5	10101.3	37573.7	221436.9
DS12	8000	0	Kill w/ DS	Casing OD	12.75	0.25	16491.5	48903.1	470527.9
DS13	8000	5000	Kill w/ DS	Casing OD	8.625	1	216	3156.2	402.5
DS14	8000	5000	Kill w/ DS	Casing OD	8.625	0.75	508.6	6488.5	1925.4
DS15	8000	5000	Kill w/ DS	Casing OD	8.625	0.5	1079.8	9246.8	5825.4
DS16	8000	5000	Kill w/ DS	Casing OD	8.625	0.25	FRICTION FACTOR FAILED		
DS17	8000	5000	Kill w/ DS	Casing OD	10.75	1	1270.4	5037.1	3733.4
DS18	8000	5000	Kill w/ DS	Casing OD	10.75	0.75	3038.4	13959.8	24746.8
DS19	8000	5000	Kill w/ DS	Casing OD	10.75	0.5	6606.7	31824.1	122667.8
DS20	8000	5000	Kill w/ DS	Casing OD	10.75	0.25	FRICTION FACTOR FAILED		
DS21	8000	5000	Kill w/ DS	Casing OD	12.75	1	4307.7	22903.8	57563.5
DS22	8000	5000	Kill w/ DS	Casing OD	12.75	0.75	9908	81039.6	468461.8
DS23	8000	5000	Kill w/ DS	Casing OD	12.75	0.5	21736.8	239273.8	3034447
DS24	8000	5000	Kill w/ DS	Casing OD	12.75	0.25	FRICTION FACTOR FAILED		
DS25	8000	10000	Kill w/ DS	Casing OD	8.625	1			
DS26	8000	10000	Kill w/ DS	Casing OD	8.625	0.75			
DS27	8000	10000	Kill w/ DS	Casing OD	8.625	0.5			
DS28	8000	10000	Kill w/ DS	Casing OD	8.625	0.25	FRICTION FACTOR FAILED		
DS29	8000	10000	Kill w/ DS	Casing OD	10.75	1			
DS30	8000	10000	Kill w/ DS	Casing OD	10.75	0.75			
DS31	8000	10000	Kill w/ DS	Casing OD	10.75	0.5			
DS32	8000	10000	Kill w/ DS	Casing OD	10.75	0.25	FRICTION FACTOR FAILED		
DS33	8000	10000	Kill w/ DS	Casing OD	12.75	1			
DS34	8000	10000	Kill w/ DS	Casing OD	12.75	0.75			
DS35	8000	10000	Kill w/ DS	Casing OD	12.75	0.5			
DS36	8000	10000	Kill w/ DS	Casing OD	12.75	0.25	FRICTION FACTOR FAILED		
DS37	12000	0	Kill w/ DS	Casing OD	8.625	1			
DS38	12000	0	Kill w/ DS	Casing OD	8.625	0.75			
DS39	12000	0	Kill w/ DS	Casing OD	8.625	0.5			
DS40	12000	0	Kill w/ DS	Casing OD	8.625	0.25			

DS41	12000	0	Kill w/ DS	Casing OD	10.75	1			
DS42	12000	0	Kill w/ DS	Casing OD	10.75	0.75			
DS43	12000	0	Kill w/ DS	Casing OD	10.75	0.5			
DS44	12000	0	Kill w/ DS	Casing OD	10.75	0.25			
DS45	12000	0	Kill w/ DS	Casing OD	12.75	1			
DS46	12000	0	Kill w/ DS	Casing OD	12.75	0.75			
DS47	12000	0	Kill w/ DS	Casing OD	12.75	0.5			
DS48	12000	0	Kill w/ DS	Casing OD	12.75	0.25			
DS49	12000	5000	Kill w/ DS	Casing OD	8.625	1			
DS50	12000	5000	Kill w/ DS	Casing OD	8.625	0.75			
DS51	12000	5000	Kill w/ DS	Casing OD	8.625	0.5			
DS52	12000	5000	Kill w/ DS	Casing OD	8.625	0.25			
DS53	12000	5000	Kill w/ DS	Casing OD	10.75	1			
DS54	12000	5000	Kill w/ DS	Casing OD	10.75	0.75			
DS55	12000	5000	Kill w/ DS	Casing OD	10.75	0.5			
DS56	12000	5000	Kill w/ DS	Casing OD	10.75	0.25			
DS57	12000	5000	Kill w/ DS	Casing OD	12.75	1			
DS58	12000	5000	Kill w/ DS	Casing OD	12.75	0.75			
DS59	12000	5000	Kill w/ DS	Casing OD	12.75	0.5			
DS60	12000	5000	Kill w/ DS	Casing OD	12.75	0.25			
DS61	12000	10000	Kill w/ DS	Casing OD	8.625	1			
DS62	12000	10000	Kill w/ DS	Casing OD	8.625	0.75			
DS63	12000	10000	Kill w/ DS	Casing OD	8.625	0.5			
DS64	12000	10000	Kill w/ DS	Casing OD	8.625	0.25			
DS65	12000	10000	Kill w/ DS	Casing OD	10.75	1			
DS66	12000	10000	Kill w/ DS	Casing OD	10.75	0.75			
DS67	12000	10000	Kill w/ DS	Casing OD	10.75	0.5			
DS68	12000	10000	Kill w/ DS	Casing OD	10.75	0.25			
DS69	12000	10000	Kill w/ DS	Casing OD	12.75	1			
DS70	12000	10000	Kill w/ DS	Casing OD	12.75	0.75			
DS71	12000	10000	Kill w/ DS	Casing OD	12.75	0.5			
DS72	12000	10000	Kill w/ DS	Casing OD	12.75	0.25			

**VITA**

Name: Samuel F. Noynaert

Parents: Mr. Chris C. Noynaert  
Mrs. Peggy K. Noynaert

Address: 4504 Ashley Stone  
College Station, TX 77845

Education: Texas A&M University  
B.S. – Agricultural Engineering, 2003

Texas A&M University  
M.S. – Petroleum Engineering, 2004